406 895

DIGITAL SEISMOGRAPH SYSTEM

FINAL REPORT

CONTRACT NO AF 19(628) 472

PROJECT NO 8652

AFCRL 63 433

TEXAS INSTRUMENTS
INCORPORATED

FINAL REPORT

DIGITAL SEISMOGRAPH SYSTEM

Bruce M. Williams, Program Manager

TEXAS INSTRUMENTS INCORPORATED

Contract AF 19(628)-472
Project 8652
Task 865205

Prepared For

GEOPHYSICS RESEARCH DIRECTORATE
AIR FORCE CAMBRIDGE RESEARCH LABORATORIES
OFFICE OF AEROSPACE RESEARCH
UNITED STATES AIR FORCE
BEDFORD, MASSACHUSETTS

29 MARCH, 1963

WORK SPONSORED BY ADVANCED RESEARCH PROJECTS AGENCY

PROJECT VELA UNIFORM

ARPA Order No. 180-61 Amendment 2

Project Code No. 8100, Task 2

SUMMARY

This report covers work done since 16 April 1962 on the research, design and construction of a prototype three-component Digital Seismograph System. This work was performed by Texas Instruments Incorporated under Contract AF 19(628)-472. The purpose of the contract was to develop a Digital Seismograph System having an output compatible with modern, high-speed computers, and to assemble and evaluate a working model.

In addition, the development included studies of the design and selection of an optimum system for digitizing the motion of seismometer masses.

An additional purpose was to demonstrate that by the utilization and exploitation of digital techniques, it would be possible to build a seismic system that had capabilities exceeding those of conventional completely analog instruments. Specifically, it was the intention of this work to develop a system with greater dynamic range (120 db), a reasonably broad frequency band (0.1 to 10 cps), good linearity and other characteristics such as temperature effects, etc., that would be within the tolerance limits of comparable conventional instruments.

A research evaluation of digital sensors produced two displacement sensors, the linear differential-transformer and the differential-capacitor types, which were acceptable from an entire systems standpoint. Each sensor was designed into a system.

Breadboard design evaluation was made with the differential transformer connected into a closed-loop, digitally encoded bridge which produced a binary floating-point output. Thirteen bits of resolution with 7 floating bits for scaling through a total 20-bit range was provided.

The approach chosen for complete system design was termed the FM-Digital approach. In this approach displacement of the boom which is attached to the differential-capacitor plates, generates a zero- to 40-megacycle FM deviation which drives a binary counter for 20 bits of digital conversion at a 40-cps rate.

In order to provide a compatible seismometer for the digital sensor, analytical appraisal of the effect of tilt on period was made for the simple pendulum, Romberg suspension, swinging gate, spring and mass, and the La Coste pendulum type spring-mass mechanism.

A new horizontal seismometer with the Romberg suspension has been designed and evaluated for the FM sensor. The Press and Ewing seismometer is used for the vertical component.

A calibrated, horizontal shake table was designed for the horizontal seismometer evaluation. Direct reading of displacement is provided.

The magnetic tape digital format is in straight binary form compatible with digital computer evaluation.

System evaluation consisted of comparison with a conventional three-component Benioff seismograph. Because of the wide dynamic range of the digital seismograph system, detailed evaluation requires the use of computer analysis of data obtained.

This seismograph system is a new tool that opens many possibilities previously considered impractical. Data transmission problems are made easier. Direct computer correlation with known signals can be considered. The early exploitation of the capabilities of this tool should contribute heavily to the seismic art.

TABLE OF CONTENTS

LIST OF APPENDICES

LIST OF APPENDICES (Cont'd)

LIST OF ILLUSTRATIONS

LIST OF ILLUSTRATIONS (Cont'd)

SECTION I

INTRODUCTION

The objective of Contract AF 19(628)-472 was to develop a three-component digital seismograph system with advanced state-of-the-art specifications for use in the VELA UNIFORM Program. The recorded information was to be in a format compatible with currently used high-speed digital computers.

An advancement in the state-of-the-art is provided by improved specifications for dynamic range, frequency response and resolution for the instrument. The basic unit of measurement can be displacement, velocity or acceleration of the earth motion. Specifications for the equipment are derived from typical amplitudes of earth motion, power spectrum of the signal and power spectrum of the noise. Information related to these subjects is presented in Appendix A. From a study of published data of ambient noise at the earth's surface and the power spectrum of recorded signals of interest to the VELA UNIFORM Program, it is concluded that an ideal instrument should contain the following specifications:

Dynamic range of a million to one (120 db or 20 binary bits).

Constant resolution.

Velocity sensing.

Broad-band recording from at least 0.1 - 10 cps. (Extension of the low-frequency end to 30 seconds possibly is desirable.)

Total recording range from 0.1 millimicrons to 100 microns. (This could possibly be from 0.2 millimicrons to 200 microns.)

Total system compatibility is required to meet these specifications; therefore, research work for this contract included the design of the seismometer, sensor and associated digital handling circuits. Without this total system approach it is believed that it would have been impossible to approach the ideal specifications.

This report presents a discussion of the reasons for selecting the final design approach, the system design and the evaluation. Details substantiating research and development work are presented in the appendices of the report. Many approaches were considered and discarded for practical

and theoretical reasons, and all of this information - including analytical work and practical design work - are included as substantiating material in the appendices.

A. RESEARCH PROGRAM

The research program is illustrated by Figure 1. A five-month research program preceded fabrication of the equipment. During the research period a study was made of various sensing methods, digitizing methods and aliasing filter problems, and breadboard design was completed for two methods of digitizing. Rice University provided consulting engineering service during this research phase. The four remaining months were used for equipment fabrication. Although the work was done primarily within the Research, Development, and Engineering Department of the Science Services division, support was provided by other groups within Texas Instruments.

Figure 2 shows the project organization with the research and engineering personnel who contributed to the fulfillment of this contract.

B. SENSOR SURVEY

In the early phase of the work approximately 20 sensor approaches were considered. A basic conclusion reached almost immediately concerned power requirements for the sensor element. Rather than let the movement of the mass generate the power required for the seismometer, it was decided to provide a basic power pump for the sensor and to allow the sensor to partition the pump power. A basic problem associated with this approach is the restoring force due to the power partitioning system. Computations and experiments relative to this effect were performed for numerous sensors, and it was concluded that the injected restoring force was negligible.

Figure 3 illustrates the sensors chosen for detailed investigation and the results of the sensor survey and sensor research. Silicon solar cells were characterized by wide dynamic range and relatively low sensitivity of 0.2 microvolts per millimicron. Cadmium sulphide photocells provided good sensitivity of approximately 40 microvolts per millimicron, but noise level was considered excessive, since it was equivalent to 40 microvolts peak-to-peak.

From the sensor study (presented in Appendix D) it was concluded that there were two basic sensors which could be used to approximate total system specifications; i.e., the linear differential transformer sensor and the differential capacitor sensor.

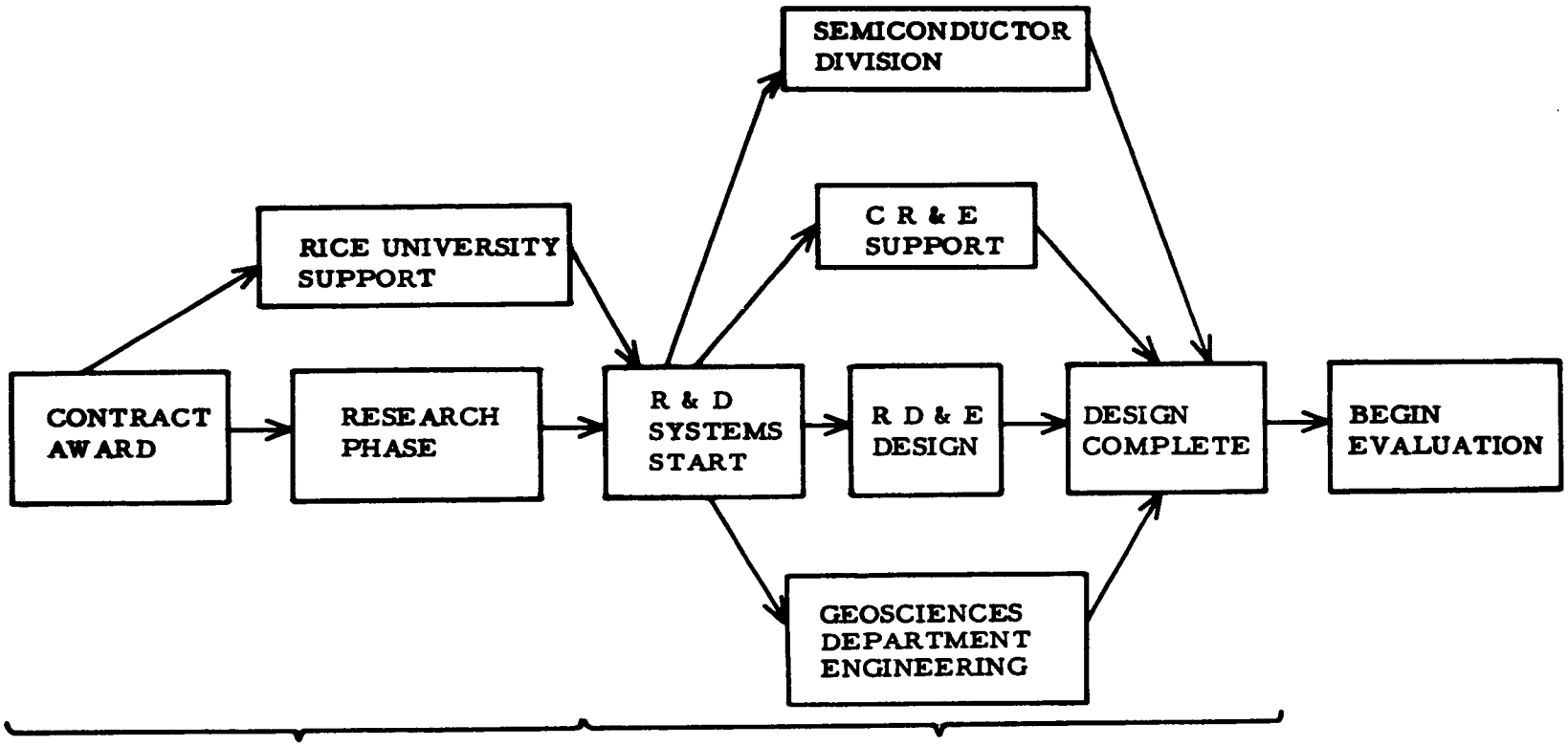

Figure 1. Research Program

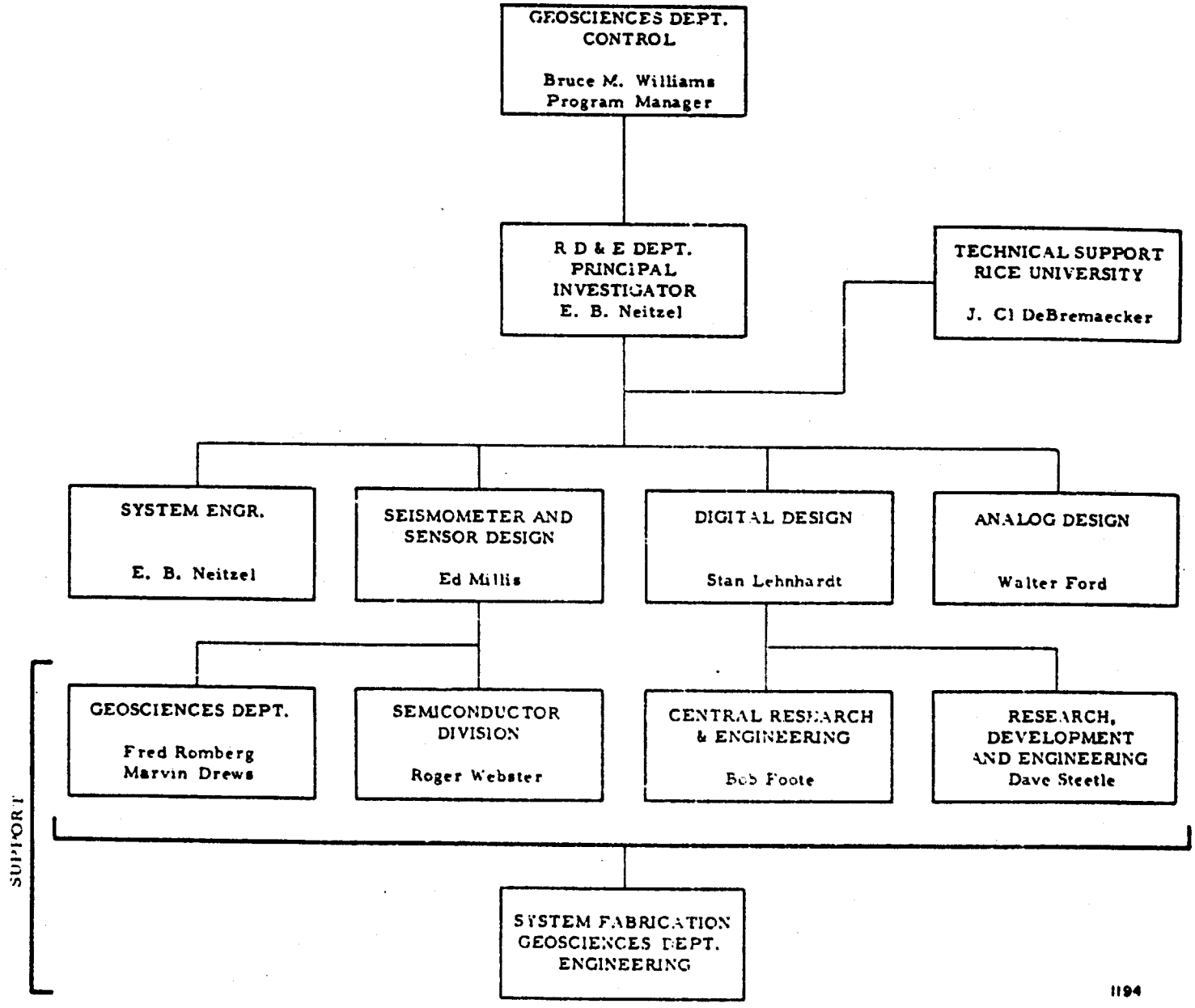

Figure 2. Research Program Personnel

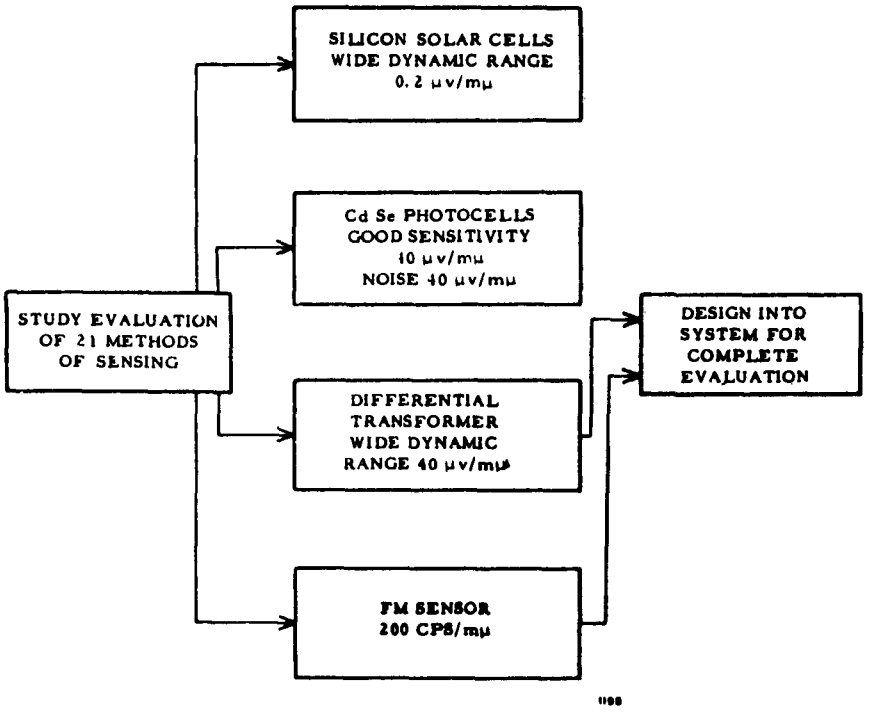

Figure 3. Sensor Research Program

A program of actual breadboard design with additional seismological specifications study was required to make a choice between the two sensors. The differential capacitor sensor was chosen, which provided a frequency-modulated signal proportional to displacement of the seismometer boom.

C. METHODS OF DIGITIZING

Figure 4 is a simplified diagram of the four methods of digitizing considered. Method 1 is considered the conventional approach. An analog sensor is connected through a filter to eliminate aliasing error, then to an amplifier to generate adequate voltage for driving a current state-of-the-art 14-bit analog-to-digital converter. Resolution of approximately 1 part in 16,000 is provided by this conventional approach.

Method 2 is a logical extension of Method 1 where greater dynamic range is required. Additional information results from the use of 6 amplifiers with gain steps of 6 db each. Outputs of the amplifiers are passed through a multiplexer to a conventional analog-to-digital converter. A data block at the output of the analog-to-digital converter would contain a reading from each of the 6 amplifiers for each sample

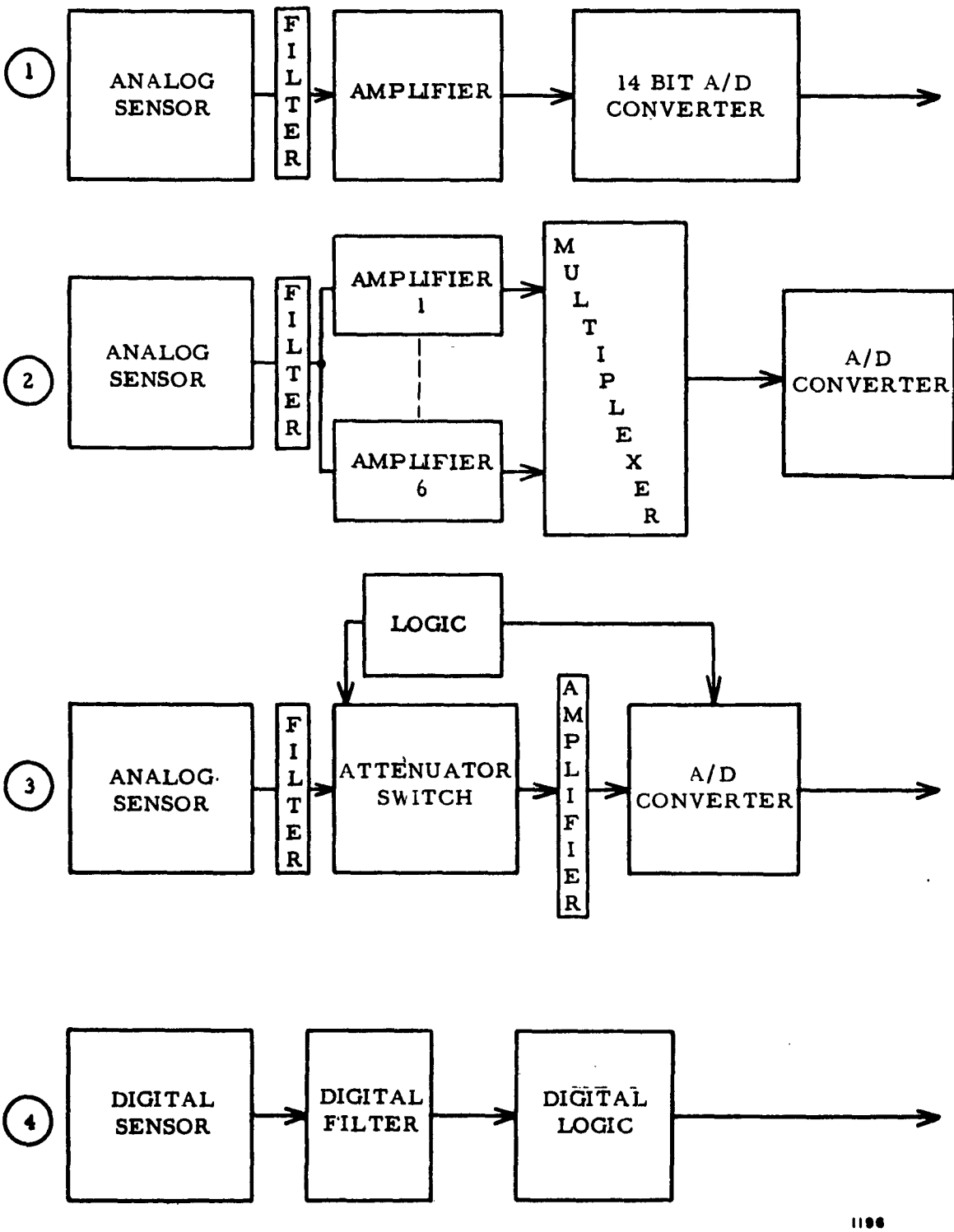

METHODS OF DIGITIZING

Figure 4. Methods of Digitizing

point of digitizing. Information for 20 binary bits is obtained since the amplifier gains are adjusted in a binary sequence. By choosing the appropriate reading from an amplifier which is within a linear region, a range of recording of over a million to 1 can be obtained. A disadvantage of Method 2 is that an editing operation is required to choose the first amplifier which is not overdriven in the data block. Another significant disadvantage of this approach is that variable resolution results since the A-to-D converter range is only 14 bits.

With Method 3, only one amplifier is used, but the setting of an attenuator at the input of the amplifier is under the control of the digital logic. The sequence of operation would be to set the attenuator scale for maximum attenuation, perform an A-to-D conversion, and allow this information to logically set the attenuator switch so that the A-to-D converter would be set near maximum for the second step in the sequence. The second step then results in the proper attenuator setting for maximum drive to the A-to-D converter. The second step provides a 14-bit reading of the input variable and the setting of the attenuator provides a binary floating-point indication which is grouped with the A-to-D converter output.

Method 4 uses a digital sensor followed by a digital filter with the appropriate logic to generate 20 binary bits of range. This last approach was the one chosen for complete system development.

The two approaches chosen for detailed analysis were logically controlled scale setting using an analog sensor driving a conventional A-to-D converter and the system utilizing an FM-Digital sensor with signal conditioning for the aliasing filter.

The first approach is the digital bridge concept and is illustrated in Figure 5. Boom displacement partitions the power from the power pump by the analog sensor. For this application the analog sensor was the linear differential transformer. Output of the low-pass analog aliasing filter passes through the multiplexing switch to the automatic scale attenuator. The first step in the timing sequence is the setting of the scale attenuator to maximum attenuation. A-to-D conversion of the signal is used to provide logic control for the setting of the scale attenuator so that the A-to-D converter can then be driven to within 6 db of the maximum signal obtainable without overdrive. After re-setting the scale-setting attenuator, another A-to-D conversion is performed and the output is gated to the digital format converter required for magnetic tape recording. The additional information is available in the scale attenuator, and this information is gated out as a floating point binary representation of the displacement of the boom. The multiplexing switch then sequences to the next sensor system and the process is repeated. (Details for the design of this system are given in Appendix E). The

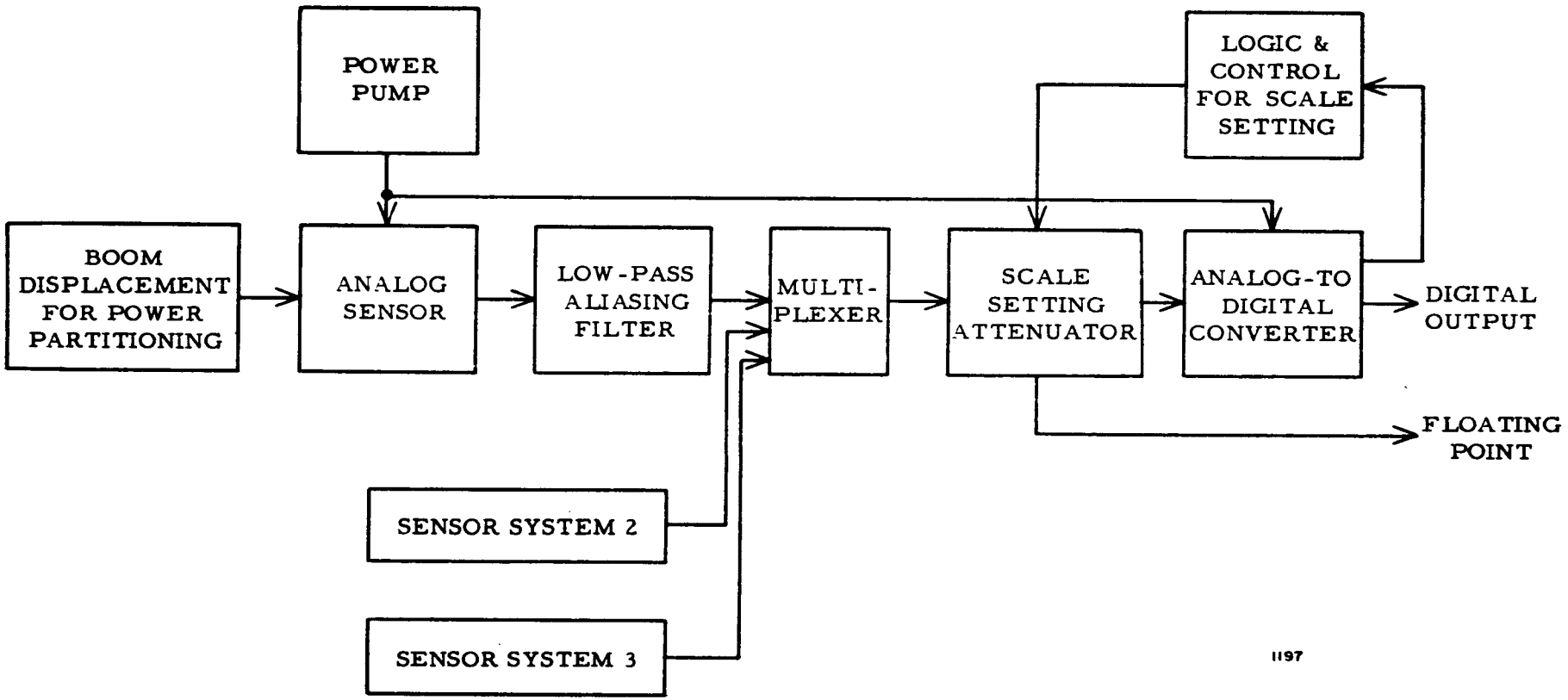
POWER PUMP
LOGIC & CONTROL FOR SCALE SETTING
BOOM DISPLACEMENT FOR POWER PARTITIONING
ANALOG SENSOR
LOW-PASS ALIASING FILTER
MULTI-PLEXER
SCALE SETTING ATTENUATOR
ANALOG-TO DIGITAL CONVERTER
DIGITAL OUTPUT
FLOATING POINT
SENSOR SYSTEM 2
SENSOR SYSTEM 3
1197

disadvantage to this approach is the resolution factor. Resolution varies by a factor of 6 db for each adjacent scale. It was concluded that this approach was satisfactory, and that it was much better than the conventional approaches mentioned above. Variable resolution was the only factor which resulted in the decision to drop this approach and to follow the FM-Digital concept.

D. FM-DIGITAL CONCEPT

Figure 6 illustrates the FM-Digital concept. An FM sensor consists of two oscillators, each connected to opposite sides of the seismometer boom. As the boom is displaced, one oscillator increases in frequency as the other oscillator decreases in frequency. By mixing the output of the two oscillators, a frequency-modulated signal of 0 to 20 megacycles is obtained from a displacement of 0.2 millimicrons to 200 microns. Resolution is increased further by a frequency-doubling circuit to provide a total FM excursion from 0 to 40 megacycles for the maximum dynamic range of the sensor. Digitizing of this signal is implemented by a binary counter which is gated ON for a total time of 6/250 second or 24 milliseconds. A significant systems feature of this approach is the low-pass

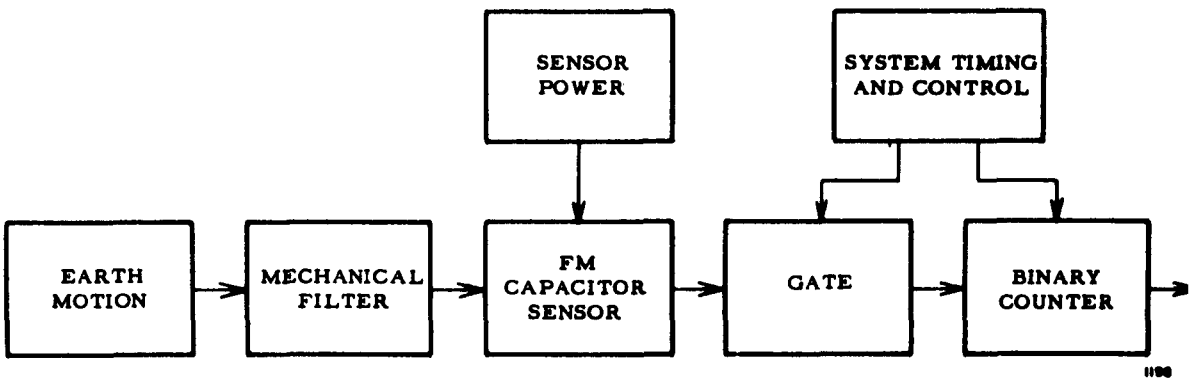

Figure 6. FM-Digital Concept

aliasing filter required. From classical sampled system theory, illustrated in Figure 7, all frequencies above 20 cps should be attenuated for a sampling rate of approximately 40 cps. (Exact sample rate is $\frac{250}{6} \cong 41.66$ cps). If these frequencies are not attenuated, they will fold back as an aliased error into the digital system. The following three approaches were considered for the low-pass filter required:

1. 6 db/octave filter due to counting for the 1/40 sec period. This is equivalent to integration of the data for 1/40 sec. Therefore, all frequencies which are multiples of 40 cps have infinite attenuation. The peaks associated with the highest signal attenuate at 6 db/octave.

2. A mechanical filter connected to the sensor for attenuation of 12 db/octave above 10 cps.

3. A closed-loop Automatic Frequency Control (AFC) filter which clamps the oscillators from frequency deviating above 10 cps. This is essentially a negative feedback with a 12 db/octave analog filter in the feedback loop. Details of this approach are presented in Appendix B and Section II, B of this report.

All three of these filters were designed and evaluated.

The final system consisted of two filters, the first due to the integration for 6/250 second, and the second provided by a mechanical filter. This resulted in an equivalent 18 db/octave low-pass filter which cuts off at 10 cps. The most critical aliased frequency would be at 30 cps which would be down approximately 46 db from the 10 cycle high-frequency cutoff. The next critical point, 54 cps, would be down 52 db. The next multiple of 40 cycles for a critical point would be at 100 cps, which is down approximately 68 db. If it is decided at a later time that additional low-pass filtering is required, the AFC negative feedback loop can be incorporated into the system with only minor change to provide a total 30 db/octave filter cutoff.

From these considerations, with substantiating details documented in the appendices of this report, it was concluded that the final system for development and evaluation would consist of the FM-Digital approach incorporating the equivalent of 18 db/octave aliasing filter, constant resolution over a dynamic range of 0.2 millimicrons to 200 microns, a band-pass from 0.1 cps to 10 cps, and displacement sensing. The only additional significant systems consideration was the effect of seismometer tilt on a displacement sensor. Therefore, a closed-loop boom-centering system

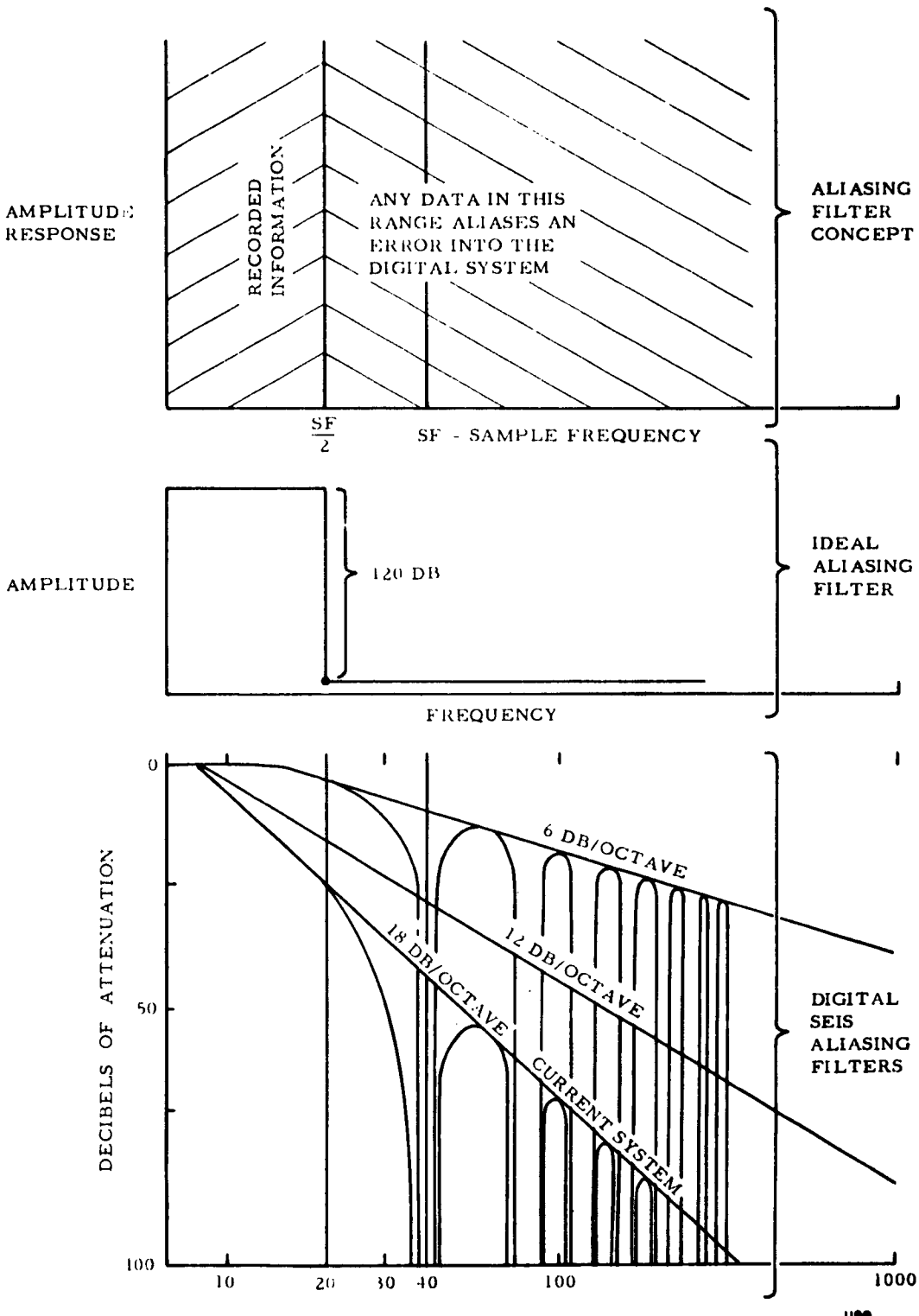

Figure 7. Aliasing Filter

was designed, resulting in a frequency cut-off of 18 db/octave below approximately 1/40 cps. Overall system cut-off on the low frequency end is 1/10 cycle per second due to the mechanical spring-mass system at 12 db/octave and 6 db/octave below 1/40 cps due to boom centering.

In its elementary form the basic concept of the FM-Digital approach is not original. The most recent exploitation of this concept was by Dr. J. Cl. De Bremaecker of Rice University.

Since the capacitor plates for this sensor design are relatively small, a special seismometer that would be system compatible with the sensor was designed. The spring-mass system was based on an original concept of Mr. Fred Romberg of Texas Instruments and was designed into a practical system by Ed Millis of Texas Instruments. For this reason, it is called the Millis-Romberg seismometer. For the vertical seismometer, the sensors were adapted to the Press and Ewing seismometer.

It was not within the scope of this contract to provide a magnetic tape compatible with all IBM or CDC computers. For this reason the data is provided in straight binary form at the output so that it could be formatted for any computer. For evaluation work magnetic tape recording was on an Ampex FR-400 in straight binary form for the three channels of the digital seismometer system. A standard multiplexer and analog-to-digital converter system, which was already available within Texas Instruments, is utilized to provide unique features for equipment evaluation. Formatting for the recording is compatible with the Texas Instruments TIAC Computer. Since a data block contains 31 channels, 28 conventional channels are available for comparison with other seismometer systems. Resolution of these test evaluation channels is 14 binary bits. Therefore, the total system for evaluation allows direct comparison between any 28 channels with other seismometer inputs with the 3 channels of the digital seismometer system, all within the same data block and the same timing reference. Details for this particular equipment are presented in Section II-E of this report.

SECTION II

SYSTEM DESIGN

A. GENERAL SYSTEM DESCRIPTION

Figure 8 is a simplified block diagram of the FM-Digital System which was designed into a completely integrated system for future evaluation.

Displacement sensing is provided by the mixing of two oscillators which are controlled by the boom position. One oscillator is connected to a capacitor coupled to one side of the boom, and the other to a capacitor connected to the opposite side of the boom. These capacitors are part of the frequency determining circuits of two oscillators. The frequencies of the oscillators are approximately 400 megacycles, but differ by 10 megacycles when the boom is in the center position. Outputs of the two

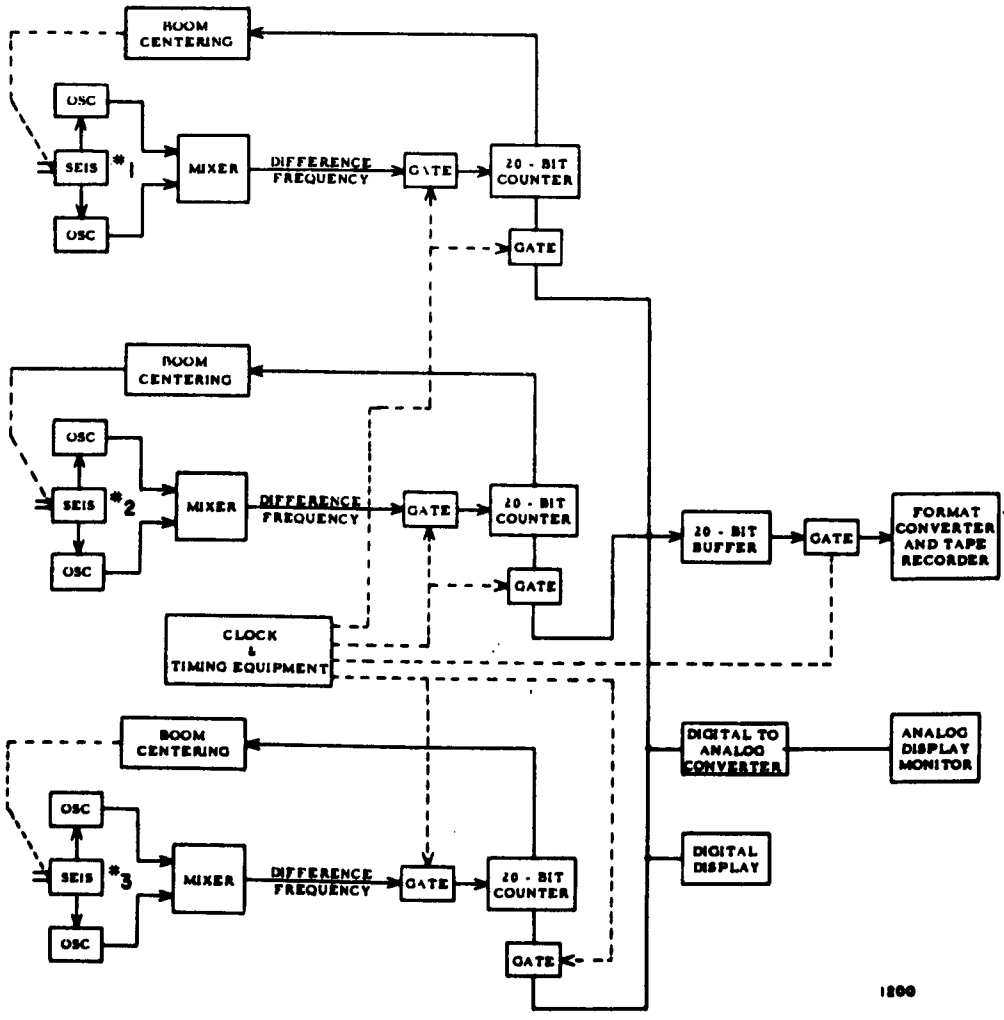

Figure 8. Simplified Block Diagram of FM-Digital System

oscillators are mixed to provide a frequency modulation range from 0 to 20 megacycles for a total boom displacement of 200 microns. Frequency doubling results in a total FM range of 0 to 40 megacycles. The same sensor concept is used for all three components of the system. For the vertical component, the sensor system is coupled to the boom of a modified Press and Ewing seismometer. A completely new seismometer was designed for the horizontal components.

The output of the sensor therefore is a frequency which varies from 0 to 40 megacycles, depending upon the displacement of the boom. This output is then gated into a binary counter for 6/250 second. The counter will fill up to 20 binary bits for the equivalent of 200 microns total displacement. Three binary counters are used, one for each of the seismometers and are gated in sequence to provide a 20-bit binary output every 6/250 second for each of the three sensors. They are, therefore, staggered by 2/250 second. After a particular counter has concluded its counting interval (and this is now called a binary word), it is gated into a buffer which connects the binary word to the output. This is followed by a reset pulse 2 microseconds later. One microsecond after the reset pulse the counter starts counting again, sampling the output of the sensor, storing it in a buffer, and so on. The logic for the total system is synchronous and is under the control of a one-megacycle clock from the chronometer system. A binary digital display is switch-selectably controlled to the output of any of the three binary counters. This provides for immediate monitoring of the binary logic. The digital output from the entire system is 20 binary bits, transferred in parallel, which could be used to drive an tape recording system.

Boom centering is maintained for frequency components below 1/40 cps. This closed-loop system takes the output of the FM sensor after the first five stages of the binary counter. The FM signal drives a circuit for producing constant-width pulses but at the FM repetition rate. These pulses are integrated and are used to drive a power amplifier which in turn allows current to flow in a heater coil connected to one leg of the horizontal seismometers. In the case of the vertical seismometer, a coil within a permanent magnetic field is driven. Heat from the coil of the horizontal seismometer increases or decreases the expansion of the leg to automatically correct for tilt. For the vertical seismometer, current through the coil deflects the boom to the center position. The signal used for boom centering of any of the three components can be selected for display on the fourth channel of the analog recorder.

A digital-to-analog conversion is made from the digital output and is used to drive an analog display. This converter is under the control of the timing logic. The analog display, therefore, tests the entire system.

The output of the summing junction in the digital-to-analog converter passes through a low-pass filter and then through an optional, continuously variable notch filter. The notch filter can be adjusted from 0.13 to 10 cps and is used to reject unwanted microseisms within this frequency range. A 6 db per step gain control is provided, and is determined in the digital logic portion of the system.

In addition, time encoding is provided on the edge of the analog record, coming directly from the chronometer system.

A picture of the digital seismograph system is shown in Figure 9. The system consists basically of three seismometers and a control console containing the chronometer, digital circuits and displays, analog circuits and displays, controls and power supplies. Specifications for the system are listed in B, following.

B. SYSTEM SPECIFICATIONS

1. Frequency 10 seconds - 10 cps.

   Low end cut off

   12 db/octave below, 0.1 cps.
   18 db/octave below, 0.025 cps.

   High end cut off

   18 db/octave above, 10 cps, with infinite attenuation at 40, 80, 120, etc.

2. Dynamic range 1,000,000 to 1 (120 db or 20 binary bits) at a sample rate of approximately 40 cps.

3. Constant resolution.

4. Displacement sensing with automatic boom centering.

5. Sensitivity - 0.2 millimicrons to 200 microns.

6. Digital display - 20 binary bits, switch selectable to any of 3 channels.

7. Analog display - 4 channel servo/riter*, 9-inch wide display with overlapping traces in multicolors. Three channels are used for the three seismic components with one channel, switch selectable, for monitoring the boom centering of any of the three components. Time encoding is on the edge of the paper.

   a. Notch filter for microseism frequencies continuously adjustable from 0.13 to 10 cps.

---

* Trademark of Texas Instruments

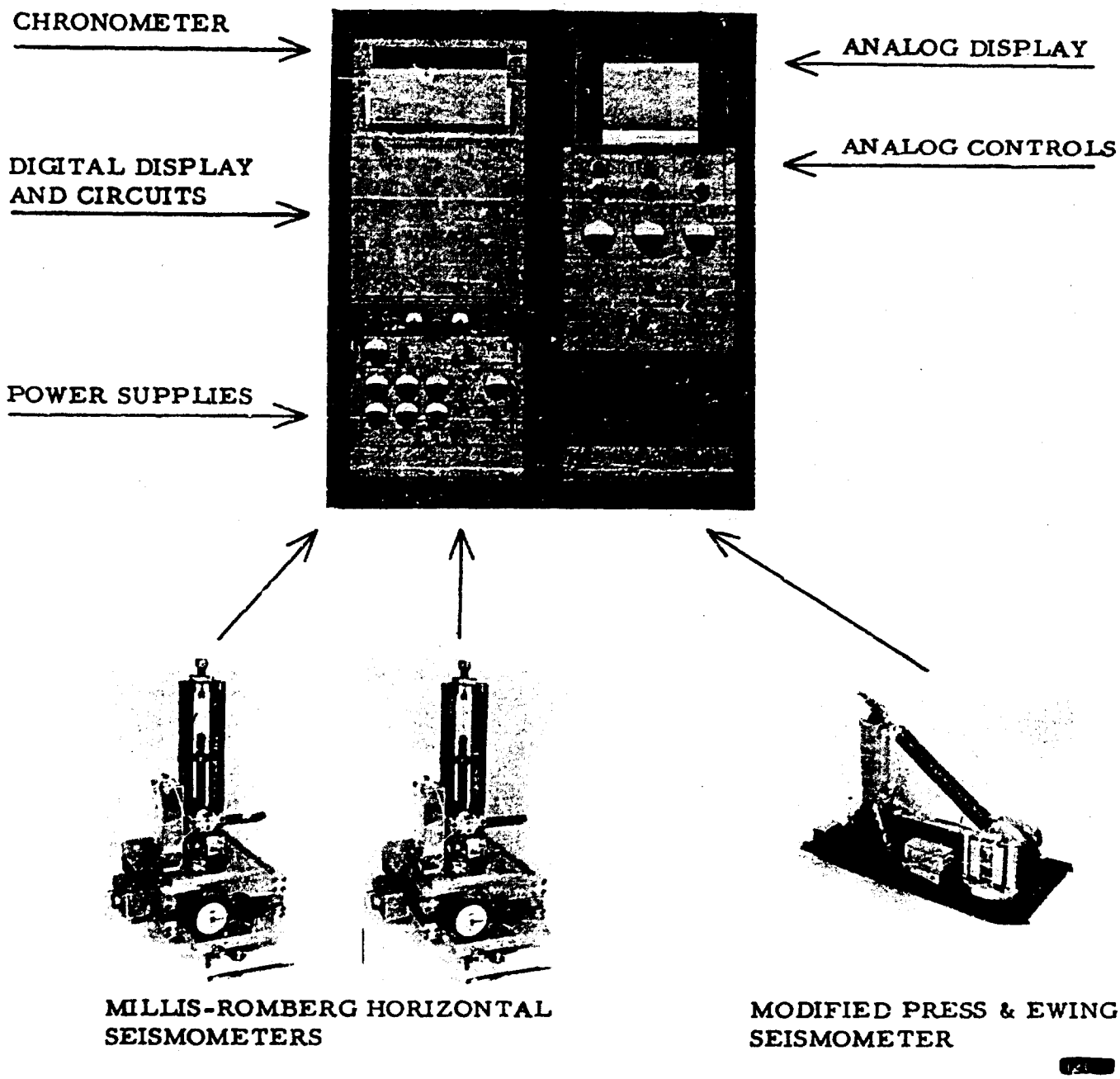

Figure 9. Digital Seismograph System

b. Gain ± 100 microns full scale with 6 db/step gain increments for 15 total steps.

8. System calibration

a. Method of clamping boom at known values of displacement for horizontal seismometer only.

b. Sensor test oscillator provided.

c. Special horizontal shake table provided for check of frequency response.

9. Seismometers

a. Millis-Romberg seismometer for horizontal components with 12 db/octave mechanical filter above 10 cps.

b. Modified Press and Ewing seismometer for the vertical component with 12 db/octave mechanical filter above 10 cps.

10. Linearity - satisfactory with micrometer test but requires computer analysis for precise linearity measurement.

11. Environmental - satisfactory operation under laboratory conditions. Additional tests are required to determine total system temperature and humidity coefficients.

12. Digital output - straight binary. Currently gated into data block of TI magnetic tape recording system for evaluation. Can be formatted to IBM magnetic tape with format converter and 1/2-inch magnetic tape recorder.

C. SEISMOMETER DESIGN

1. Vertical Seismometer

The vertical seismometer chosen for use in this program is a Press and Ewing model built by Lehner-Griffith. It is shown in Figure 10 with the sensor package installed.

This seismometer has a mass of approximately 6.9 kilograms and a boom length of 35 centimeters. It is designed for a maximum period of 30 seconds and is thus easily set to 10 seconds.

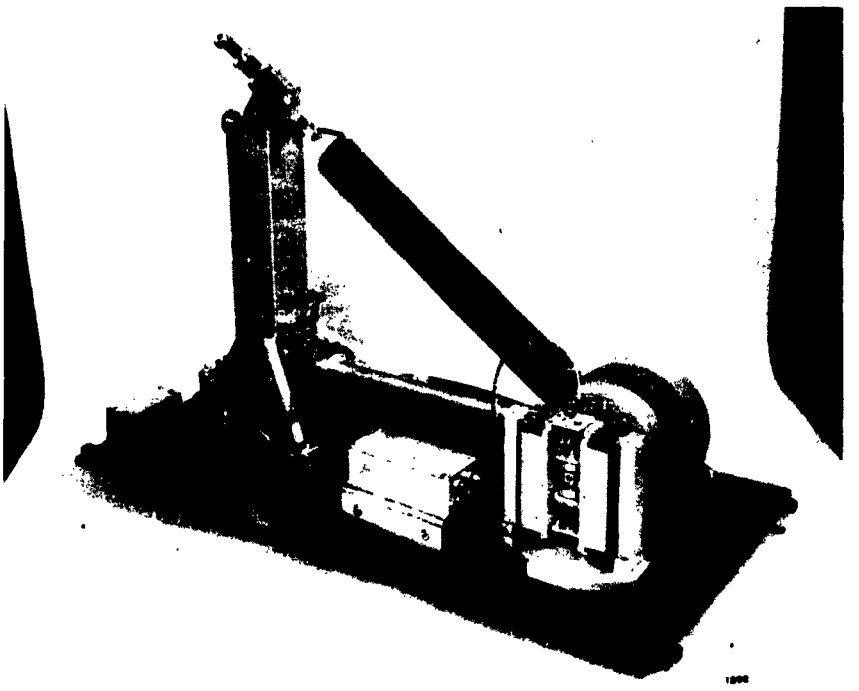

Figure 10. Press-Ewing Vertical Seismometer

Since this seismometer was designed for a permanent installation in concrete with lead "tampins," a temporary steel base was affixed. The instrument can now be used on any flat surface and levelled with three screws in the temporary base.

2. Horizontal Seismometer

A survey of the available horizontal seismometers showed none particularly suited to this project. The primary problems were the large size and difficulty of initial adjustment of the swinging-gate type instrument. Included in the set-up difficulties is the sensitivity of the period to tilt.

The Romberg suspension appeared to be an excellent configuration for this project and was consequently adapted to fit the specific needs. The Romberg suspension instrument is not as familiar as the Press and Ewing instrument, therefore, design details are included.

a. General

The basic configuration for the Romberg suspension is shown in Figure 11. It consists of a simple pendulum whose restoring force is

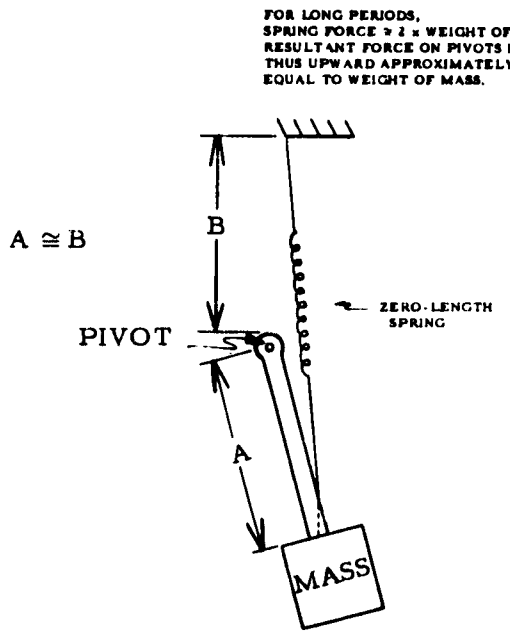

Figure 11. Basic System of Romberg Suspension

partially balanced by a spring, thereby lengthening the natural period.*

This instrument is relatively insensitive to transverse tilting and also lends itself to compact construction.

b. The Millis-Romberg Seismometer

1) Physical Size

The baseplate of the seismometer is 8 x 14-1/4 inches. The main frame is 3 inches in diameter and 12 inches tall. The pendulum has a mass of about 250 grams and a physical length of about 4-1/4 inches from the pivots to the center of gravity.

The assembled instrument stands 19-3/4 inches high to the top of the thermal box. Total weight is 13 kilograms.

2) Construction Details

a) Main Frame Assembly (Figure 12)

The main frame (301), pendulum (302), and spring adjuster (306) are machined from Invar for thermal stability. These pieces determine the geometry of the moving system, and thus, with the spring, determine the period. Calculations show that the period of this instrument will change about 0.02% per degree Centigrade due to the change in geometry of the Invar pieces. As a matter of interest, if brass were used in place of Invar, the temperature coefficient of the period would be 0.3% per degree Centigrade, again assuming a perfect spring.

* Romberg, F. E., "An Oscillating System for a Long-Period Seismometer for Horizontal Motion," Bull. of the Seis. Soc. of Amer., Vol 51, No. 3, pp. 373-379, July, 1961.

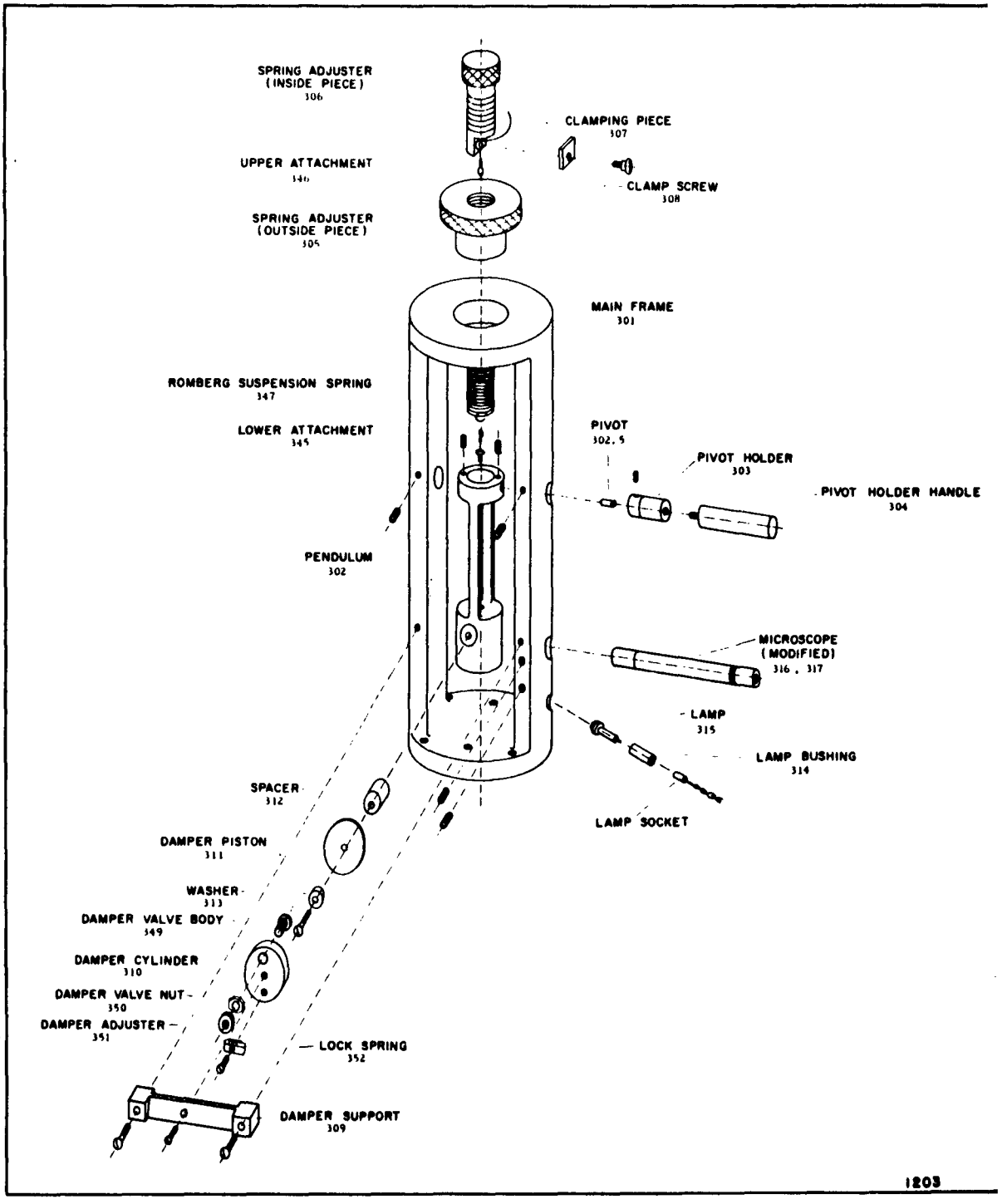

Figure 12. Main Frame Assembly

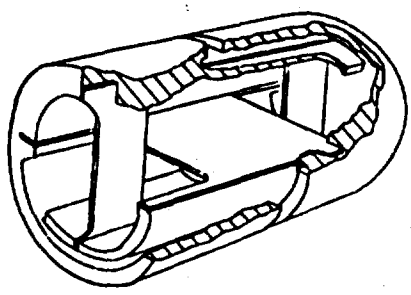

Figure 13. The Pendulum Support Pivot

The pendulum support pivots (302.5) are Bendix "Free-flex" Flexural Pivots, type 5004-800. They are 0.125 inches in diameter and 0.200 inches long and will each support 0.31 pounds in compression or 6.2 pounds in tension. A cut-away drawing from the Bendix catalogue is shown in Figure 13.

The nominal restoring rate of each pivot, with no load applied, is 0.011 inch-pounds per radian. However, loading the pivots in tension, as is done in this model, decreases the restoring force in an approximately linear fashion.* Restoring rate goes negative for loading values above 318 grams. The actual loading in this case reduces the restoring rate of the pivots to about 0.002 inch-pounds per radian per pivot.

The main suspension spring (347) is the most critical part of the instrument. The springs being used were made by Mr. Fred Romberg of TI who has a number of years experience in making similar springs for the LaCoste-Romberg gravity meter.

The springs are wound from 0.035 diameter Ni-Span "C" wire. They are lathe-wound with no pre-tension on a 7/16" diameter mandrel. The length of these spring blanks is about 4 inches, or somewhat longer than the finished spring. After winding, the spring blanks are turned inside-out with a special tool to make them approximately zero-length.

The blanks are then sealed in a quartz tube which is evacuated and tipped-off. This assembly is heat-treated for 5 hours at the exact temperature as specified by Engelhard Industries for the batch of wire being used. This gives a thermoelastic coefficient of zero, with a possible error of about $\pm$ 4 x 10^{-6} per degree Centigrade.

After heat treating, the spring blanks are turned inside-out several more times to cold-work the material slightly, and are left in the zero-length condition. It has been Mr. Romberg's experience that this tends to make the spring more stable with respect to creep over a long time interval.

The spring is then cut to the correct length and the ends formed into hooks for attachment.

* Technical Information for Bendix "Free-flex" Pivots, Pub. No. 19V-6-629A, The Bendix Corporation, Utica Div., Utica 1, N. Y.

The spring attachment wires (345 and 346) are 0.0035 diameter stainless steel. The loops in the ends are secured by wrapping with No. 36 tinned copper wire and soft soldering, using a suitable liquid flux.

Two air-cup dampers are used in a push-pull configuration to eliminate the possibility of a directional difference in damping. The damper cylinders (310) are 1.44 inches in diameter, inside, with the diameter of the pistons (311) allowing a 0.006-inch radial clearance. Damping is set by adjusting an air bleed valve (349 and 351) on each cylinder. The mechanical stops which limit pendulum displacement are also incorporated in the damper cylinders. The stops can be set to limit the swing of the pendulum over wide limits.

The spring adjuster (306) is used to adjust the period of the instrument by varying the tension on the spring. In practice, the inner piece (306) is held stationary and the outer piece (305) is rotated. This moves the inner piece up or down without rotation. The two pieces are rotated together to take any residual twist out of the suspension spring without changing the tension.

A small measuring microscope (316) is set in the main frame, and is focused on a scribed line on the pendulum mass. The microscope is calibrated in one-thousandth-inch increments and is used to define the mechanical zero of the instrument as well as for leveling the instrument in the direction of motion. A lamp (315) is used to illuminate the pendulum.

b) Base Assembly (Figure 14)

The main frame assembly bolts to the base assembly as shown in Figure 14. This base assembly consists of a base plate (322) supported from the lower stand (333) by four beryllium-copper leaf springs (323). A silicone oil dashpot is also connected between these two members.

Leveling the instrument is accomplished with three adjustable feet. Two of these are standard leveling legs, and in conjunction with a bubble level (319) serve to level the instrument in the plane transverse to the direction of motion.

For the more critical leveling in the direction of motion, a vernier leveling leg (334 through 338) is used. The leg (336) has a 1/4-20 thread which screws into the leveling screw (335). The outside of this leveling screw is threaded 5/8-18 and screws into the seismometer stand (333).

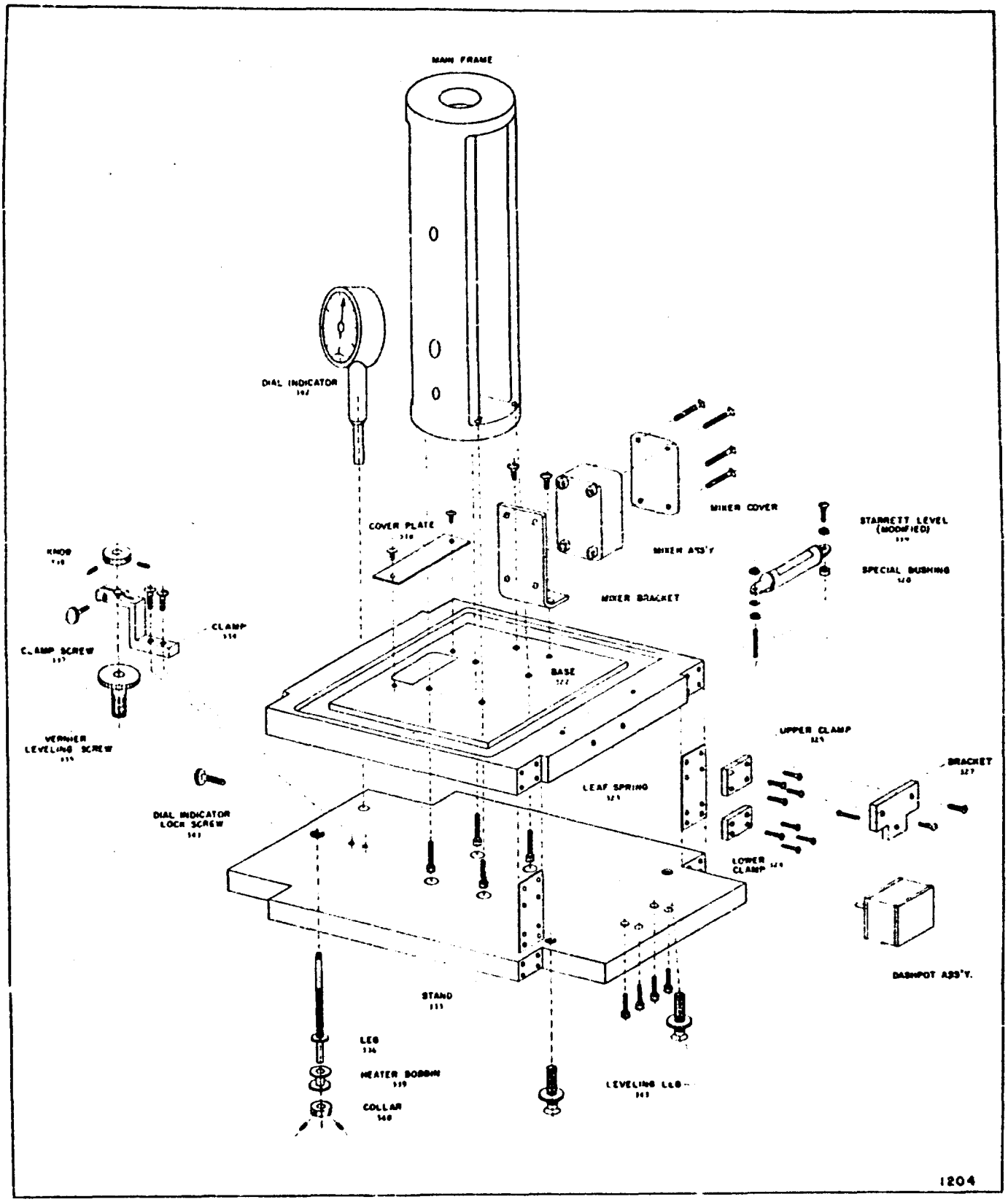

Figure 14. Base Assembly

If the clamp screw (337) is loose, the knob (338) on the leg will coarsely adjust the level of the instrument as it moves through the stationary leveling screw (335). For fine adjustments, the clamp screw (337) is tightened, and the leveling screw (335) is turned to make the adjustment. If the leveling screw is turned clockwise, it screws down into the stand with a pitch of 18 threads per inch. At the same time, the leveling screw raises the leg (336) at a pitch of 20 threads per inch. The net result is a vernier action with the equivalent pitch of $\frac{(20)(18)}{20 - 18}$ or 180 threads per inch.

The clamp (334) is flexible purposely, in the vertical direction, and will accommodate several turns of the leveling screw before the clamp screw (337) must be loosened and re-tightened to take care of the change in length of the leg above the stand.

Also on this leveling leg is the heater coil for the automatic boom-centering. The heater coil (339) is positioned on the leg (336) by a collar (340). The heater bobbin is free to rotate on the leg to allow the leg to be turned for adjustment without twisting the heater wiring.

A dial indicator (342) can be installed in the stand (333) to observe the operation of the automatic leveling or as a means of putting calibrated tilts into the instrument. The presently used dial indicator is a Federal C 1/2 K, with 50-microinch minor divisions. (A dial indicator with more sensitivity would be desirable).

The electrical wiring from the sensor passes through rubber grommets in the cover plate (318) and terminates in a junction box (not shown) on the far side of the stand.

The completed seismometer with the cover removed is shown in Figure 15.

Figure 16 shows the Styrofoam cover in place.

c) Shipping Considerations

It is proposed to ship this seismometer with the pendulum in place. The pivots can be easily removed, and replaced with a set of solid steel "shipping pivots." The suspension spring will be left in place and secured with balsa wood wedges where it passes through the top of the pendulum. The pendulum stop adjustment screws will be carefully tightened to clamp the pendulum and eliminate free play. This method of shipping does not interfere with the setting of the dampers or the period adjustment; therefore, the instrument should require minimum calibration and readjustment after shipping.

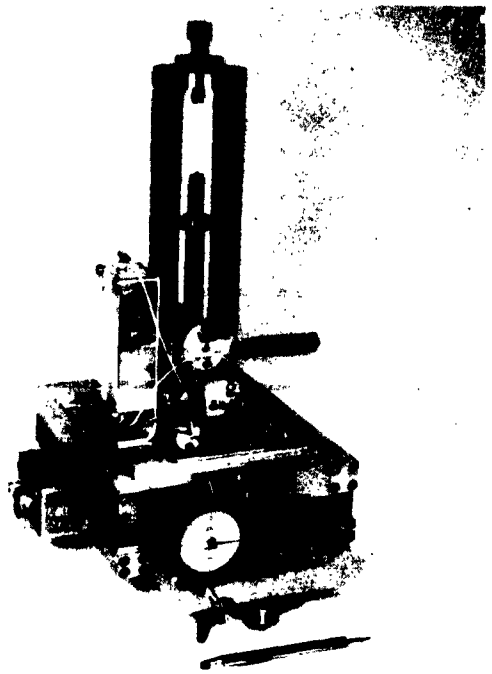

Figure 15. Millis-Romberg Horizontal Seismometer End View

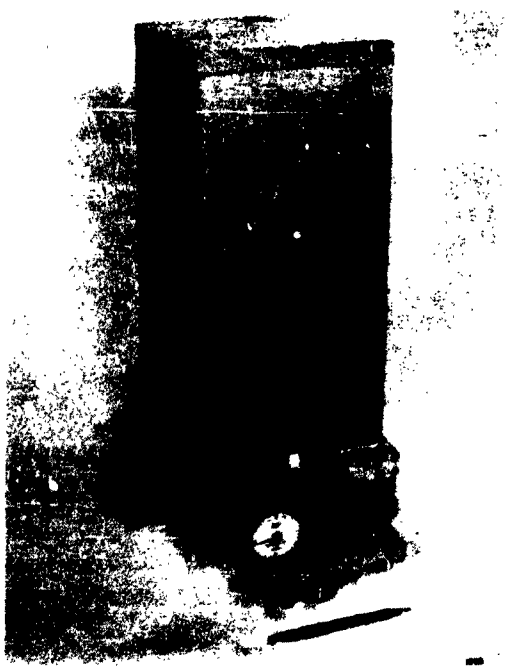

Figure 16. Complete Assembly for Millis-Romberg Horizontal Seismometer

3. Mechanical Filter

A mechanical filter was designed to provide 12-db-per-octave high-cut filtering to each component of the seismograph system.

Figure 17 is a mechanical schematic of the approach used for the horizontal system and Figure 18 is a force-voltage electrical analogy of the mechanical system. M_2 is the mass of the moving pendulum resonant at 1/10 cps damped by D_2. M_1 is the mass of the movable platform, resonant at 10 cps damped by D_1. The movement of M_2 is determined by the resonances of each spring mass. M_2 was much smaller than M_1 eliminating the interaction problem.

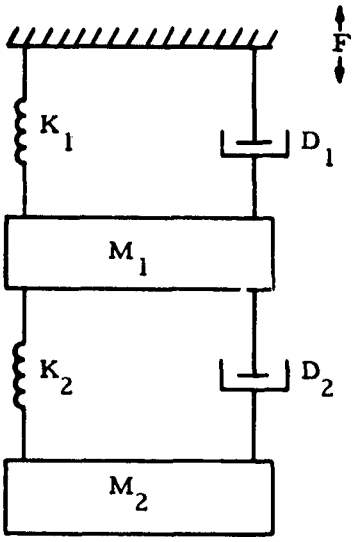

Figure 17. Horizontal System

The system described was built and tested on a horizontal shake table, Figure 43, designed for this project. The platform is suspended on flat leaves thick enough to raise the table frequency considerably above 10 cps. The platform is driven by a loudspeaker driver unit.

A similar mechanical filter was designed for the vertical seismometer. Suspending the entire seismometer did not appear to be very practical because of size. The pickoff (oscillator assembly) was suspended at a 10 cps resonance. Figure 19 is a schematic of the vertical system. M_2 is the seismometer moving mass resonant with its spring at 0.10 cps and M_1 is the sensor and mechanical mounting resonant at 10 cps. The difference in movement of M_1 and M_2 is the desired signal.

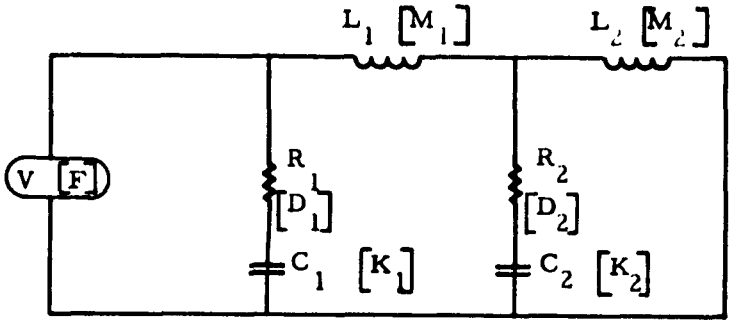

Figure 18. Electrical Analogy of Horizontal System

4. Sensor

a. Concept

The variable-frequency concept of the sensor is shown in the block diagram of Figure 20. The two variable-frequency oscillators have nominal center frequencies of 420 and 430 megacycles. Seismometer boom movement varies the capacity of the oscillator tank circuit, thus varying the frequency. The frequency difference between the two oscillators is developed in the mixer and amplified to a reasonable level. A coaxial cable carries this signal to the console.

A boom movement of 100 microns causes the difference frequency to shift about 10 megacycles. The difference

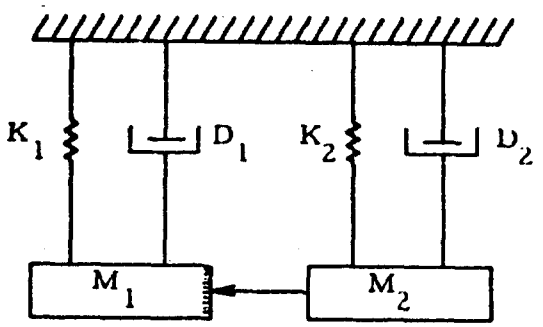

Figure 19. Vertical System

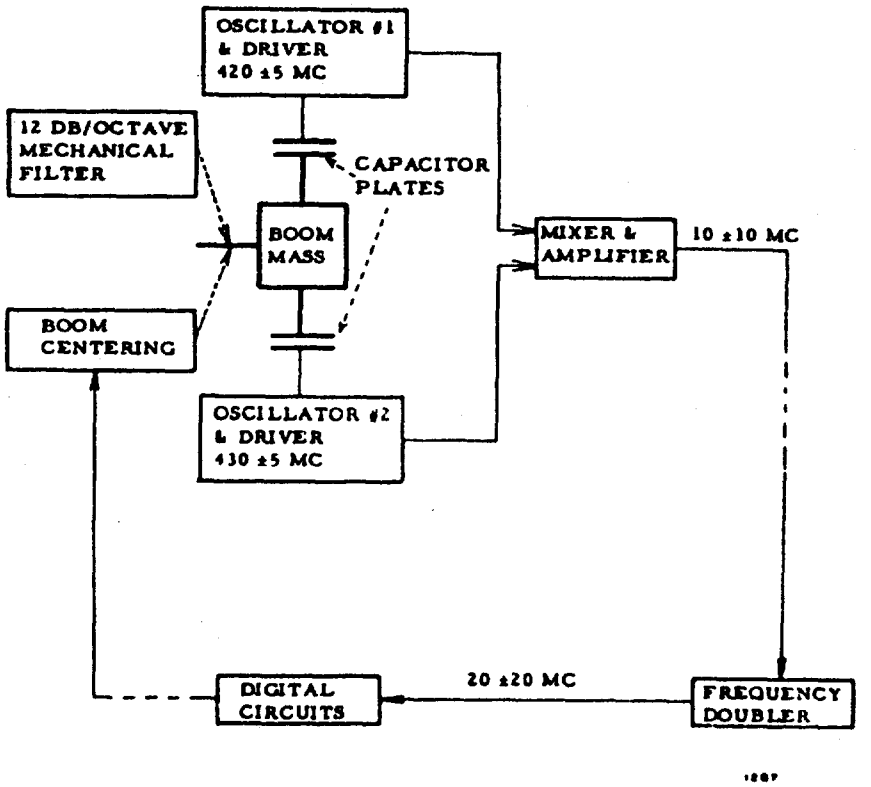

Figure 20. Basic Sensor Diagram

frequency will then approach either zero frequency or 20 megacycles, depending upon the direction of movement. In the console, this frequency is doubled and counted for 24 milliseconds (about 41 times per second). The theoretical least-detectable boom movement is thus one cycle change per sampling period, or about 41 cycles per second. This corresponds to approximately 0.2 millimicron.

b. Oscillators

The oscillator schematic diagram is shown in Figure 21. Feedback for the oscillator is supplied by the collector to emitter capacitance of the transistor header, and also by the internal collector to base capacitance of the transistor. The internal base resistance is high enough to allow this feedback to be effective.

The 2N2415 was chosen for use because of its 1.1 kmc alpha cut-off frequency, which suggests that the critical transistor parameters are relatively stable at 430 megacycles. Operating levels of current and voltage were chosen to be in the specified range for minimum noise.

The collector is tapped into the center of the tank coil, which is as near the ground end of the coil as was consistent with stable oscillation. This tapping down on the inductor minimizes the effect of transistor parameter variations on the oscillator frequency.

The oscillator signal is taken off the emitter of the oscillator transistor and direct-coupled to an emitter-follower. The emitter-follower is then direct-coupled to a "Microdot" coaxial fitting on the oscillator case.

All biasing resistors are enclosed in a separate compartment. Bypassing of various points of the circuit is done with ceramic feed-through capacitors.

The oscillator package without the cover is shown in Figure 22.

c. Mixer

The schematic diagram of the mixer and amplifiers is shown in Figure 23. The high-frequency amplifiers boost the signal from the oscillators to a level sufficiently high for proper mixer operation.

The mixer stage operates by virtue of the non-linear characteristics of a grounded-emitter amplifier stage. Both oscillator signals are brought in to the base of the mixer transistor. This base circuit presents a

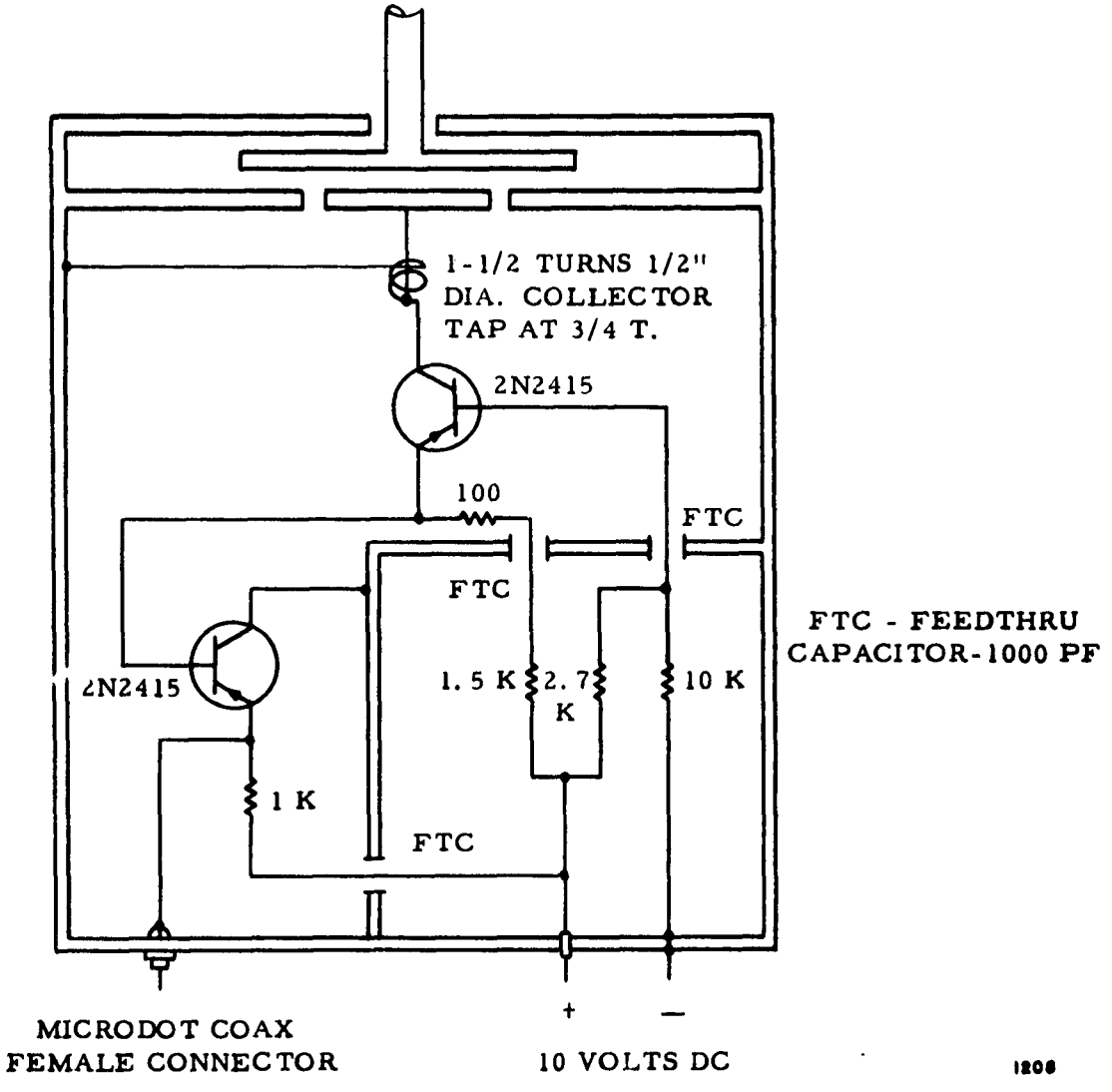

Figure 21. High-Frequency Oscillator

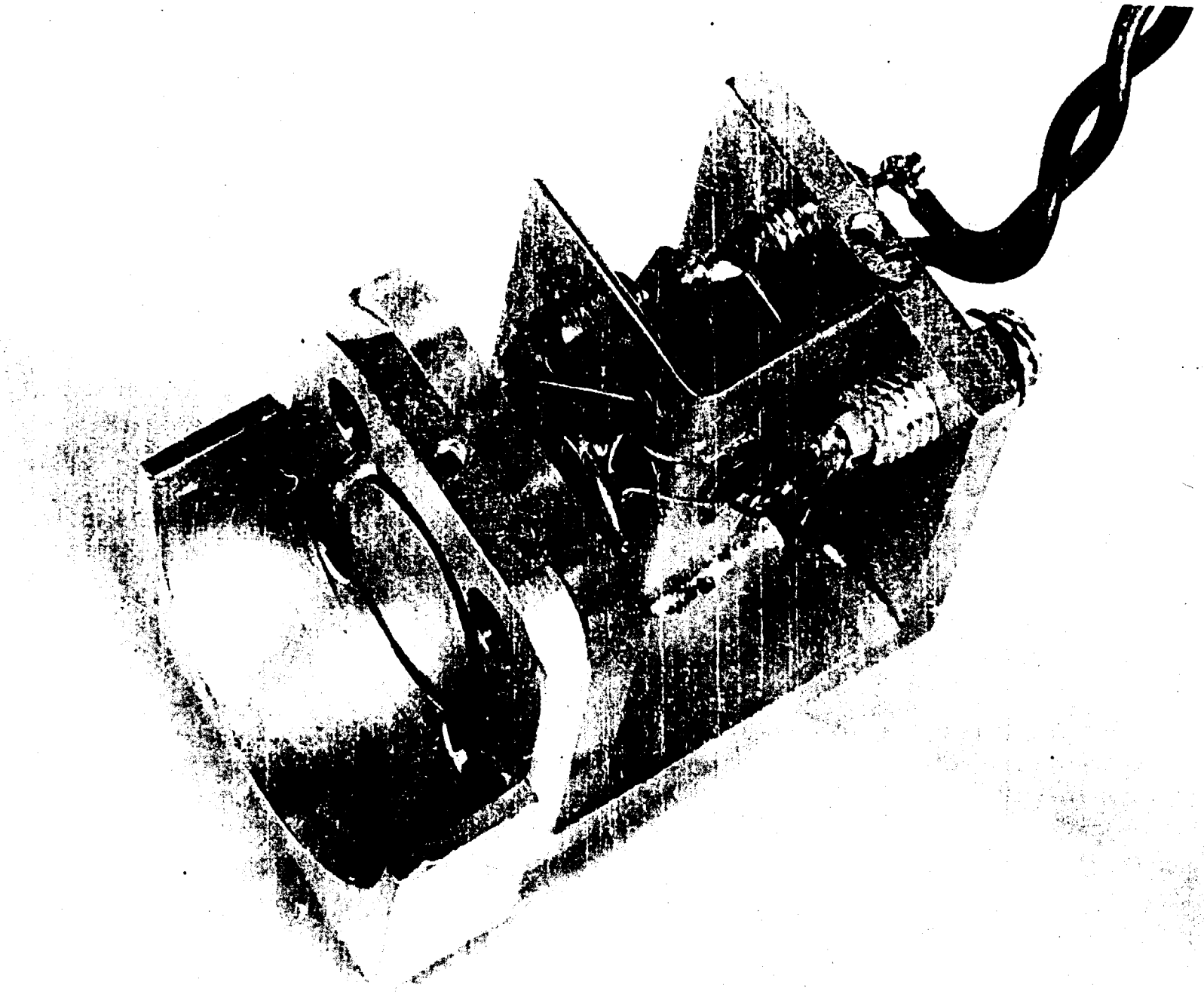

Figure 22. 430-Megacycle Oscillator Package

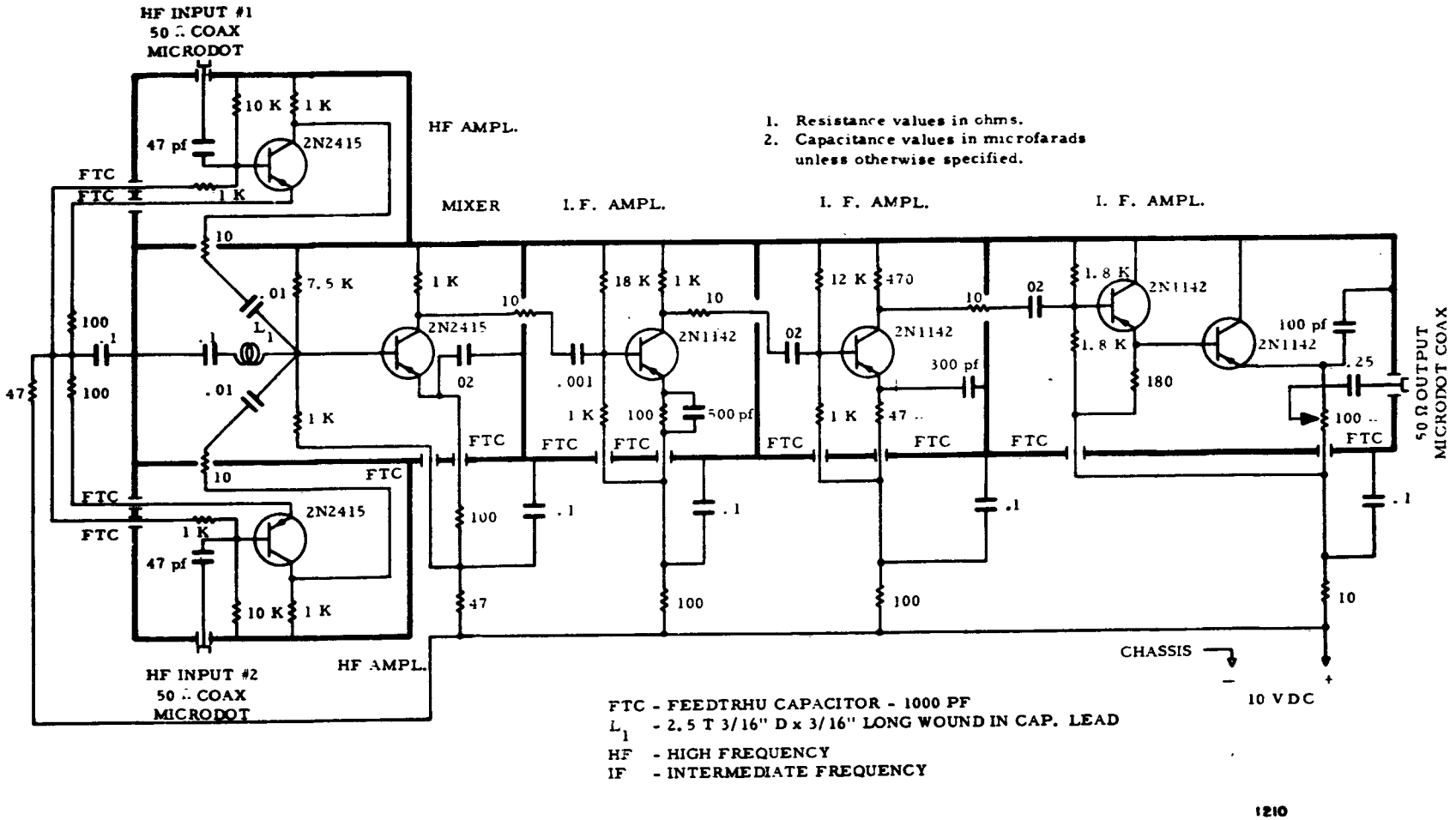

Figure 23. Mixer and Amplifier Circuit

high impedance to the high-frequency oscillator signals because of L_1. At the difference frequency, however, L_1 is too small for any appreciable effect, and the base is bypassed to ground. This greatly enhances the gain of the mixer stage at the difference frequency.

The difference frequency is then amplified by two grounded-emitter stages which are carefully bypassed to level out the gain of the mixer assembly over the wide frequency range.

Two cascaded emitter followers are used to provide a low-impedance source to drive the 50-ohm coaxial cable to the console. The potentiometer in the last stage is used to set the proper voltage level at the console to compensate for losses in the coaxial cable .

B+ decoupling is used in all stages to eliminate any tendency toward instability.

Figure 24 shows the mixer-amplifier package.

5. Mechanical Considerations

a. Sensor Mounting

The oscillators are mounted on the Millis-Romberg horizontal seismometer as shown in the exploded view, Figure 25. The capacitor plate assembly fastens to the bottom of the pendulum. The oscillators are mounted on slides (503) which allow mechanical adjustment in the direction of capacitor plate movement.

Figure 26 shows one oscillator package in place with the movable capacitor plate in position. (Refer to Figure 10 for a similar installation for the vertical seismometer sensor).

b. 10-Cycles Cut-Off Mechanical Filter

1) Horizontal Seismometer

The 10-cycle per second cut-off low-pass filter on the horizontal seismometer can best be seen in Figure 15. The entire active portion of the seismometer is mounted on the four beryllium-copper leaf springs. The springs were designed to make the supported portion resonant at 10 cycles per second. The silicone oil damper, which can be seen on the right edge of the instrument, is set to give critical damping to the assembly.

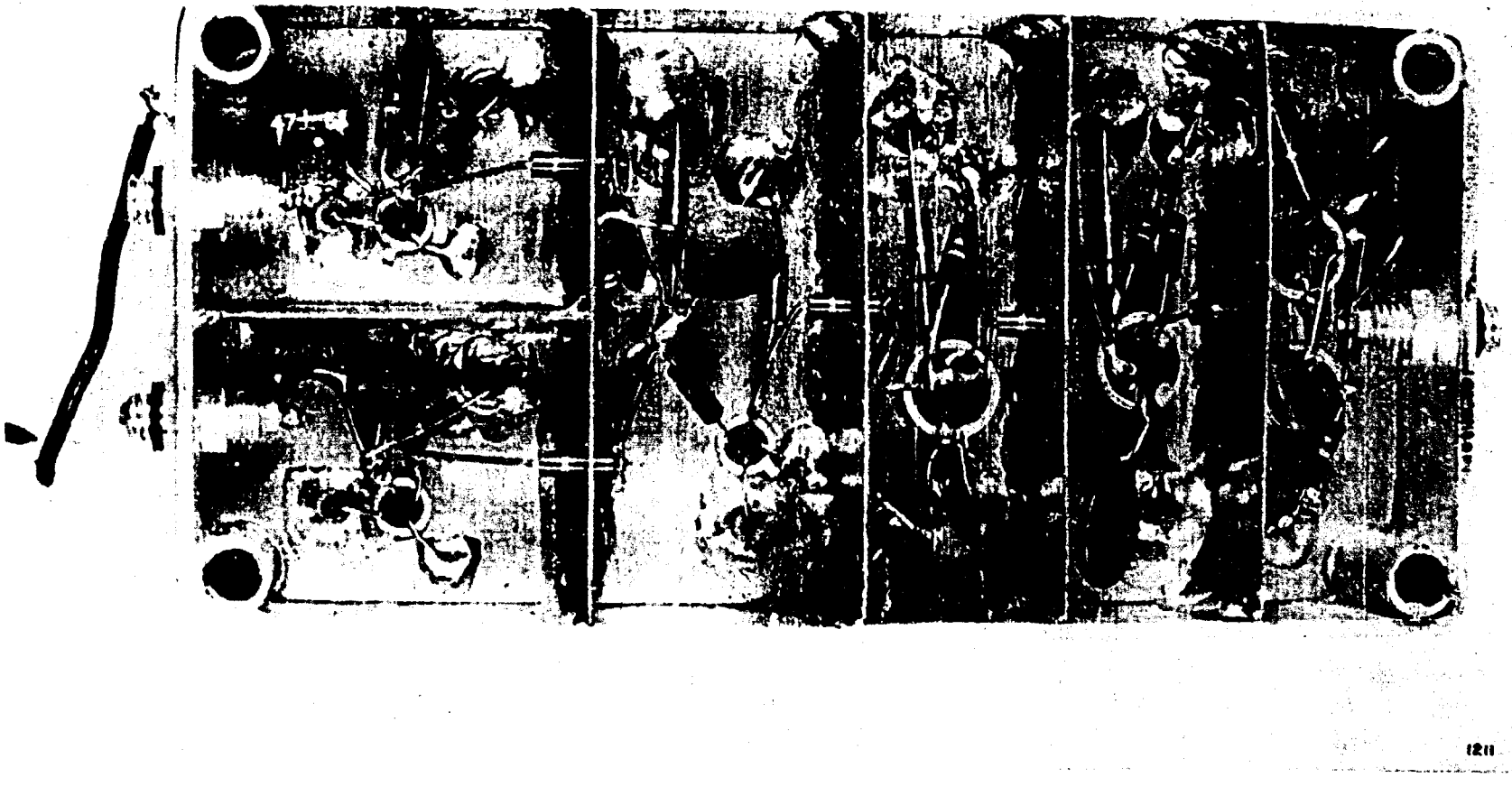

Figure 24. High-Frequency Mixer-Amplifier Package

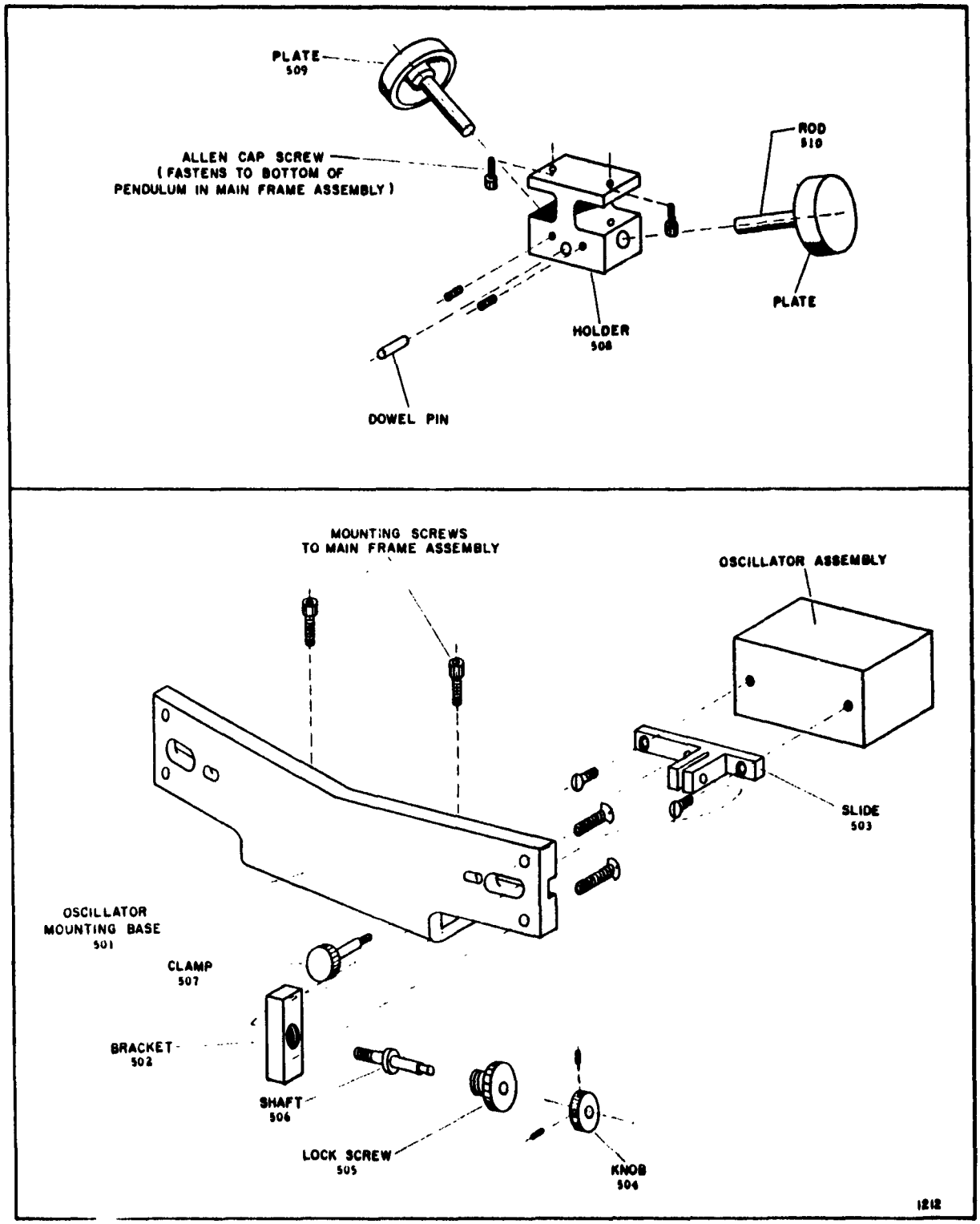

Figure 25. Mounting of Oscillator Assembly

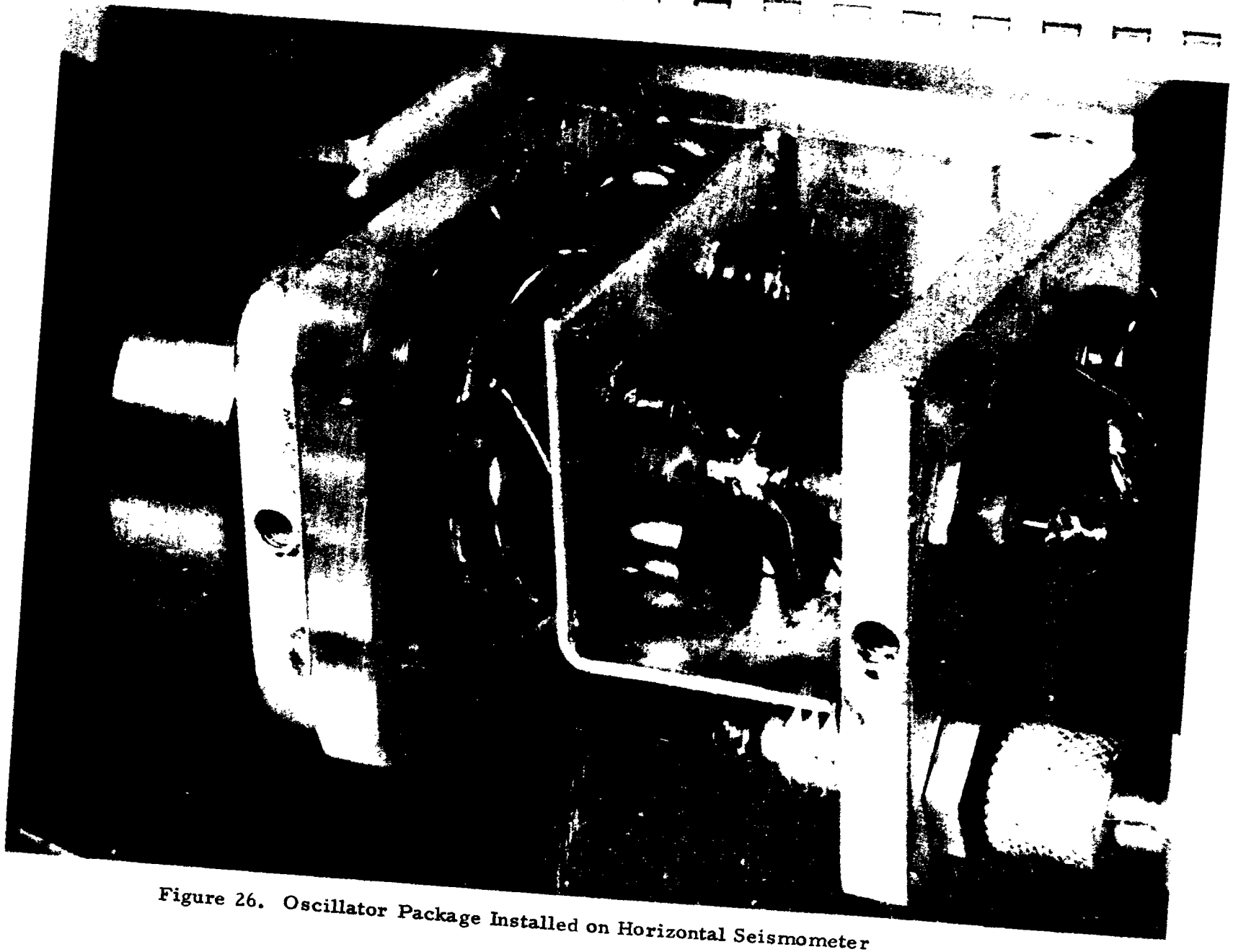

Figure 26. Oscillator Package Installed on Horizontal Seismometer

A 12-db per octave fall-off in response above 10 cycles per second has been verified with shake table experiments.

2) Vertical Seismometer

As it did not appear practical to support and tune the entire vertical instrument as was done with the horizontal, only the sensor package is tuned.

Figure 10 shows the sensor package supported by four horizontal leaf springs. The damper, which is similar to the one on the horizontal, was removed for the photograph.

At frequencies above 10 cycles per second, the sensor package moves up and down with the boom, thus reducing the relative motion between the boom (and capacitor plates) and the oscillator packages.

D. DIGITAL DESIGN

Digital logic for the entire system is synchronous and is under the control of a 1-megacycle clock from the chronometer system. Logic speeds divide into three general categories: (1) circuits that work to 40 megacycles, (2) circuits to 5 megacycles, and (3) 1-megacycle circuits. Both the 5-megacycle circuits and the 40-megacycle circuits were designed specifically for this contract.

Figure 27 is the logic design for the entire system. Numbers indicated in each of the blocks correspond to circuit diagram numbers which are included in detail in Appendix I. Numbers also designate physical location of boards. For an explanation of the digital seismograph system it is necessary to refer to Figure 28, the Timing Diagram; Figure 27, the Basic Logic Design Circuit; and Figure 29, the Basic Logic Timing Circuit.

The logic merely provides the electrical circuitry for gating the 20-bit binary counter for 6/250 second for converting the sensor FM signal to a digital output. A separate binary counter is utilized for each of the three sensors. Gating and readout of the binary counters are staggered in time so that each counter is sampled every 6/250 second. After a counter has concluded its counting period, it is gated to an output buffer. A readout strobe pulse is applied 1 microsecond following the counting interval. Two microseconds later, the counter is reset to zero. One microsecond following the reset pulse, the gate is again turned on at the counter input so that the next digitizing sequence will start. Figure 28 illustrates this sequence.

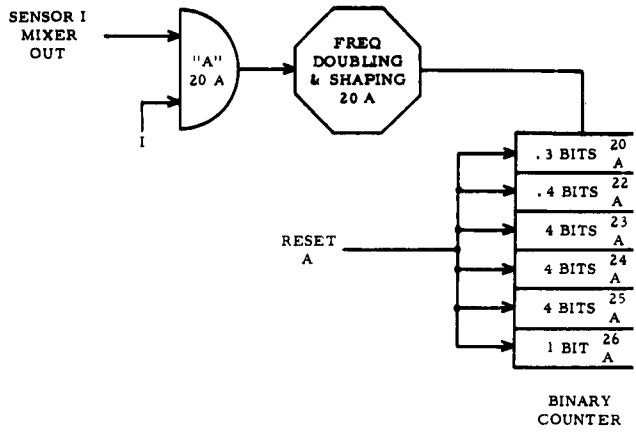
SENSOR I
MIXER
OUT
"A"
20 A
I
FREQ
DOUBLING
& SHAPING
20 A
.3 BITS 20 A
.4 BITS 22 A
4 BITS 23 A
4 BITS 24 A
4 BITS 25 A
1 BIT 26 A
RESET
A
BINARY
COUNTER

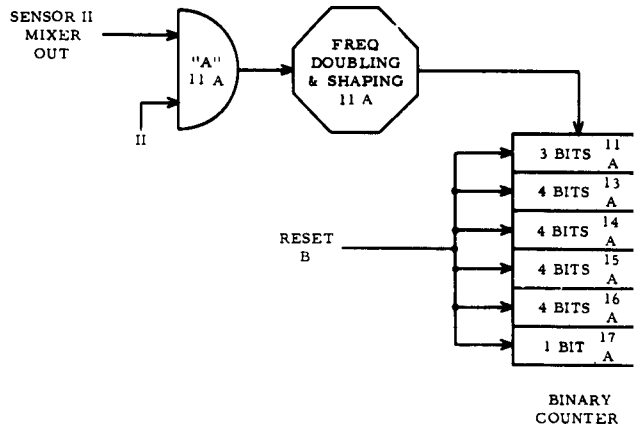
SENSOR II
MIXER
OUT
"A"
11 A
II
FREQ
DOUBLING
& SHAPING
11 A
3 BITS 11 A
4 BITS 13 A
4 BITS 14 A
4 BITS 15 A
4 BITS 16 A
1 BIT 17 A
RESET
B
BINARY
COUNTER

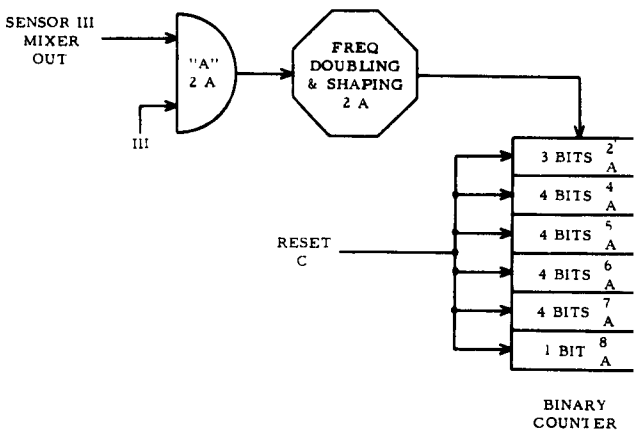
SENSOR III
MIXER
OUT
"A"
2 A
III
FREQ
DOUBLING
& SHAPING
2 A
3 BITS 2 A
4 BITS 4 A
4 BITS 5 A
4 BITS 6 A
4 BITS 7 A
1 BIT 8 A
RESET
C
BINARY
COUNTER

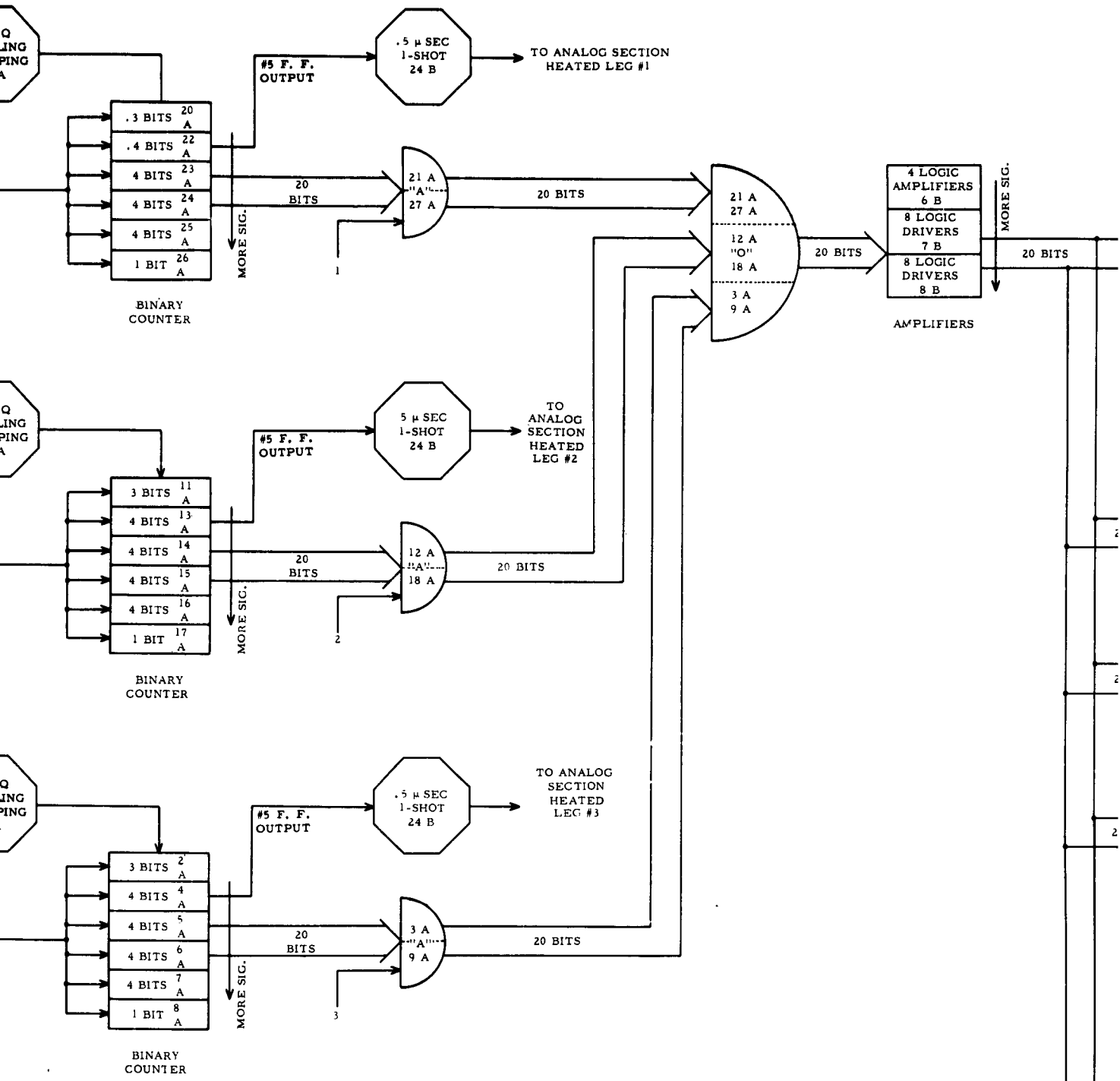
.3 BITS 20 A
.4 BITS 22 A
4 BITS 23 A
4 BITS 24 A
4 BITS 25 A
1 BIT 26 A
BINARY COUNTER
#5 F. F. OUTPUT
.5 μ SEC 1-SHOT 24 B
TO ANALOG SECTION HEATED LEG #1
MORE SIG.
20 BITS
21 A "A" 27 A
1
20 BITS
21 A 27 A
12 A "O" 18 A
3 A 9 A
20 BITS
4 LOGIC AMPLIFIERS 6 B
8 LOGIC DRIVERS 7 B
8 LOGIC DRIVERS 8 B
AMPLIFIERS
MORE SIG.
20 BITS
3 BITS 11 A
4 BITS 13 A
4 BITS 14 A
4 BITS 15 A
4 BITS 16 A
1 BIT 17 A
BINARY COUNTER
#5 F. F. OUTPUT
5 μ SEC 1-SHOT 24 B
TO ANALOG SECTION HEATED LEG #2
MORE SIG.
20 BITS
12 A "A" 18 A
2
20 BITS
3 BITS 2 A
4 BITS 4 A
4 BITS 5 A
4 BITS 6 A
4 BITS 7 A
1 BIT 8 A
BINARY COUNTER
#5 F. F. OUTPUT
.5 μ SEC 1-SHOT 24 B
TO ANALOG SECTION HEATED LEG #3
MORE SIG.
20 BITS
3 A "A" 9 A
3
20 BITS

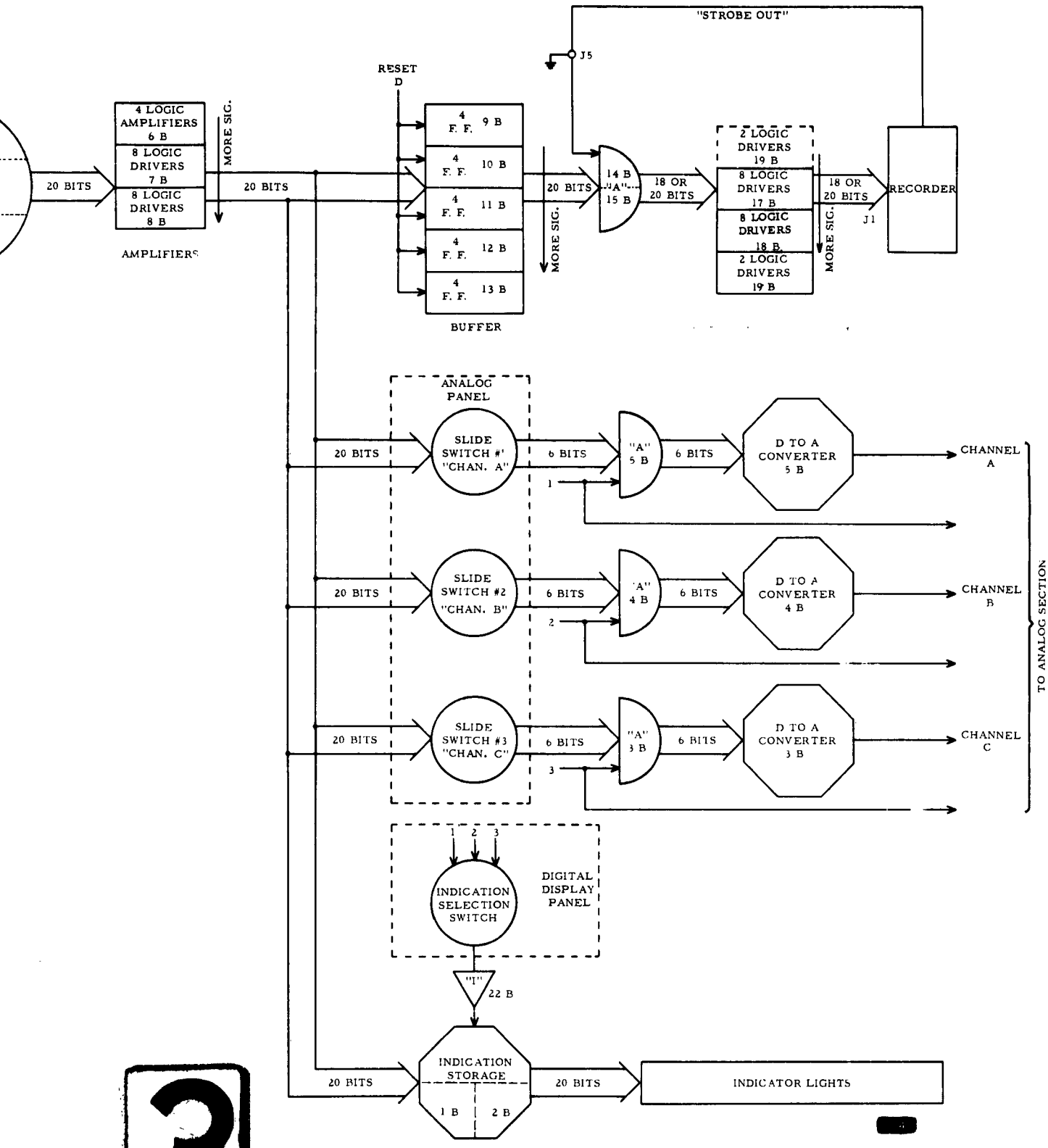

Figure 27. System Logic Design

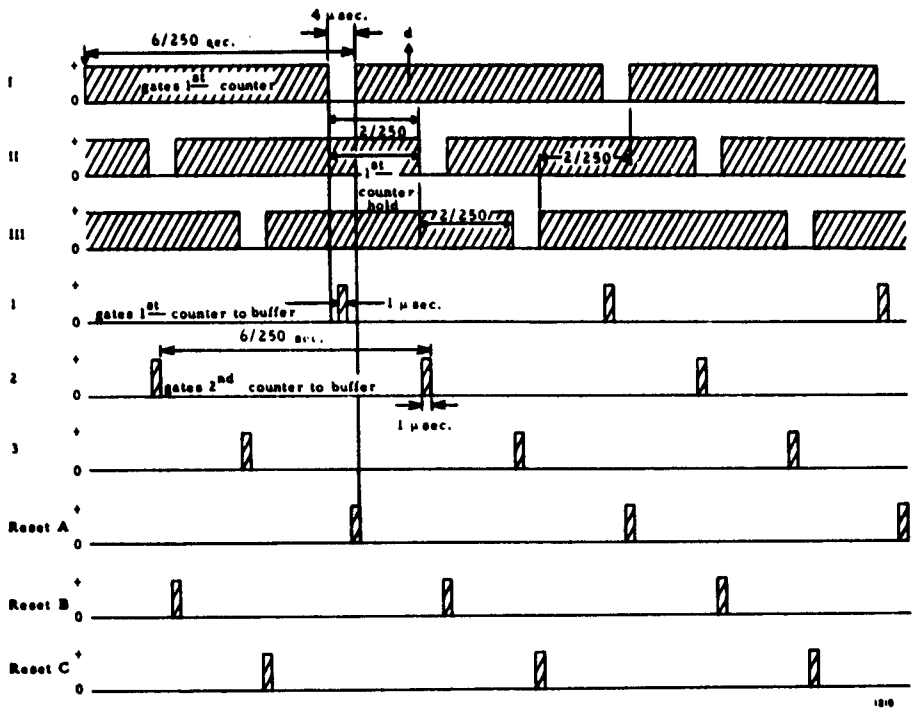

Figure 28. Time Chart for Timing Circuit (not to scale)

Resolution to 1/2 cycle of the input signal is obtained by frequency doubling the output of the "AND" gate at the counter input before application to the first binary counter stage. The output of the frequency doubler drives a Schmidt trigger circuit for pulse shaping to drive the first binary stage.

The output from each of the binary counters passes thru an "OR" circuit and logic drivers for connection to an output 20-bit buffer. The output of the buffer register passes through an "AND" gate and logic drivers to the format converter of the tape recorder. Exact strobe-out time of the buffer register is under control of the tape recorder logic to maintain proper formatting and packing density on the magnetic tape.

The 20 binary bits which drive the buffer register also drive the two monitor displays. The digital display consists of binary coded indicator lights. Since the output of a counter is only available for one microsecond, indicator storage is implemented by capacitors which are analogous to the sample and hold circuit of an analog-to-digital converter. The one set of indicator lights for the 20 binary bits can be connected to any of the three seismometers by the Indicator Selector switch. This merely controls the logic time for connection of the indicator lights to the input of the buffer register.

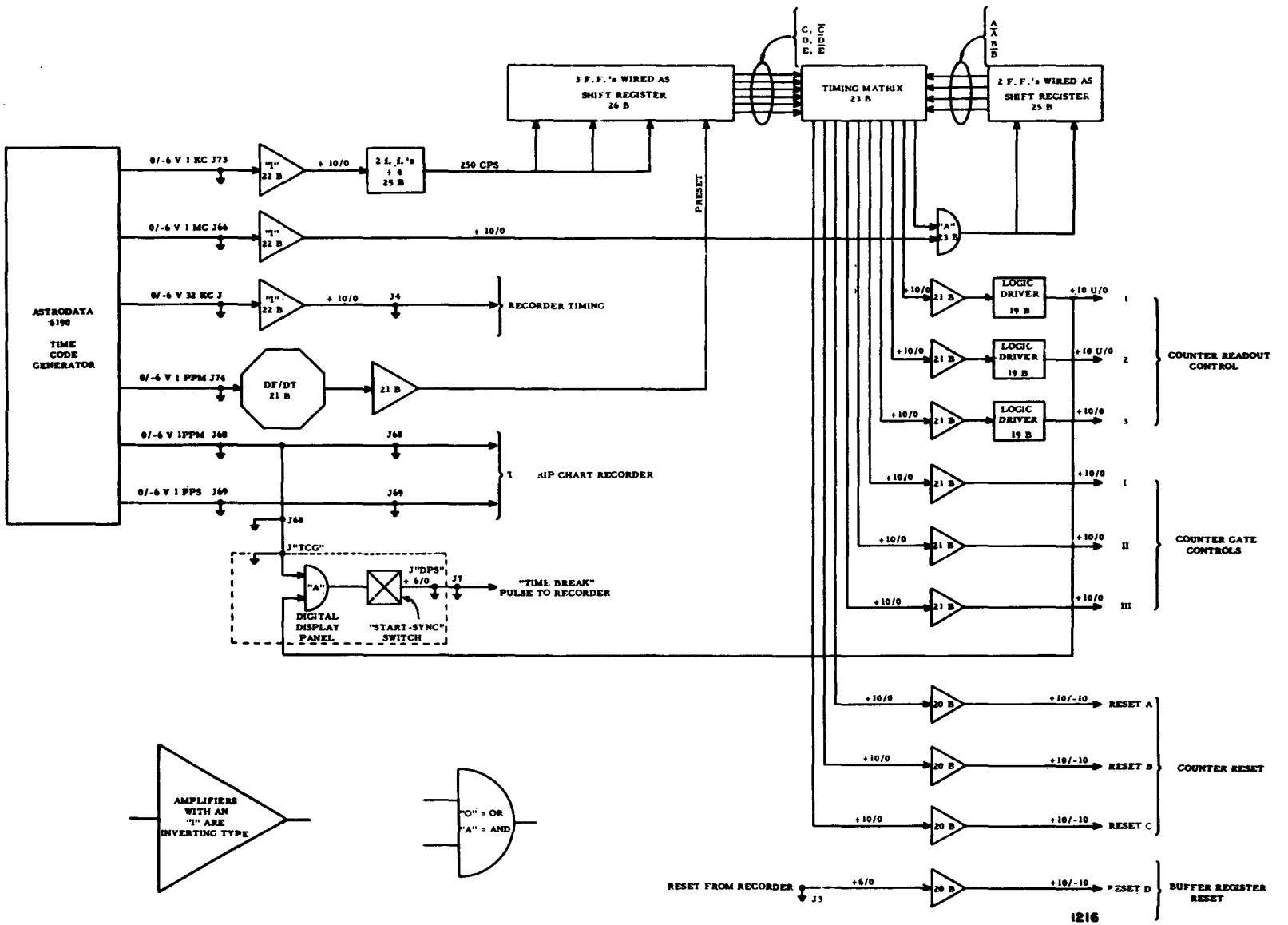

Figure 29. Logic Timing System

In parallel with the buffer register input is a digital-to-analog converter to drive the strip-chart monitor recorder. D-to-A conversion is made on 6 binary bits, but these can be placed at any point in the 20-bit scale by sliding as a 5-bit sequential group plus a sign bit. Fifteen binarily weighted scale changes are provided, so that the strip-chart monitor can be driven to full scale for any signal input range. The "AND" gate at the input of the D-to-A converters is needed to connect the proper multiplexed word into the channel. Since the buffer register input consists of the three time-multiplexed words from the three binary counters, the "AND" gate is required.

In addition to the functions of digital conversion, gating, buffering, and drive to the display monitors, the logic also provides the signal for boom centering. The output of the fifth binary stage of each of the three counters connects to a 0.5 microsecond one-shot multivibrator. The output of this circuit is therefore a pulse frequency modulated signal (PFM), which can be passed through a low-pass filter for conversion to an analog signal to drive the boom centering circuitry.

Timing for the above functions is synchronous under control of the one-megacycle clock in the chronometer system, as shown in Figure 29. The Astrodata Model 6190 Chronometer or time code generator has six outputs for time control of the entire digital logic. The 250 pulse-per-second requirement for the counter gating is obtained by dividing 1000 cycles per second by 2 binary flip-flops. This signal drives three flip-flops wired as shift registers for division by three to obtain the basic counting time for the binary counters. The true and complement output of each of the three flip-flops control the timing matrix for reset and control pulses for the digital logic. Pulses for binary counter readout and reset are generated by the "AND" circuit at the output of the timing matrix and are synchronous with 1-megacycle pulses from the chronometer. The control pulses are actually generated from two flip-flops wired as shift registers under control of the 1-megacycle clock and logic pulses from the matrix. Circuitry is shown in more detail on Figure 30 for the timing reset and readout logic.

Time encoding for the analog display is derived from the chronometer output. A pulse of 10-seconds duration every minute and a pulse of 10-milliseconds duration every second drive a marker pen on the edge of the paper of the analog monitor.

Time encoding of the magnetic tape recorder is also under control of the chronometer system. After locking the chronometer reading with a WWV receiver, the system tape recorder can then be time encoded in real time by the following system. A few seconds preceding an exact minute mark from the chronometer, the Start-Sync switch is depressed. After the tape recorder is up to speed, the first timing word is written at the exact minute under control of the 1-pulse-per-minute signal from the chronometer

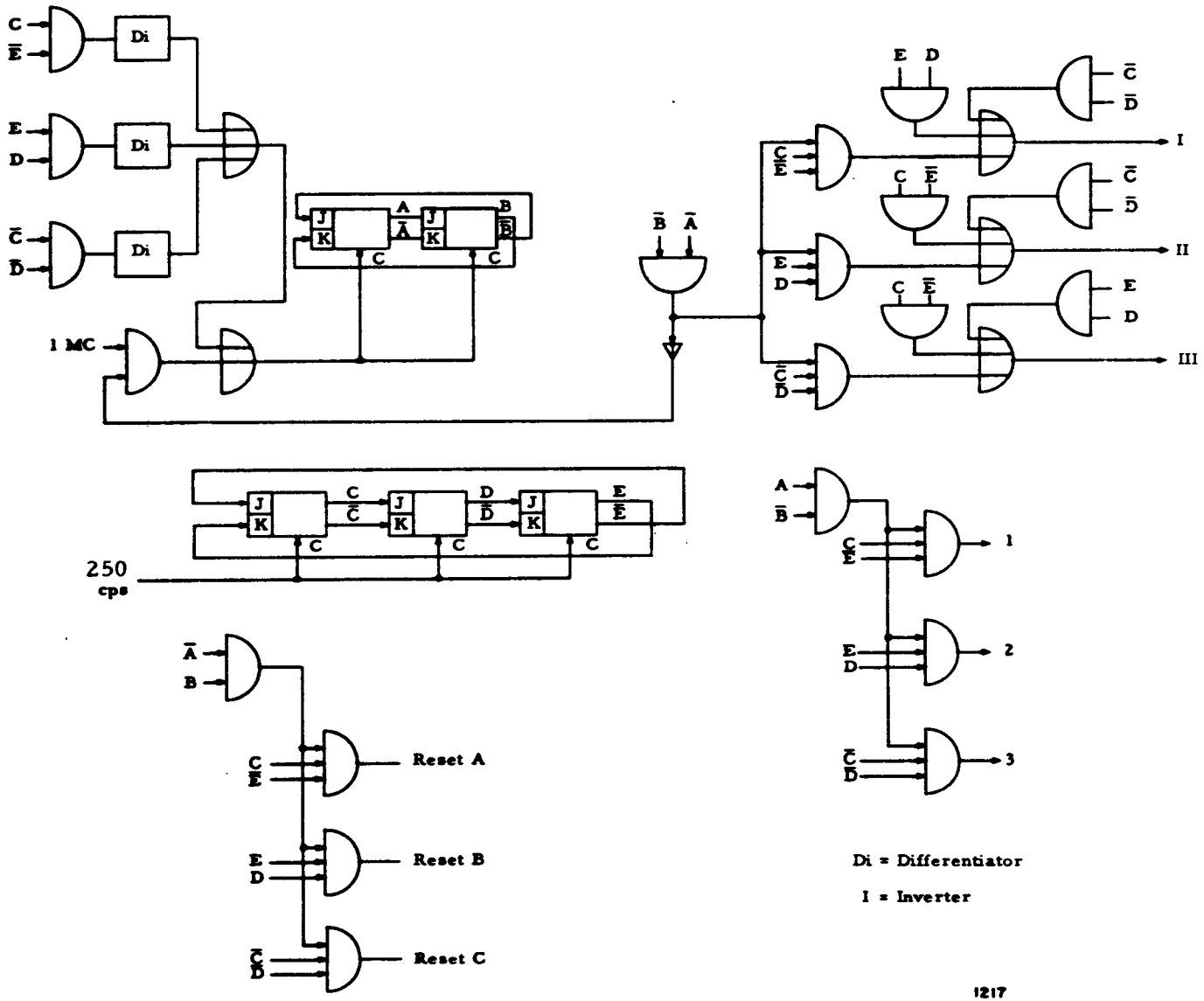

Figure 30. Timing Circuit for All But Buffer Control

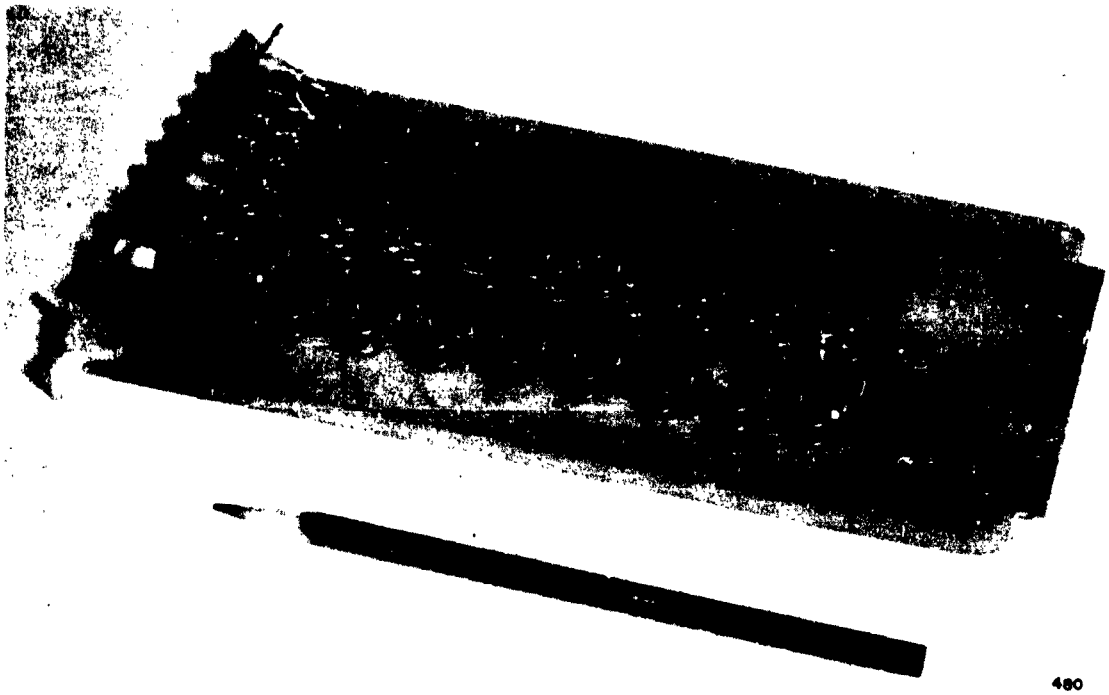

Figure 31. Logic Driver Circuit Board

in exact synchronization with the readout pulse from the first binary counter. Within the tape recorder, each data block is preceded by a timing word which is synchronous from the chronometer. The binary counter within the tape recorder system which generates the timing words is driven by the 32 kc system from the chronometer. To insure synchronization of the digital logic with the logic of the tape recorder, the complement of the one-pulse-per-minute signal from the chronometer is differentiated and presets the time-generating logic. This insures a positive lock between the tape recording logic and the digital seismograph logic. Detailed circuit diagrams for the individual logic circuits for implementation of the functions described above are presented in Appendix I.

The mechanical arrangement of components for the logic are illustrated by the following three figures. Figure 31 shows a typical logic card, Figure 32 illustrates the logic rack from the front with the door removed, and Figure 33 shows the logic rack from the back with the doors removed. Packaging of the system was dictated by the requirement for maximum flexibility. Test points are provided for all pertinent logic signals at the front of the logic cards. Point-to-point wiring at the back of the cards was used because of the high-frequency logic signals. It is obvious that production re-packaging could reduce the size of the overall electronics package by approximately a factor of 4.

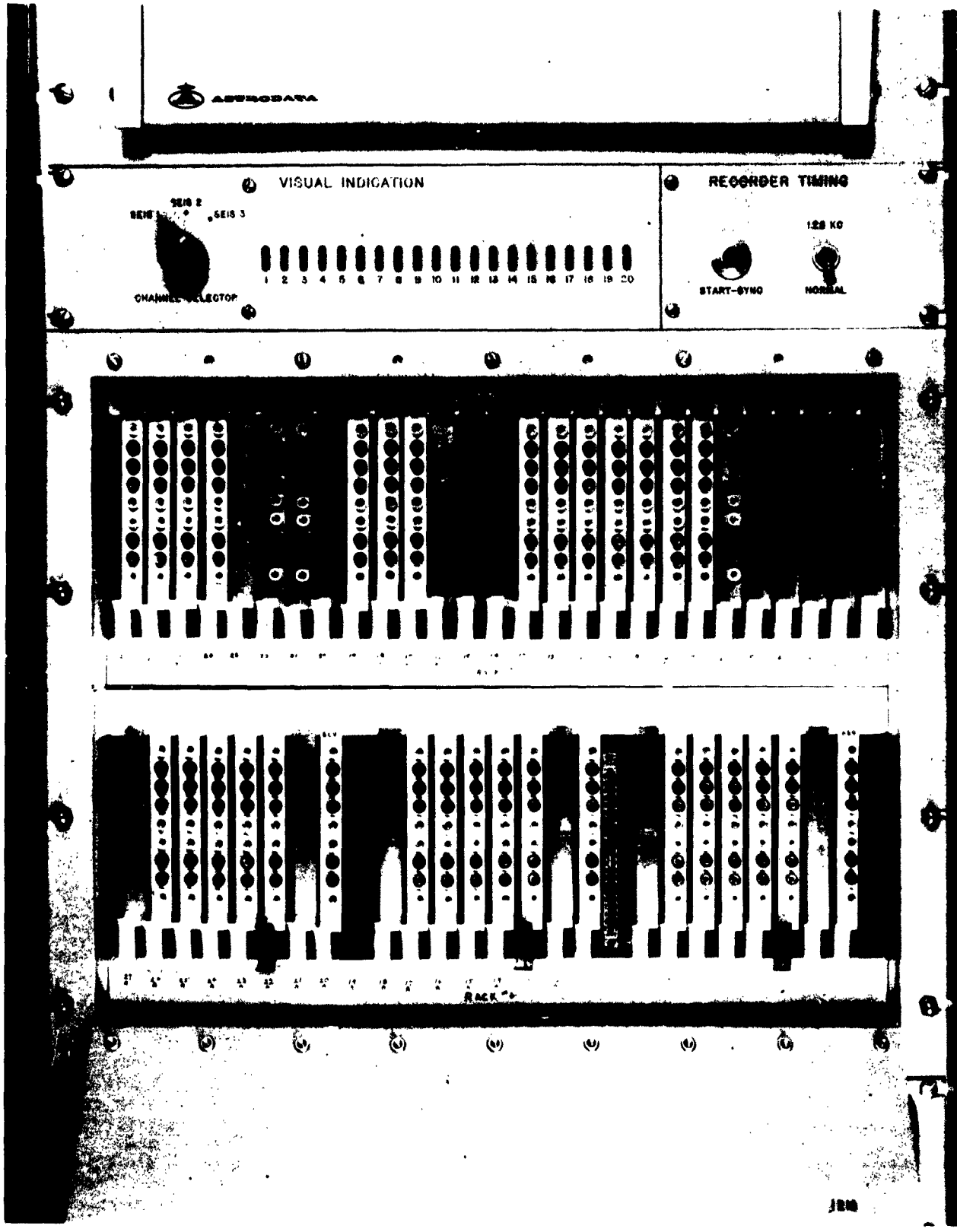

Figure 32. Front View of Logic Rack

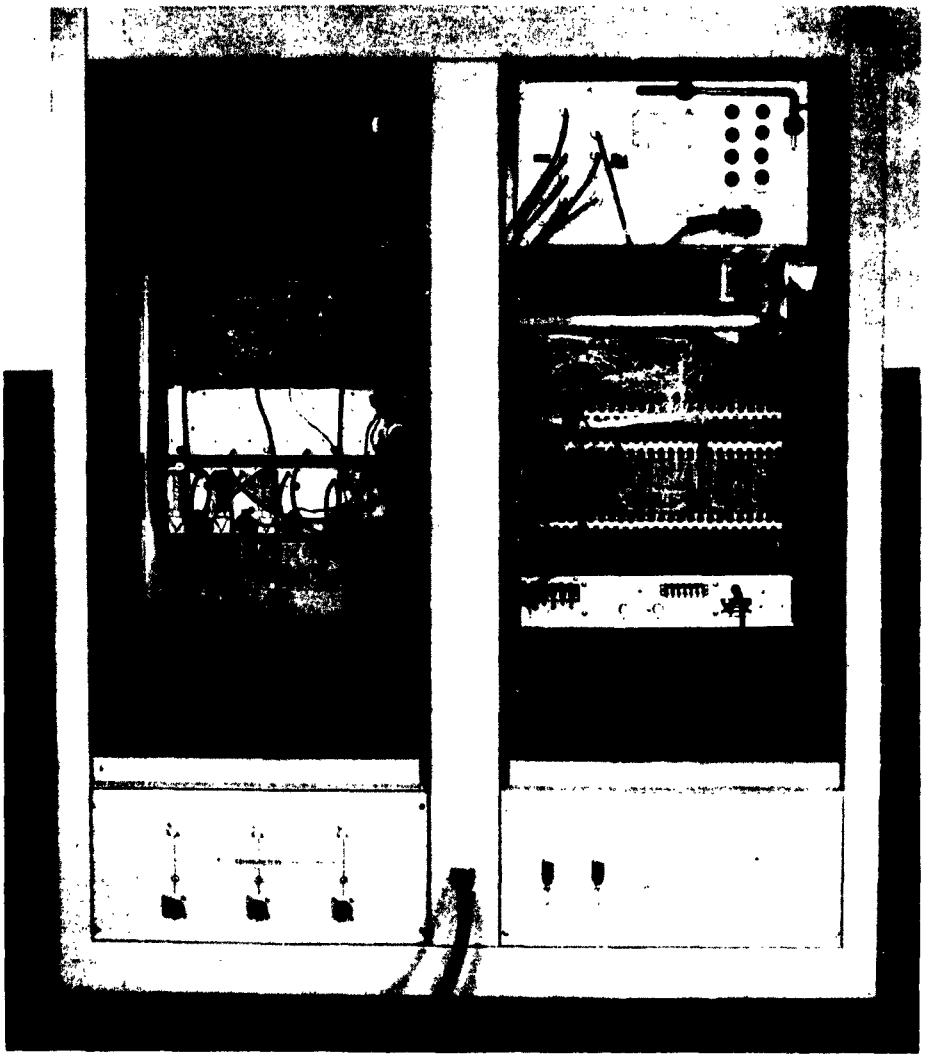

Figure 33. Back View of Logic Rack With Doors Removed

E. BOOM CENTERING AND ANALOG DISPLAY MONITOR

The analog circuit portion of the total system provides the functions of automatic boom centering and strip-chart display monitoring. Boom centering is maintained for displacement frequencies below 0.025 cycles per second.

A basic block diagram for the total analog system is shown in Figure 34. The output of the FM sensor with a frequency deviation of 0 to 40 megacycles is divided down to 0 to 1.25 mc by the first five stages

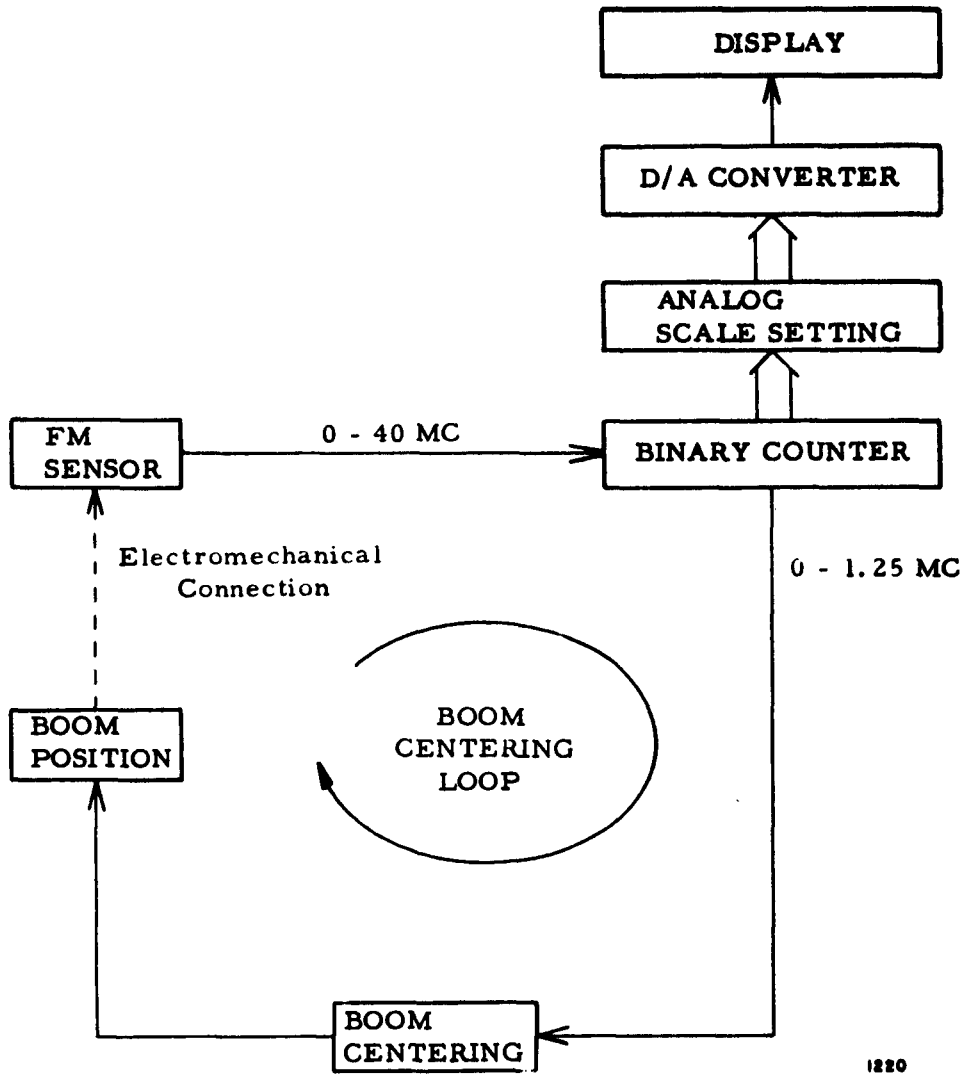

Figure 34. Analog System Block Diagram

of the binary counter. The boom centering circuitry converts the 0-to-1.25-mc FM to pulse frequency modulation (PFM). Integration of the PFM signals results in an analog signal to drive the boom centering mechanism. As previously described, boom centering for the horizontal seismometer is adjusted by the thermal bias applied by a heater coil on one leg of the seismometer.

For the vertical seismometer, deflection of the boom results from current through a coil in a magnetic field. The conventional output coil of the Press and Ewing seismometer is used for this application.

Analog display for monitoring is driven from the output of the individual binary counters. Any six consecutive bits can be switch selected for gain adjustment. Voltage for the 6 bits drive binary weighted resistors for digital-to-analog conversion.

1. Boom Centering

The boom centering block diagram in Figure 35 and the schematic diagram of Figure 36 show details of the boom centering system.

The PFM signal with a pulse width of 0.5 microseconds is integrated by a low-pass filter with a cut-off of 10 cycles per second. This output is added to a reference voltage. A reference voltage of 7 volts results in a constant expansion of the leg of the seismometer. Therefore, correction for tilt of the horizontal seismometers can be applied in both directions - that is, expansion or contraction from the bias value.

Sums of both the reference voltage and the closed loop correction voltage are amplified and phase corrected. A Philbrick P2 operational amplifier with phasing in the feedback loop produces phase correction for the total loop. Power amplification drive comes from a Darlington type emitter-follower with the heater coil in the emitter circuit.

To monitor any of the three closed loop systems the output of the power amplifier is switch selected for the fourth channel of the servo/riter.

For the vertical seismometer the reference voltage is not required; the P2 operational amplifier is used merely for symmetry loop phasing.

Additional investigation could considerably reduce the complexity of the loop circuitry. Linearity and long-time drift of the circuits are of little significance because of the self-correcting nature of the closed loop. A most significant requirement is that the circuitry should not inject any noise into the seismometer reading. This is particularly important with 20 binary bits of range.

Figure 37 illustrates the operation of the circuit for approximately one hour with the horizontal seismometer in an area of high seismic noise.

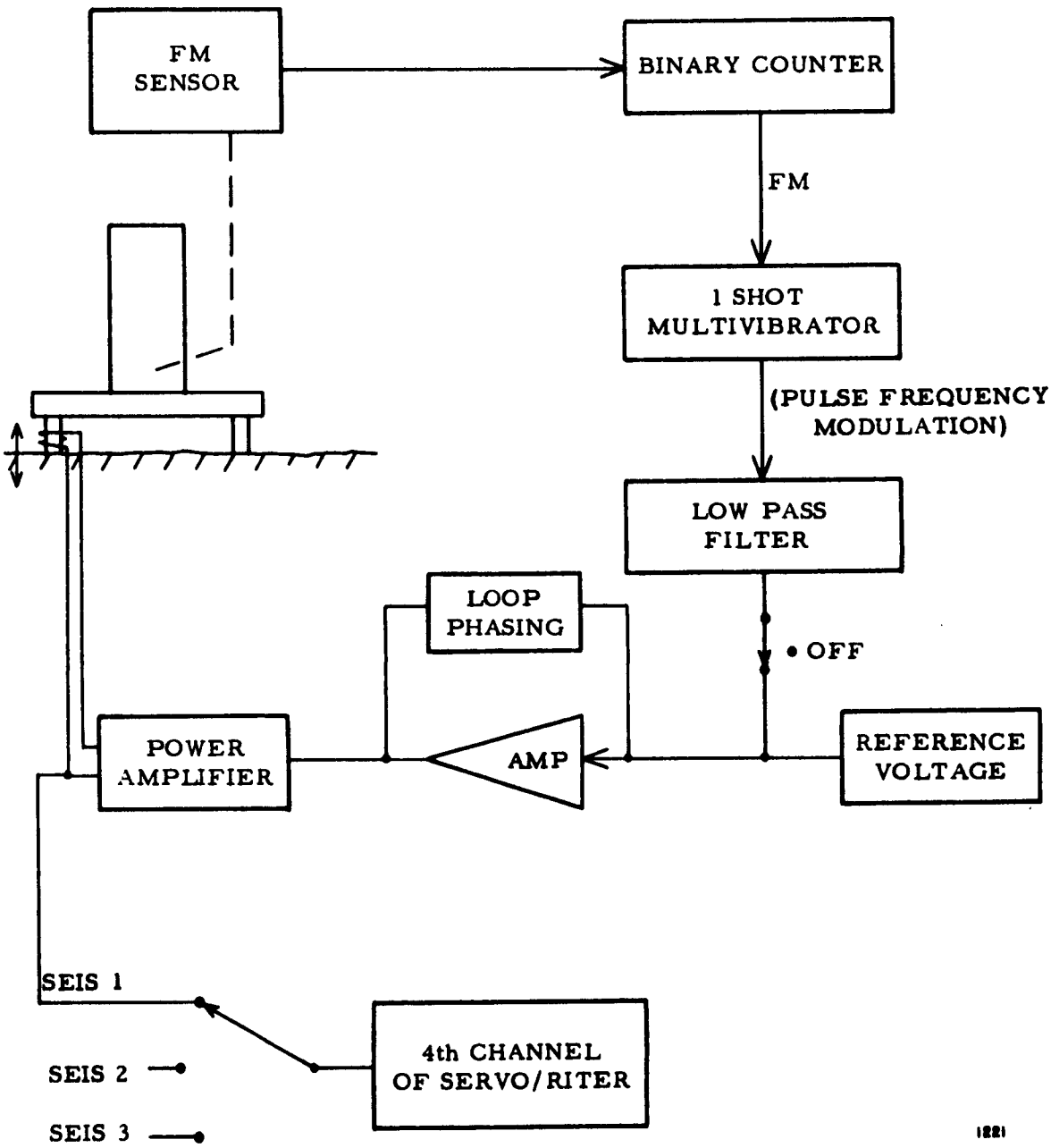

Figure 35. Boom Centering

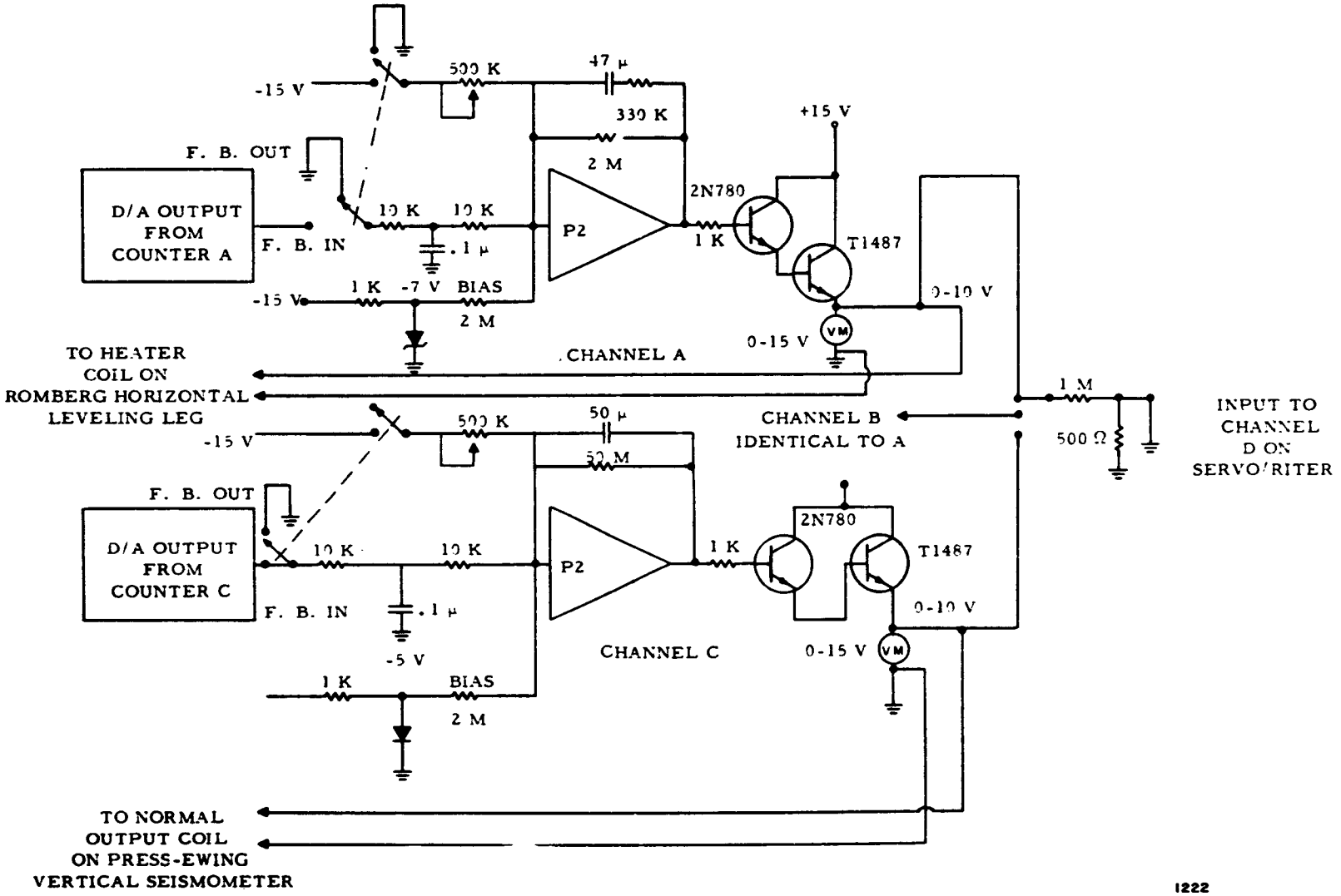

Figure 36. Boom Centering Schematic

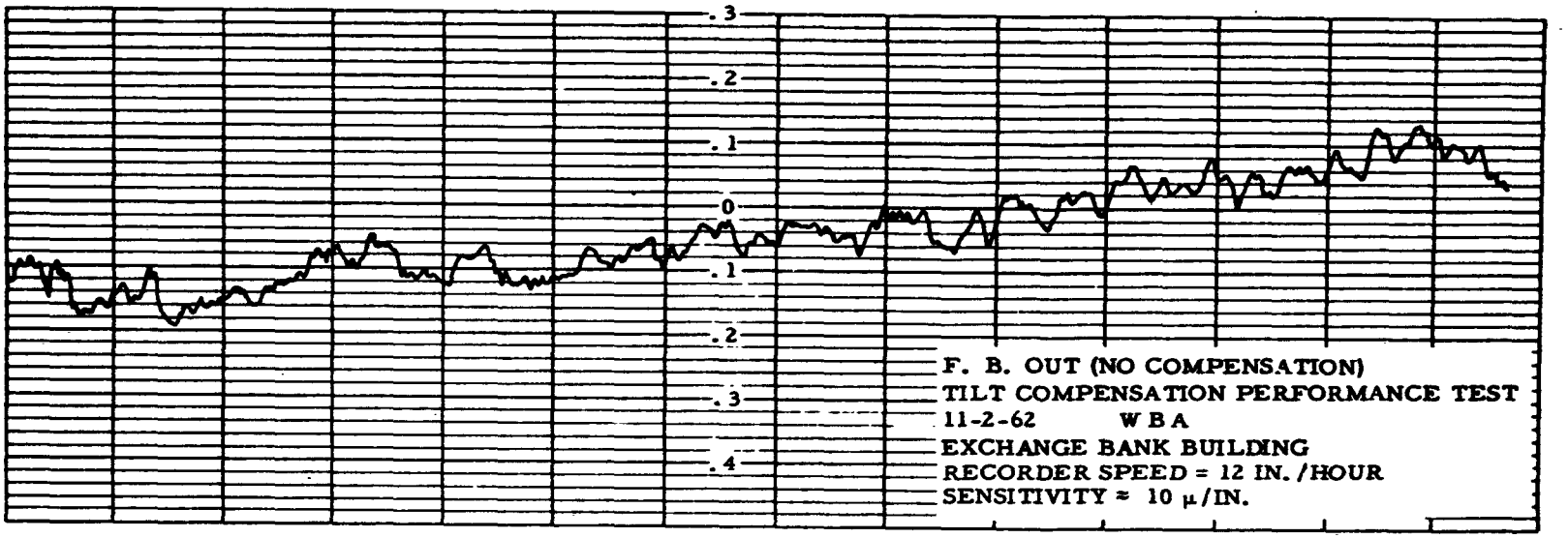

NO BOOM CENTERING

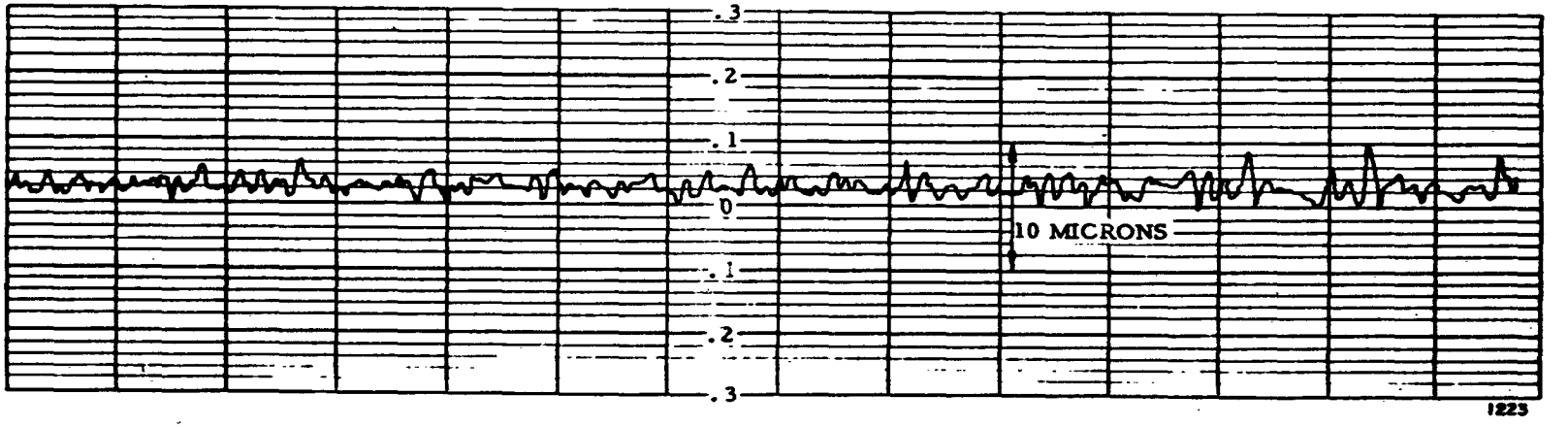

WITH BOOM CENTERING

Figure 37. Boom Centering Test Data

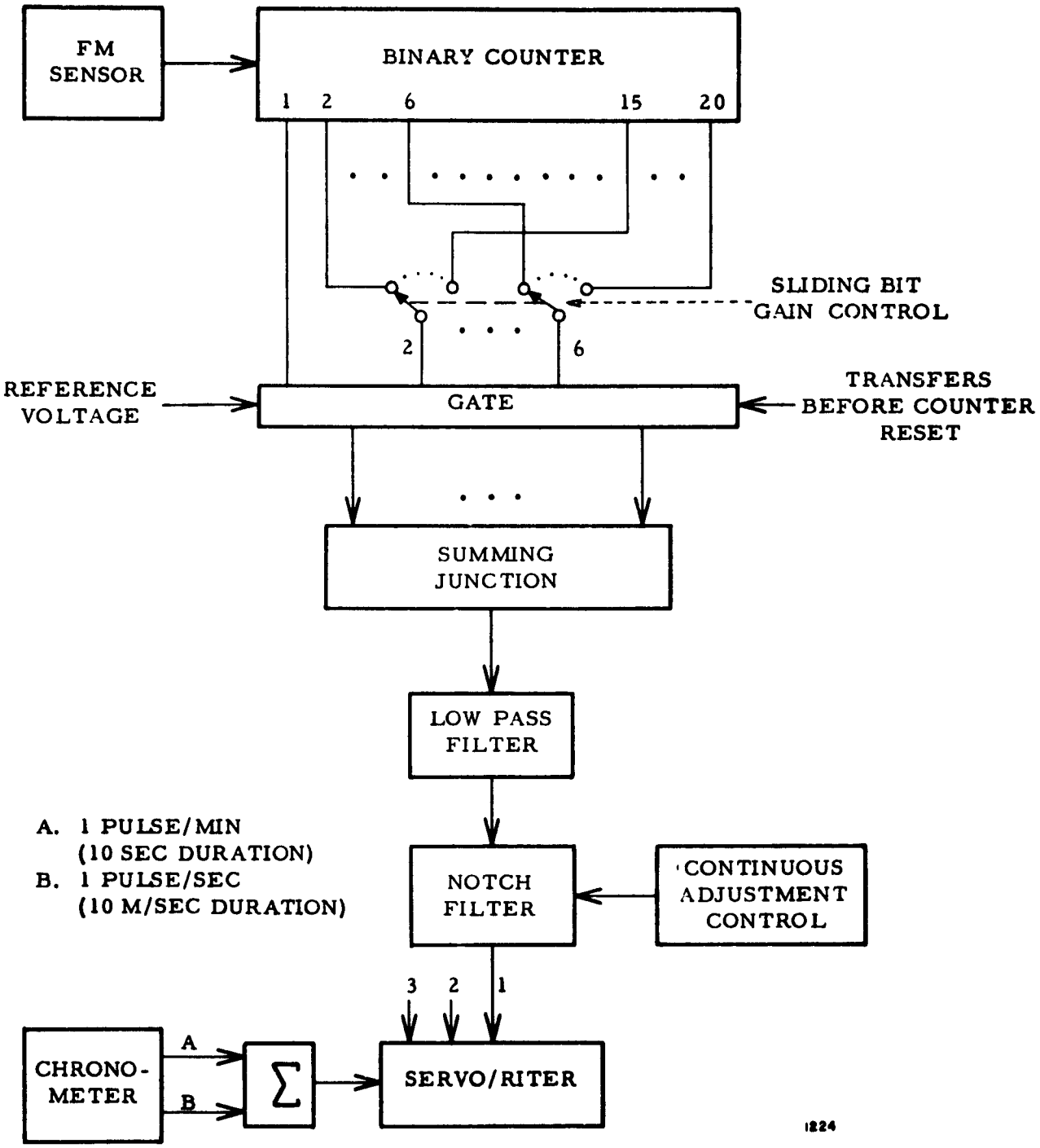

Figure 38. Analog Display

2. Analog Display

The block diagram for the analog display is shown in Figure 38. Two microseconds after the termination of a counter cycle, data is gated to the buffer register, digital display, and analog display circuitry. As previously discussed, gain selection for analog display is implemented in 6 db steps by sliding five consecutive bits along the total 20-bit range. (The first bit to drive the digital-to-analog converter remains the same for all gain settings, since it is the sign bit.)

By referring to the analog display block diagram, Figure 38, and the schematic, Figure 39, the system works as follows. Data is passed from the sliding bits to the resistor summing junction under the control of the strobe pulse. For a binary zero condition on one of the input lines, the input to the resistor summing junction is strobed to a ground condition. When a "1" is on the input, the strobe connection results in the connection of the 10-volt reference voltage to the resistor summing junction. Voltage summing at the summing connection is obtained by a resistor ladder network. The output of the summing junction is passed through an emitter-follower to obtain adequate power for charging a capacitor. Since data is available only for one microsecond out of approximately 1/40 second, the time constant for the capacitor discharge is maintained at a high value by back-biasing the diode and by the high-impedance emitter-follower load on the capacitor. The RC time constant on the capacitor discharge acts as a low-pass filter, the output is then passed through an emitter-follower to the notch filter. This is a conventional, parallel-T notch filter for rejection of microseism frequencies on the analog display monitor. Total range is 0.13 to 10 cycles per second. All potentiometers are ganged for ease of setting a particular reading. The notch filter is calibrated and can be set to any value by use of the scale of the 10-turn ganged potentiometer. The notch filter output drives one of the servo/riter strip-chart channels for display. The servo/riter has four overlapping pens for a maximum scale of 9.5 inches total deflection for each channel. Three channels are used for the monitoring of the three components of the seismograph system and the fourth channel is switch selectable to any of the three boom centering channels.

Time encoding on the strip-chart recorder is furnished by a pen marker at the edge of the paper. A pulse of 10 seconds duration is applied at 40 minute intervals. At 1-second intervals, a pulse of 10-milliseconds duration is applied. Figure 40 is a picture of the control panel for the analog display and boom centering system. Switches are used for placing the notch filter in or out of each of the seismic channels. The feedback loop for the boom centering also can be switched in or out of the circuit. Boom centering signal is monitored by the tilt-control voltage meters. The one additional selector switch is the channel selection for channel D or the fourth

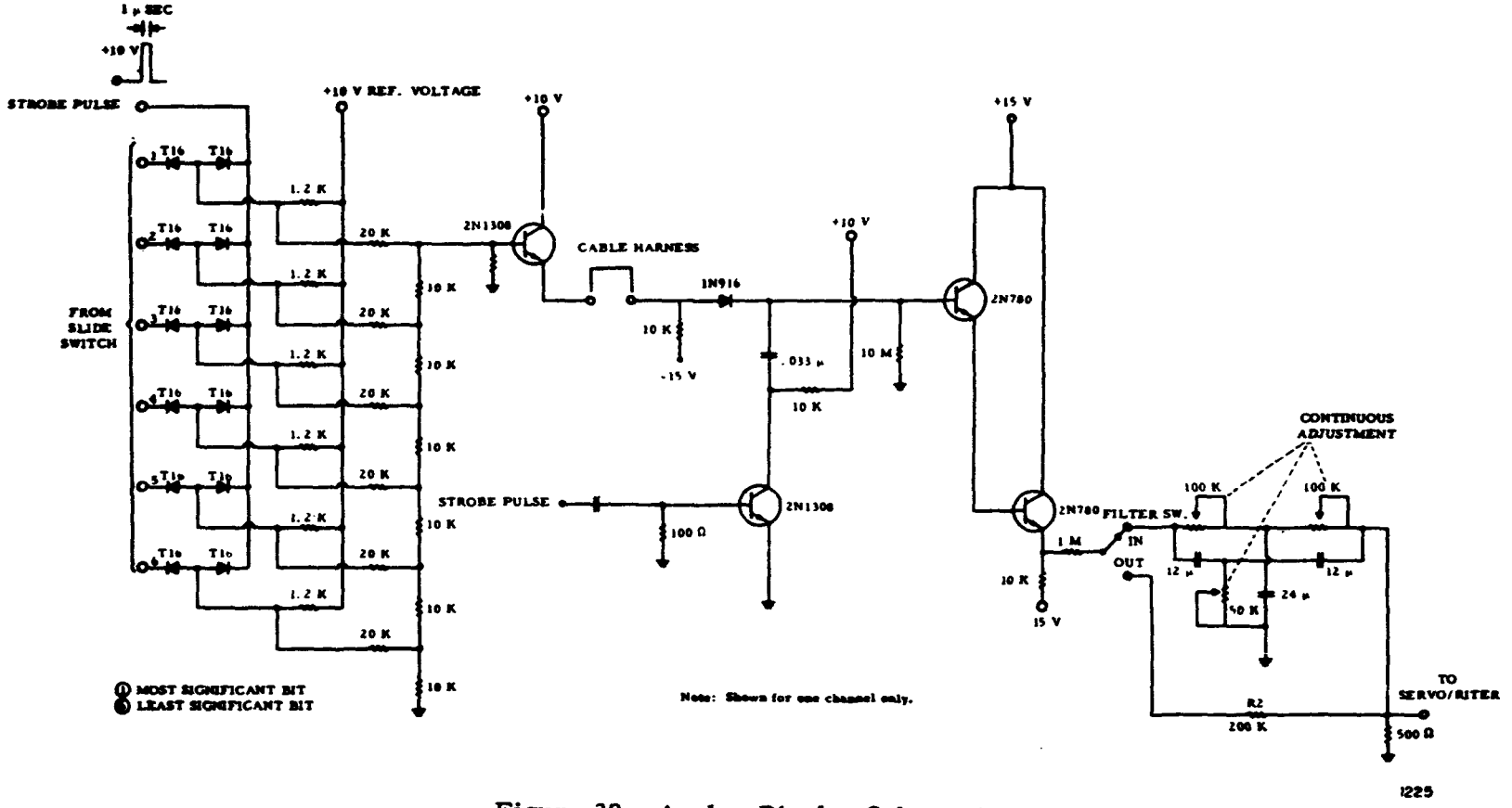

Figure 39. Analog Display Schematic

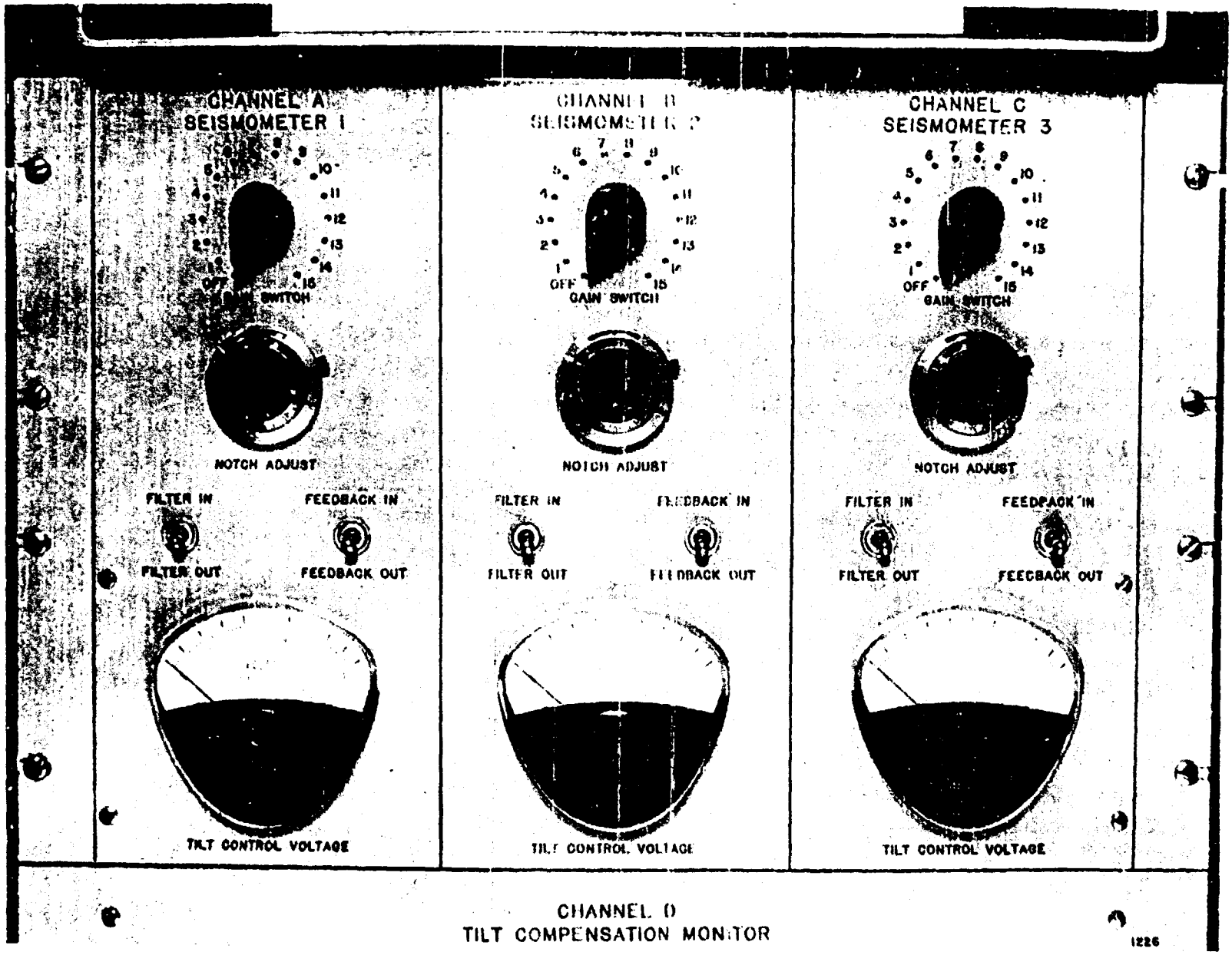

Figure 40. Analog Panel

channel of the strip-chart recorder. This switch allows selection of one of the tilt-control voltages for display on the strip-chart recorder. The control is directly beneath the center channel control.

F. DIGITAL RECORDING

The tape recording system works as follows. The record identification number is entered as a keyboard setting on the left side of the TI digital tape recording system as illustrated on Figure 41. The start button is pressed on the tape recording system. Under control of the tape logic, a specific code for "start-of-data" is written for a short period of time, after which blank codes are written until information about the digital seismograph system is fed into the recorder. The tape recording logic now waits for a synchronizing signal from the digital seismograph system. A SYNC PULSE switch is depressed approximately five seconds prior to a minute marker from the chronometer. This assumes that the chronometer has already been synchronized with WWV. Within one microsecond after the minute marker, the zero timing word is written on the magnetic tape and the 14-bit analog-to-digital converter starts functioning to convert any of the 19 comparison or evaluation signals to a 14-bit digital number. Simultaneously, the first data word from seismometer no. 1 is transferred into the data block as shown on Figure 42. Seismometers 2 and 3 are simultaneously gated into the same data block. Timing word identification for the next data block, which comes 24 milliseconds later, is indexed by one count.

Total recording time can be any value up to the maximum time for one reel of tape. When it is decided to terminate a recording, the STOP switch on the tape recording system is pressed. End of data code is written for a finite time, starting at the next block position. Next, the tape transport stops for unloading the tape. The tape is then manually transferred to a playback facility which is available within Texas Instruments for either data presentation or for computer analysis. Formatting is compatible with the Texas Instruments TIAC* computer, and the data can be analyzed by the computer.

Programs are already available for such computer analysis as Fourier transform computations or frequency analysis, filtering with up to 42 operator points, and various signal-enhancement techniques.

---

* Trademark of Texas Instruments Incorporated

Figure 41. Texas Instruments Digital Tape Recording System

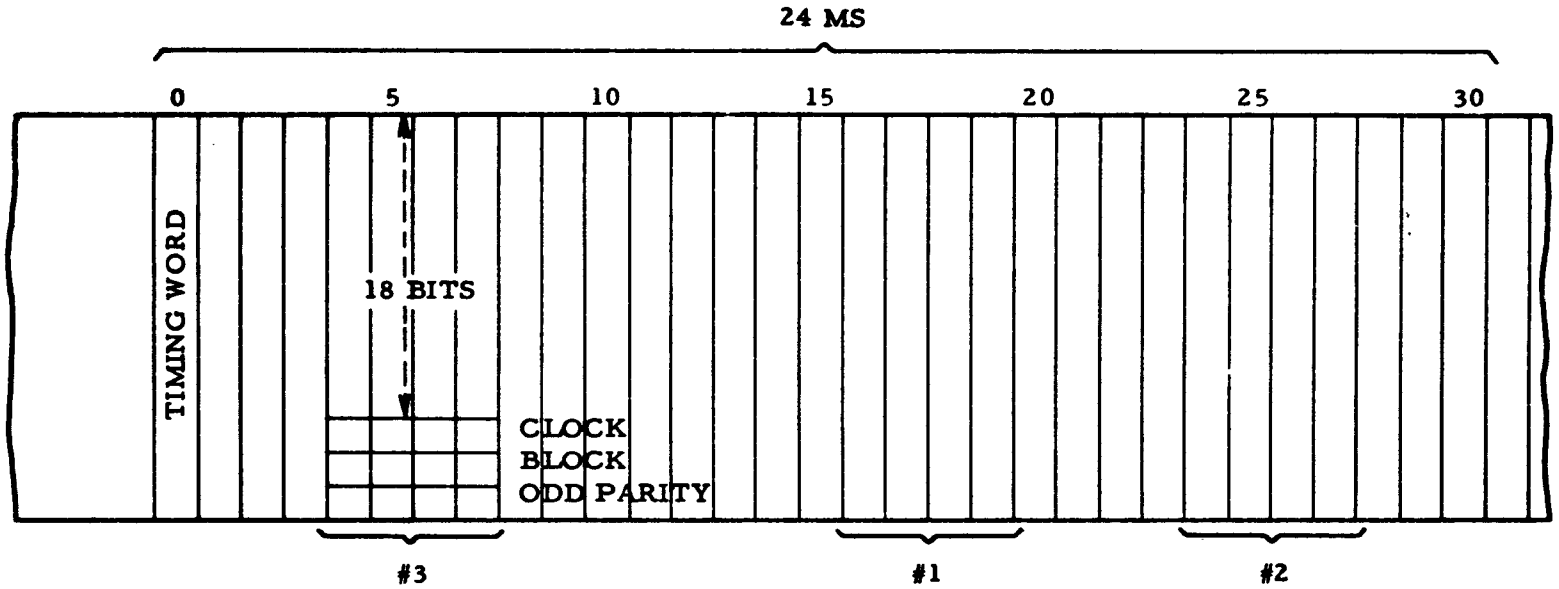

TIAC DATA BLOCK

Figure 42. TIAC Data Block

SECTION III

EVALUATION

As the design of the elements of the Digital Seismograph System has progressed, it has been necessary to evaluate several of these elements. The results of these evaluations are described below.

A. TILT COMPENSATION FOR HORIZONTAL COMPONENTS

A very thorough theoretical study was made of three horizontal oscillating systems. The systems considered were the simple pendulum, swinging gate and Romberg suspension.* This is reported in detail in Appendix C. The conclusions drawn were:

1. The period of the swinging gate and the Romberg suspensions are almost identically affected by tilt in the plane of oscillation. Tilt in the transverse plane in either direction will cause the period of Romberg suspension to become infinite, but the rate of change of tilt sensitivity is zero when the instrument is level. The period of the swinging gate becomes infinite only when the tilt brings the plane of oscillation horizontal (negative tilt), but there exists no condition where the rate of change of tilt sensitivity is zero. Also, a 20-second-period Romberg must be tilted .045 radians to reach the infinite period condition, while an equivalent-period swinging gate instrument goes to infinity at a tilt of only 0.001 radians.

2. In horizontal-motion seismometers the sensitivity of the mass position to tilt and the sensitivity to long-period horizontal motion are directly related. A similar condition exists in vertical-motion seismometer between the sensitivity to long-period motion and mass displacement. Because of this, boom centering systems were devised and evaluated.

Figure 43 is the record of a step input function into the horizontal seismometer to test the boom centering loop response. The step function was generated by suddenly tilting the base of the seismometer a small amount.

Referring to this figure, the seismometer boom was resting at 3.5 microns above the chart center before the step function. The step function was about 48 microns in amplitude. After two minutes, the boom had again come to rest, this time at 4 microns above zero. This

* Romberg, F. E., An Oscillating System for a Long-Period Seismometer for Horizontal Motion; Bulletin, Seismological Society of America, July 1961.

gives a boom drift reduction of about 100:1.

The period of the first cycle of boom oscillation was 46 seconds, and the second cycle about 41 seconds. The boom centering loop was purposely left underdamped for these tests to facilitate the observation of its natural frequency. In actual operation the loop is approximately critically damped.

The boom centering voltage, as shown in this figure, was initially 6.45 volts. The final value, which is not shown in the figure, was 6.95 volts.

Since the change in length of the heated leg on the horizontal seismometer is proportional to temperature, and the temperature of its leg is proportional to the power applied to the heater coil over this small range, the boom centering mechanical sensitivity would be:

$$\frac{48 \text{ microns (boom correction)}}{\frac{(6.95)^2 - (6.45)^2}{25 \text{ ohms}} \text{ (change in heater power)}} = 180 \text{ microns/watt}$$

Four watts of controlled heater power is available; thus the boom centering loop should be able to correct for a total boom drift of 720 microns. This is equivalent to a base-plate tilt on the Millis-Romberg seismometer of 2.3×10^{-5} radians, or 4.7 seconds of arc.

B. THEORETICAL SENSOR LINEARITY

The frequency of oscillation of the FM system oscillators is determined by the relation:

$$f = \frac{1}{2\pi\sqrt{LC}}$$

where C is varied by the boom position.

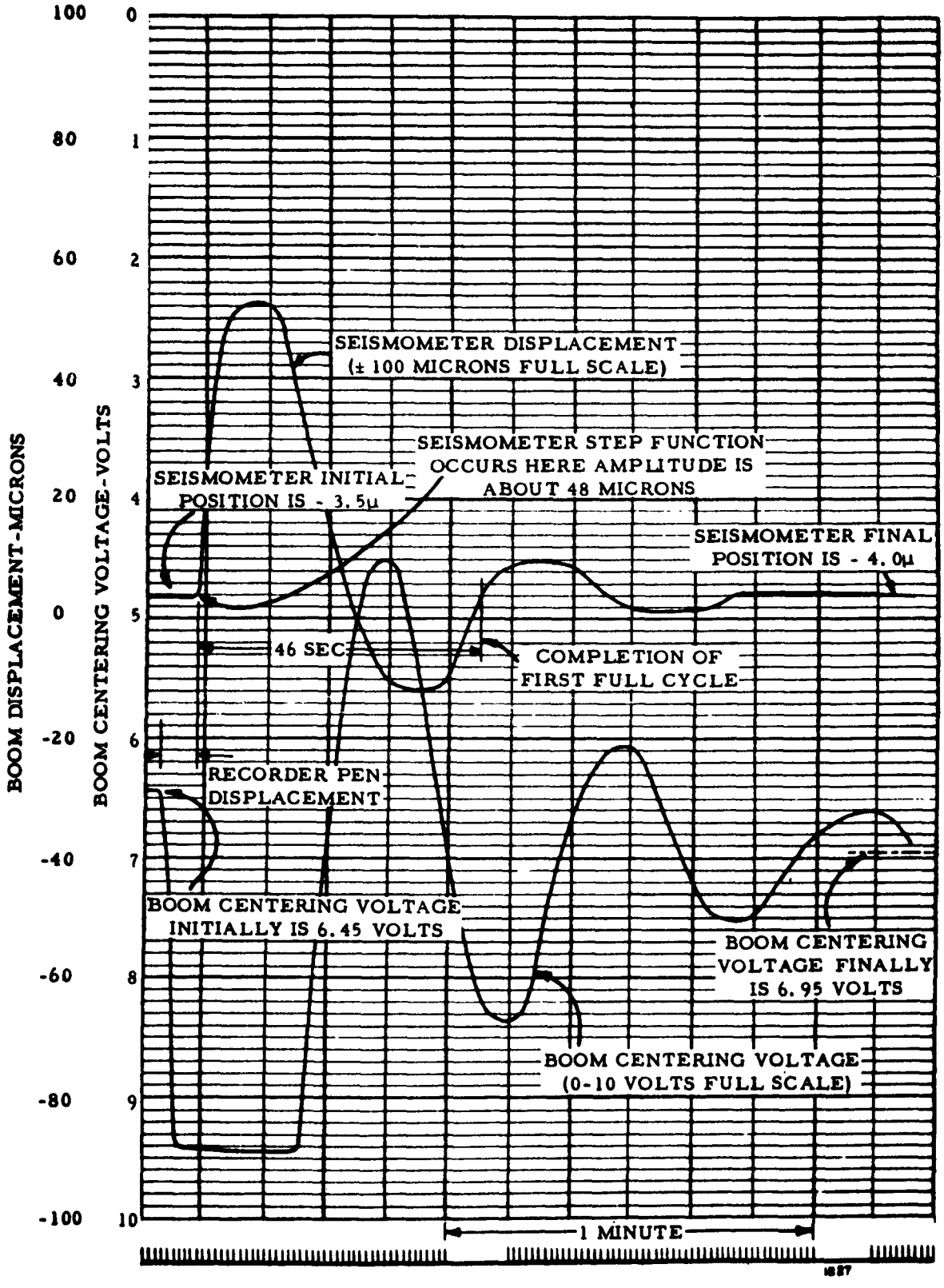

Figure 43. Boom Centering Test-Horizontal Seismometer

If d_c is the plate spacing, then C is proportional to $1/d_c$.

Letting d be the incremental movement of the plate spacing,

Frequency is proportional to $\frac{1}{2\pi\sqrt{L}} \cdot \sqrt{d_c + d}$

For two oscillators, the difference frequency would be:

$$\frac{1}{2\pi\sqrt{L}} \left[\sqrt{d_c + d} - \sqrt{d_c - d} \right]$$

To determine the linearity and distortion over a wide range of d, $\frac{1}{2\pi\sqrt{L}}$ may be considered a constant and arbitrarily set equal to 1. d_c is also constant, and values of d from 0 to d_c may be used.

The spacing between capacitor plates in the system is 1 millimeter. The extreme operating range of ± 100 microns will give a frequency variation from the mixer which is calculated to be linear with respect to boom movement to within approximately 0.15 per cent.

Since the boom centering circuit will also compensate for drifts in the oscillator beat frequency, it is possible that the boom will move off from the mechanical center position. This drift is expected to be less than 50 microns. If it should drift as much as 100 microns from the center, the linearity will be degraded to about 0.54 per cent. At 100 microns off the center, 3rd harmonic distortion of an incoming sine wave will be approximately 0.13 per cent. It is possible to remove this distortion in computer analysis of the data.

C. BENIOFF-DIGITAL SEISMOGRAPH COMPARISON

The experimental set-up is shown in the block diagram of Figure 44. This allowed simultaneous digital and analog recording of the two separate three-component seismograph systems.

In addition, the digital seismometer analog output was filtered with Krohn-Hite bandpass filters. These filters were set to give a bandpass of 1.6 to 8 cycles per second with a roll-off of 24 db per octave on both ends. Bandpass was determined experimentally by simultaneously observing a Benioff seismometer output and the equivalent filtered digital seismometer output on a dual-beam long-persistence oscilloscope. The filter was adjusted to give maximum correlation between the two traces.

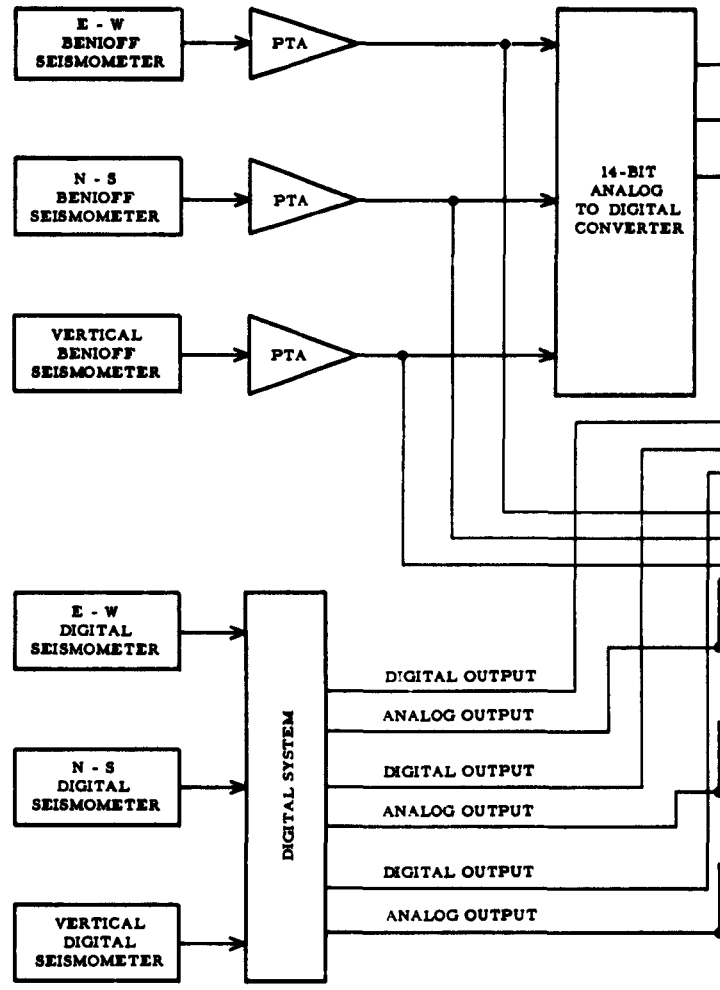
E - W
BENIOFF
SEISMOMETER
PTA
N - S
BENIOFF
SEISMOMETER
PTA
VERTICAL
BENIOFF
SEISMOMETER
PTA
14-BIT
ANALOG
TO DIGITAL
CONVERTER
E - W
DIGITAL
SEISMOMETER
N - S
DIGITAL
SEISMOMETER
VERTICAL
DIGITAL
SEISMOMETER
DIGITAL SYSTEM
DIGITAL OUTPUT
ANALOG OUTPUT
DIGITAL OUTPUT
ANALOG OUTPUT
DIGITAL OUTPUT
ANALOG OUTPUT

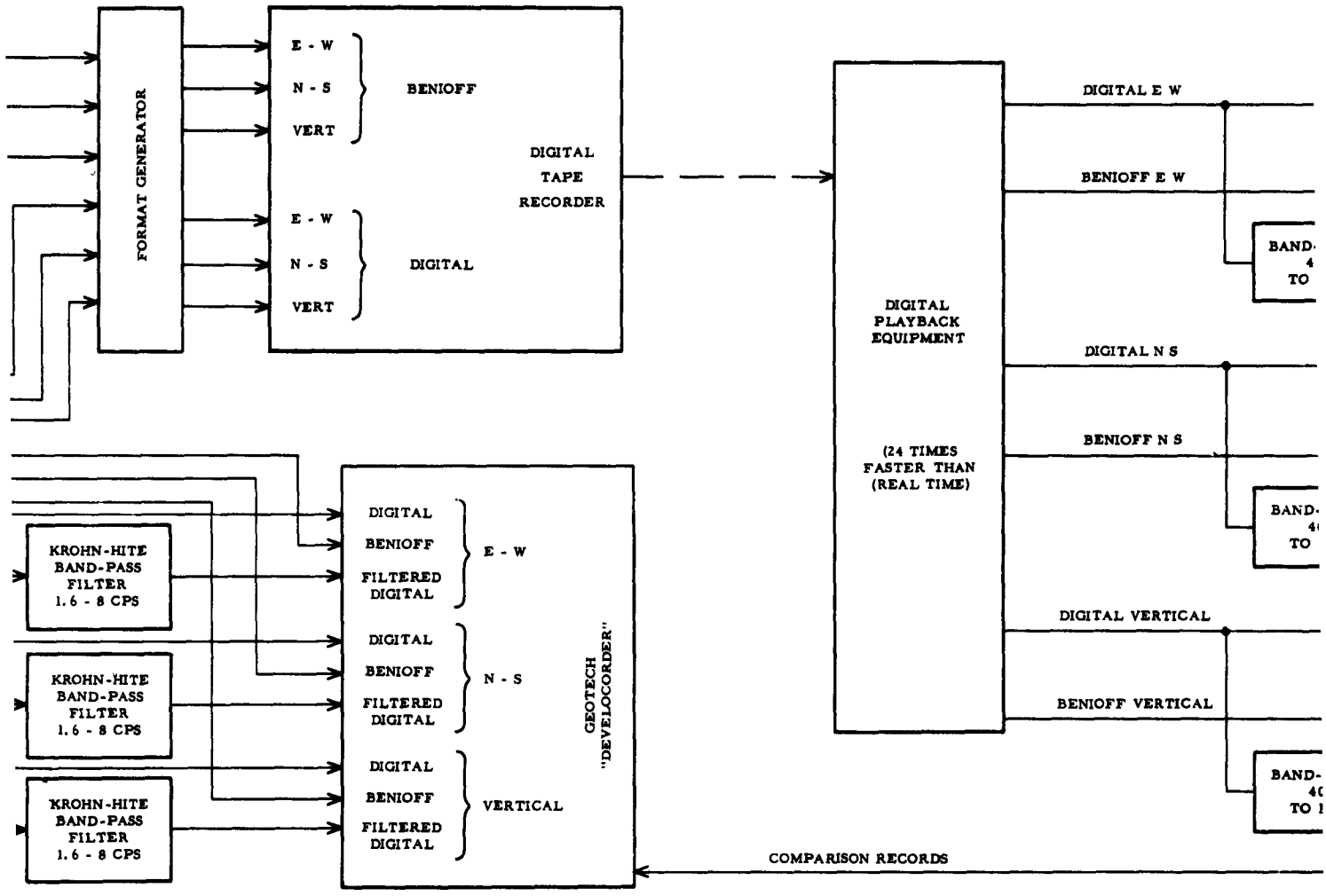

2

Figure 44. Experimen

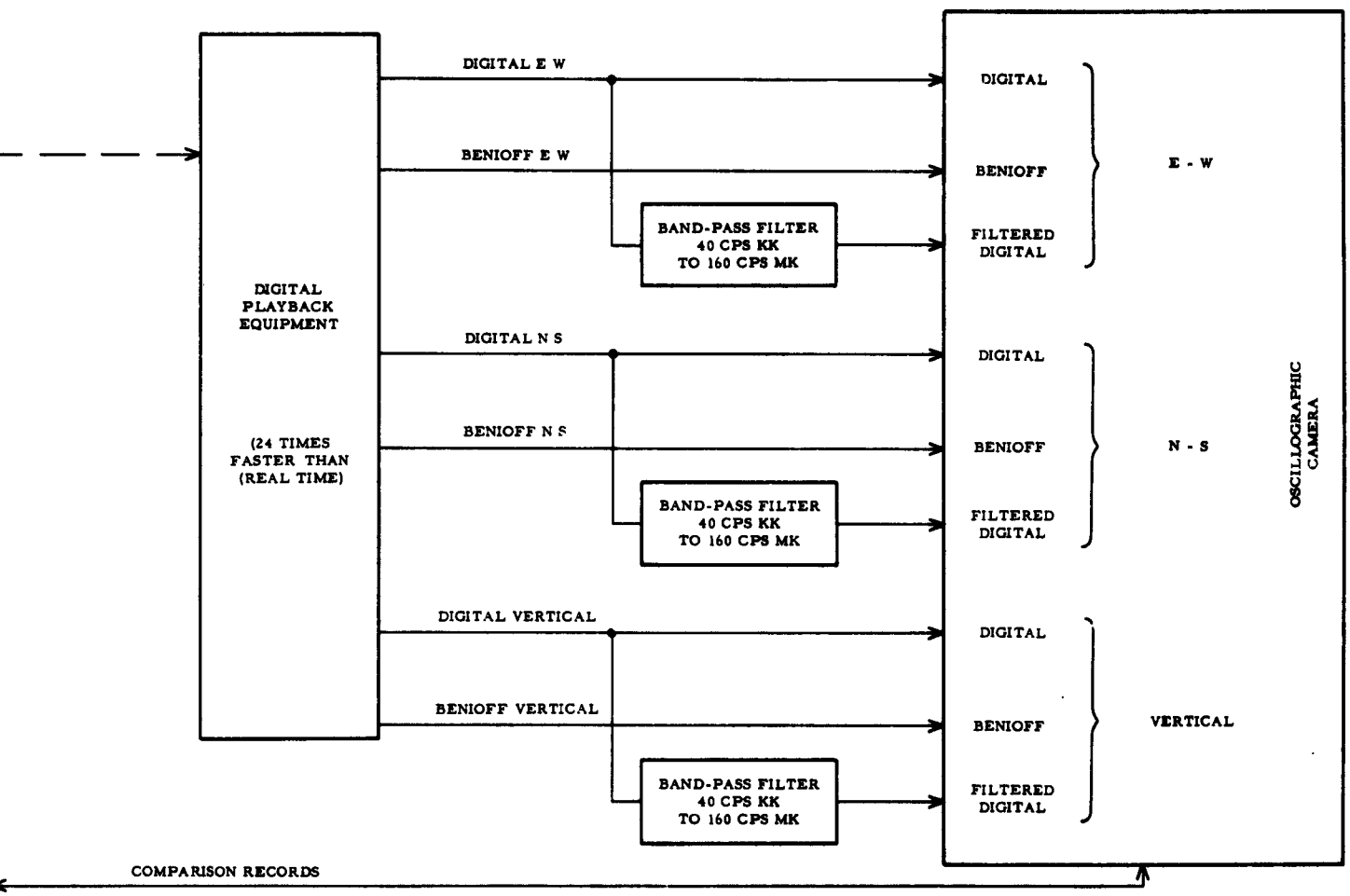

Figure 44: Experimental Set-up for Seismograph Evaluation

Real-time analog recording was made on a Geotech "Develocorder." In addition to the timing marker, nine signals were recorded. Each of the three seismic components was recorded under three conditions. The upper trace of each component group is the straight unfiltered digital seismometer output. The middle trace is the output from the photo-tube amplifier, which is driven by a one-cycle-per-second period Benioff seismometer. The bottom trace of each group is the filtered digital seismometer signal. A section of this record is shown in Figure 45.

While analog recordings are being made, a digital tape recording also is being made of the three digital seismometer outputs and the three Benioff outputs. The Benioff outputs are digitized separately in a 14-bit analog-to-digital converter which is compatible with the digital seismograph tape format. No filtering is used on either group.

The digital tape thus generated is played back on similar equipment at 24 times real time. The six analog outputs from the playback equipment are fed to a multi-trace oscillographic camera. In addition, the three digital seismometer outputs are carried through a filter bank to form a third set of outputs. These bandpass filters are set up to approximate the Krohn-Hite filters used in the real-time filtering for the analog recording. The low end of the pass band is a double section constant-K filter set to cut at 40 cycles per second. This is equivalent to about $\frac{40}{24}$ or 1.7 cycles per second. The high end is cut off with an M-derived section followed by a constant-K filter set to 160 cycles per second. This is equivalent to about 6.7 cycles per second in real time.

These three groups of three traces each were set up in the same pattern as in the analog recording. This recording is shown in Figure 46 and represents the same real-time period as the analog recording, Figure 47.

This comparison is judged to be satisfactory, since analog filters are used. By the use of digital filtering it is possible to "map" the broad-band digital data into the equivalent several different narrow-band seismometer systems. The research approach for this work is outlined in Appendix H.

D. MECHANICAL FILTER EVALUATION

The frequency response of a digital seismograph system is of greater interest than the response of an analog-type seismograph. This is due to the high resolution and therefore the possibility of aliasing signal distortion near the sampling frequency. It is particularly important to know the exact response of the developed system, because of the new method being used to eliminate the seismic frequencies above 10 cycles per second.

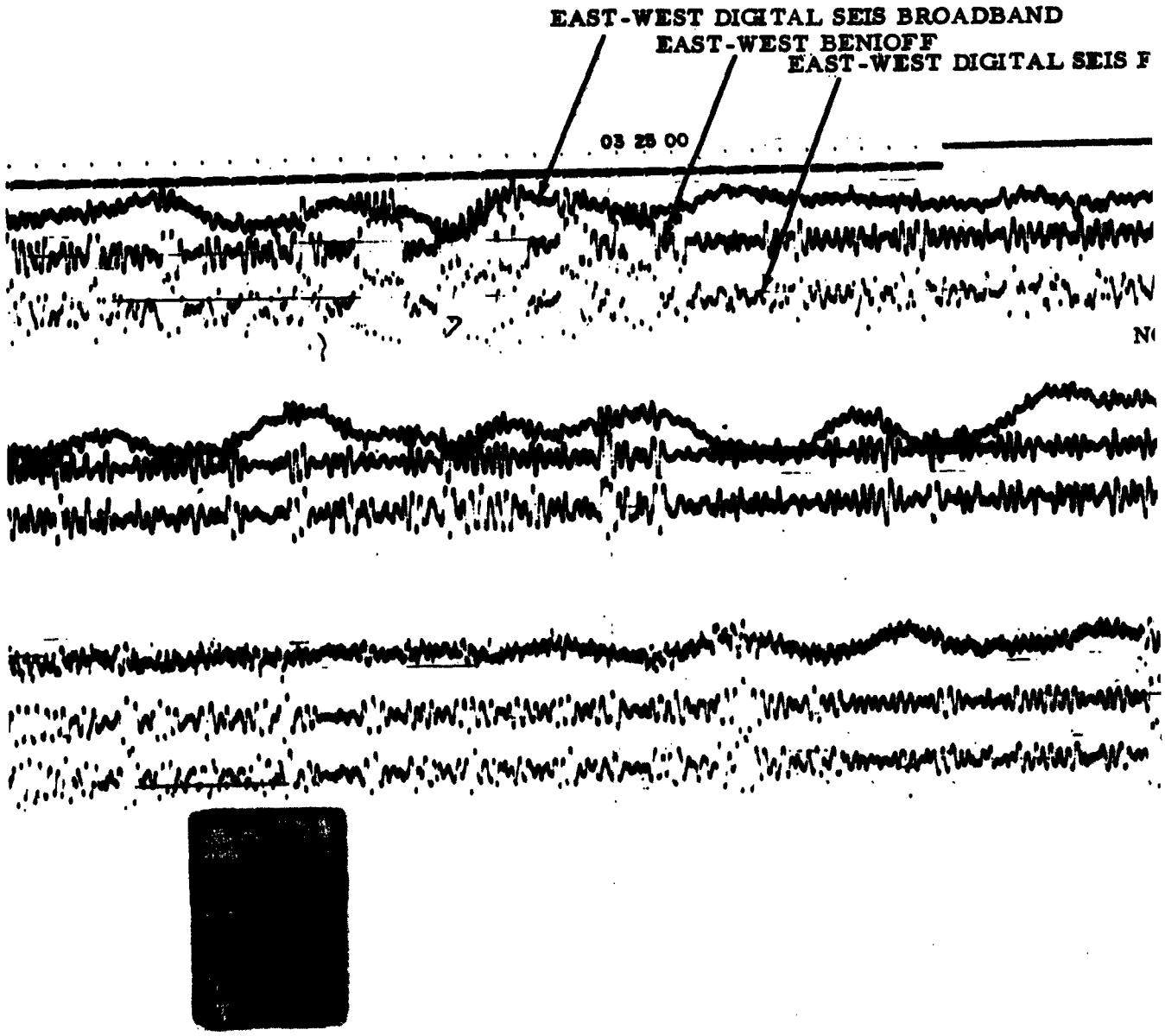
EAST-WEST DIGITAL SEIS BROADBAND
EAST-WEST BENIOFF
EAST-WEST DIGITAL SEIS F
03 25 00

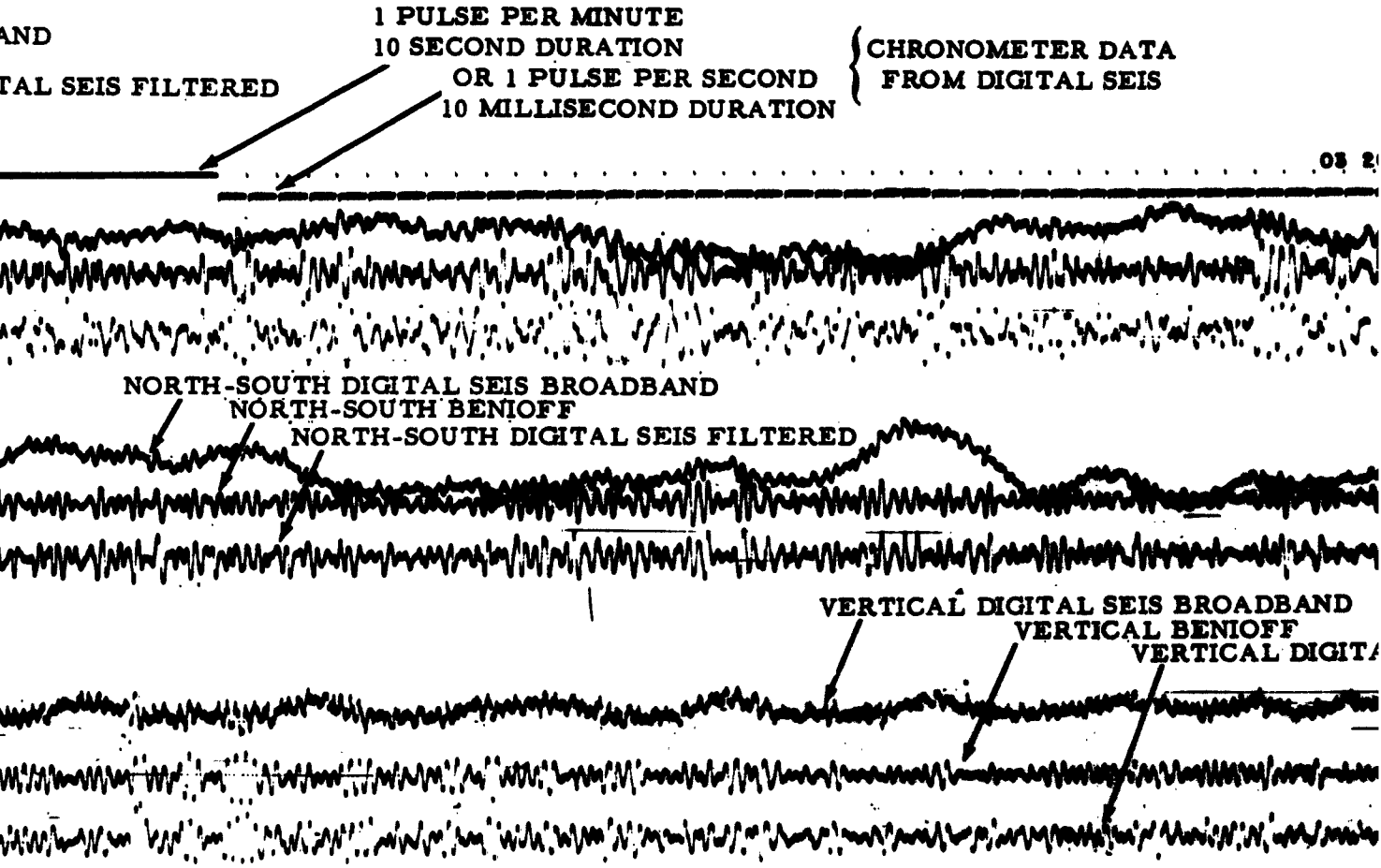

Figure 45. Analog Comparison of Benioff and Digital Sei

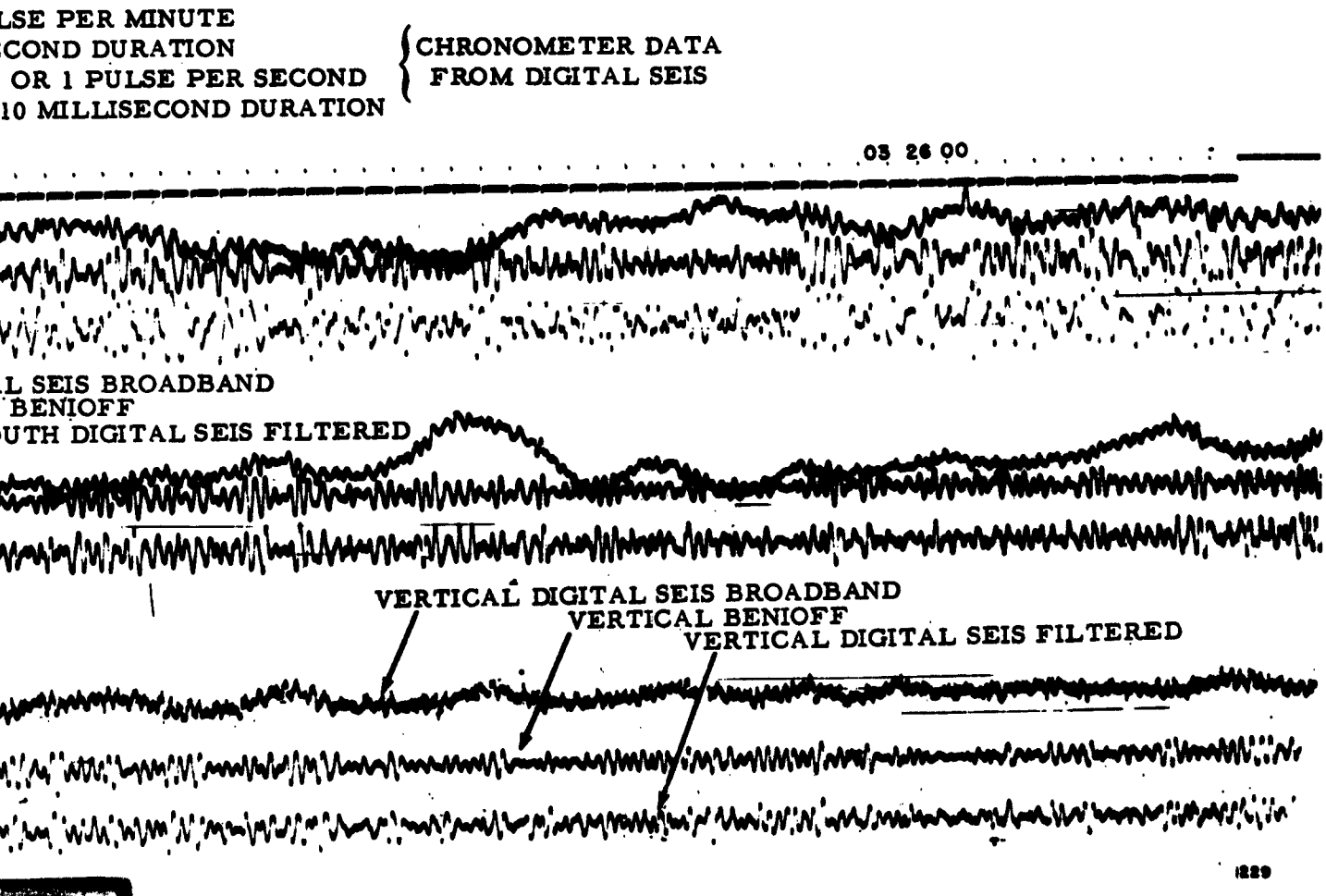

Figure 45. Analog Comparison of Benioff and Digital Seismograph Records

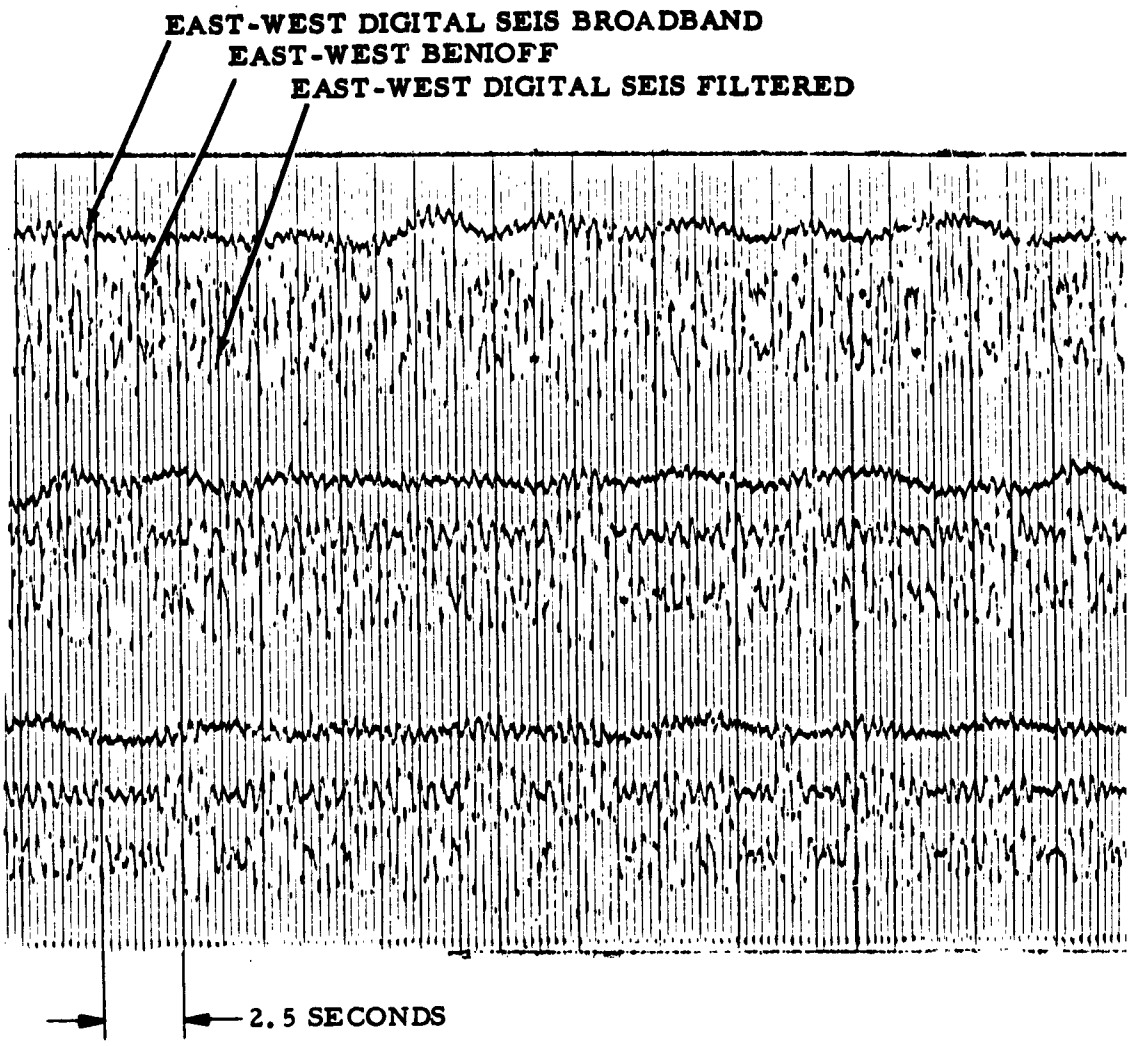
EAST-WEST DIGITAL SEIS BROADBAND
EAST-WEST BENIOFF
EAST-WEST DIGITAL SEIS FILTERED
2.5 SECONDS

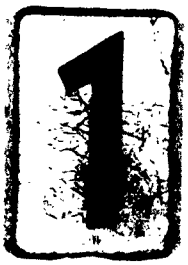

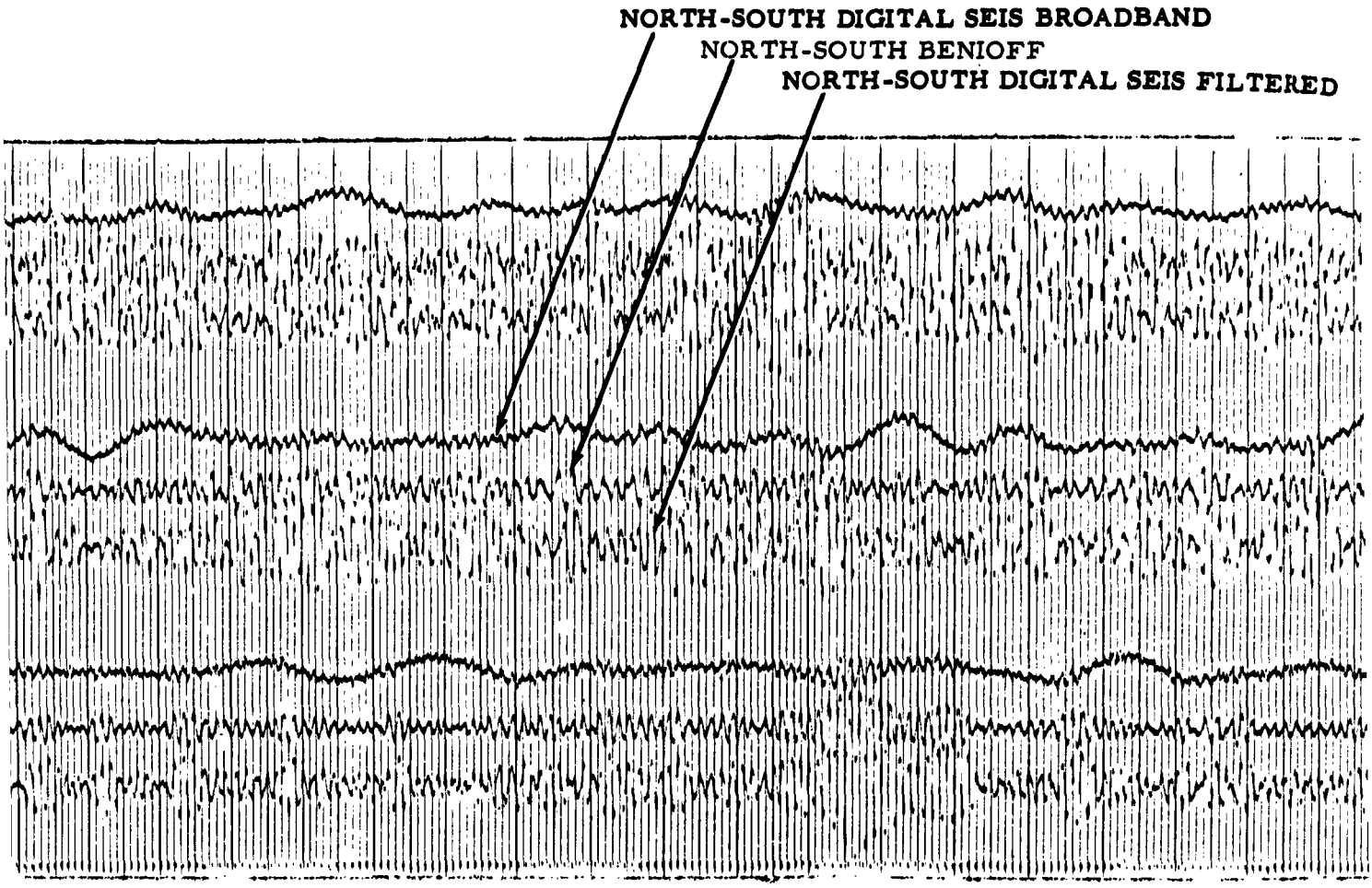
NORTH-SOUTH DIGITAL SEIS BROADBAND
NORTH-SOUTH BENIOFF
NORTH-SOUTH DIGITAL SEIS FILTERED

2

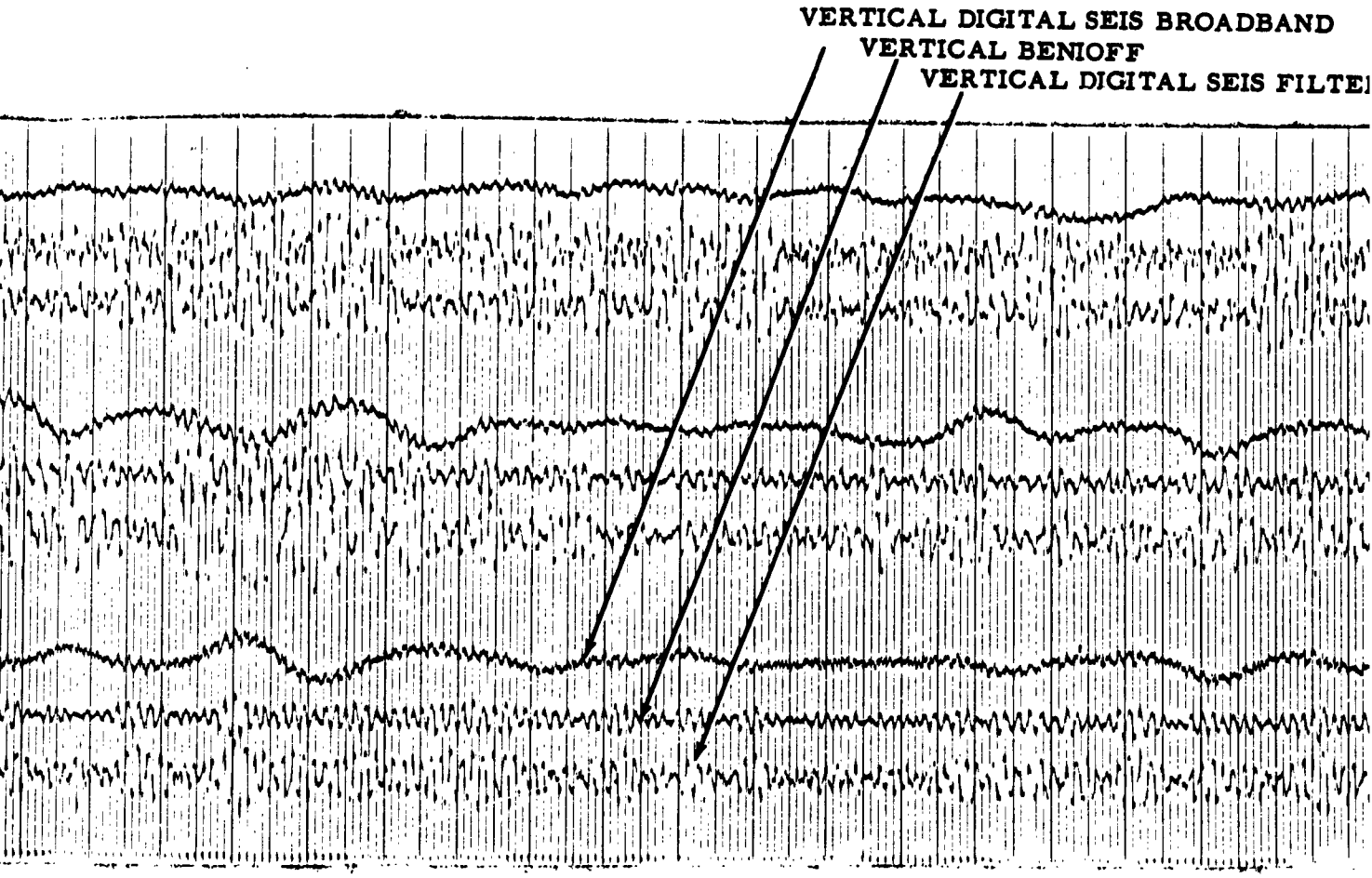

3

Figure 46. Digital Playback Comparison R

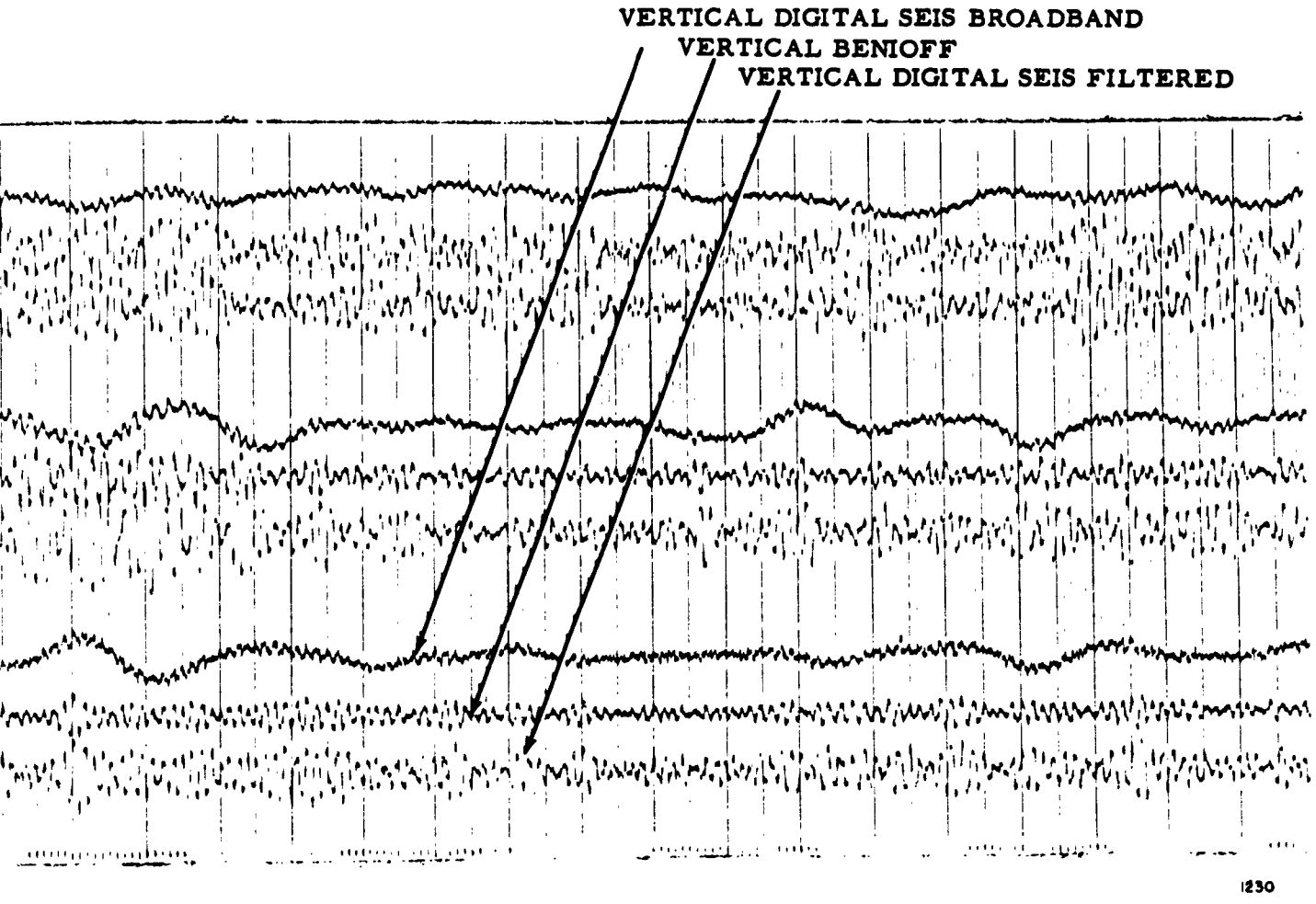

4

Figure 46. Digital Playback Comparison Record

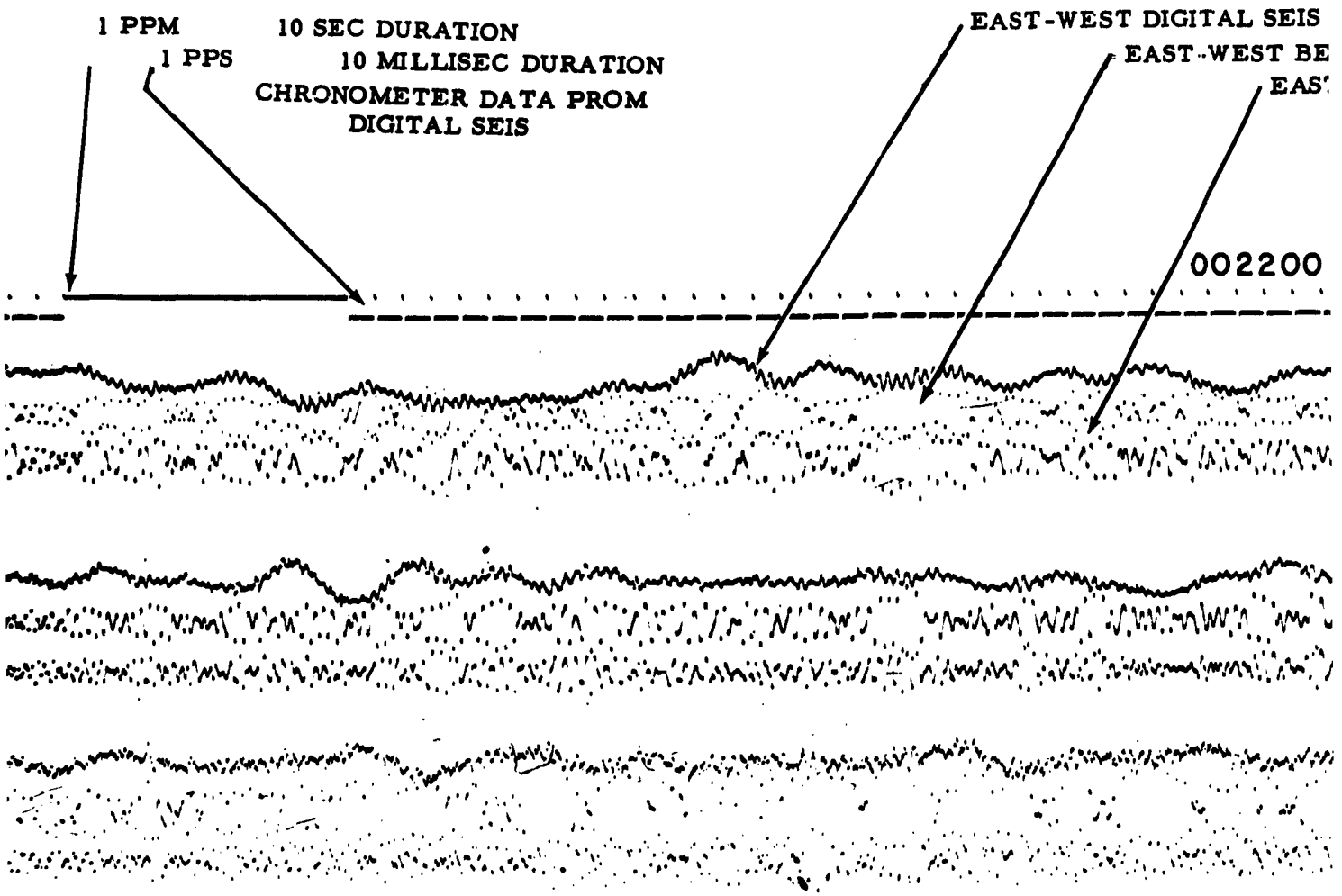
1 PPM
1 PPS
10 SEC DURATION
10 MILLISEC DURATION
CHRONOMETER DATA PROM
DIGITAL SEIS
EAST-WEST DIGITAL SEIS
EAST-WEST BE
EAS
002200

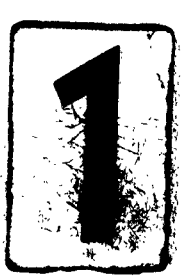

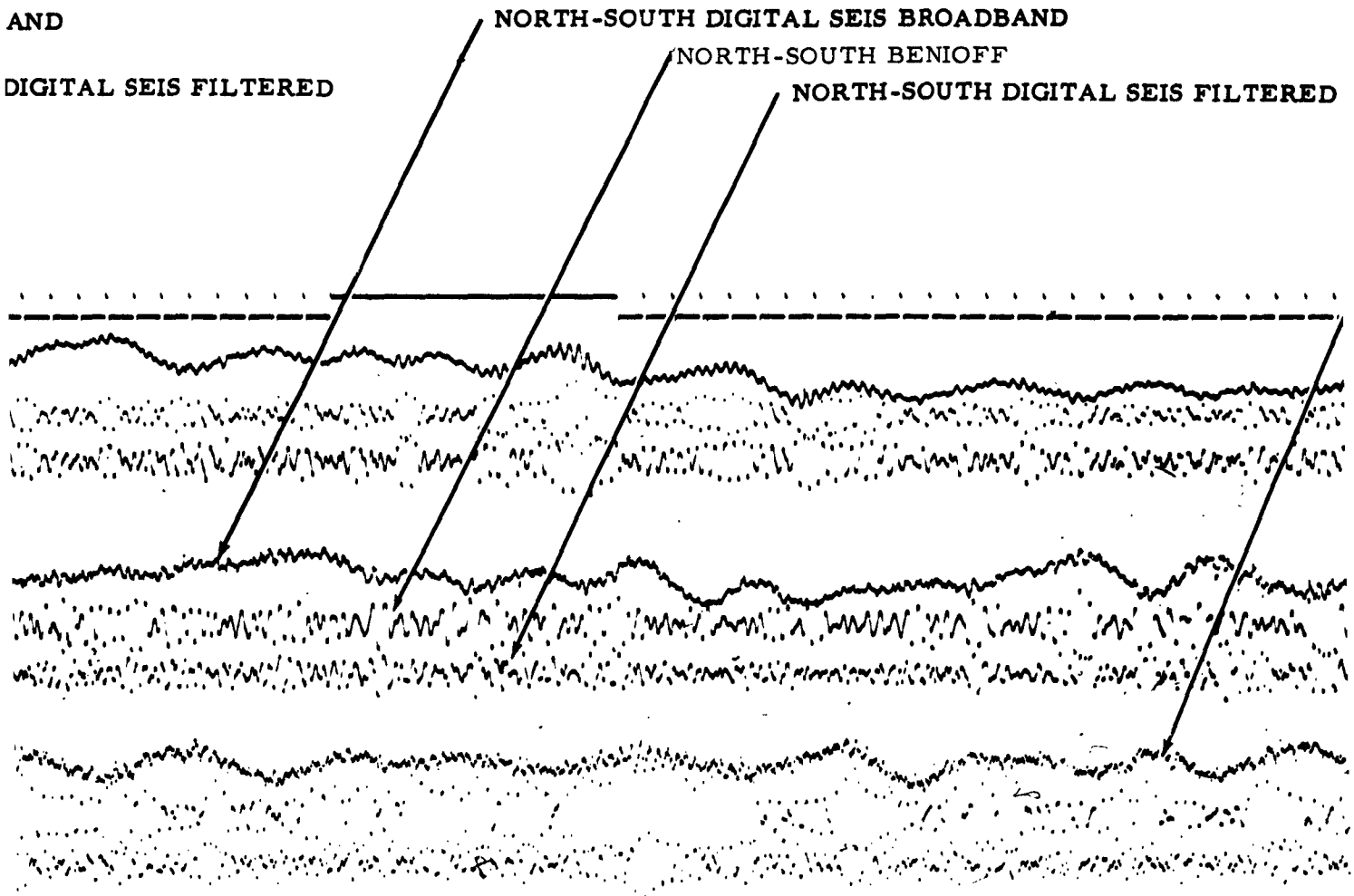
AND
DIGITAL SEIS FILTERED
NORTH-SOUTH DIGITAL SEIS BROADBAND
NORTH-SOUTH BENIOFF
NORTH-SOUTH DIGITAL SEIS FILTERED

2

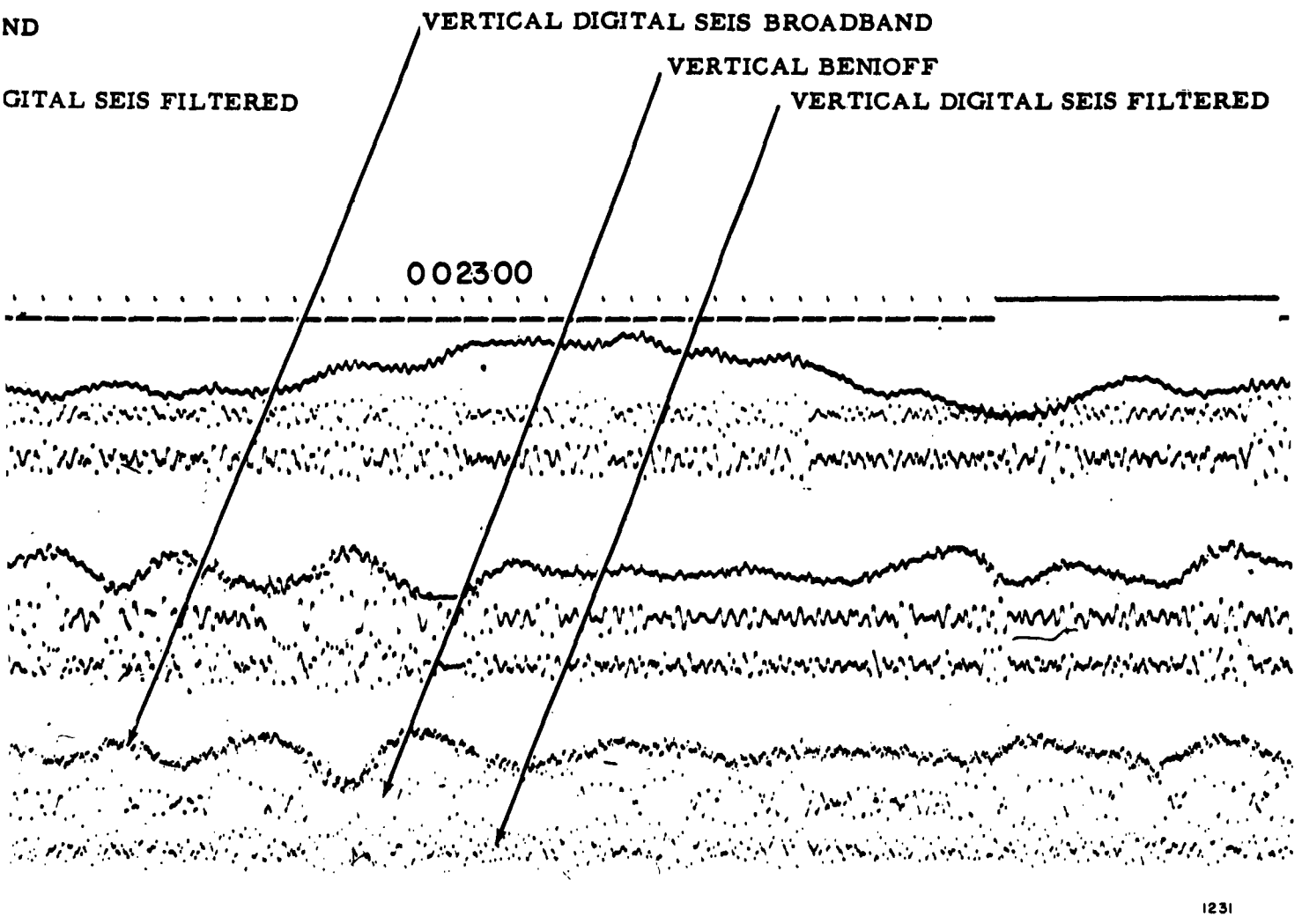

Figure 47. Analog Comparison Record

3

Specifically, inclusion of a mechanical filter to control the system frequency response requires actual movement of the seismometer for testing.

The horizontal shake table designed for the evaluation of the mechanical filter and complete seismometer consists of a moving table 11 x 15 inches supported by three vertically mounted steel leaf springs. Driving force is provided by a loudspeaker driving unit mounted on the base plate. The driver is fed by a transistor amplifier capable of supplying about three watts power.

Calibration of the table movement is accomplished with a microscope of 100 times magnification focused on a microscope stage micrometer slide mounted on the table. Amplitude reading accuracies of about 2 microns are possible when sighting through a crosshair onto slides with 10-micron divisions. At frequencies above several cycles per second, a strobe light is used to read the moving scale.

In operation, the Millis-Romberg seismometer is placed on the table. After leveling and stabilizing the seismometer, the table is driven through the desired frequency range.

At each test frequency the driver amplifier gain is adjusted to maintain a fixed amplitude of table movement. Output of the seismometer then becomes a direct plot versus frequency at constant amplitude.

With a sufficiently large coupling capacitor from the driving oscillator, the table may be driven down to 0.1 cycles per second. The resonant frequency of the table when loaded with the Millis-Romberg seismometer is about 35 cycles per second, which allows satisfactory operation to about 20 or 25 cycles per second.

The shake table was used for tests to determine the frequency characteristics of the mechanical filter for the horizontal spring-mass systems. The results show the response to be 15 db down at 20 cps with an effective cut-off at 10.5 cps.

SECTION IV

CONCLUSIONS

The effectiveness of any new tool in science depends on the intelligent use of that tool. The digital seismograph system can be properly exploited only by developing new techniques in analysis which require the large dynamic range available in this system. By the use of digital computers and a recording system having a dynamic range of 1 million to 1 with broad-band frequency content, it is estimated that new seismological analysis techniques for nuclear blast detection can be derived. It is for this reason that the system should be exploited to its utmost.

Certain advances in the seismological art are now possible because of the capabilities of the Digital Seismograph System. It is now quite feasible to telemeter seismic data, in broad band and with wide dynamic range, over distances of thousands of miles. This cannot be done with analog systems, because of inherent transmission problems. It cannot be done with most "digital seismometer systems" because they do not have the advanced capabilities of the Digital Seismograph System described below.

Another possible extension of the art relates directly to the basic VELA UNIFORM problem. This is direct computer identification of explosions and earthquakes. This possibility exists only because of the broad frequency band and wide dynamic range of the Digital Seismograph System. If an explosion can be identified and if an earthquake can be identified, there should be certain characteristics -- such as frequency content, first motion, power envelope, etc. -- which could, if properly handled, be placed into the memory of a computer. The output of the seismograph could then be fed directly into the computer and the signals compared with the stored signals. If there is correlation with either stored signal, identification is established. Of course, this has not been done but with this new tool it is closer to realization.

The completed digital seismometer system has been demonstrated to be equivalent to the conventional Benioff seismometers. This demonstration illustrated the equivalent of an unfiltered Benioff output with the digital seismometer output subjected to an analog filter. That is, the digital output was converted back to an analog signal and passed through an analog filter with the appropriate band pass to simulate the Benioff output. It is estimated that only 10 to 12 bits of resolution are required for this demonstration. An obvious extension of the analog experiment is digital filtering to simulate response of several narrow-band systems with recordings at the same location as the digital seismometer system. This can be implemented by deriving the response of the digital seismometer and Benioff systems with

a large sample of data. An analytical relation can be determined to map the digital seismometer output into the narrow-band systems as discussed in Appendix H. This work is the recommended initiation of the computer analysis of the system. Other factors such as dynamic range, linearity, and frequency response should also be determined in a precise manner by computer analysis of the appropriate test experiments as outlined in the proposed evaluation phase of this contract.

In conclusion, a digital seismograph system has been developed with the following properties:

1. A dynamic range of 120 db or 1 million to 1.
2. Broad-band frequency recording from 10 seconds to 10 cycles per second.
3. Special design of band-pass filters for cut-off of 18 db per octave below frequencies corresponding to a period of 40 seconds.
4. Filter cut-off of 18 db per octave above frequencies of 10 cycles per second.
5. A unique closed-loop boom centering system which results in boom centering for frequencies below approximately 40 seconds. Such data as moon tides can be recorded from the correction voltage for boom centering.
6. A new horizontal seismometer designed to provide complete system capability with the FM-digital approach for digitizing.
7. A unique method of analog presentation which results in complete systems monitoring from the seismometer through the digital translation equipment. This is unique to any digital seismometer system currently being evaluated.
8. A magnetic tape recording subsystem for system evaluation which allows the digital seismograph system data to be compared with conventional seismometer data recorded through 14 bit analog-to-digital converters with all information in the same data block and compatible with the Texas Instruments TIAC digital computer.

It is highly advantageous to exploit this new seismological tool for the development of new seismological nuclear blast detection techniques. However, before this is feasible, the new system must be evaluated by utilizing digital computers for analyzing the data produced by the system.

APPENDIX A

SYSTEM ENGINEERING CONSIDERATION

Such values as dynamic range, frequency response, and resolution specifications data are required for instrumentation design. For a seismometer, the basic unit of measurement can be displacement, velocity, or acceleration of the earth motion. To consider specifications we must examine such information as typical amplitudes, power spectrum of the signal, and power spectrum of the noise.

A. SIGNAL AND NOISE POWER SPECTRA

Power spectra of seismic signals and noise are of value in a study of the mode of sensing. The advantages and disadvantages of displacement, velocity, and acceleration sensing are derived from this type of study.

Noise in the range from 0.1 to 10 cps may be categorized as follows:

1) Ambient microseism noise.

2) Relatively coherent, often intermittent noise from nearby sources.

3) Local wind noise, and other locally induced "random" noise.

4) Cultural noise such as highway traffic, railroads, machinery, etc.

5) Instrumental noise and pickup.

Brune and Oliver (1959)* presented a summary of published data on the level of ambient seismic noise, excluding wind noise and clearly local noise sources. Their study is shown in Figure A-1 and has been widely used as a basis for other studies since its publication. Figure A-2 is a plot of the average Brune and Oliver curve referenced to displacement, velocity, and acceleration.

* Brune, J. and Oliver, J., "Seismic Noise of the Earth's Surface," Bulletin Seismological Society of America, Vol. 49, No. 4, pp. 349-353, October, 1959.

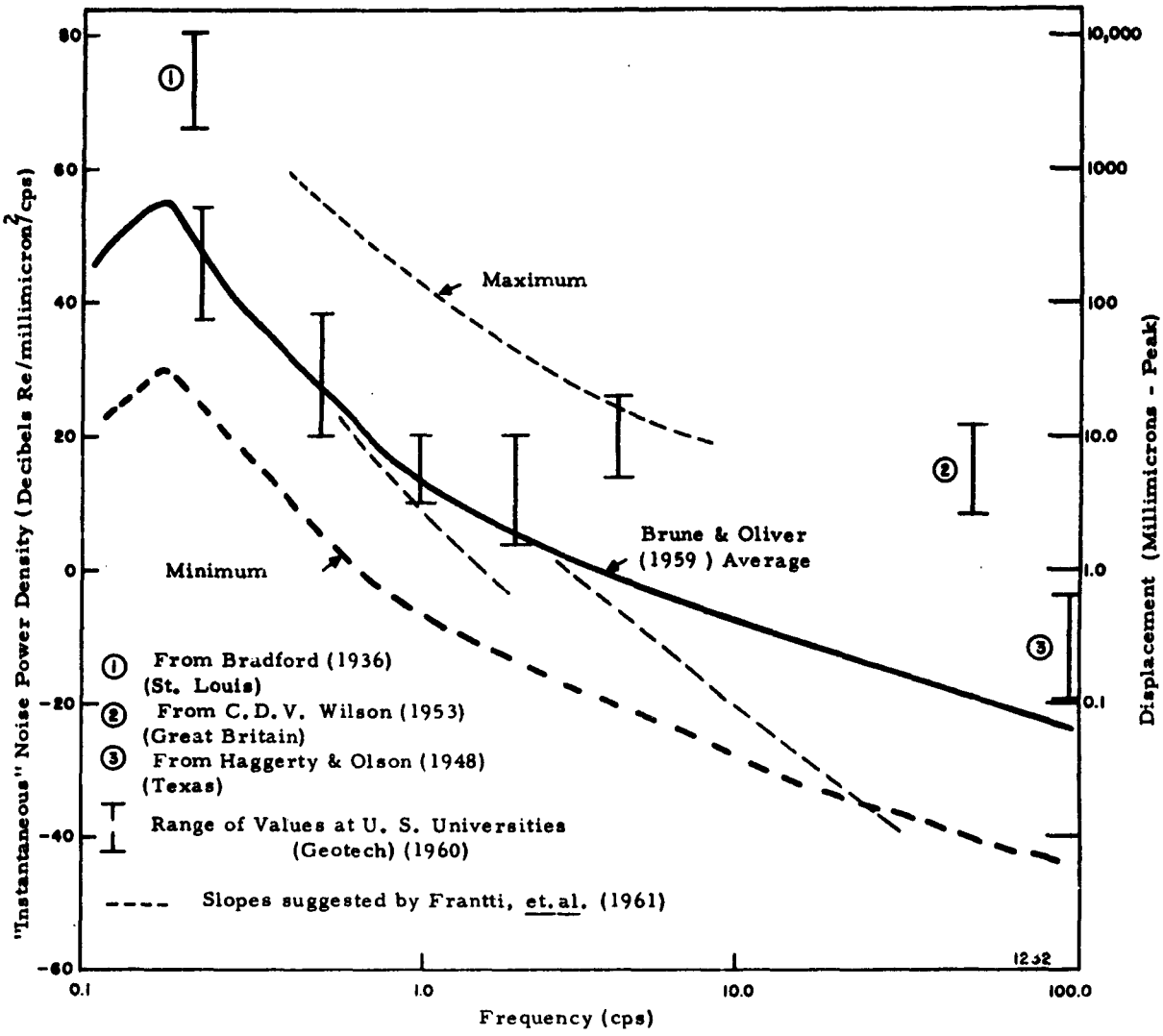

Figure A-1. Published Data of Ambient Noise at the Earth's Surface

If the power spectrum of the seismic signal is approximately the same as that of the noise, it is obvious from the curves presented that velocity sensing provides the best approach for pre-whitening the entire band of recorded data.

Power spectrum of the signal is difficult to define due to the ambiguity in the term, "signal". If we consider a broad-band seismic system, we are interested in recording three basic ranges of information.

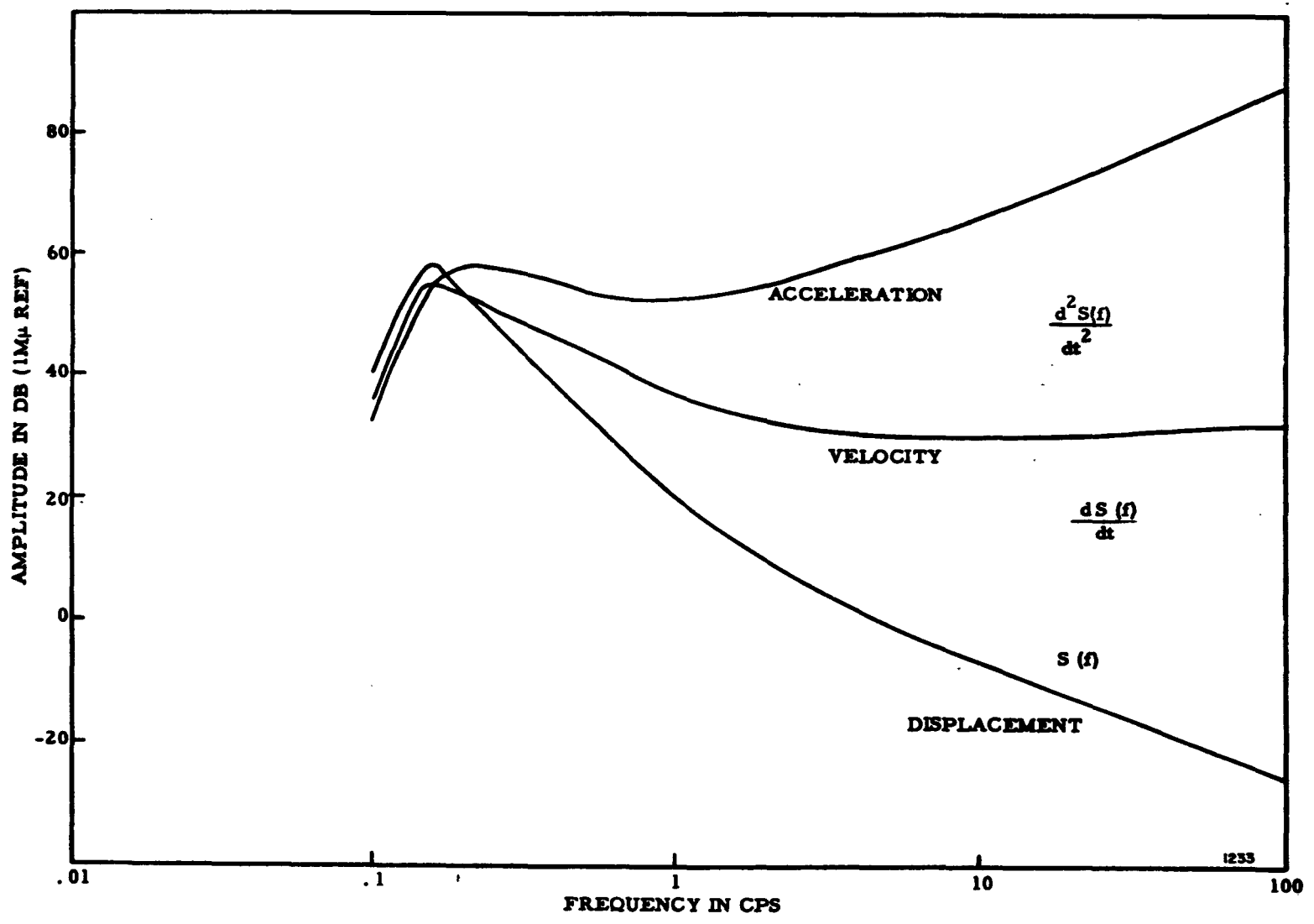

Figure A-2. Brune and Oliver Curve Referenced to Displacement, Velocities, and Acceleration

1) Low-frequency surface waves with periods of 30 seconds to 2 seconds.

2) The microseism range with periods of 4 seconds to 8 seconds.

3) First-arrival events, such as PN arrival, in the frequency range of 1 to 10 cps.

Because of the limited dynamic range of conventional seismic instruments, many narrow-band systems, each with a wide range of sensitivity, are required to cover the seismic spectrum. Figure A-3 shows response curves for typical narrow-band systems in conventional wide-band recording. Notice that the relative amplitude response of this group tends to approximate the Brune & Oliver curve.

B. SPECIFICATIONS OF A NEW SEISMOGRAPH SYSTEM

The purpose of this contract is the development of a digital seismic system. Digitizing alone is of minor significance if we are interested only in taking the output of the conventional narrow-band systems and formatting for digital computer input. Since the dynamic range of A-to-D converters is only approximately 13 bits (1 part in 8,000) we still have a relatively limited dynamic range. A logical extension of the use of conventional A-to-D converters is multichannel recordings with each channel handling a different range scale. By the use of 7 different scales with 6 db differences between them, digital data can be obtained over a 120 db range. If it is assumed that each range has 13 bits of resolution, the resolution is different for each scale as shown in Figure A-4. In addition to the variable resolution problem, a separate analog amplifier is required to drive each range of A-to-D conversion. The conclusion is that the conventional approach leaves much to be desired.

An extension of this approach is the use of logically controlled automatic scale switching at the input of a single analog amplifier which drives a single A-to-D converter. The setting of this range scale switch provides the binary floating point for scaling the 13 bits through the entire 20 bits of dynamic range. A description of actual equipment which was designed utilizing this approach is described in detail in Appendix E. This is a somewhat more sophisticated approach, but the variable resolution factor is still an inherent feature.

To provide a system which goes beyond the conventional A-to-D converter approach, consider the idealized specifications.

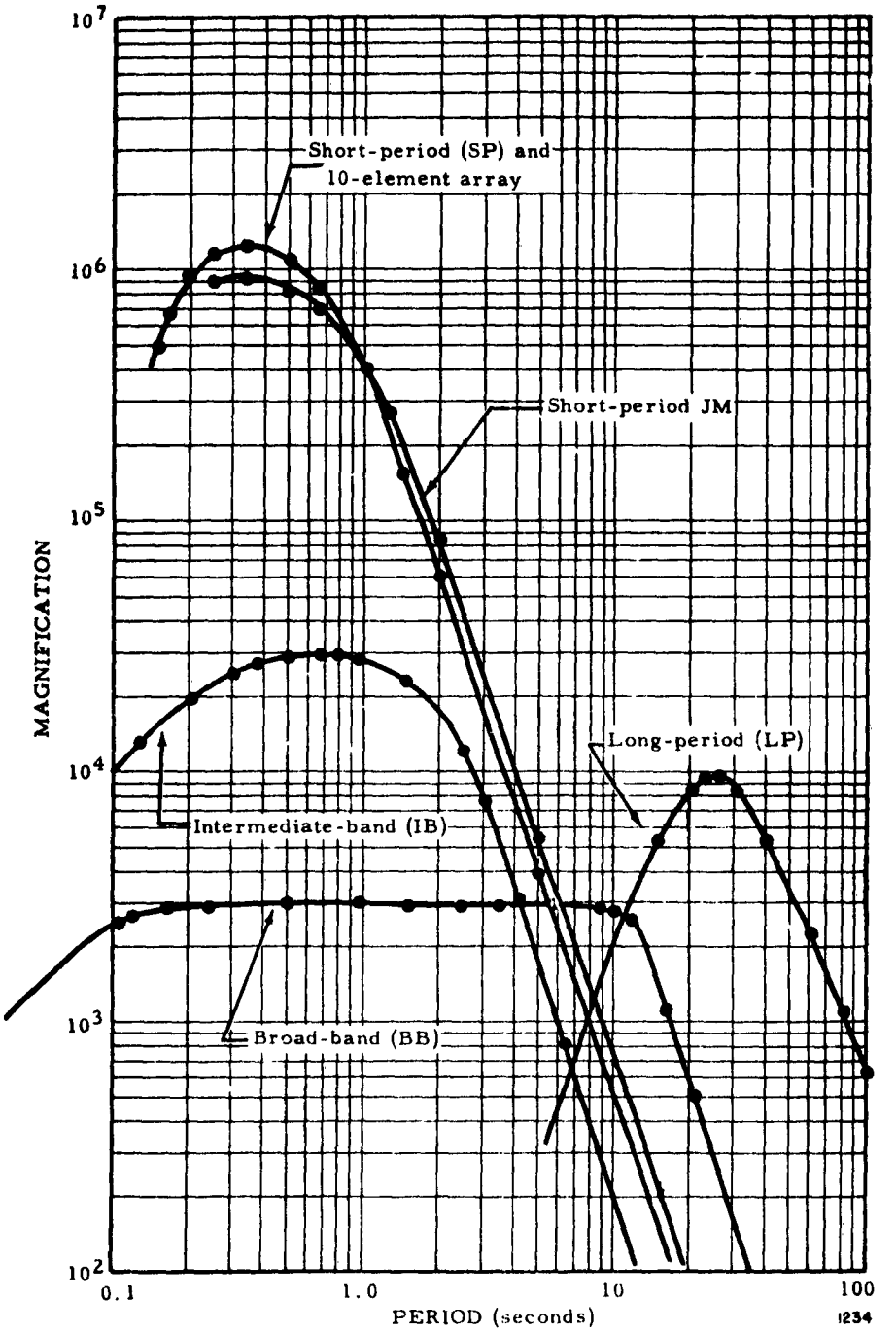

Figure A-3. Response Characteristics of Seismographs

1) Broad band recording from 0.1 to 10 cps (the 0.1 should possibly be extended to 0.03 cps).

2) A dynamic range of a million to one (120 db or 20 binary bits).

3) Constant resolution.

4) Velocity sensing.

The approach being used in the engineering and fabrication phase fulfills most of these specifications. The specifications can be met with the exception of the substitution of displacement sensing for the

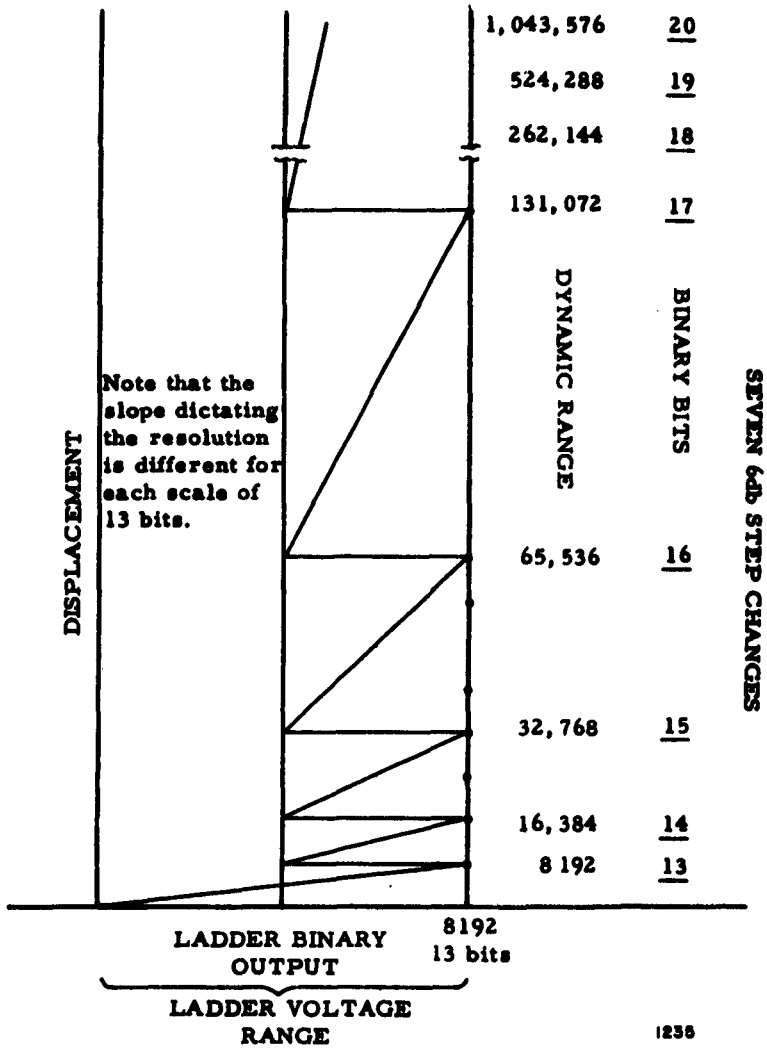

Figure A-4. Analog-to-Digital Converter Concept

idealized velocity sensing. The approach which has been chosen is not original. It has been used in several experimental systems during the past 10 years. The most recent practical exploitation of the sensing method is that of the Rice University seismograph system, designed by Dr. J. Cl. De Bremaecker. It consists of a differential-capacity displacement sensor. Each of two capacitor plates controls the frequency of an oscillator. Mixing of the two oscillator outputs furnishes a broad-band FM signal proportional to the displacement of the seismometer boom. Counting the FM pulses for a specific period of time generates the digitized binary number proportional to displacement. Even though this approach is relatively simple in principle, engineering the approach into a practical system requires several advancements in the state of the art. The required advancements are the subject of this contract.

C. SAMPLING-SYSTEM PROBLEMS

A primary consideration in reading any function as a serial sequence of sampled quantized amplitudes, spaced evenly in time, is the problem of the generation of aliasing error. If it is assumed that the highest frequency of interest is 10 cps, sampled-system theory states that the function must be sampled or read at a minimum rate of 20 cps. With a 20-cps sampling rate, the folding point for aliased or error fold-back is 10 cps. Therefore, any amplitudes of frequency components above the fold-over point of 10 cps will generate an error in the 0 to 10-cps range of interest. If the power spectrum of the data was flat up to frequencies higher than 10 cps, and 20 bits of accuracy are required, a flat system response would be required up to 10 cps, and all frequencies above 10 cps should be attenuated by 120 db. A system of this type is obviously impossible from a practical design standpoint.

A practical system, therefore, utilizes a quantitizing sample rate in the range of 2 to 5 times the highest frequency of interest in the function. Sampling at a rate of 40 cps or 4 times the highest frequency of interest has been chosen for the digital seismograph work. An aliasing or low-pass filter should therefore be utilized to reject frequencies above 20 cps, the fold-over frequency.

An aliasing filter for the FM system utilizes a binary counter for summing or integrating the total number of pulses generated by the displacement sensor within a specific period of time. Integration for a specific period of time is equivalent to a low-pass filter with the following characteristics.

$$A(f) = \frac{\int_0^T \sin \omega t \, dt}{\sin \omega \frac{T}{2}} \qquad (A-1)$$

where

$A(f)$ = Amplitude response of the filter

T = time interval of counting

$\omega = 2\pi f$

f = frequency of the function or the frequency deviation

This merely states that the output of the filter for a specific frequency of the input function is proportional to the integrated value of the frequency for the gated time period divided or referenced to the actual value of the function of one half the gate time. A plot of the function shows a notch or zero value for all frequencies which are integrated for an integral number of cycles. Figure A-5 shows this curve with comparison to a typical analog filter curve. Notice the fall-off of the peaks of the curve at 6 db per octave. This is obviously a poor aliasing filter. Two additional filters could provide an additional 24-db-per-octave attenuation. A total resultant 30 db per octave results. Mechanical filtering provides 12 db per octave. A closed-loop filter of 12 db per octave in an Automatic Frequency Control (AFC) loop could furnish the remaining 12 db per octave.

With this combination of low-pass filtering at 10 cps cut-off, the system is satisfactory. The remaining decrease in aliased frequency components can be attributed to the decrease in power spectrum of noise with increasing frequency.

D. DATA-HANDLING CONSIDERATIONS

To provide a significant digital seismograph system, the entire data-handling system must be considered. Figure A-6 illustrates a generalized concept for digital data handling. If the characteristics of the seismometer sensors are such that they do not have to generate appreciable power, the spring-mass system can be miniaturized. All sensors which have been considered in this R&D program are power-partitioning sensors. External power is furnished to the sensor and the boom of the spring-mass system merely modulates the applied power. The digital seismometer problem therefore includes research considerations for the spring-mass system as well as the digital sensors.

Digital output from the sensors is multiplexed, converted to a 20-bit binary number in the digital converter system, then formatted and stored on magnetic tape.

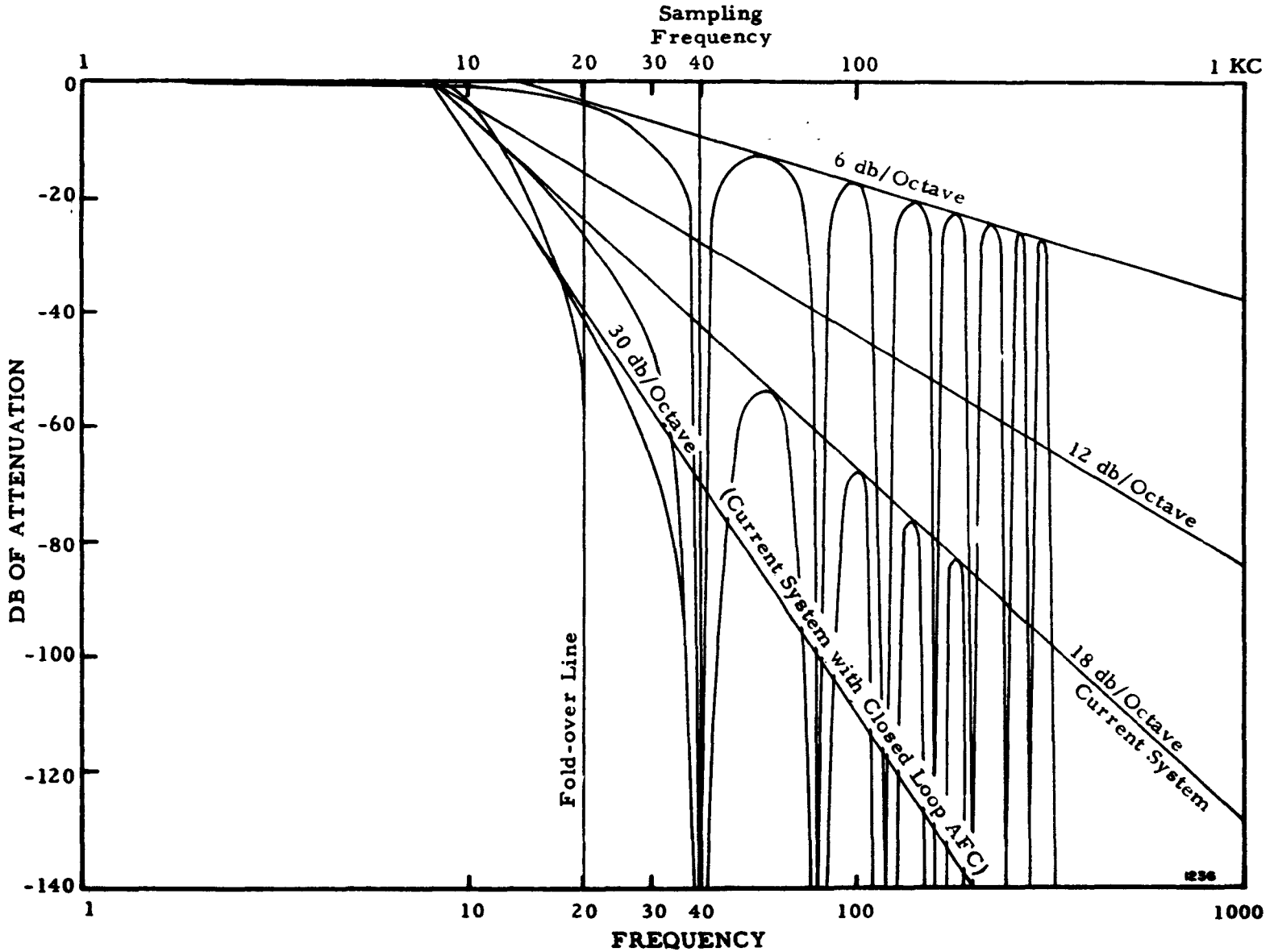

Figure A-5. Digital Aliasing Filter Compared with Typical Analog and 12 db/Octave Filters

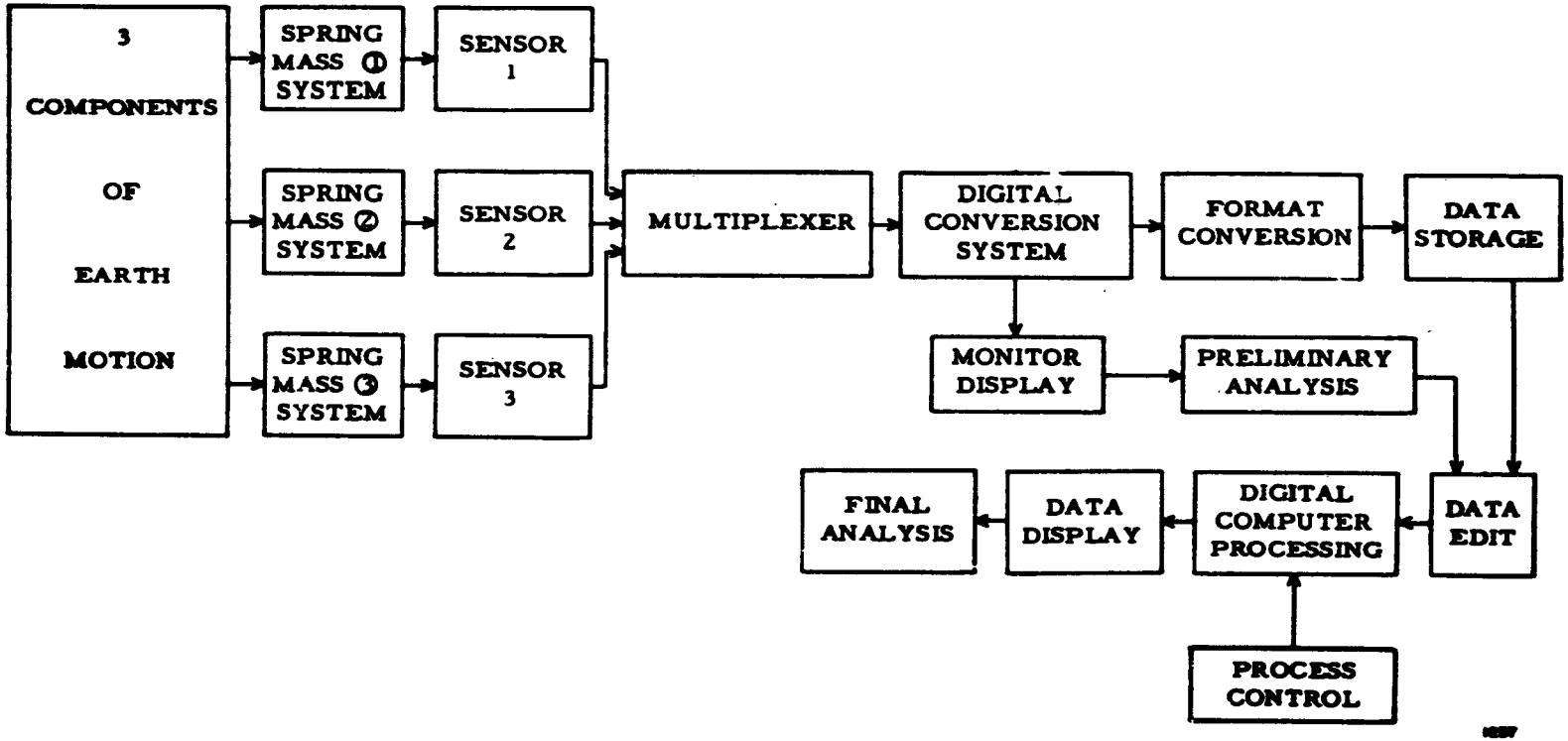

Figure A-6. Generalized Concept for Digital Data Handling

The analog monitor display, with the appropriate digital-to-analog converters, should be connected as close to the output of the digital seismometer system as is practicable. Two features of the monitor display are monitoring of the entire digital system and presenting data for preliminary analysis. Preliminary analysis is used for editing the digitally stored magnetic tape before computer processing.

With the exception of the digital system evaluation; the digital computer processing, program control, computer data display, and final analysis were not considered to be within the scope of this contract.

Ultimate formatting should be compatible with commercial digital computers, especially those associated with VELA UNIFORM Central Computer Center. This requires IBM-compatible magnetic tape for straight binary recording mode. Compatibility should be provided with such computers as the IBM 7090 and the CDC 1604. To conserve magnetic tape the higher packing density of approximately 556 bits per inch should be used. One-half-inch-wide magnetic tape with character serial recording for 6 straight binary bits per character, plus parity, is used.

Normal formatting requires the 3/4-inch inter-record gaps for computer program control and other reasons. Each serial grouping of characters is followed by a longitudinal parity character. Generation of inter-record gaps at the seismometer station requires complex buffering equipment. Because of this equipment complexity, two format tape recording systems are under consideration.

The first system employs recording of all data in binary serial form on a single track of a tape recorder. Word data from the three sensors would be multiplexed in a serial form on this track. This permits an extremely simple tape recording system at the seismometer station. Three auxiliary tracks would also be used: (1) block pulse data to identify the grouping of sensor values, (2) clock pulse data for decoding purposes, and (3) possibly a voice track for miscellaneous information. Such data as real-time chronometer setting, seismometer location information, etc. are recorded in bit serial form as the magnetic tape heading. Four tracks of recording can be easily made on 1/4-inch-wide magnetic tape. Further reduction in tape requirements should be made by the use of relatively high bit-packing densities. Twenty-four hundred bits per inch is considered reasonable. If tape skew problems are intolerable between the data and adjacent clock track, the clock track can be removed. The playback clock for decoding would be generated by a phase lock from the signal data pulses. This system is commonly used in digital missile-telemetry systems. A discussion has been presented for a simple tape recording system at the

seismometer location. If this approach were used, a format converter is required at the computer center for formatting the special-purpose digital tape to the computer-acceptable digital tape with inter-record gaps. This format converter could be used at 30 to 50 times real time to serve many seismometer systems.

The second approach for tape formatting at the seismometer location requires recording data in computer-acceptable character-serial form. The only difference between this tape and computer-generated tape is the elimination of the inter-record gaps. One track of the 7 track tape would be reserved for block pulse identification. A relatively simple adapter is required to read this data into the IBM 7090.

APPENDIX B

AUTOMATIC FREQUENCY CONTROL FILTER DESIGN

Since it is not possible to filter the FM output from the seismometer sensor in the conventional manner to obtain the desired frequency spectrum, a method of cutting off the high-frequency response of the sensor system was investigated. This investigation was initiated by the aliasing problem as described in Appendix A of this report.

This method was not used in the final system because of technical problems encountered at the frequencies being used and the consideration of FM noise injection into the oscillators. A mechanical filter, described in Section II, C, 3 of the report was used instead to provide a 12-db/octave roll-off in response above 10 cps.

The basic idea is shown in Figure B-1. The difference frequency from the mixer is fed to a discriminator to obtain an analog output from the sensor. This signal is then passed through a high-pass filter (2 RC sections) and the resultant voltage used to operate a variable-capacity diode in the tank circuit of one oscillator.

The output from the discriminator is phased such that a change in mixer output frequency necessarily drives the controllable oscillator frequency in the direction tending to cancel the initial frequency variation. If the deviation frequency is appreciably below 10 cps, the discriminator voltage will not pass through the filter and thus will not affect the operation of the oscillator. If the deviation frequency is near 10 cps or higher, the filter will pass a signal which will tend to change the frequency of the oscillator in opposition to the original deviation. With a two-section RC filter, the sensor FM output response will fall about 12 db per octave above about 10 cps. Since this is a closed loop system, no faster fall-off in response is permissible or loop oscillation will result from excessive phase shift in the filter.

A breadboard mockup of an equivalent but simplified closed loop system was constructed. The schematic is shown in Figure B-2.

Referring to the schematic, the oscillator frequency is determined by the tank circuit which consists of a slug-tuned inductor and two voltage-variable capacitors. A battery and potentiometer are used to set the initial tuning of the tank circuit.

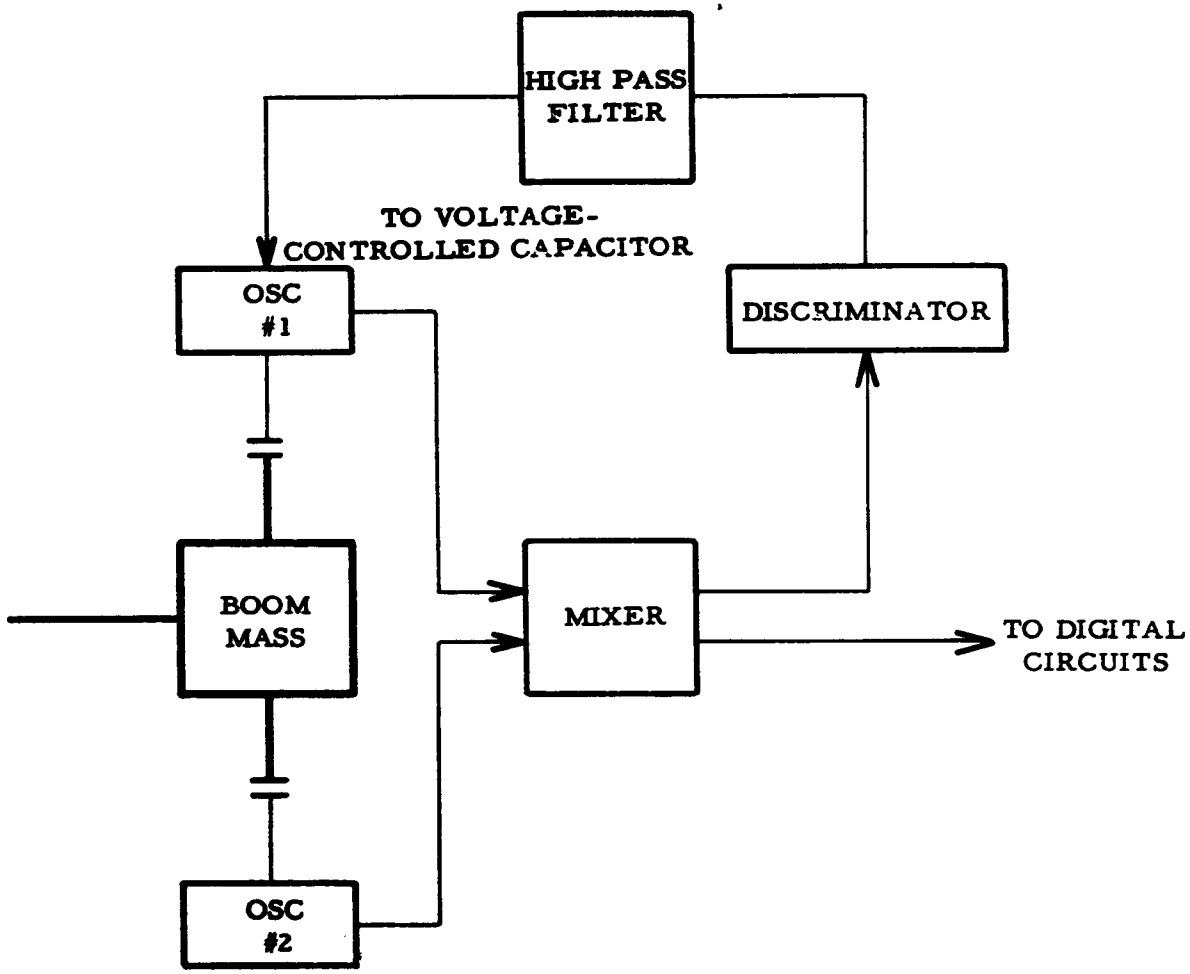

Figure B-1. AFC Aliasing Filter Block Diagram.

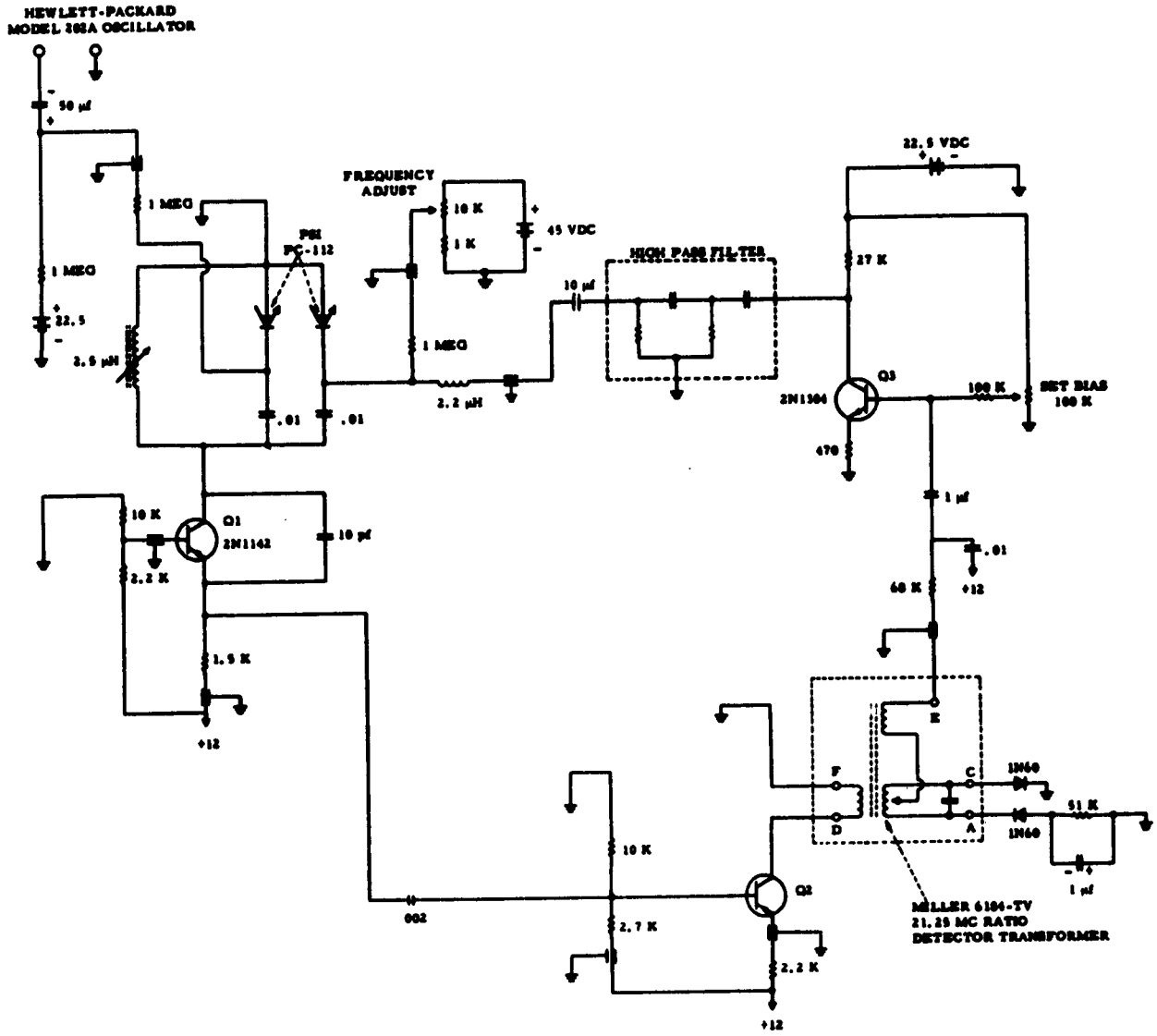

Figure B-2. Experimental Circuit for AFC Aliasing Filter.

The output of the oscillator feeds transistor Q2 which drives a 21.25-mc ratio detector. The output from this is amplified by transistor Q3. Q3 then drives one of the voltage-variable capacitors in the oscillator tank after passing through a high-pass filter.

A Hewlett-Packard 202A low-frequency oscillator is used to modulate the oscillator by means of the other voltage-variable capacitor and provide the FM equivalent of a sinusoidal seismic signal. The output of the ratio detector is monitored with an oscilloscope to determine the response of the system.

After initially setting the frequency of the circuit oscillator to 21.25 mc, the Hewlett-Packard oscillator is connected and set to provide an acceptable FM deviation at a frequency of 1 cycle per second. A frequency response curve is then run in the usual way.

The resulting response curve showed a slight peaking at about 6 cps, then a falling off at all higher frequencies. The filter was designed to make the response down 3 db at 10 cps. Above 10 cps the response falls off at the predicted 12 db per octave rate.

APPENDIX C

DISCUSSION OF OSCILLATING SYSTEMS FOR DETECTING EARTH MOTION

I. BASIC REQUIREMENTS

Sensors for detecting earth motion usually consist of a mass suspended in such a way that it may oscillate about a point of zero displacement with respect to the frame of the suspension. Earth motion can be measured if the frame is coupled to the ground and a device for recording the displacement is present. When the earth moves back and forth or up and down, as it does in an earthquake, the displacement of the suspended mass from its zero point will be a measure of the earth's motion, provided the period of the earth motion is substantially shorter than the natural oscillation period of the mass. In practice, motion sensors are always damped. In this discussion we shall ignore the damping since, while it affects the period to some extent, it is not necessary to the argument.

The simplest example of a suspended mass for measuring earth motion is the ordinary vertical pendulum. If the frame of the pendulum is moved back and forth, the displacement of the pendulum bob will be a measure of the horizontal component of earth's motion in the plane of oscillation of the pendulum. Another simple example is a weight suspended from a spring; this system measures the vertical component of earth motion. Both systems are useful for measuring earth movements whose periods are of the order of one second or less, but it is difficult to adapt them to movements with periods longer than a few seconds because they would have to be so large in size. From the well-known relation

$$t = 2\pi \sqrt{\frac{\ell}{g}} \qquad \text{(C-1)}$$

where t is the period of a pendulum, ℓ its length, and g the acceleration of gravity, a pendulum suited to recording waves with 20-second periods would have to be well over 100 meters long. The same relation, and the same conclusion, holds for the vertical-motion sensor, where ℓ is the extension of the spring.

II. LACOSTE SUSPENSION

Since in order to sense the surface waves of earthquakes the elementary oscillating devices would have to be made inordinately long, systems have been developed whose periods are independent of their size, at least in principle. For long-period vertical motion, a suspension described by LaCoste (1934, 1935; see Coulomb, 1956) has become almost standard, and is used in the well-known Sprengnether and the Press-Ewing vertical seismometers. Figure C-1 shows the principle of this suspension. The mass M,

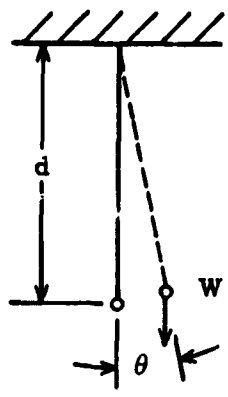

Figure C-1. Simple Pendulum

at the end of a beam of length d, oscillates about a hinge with an angular displacement ϕ from the horizontal. The beam is supported by a spring whose extended length is r, attached at a point a distance a above the hinge. Gravity acting on the mass produces the torque

$$T_g = -Mgd \cos \phi \qquad (C-2)$$

while the torque exerted by the spring is

$$T_s = k(r-c)s \qquad (C-3)$$

where k = the spring constant
r = extended length of spring
c = length of spring if stress is zero.

Now by geometry $s = a \sin \beta$

$$\sin \beta = \frac{b}{r} \sin \left(\frac{\pi}{2} - \phi \right)$$

thus

$$T_s = kab \cos \phi \left(1 - \frac{c}{r} \right) \qquad (C-4)$$

and the total torque is

$$T = T_g + T_s = \cos \phi \left[kab \left(1 - \frac{c}{r} \right) - Mgd \right] \qquad (C-5)$$

Equation C-5 means physically that the equilibrium point is determined by the condition T = 0, which implies that

$$kab \left(1 - \frac{c}{r} \right) = Mgd \qquad (C-6)$$

This determines r and therefore ϕ for the equilibrium position. The important thing is that if c could be made to be zero, the torque could be made to be zero regardless of ϕ and the system would then have an infinitely long period.

What happens in practice is that c can actually be made quite small, by pre-stressing the spring in winding and by adjusting the length of the hangers.

Then since

$$r = \sqrt{a^2 + b^2 - 2ab \sin \phi}$$

we have to a first approximation

$$\frac{1}{r} = \frac{1}{\sqrt{a^2 + b^2}} + \frac{ab \sin \phi}{(a^2 + b^2)^{3/2}} \qquad \text{(C-7)}$$

so that

$$T = \cos \phi \left[kab - Mgd - \frac{kc}{\sqrt{a^2 + b^2}} - \frac{kca^2b^2}{(a^2 + b^2)^{3/2}} \sin \phi \right] \qquad \text{(C-8)}$$

Then if we adjust the components so that

$$kab = Mgd + \frac{kc}{\sqrt{a^2 + b^2}} \qquad \text{(C-9)}$$

for small ϕ we may write the differential equation of motion

$$Md^2 \frac{d^2\phi}{dt^2} = -B\phi \qquad \text{(C-10)}$$

where $B = kca^2b^2/(a^2 + b^2)^{3/2}$. If c is negative, the system is not oscillatory. If $c = 0$, the system is unstable. If c is positive, the system will oscillate about the position $\phi = 0$, and according to Equation C-9 the period is given by

$$t = 2\pi \sqrt{\frac{Md^2}{B}} \qquad \text{(C-11)}$$

which shows that t can be made long by making c small, regardless of whether the dimensions of the system are small or large.

Long-period instruments are in general sensitive to tilt in the frame, and the degree of this sensitivity can of course be found by writing the equation of motion for a small angle of tilt and differentiating with respect to the angle. Tilt may affect the period and the zero point. The period of the LaCoste suspension is not appreciably affected by small tilts in the plane perpendicular to the plane of oscillation if it is almost level; this can be shown by the fact that the derivative goes through a minimum at zero tilt. The period is affected by tilt in the plane of oscillation, and the final adjustment for period is often made by adjusting the tilt. An ordinary twenty-second seismograph should be leveled to about plus or minus half a minute of arc to retain its period.

The equilibrium position of the LaCoste suspension is also affected by tilt in either plane, but the effect goes through a minimum of zero if the frame is exactly vertical and the center of the beam is exactly in a horizontal plane with the hinge. Once the frame is properly leveled the effect of tilt is not important.

III. SWINGING-GATE SUSPENSION

The device most commonly used at present for sensing the horizontal components of long-period earth motion is the so-called swinging-gate system (Figure C-2) This system consists essentially of a pendulum constrained to oscillate in a plane which is not vertical but almost horizontal. This means that the restoring force in the pendulum equation is reduced by a factor cos θ, where θ is the angle of tilt from the vertical. This changes Equation C-1 for the period of an ordinary pendulum to the form

$$t = 2\pi\sqrt{\frac{\ell}{g}\cos\theta} \qquad \text{(C-12)}$$

for the period of the swinging-gate system; if θ is made almost a right angle, the period becomes very long.

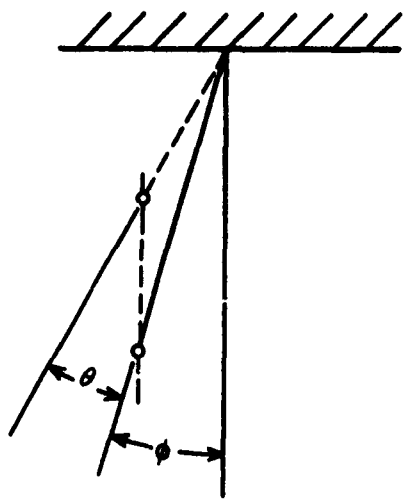

Figure C-2. Simple Pendulum Tilt, ϕ, Perpendicular to Oscillations

The defect of this system in practice is that as the period is lengthened, it becomes extremely sensitive to tilt. This is shown by differentiating Equation C-12 with respect to θ. The result is

$$\frac{dt}{d\theta} = \pi\sqrt{\frac{\ell}{g}}\,\frac{\sin\theta}{(\cos\theta)^{3/2}} \qquad \text{(C-13)}$$

which for θ near $\pi/2$ is very large. For instance, if a system in which ℓ = 20 centimeters is to have a period of 30 second, then according to Equation C-12, θ must be about 3 minutes of arc, and a tilt of 5 seconds of arc would reduce the period by one second. Tilt of this magnitude may result from earth tilt or from temperature gradients in the frame.

The zero position of the swinging-gate system is not affected by tilt in the plane of the beam, but is critically affected by tilt in the plane perpendicular to the plane of the beam. This in inherent in suspended instruments for detecting horizontal motion and in general a feedback correction must be made to hold the beam close to its zero position.

IV. VERTICAL PENDULUM-AND-SPRING SUSPENSION

A suspension described by Romberg (1961), in which the restoring force of a vertical pendulum is almost cancelled by a vertical spring, can be used to sense horizontal earth motion. The advantage of this system over the swinging-gate system is that its period is relatively insensitive to tilt. A minor advantage is that is has no long horizontal members, so that is could be put into a bore hole. The oscillating system is shown schematically in Figure C-3. The mass M is at the end of a beam of length d which swings about a hinge; its displacement is ϕ and its gravitational torque is

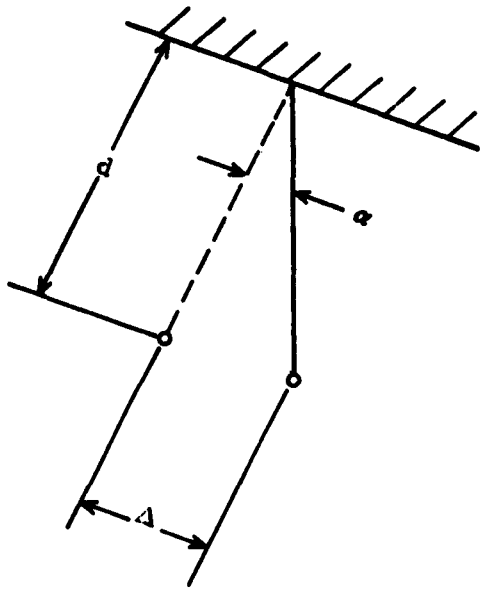

Figure G-3. Simple Pendulum Tilt α, In Plane of Oscillations

$$T_q = -Mgd \sin \phi \qquad (C-14)$$

The beam is shaped like an inverted U so that the spring can pass the zero position. The spring is attached to a point on the frame a distance a directly above the hinge, and to the beam at a distance b from the hinge, thus pulling the beam upwards against the gravitational torque. By analogy with Equations C-3, C-4, and C-5, we have for the total torque

$$T = \sin \phi \left[kab \left(1 - \frac{c}{r} \right) - Mgd \right] \qquad (C-15$$

As in the LaCoste suspension, c can be made zero; the torque can then be adjusted to be very small, so that for small values of ϕ we have the differential equation

$$Md^2 \frac{d^2\phi}{dt^2} = (kab - Mgd) \phi \qquad (C-16)$$

and the period of the system is

$$t = 2\pi \left[\frac{d}{g - \frac{kab}{Md}} \right]^{\frac{\ell}{2}} \qquad \text{(C-17)}$$

Suppose now that there is a tilt γ in the vertical plane perpendicular to the plane of motion. This case is analogous to tilting the pendulum (except that the tilt will be small) which resulted in Equation C-12. In this case Equation C-17 goes to

$$t = 2\pi \left[\frac{d}{g \cos \gamma - \frac{kab}{Md}} \right]^{\frac{1}{2}} \qquad \text{(C-18)}$$

and the rate of change of period with tilt is found by differentiating, so that

$$\frac{dt}{d\gamma} = \pi g \sin \gamma \sqrt{\frac{d}{(g \cos \gamma - \frac{kab}{Md})^3}} \qquad \text{(C-19)}$$

which shows that when γ is zero the rate of change of period is also zero. By comparison with the swinging-gate model, if the system is upright, with a period of 30 seconds and an effective beam length of 20 centimeters, the tilt required to change the period by one second will be 36 minutes rather than five seconds.

The equilibrium position, as explained in the previous section, is inherently sensitive to tilt in the plane of oscillation. It is not sensitive to tilt in the plane perpendicular to the plane of oscillation if the frame is accurately vertical.

APPENDIX D

SENSOR SURVEY

A preliminary evaluation of sensors was conducted to provide a basis for selection of the sensor which would work best in the digital seismograph system. Some of the sensors considered were obviously unsuited to the project purposes and were eliminated from a more detailed evaluation. Below is a complete list of the evaluated sensors.

1. Differential transformer

   a. Offers best sensitivity (up to 1000 V/in) of any transducer investigated.

   b. Operates at high temperatures.

   c. Requires higher displacement forces than capacitor plates or optical systems.

   d. Linearity better than 1% over wide range.

   e. To achieve 10^6 dynamic range, a power amplifier with this same range would be required, if range changes cannot be automatically made.

2. Capacitance - FM and closed-loop bridge

   a. Very small displacement measurements are possible at an accuracy dependent upon standard capacitor or oscillator stability.

   b. Stable and repeatable.

   c. Extremely good resolution possible.

3. Resistance types

   a. Maximum range of displacement about 70μ with 10 to 100 ounces force required.

   b. Sustained stress will yield plastic deformation.

c. Temperature and humidity sensitive.

4. Hall-effect Generator

   a. Seismograph has been built and operated with very few specifications being made available (Polish patent application).

   b. Has roughly same output level range as silicon solar cells and would therefore require external noise-free amplification.

   c. Appea ; to present large restoring forces problems.

   d. Theoretical measurements to 1 Å.

   e. Would require high field strength for required sensitivity.

5. Optical Interferometer

   a. Accurate but requires very short wavelengths for small displacements

   b. May require very long optical arms.

6. Cryogenic strain gauge

   a. Offers very low noise and thermally stable system.

   b. Would require considerable amount of apparatus.

7. Change in Beta of transistors with stress

   a. Measurements would be required for such items as sensitivity, linearity, noise characteristics, etc.

8. Magnetoresistance

   a. Similar to Hall effect device in requirements and characteristics

   b. Has wide dynamic range.

   c. Would require amplifier of wide dynamic range.

   d. Requires uniform magnetic field.

9. Magnetostrictive

   a. Requires large forces.

   b. Temperature sensitive.

   c. Non-linear characteristics

   d. Long term instability.

10. Photoresistive and Photovoltaic

   a. Solar cells

      1) Linear over wide range.
      2) Low sensitivity (0.2 μv /mμ) would require amplifier with excellent signal-to-noise characteristics as well as wide dynamic range.
      3) Requires very little force since it is an optical system.

   b. CdSe Photocells in bridge arrangement

      1) Very good sensitivity: 40 μv /millimicron.
      2) Noise high for the above sensitivity (40 μv /P-P).

11. Piezoelectric - Barium titanate

   a. Requires large forces.

   b. Poor low-frequency response.

   c. Rugged and simple.

   d. Generally poor temperature characteristics.

12. Solion chemical transducer

   a. Has excellent threshold sensitivity.

   b. Extremely sensitive to environmental conditions.

13. Eddy Current

    a. Essentially non-linear displacement vs inductive change.

    b. Will measure 250 millimicrons or better.

    c. Requires about 10 dynes restoring forces.

    d. May not be applicable in low-frequency measurements.

14. Frequency resonance in thin film (permalloy).

    a. Working model in use by TI.

    b. Has 75-db range.

    c. Maximum sensitivity is 10^{-7} radians (measures small angles).

15. Nuclear resonance.

16. Paramagnetic resonance - Helium metastable magnetometer.

17. Laser.

18. Radioactive measurements.

19. Infrared detection with heat source.

20. Borg-Warner Vibratron.

    Primarily a pressure transducer.

21. Acoustical Interferometer.

Sensors which were selected for a more thorough evaluation and the Romberg seismometer are discussed below.

A. SENSORS

1. Analog output type

    a. Differential transformer

This appears to be the best of the so-called analog output sensors. The particular model under consideration was the IRC 70-3912 with a maximum

sensitivity of 700 volts per inch, about 30 μ volts per millimicron, which is about 3.6×10^{-15} watts per millicron.

The restoring rate of this transformer is a maximum of 50 dynes per meter, which is insignificant compared to the 8,800 dynes per meter gravitational restoring force on the Romberg seismometer. Verification tests were run on this differential transformer, and, as predicted, no measurable effects were observed on the period or damping of the Romberg seismometer.

b. Closed-loop Capacitance Bridge

This method was investigated primarily because commercial equipment is available which will measure capacity differences of the same order of magnitude as those generated by the seismometer. However, it became readily apparent that the problems associated with high-speed automatic bridge balancing (which would have to be performed at the sensor because of the capacity levels involved) would be extremely difficult if not unsolvable.

c. Light Beam and Photoresistive

This method looked attractive because of the relatively large output. Tests conducted with a pair of Clairex CL 603A Cadmium Selenide photo-resistive cells showed a maximum possible sensitivity of about 100 microvolts per millimicron from a 50,000-ohm source which would be 2×10^{-13} watts per millimicron. This sensitivity is accomplished by using the cells in a relatively high-voltage bridge circuit, and with the addition of an optical lever arm with a gain of 10.

Unfortunately, cell noise at room temperature in the bridge circuit was about 250 μv peak to peak. Even more critical was the drift of the cells, which exceeded 150 millivolts during one of the overnight tests.

d. Light Beam and Photovoltaic Cells

Silicon solar cells were tested similarly to the photoresistive cells. Results showed that with a gain of 10 from an optical lever arm, an ultimate sensitivity of about 2 μv per millimicron might be achieved with 10,000-ohm load, which is 4×10^{-16} watts per millimicron. It seemed only remotely possible that the voltage levels available at the submillimicron displacement region could be switched and digitized. The noise levels were satisfactory, however, being appreciably less than 50 μv, which was the limit of our measuring equipment. Drift characteristics were not measured.

e. Hall-Effect Generator

Although a seismograph has been built using a Hall-effect generator, calculations show that to achieve our level of sensitivity, the restoring force would be excessive. Also, the generation of a steep linear magnetic gradient appeared to be impractical.

2. "Digital" Output Type

a. Optical Interferometer

Optical fringe counting techniques appeared to lack sufficient resolution by about three orders of magnitude, even using ultraviolet light. Wavelengths of 100 Å could possibly be used but with difficulty; however, this would still fall short of the desired 1 Å.

b. FM Oscillators

The use of two high-frequency oscillators controlled by the seismometer boom appears to be the best method of achieving the required sensitivity and dynamic range. By proper choice of sensor dimensions such as spacing, displacement and area, the linearity can be kept within the accuracies required for this application. Restoring forces should be essentially zero since there is no d-c voltage difference between the plates. A detailed description of this approach is covered in Section VIII of this report.

APPENDIX E

THE DIGITAL BRIDGE CONCEPT

A. SIGNIFICANT FEATURES

The Digital Bridge Concept provides two significant features:

1. The bridge reference oscillator is used to power the linear differential transformer and to convert to the dc reference supply for the analog-to-digital converter.

2. A floating point type of analog-to-digital conversion for sensor displacement is provided by the use of automatic scale switching.

B. SYSTEM OPERATION

The block diagram (Figure E-1) will aid in following this discussion.

1. Oscillator and Amplifier

The 38-kc oscillator drives the primary of the differential transformer for each of the three seismic sensing components of boom displacement. The 38-kc signal is also converted from ac to dc voltage for the reference source for the A-to-D converter. The outputs from each of the secondary windings of the differential transformer are bridge rectified and summed. Conversion is therefore made from the 38-kc amplitude modulation to analog voltage modulation. The analog voltage thus produced passes through appropriate filters to eliminate aliasing errors due to the sampled system. Dynamic range at this point is at least 120 db or 20 binary bits. Signal level for a displacement range of 0.5 to 500 millimicrons is 8 microvolts to 8 volts. To provide a large enough least-significant-bit voltage for measurement with the A-to-D converter system, it is necessary to pass the voltage through a low-noise constant-gain preamplifier. A TI reactance amplifier and a Philbrick operational amplifier were considered for this application.

2. Analog-to-Digital Converter

Outputs of the preamplifier are multiplexed into the A-to-D converter at a 30-cps rate. The dynamic range of the reactance amplifier is 60 db or approximately 10 binary bits. Extension of the dynamic range to 13 bits is possible with extensive circuit modification. Use of this circuit over a 120-db range or 20 binary bits, requires appropriate scale switching at the amplifier input.

Information required for scale switching is obtained by an A-to-D conversion first-look at the input voltage with a low-gain system. This low-gain

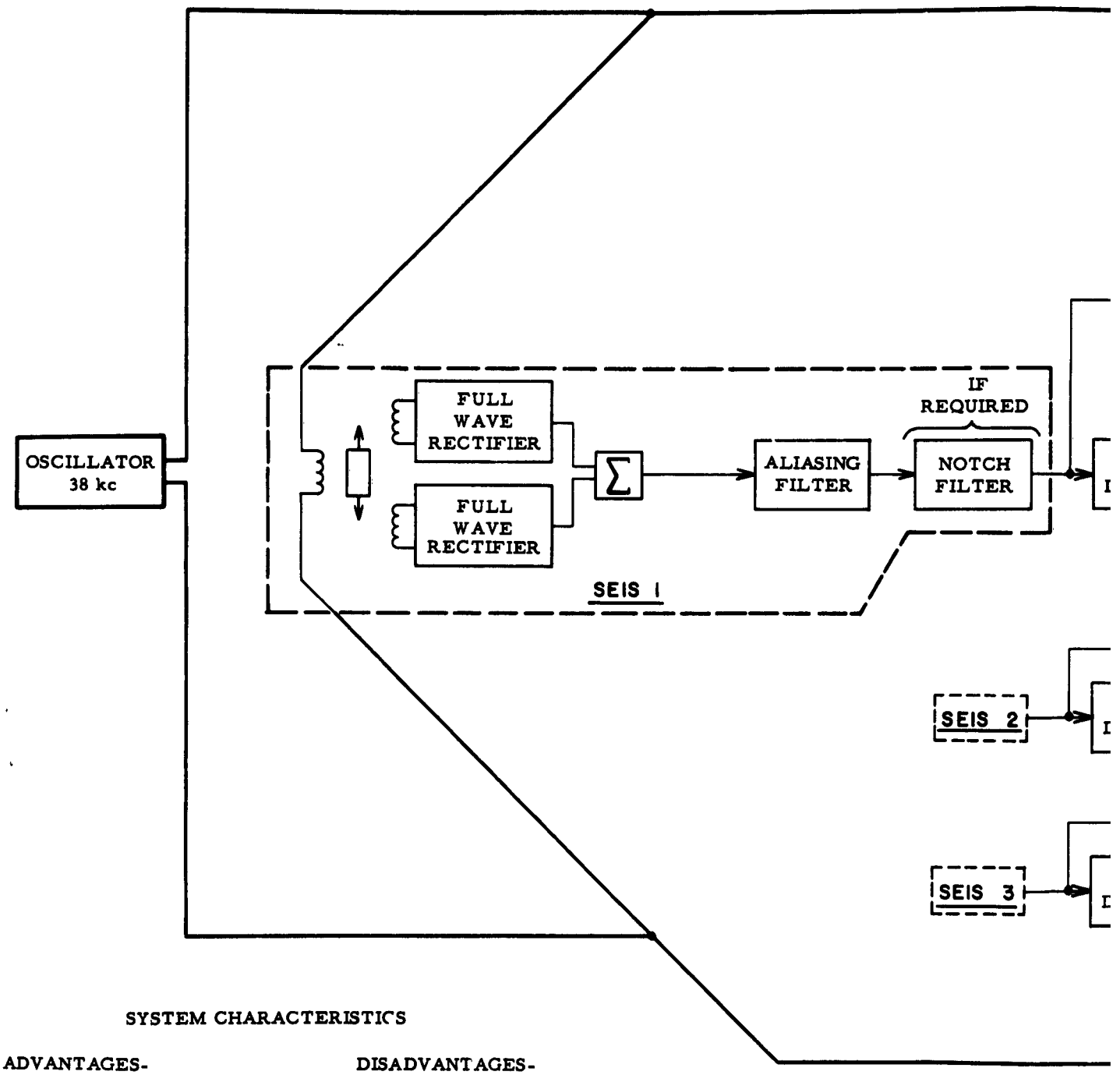

SYSTEM CHARACTERISTICS

ADVANTAGES-

1. Analog Filter Flexibility
2. Compatible With Many Sensors
3. Floating Point Saves Tape
4. Prewhiting Filter Allowed

DISADVANTAGES-

1. Relay Switching - Reliability
2. Dynamic Range of Preamp 10 Bits Now
3. Variable Resolution
4. Limited Sensitivity ($\pm$.4 mμ)

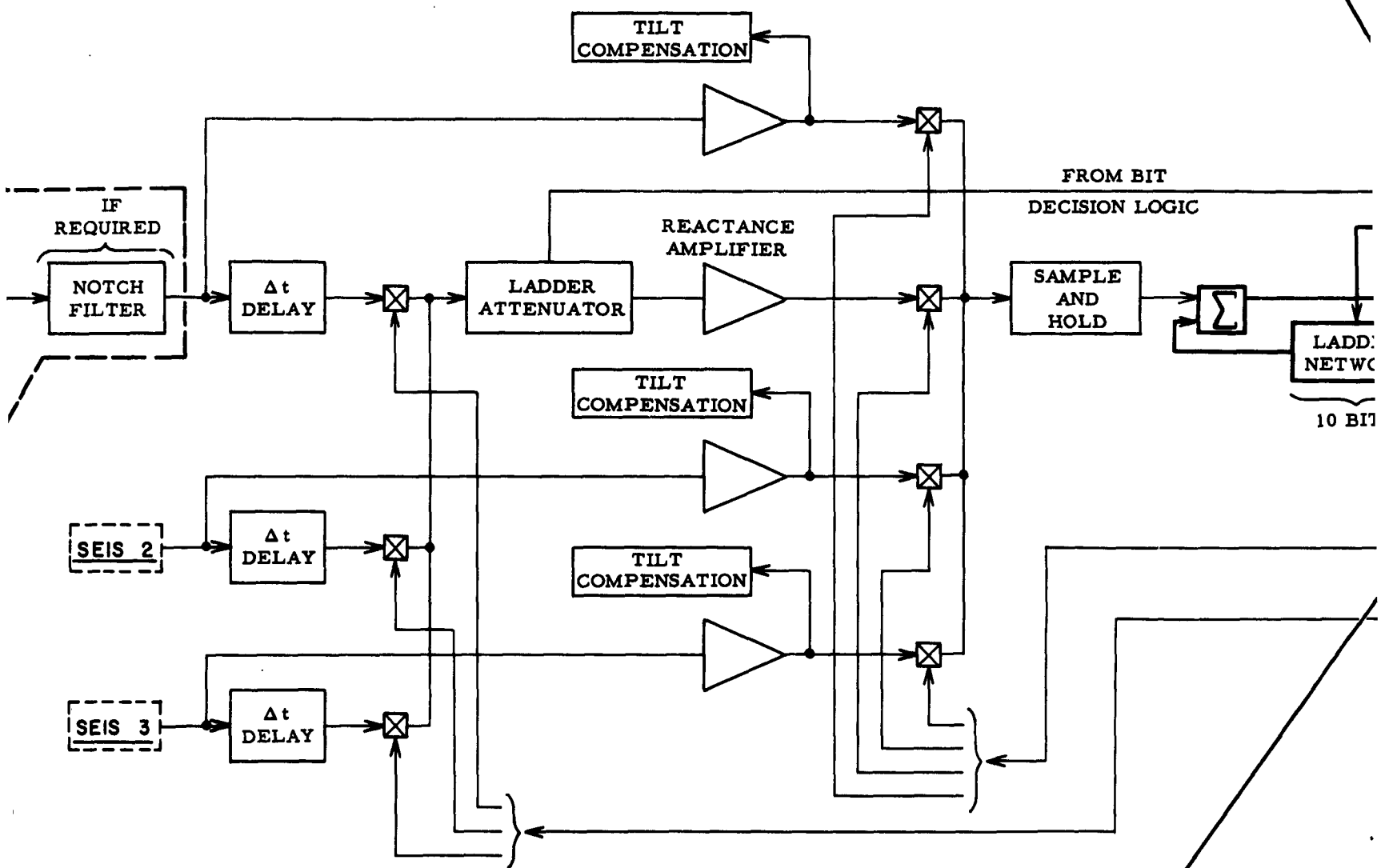

NOTE: HEAVY LINES INDICATE PARTS OF SYSTEM DESIGNED, FABRICATED AND EVALUATED

2

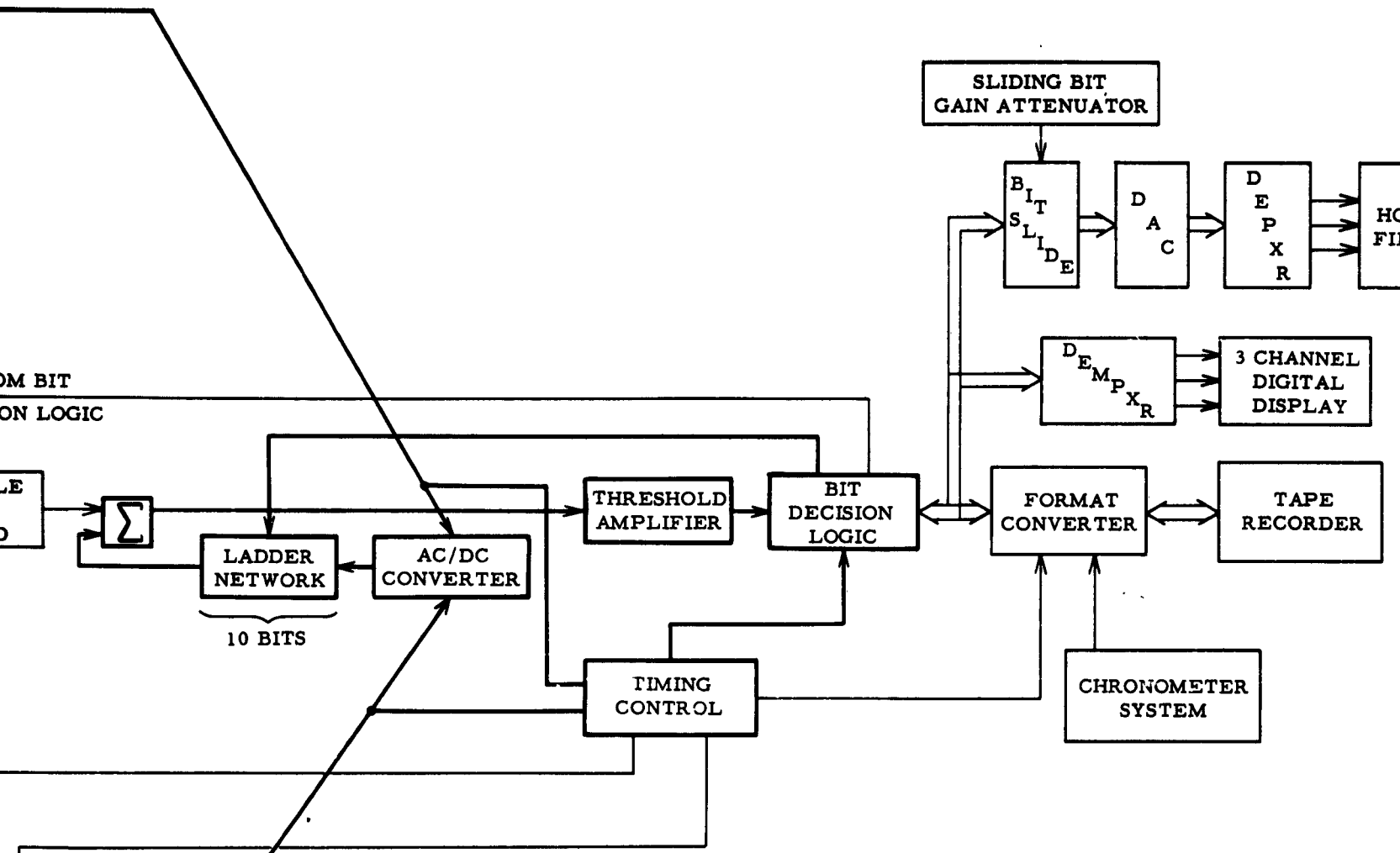

STEPS IN DIGITIZING

1. Set Gain Attenuator Amplifier To Low G
2. Use 10 Bit Ladder Network To Determi Switches
3. Throw All Bits For Gain Switching Simu
4. Wait For Reactance Amplifier To Stabil
5. Digitize Output Of Amplifier With 10 Bi

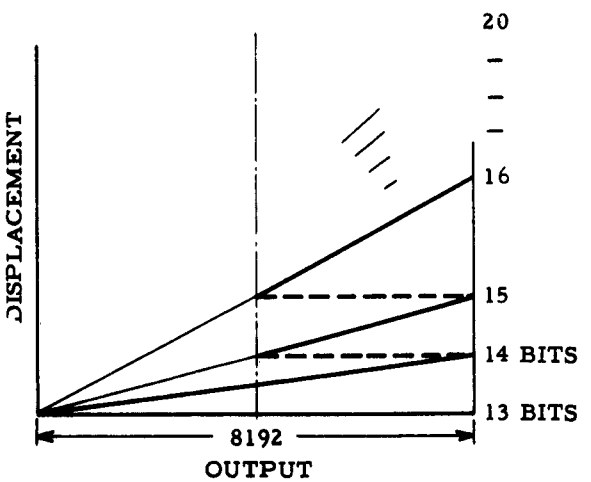

DIGITAL BRIDGE CONC

CONTRACT AF 19 (6

ARPA ORDER 292-62

5 SEPT 1962

PROJ

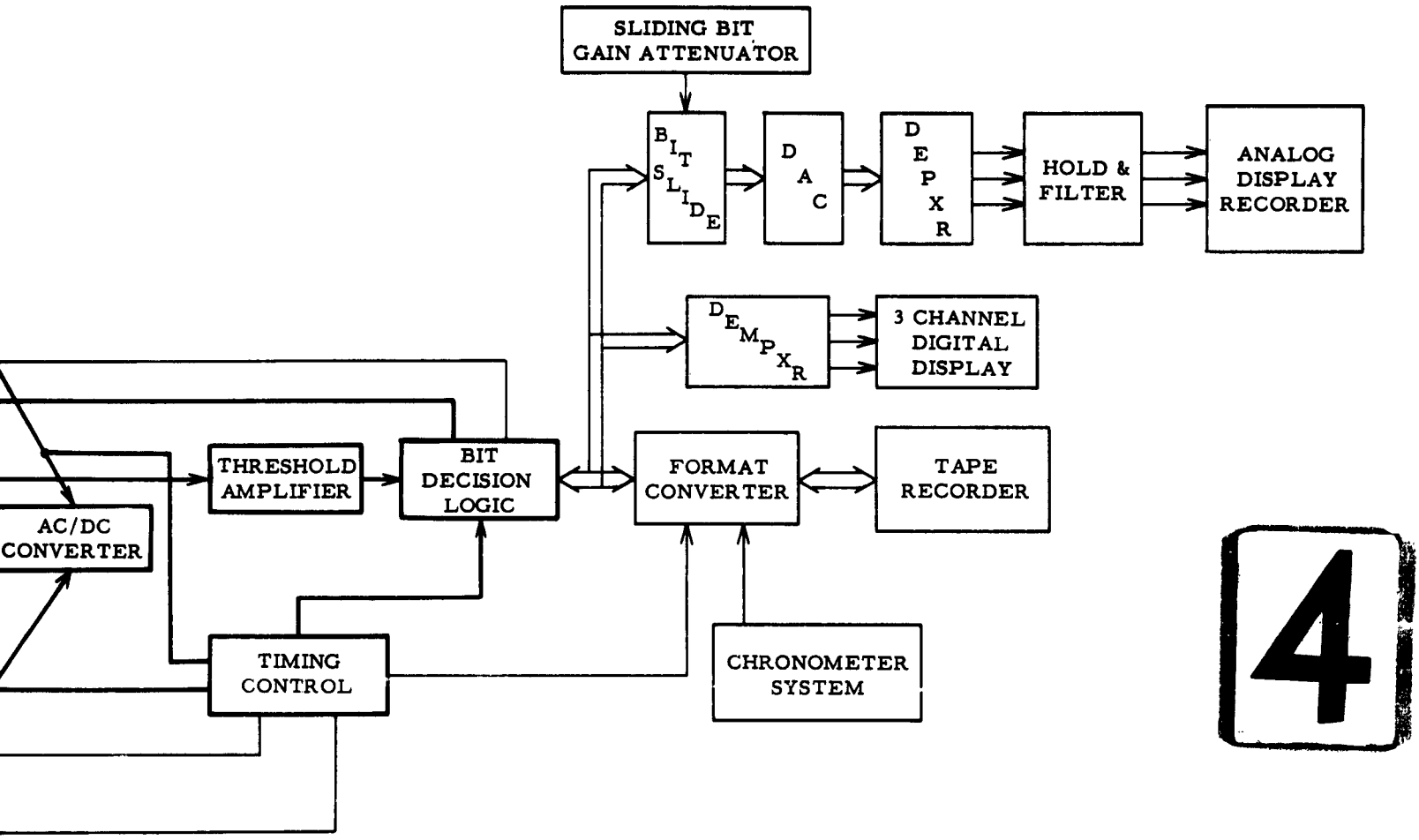

4

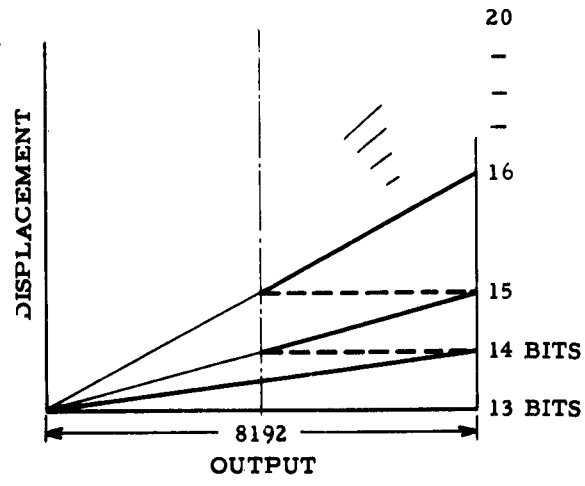

STEPS IN DIGITIZING

1. Set Gain Attenuator Amplifier To Low Gain
2. Use 10 Bit Ladder Network To Determine Setting of Mechanical Switches
3. Throw All Bits For Gain Switching Simultaneously
4. Wait For Reactance Amplifier To Stabilize (1.5 MS)
5. Digitize Output Of Amplifier With 10 Bit Circuit

DIGITAL BRIDGE CONCEPT DIAGRAM

CONTRACT AF 19(628)-472

ARPA ORDER 292-62 PROJECT 8652

5 SEPT 1962 PROJECT MGR.- B. WILLIAMS

Figure E-1

voltage is switched directly into the sample and hold and an A-to-D conversion performed.

First-look reading provides the necessary information for setting the appropriate scale swtiches at the input of the reactance amplifier. Seven-bit ladder-attenuator switches are engaged simultaneously. The signal level at the input of the reactance amplifier is now at the proper level to utilize the amplifier's limited dynamic range. Since a step change in level has been made at the input, approximately 1.5 milliseconds must be allowed to reach stability due to the 1-kc bandwidth of the amplifier. Since approximately 10 milliseconds has passed after the initiation of the convertor sequence, the voltage of the displacement function could possibly change by a significant amount. To alleviate this problem, the function has passed through a precise 16-millisecond delay unit (an m-derived, low-pass filter) so that the scale setting is correctly referenced to the analog voltage as it is connected into the A-to-D converter. The reactance amplifier transforms the voltage to a level high enough at its output for conventional A-to-D conversion. With the present system this provides 13 bits of resolution with 7 bits for scale switching. Floating point information is provided by the scale switch setting.

A system feature of this method of A-to-D conversion is that resolution is dependent on the amplitude of the signal. A single binary bit is equivalent to 0.5 millimicrons for the lowest scale setting but is equivalent to 500 millimicrons for the highest scale setting.

The system described above is a completely workable and adequate system. Critical parts of the system have been designed, fabricated, and evaluated. Areas of this investigation are indicated with heavy lines on the block diagram in Figure E-1.

C. DIGITAL BRIDGE CIRCUIT DETAILS

1. Analog Circuits

Engineering details related to the evaluation of the digital bridge concept are presented below.

a. Bridge Oscillator

The 38 kc oscillator schematic, shown on Figure E-2, drives the three differential transformers and the bridge reference source. Ten volts rms at 250 milliwatts is required for each of the IRC 70-3912 differential transformers. Ten volts rms at 1 watt is the total output requirement.

Transformer T1, designed and fabricated by Texas Instruments, operates at 38 kc with a primary unbalance of 125 ma. One of the secondary

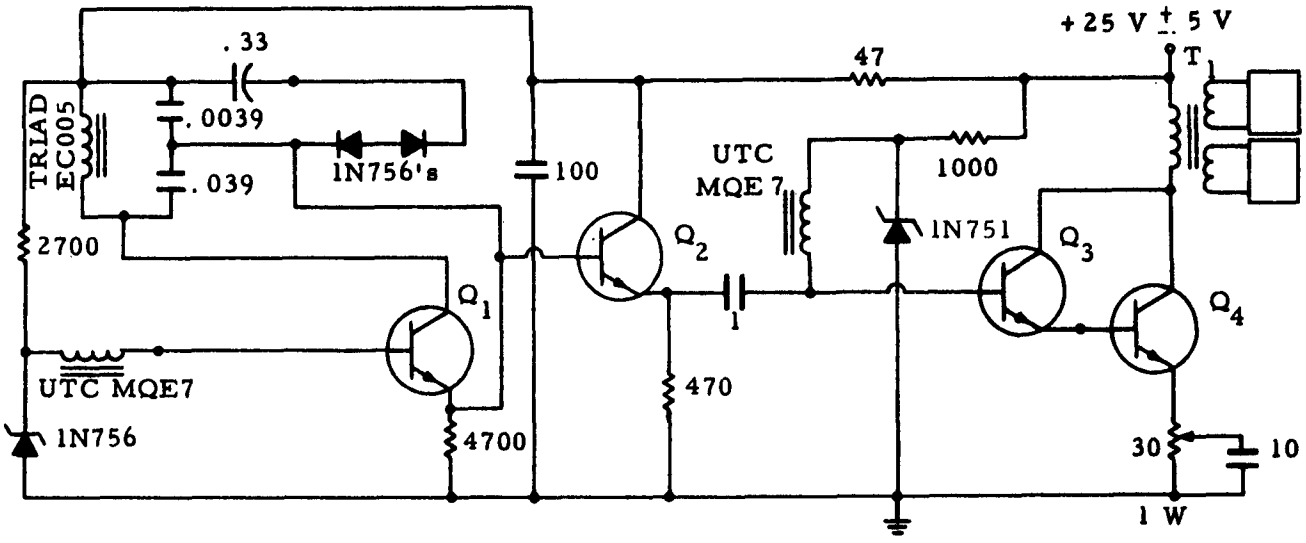

Capacitors are in microforads.
Resistors are in ohms 1/2 W 5% unless specified otherwise.
Q_1, Q_2, Q_3 are npn mesa-planar silicon transistors.
Q_4 is a 2N389.

1238

Figure E-2
38-KC Oscillator

windings furnishes power for the differential transformers. The other transformer secondary drives the circuit which generates the digital reference voltage.

A primary consideration is that secondary output voltage be independent of supply voltage variations. A one-volt power supply variation causes 1-millivolt oscillator output voltage variation with negligible frequency change.

b. Differential Transformer

The IRC type 70-3912, nominally rated at 1,000 volts per inch, was chosen because of its extremely high sensitivity. Maximum sensitivity is obtained with a 38-kc signal at 10 volts rms, primary supply. Under these conditions output impedance is 250,000 ohms for each secondary winding. Linearity is ± 1 per cent for 0.1-inch displacement of the core from its null position. Linearity for the seismometer application is much higher than ± 1 per cent since the core travel is limited to ± 0.020 inch. Testing of the purchased unit showed 700 volts per inch sensitivity.

c. Rectifier Circuit for Differential Transformer

To eliminate phase-shift problems around the null position, both secondary voltages are bridge rectified and then nulled, as shown on Figure E-3.

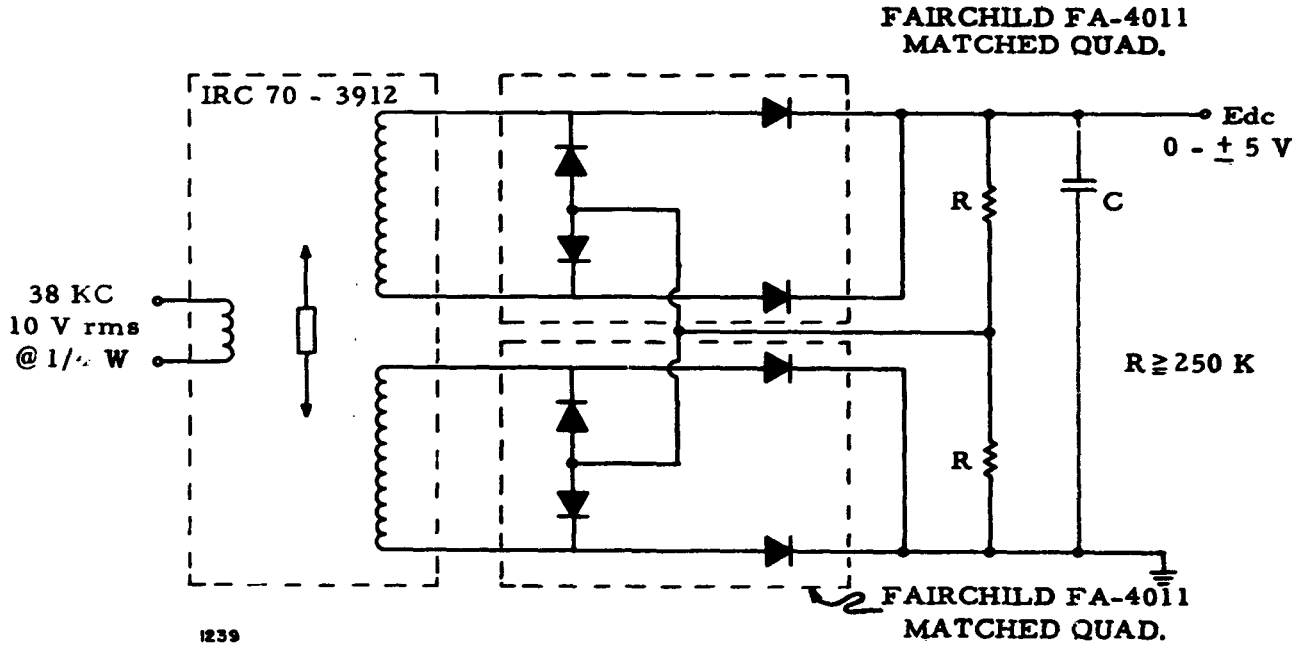

Figure E-3
Rectifier Circuit for Differential Transformer

Testing showed diode noise of approximately 0.3 microvolts rms with 3 ma. dc current through the diodes. A 0.1 millimicron displacement should produce approximately 3 μ volts output from the circuit.

d. Filters

A UTC LLP-10 m-derived low-pass filter with a cutoff of 10 cps was used for the aliasing filter. The 100,000 Ω input impedance of the filter matches approximately the output impedance of the rectifier circuit.

The variable twin-T notch filter, shown on Figure E-4, follows the aliasing filter and is adjustable from 0.16 to 10 cps. Maximum attenuation at the notch was approximately 50 db.

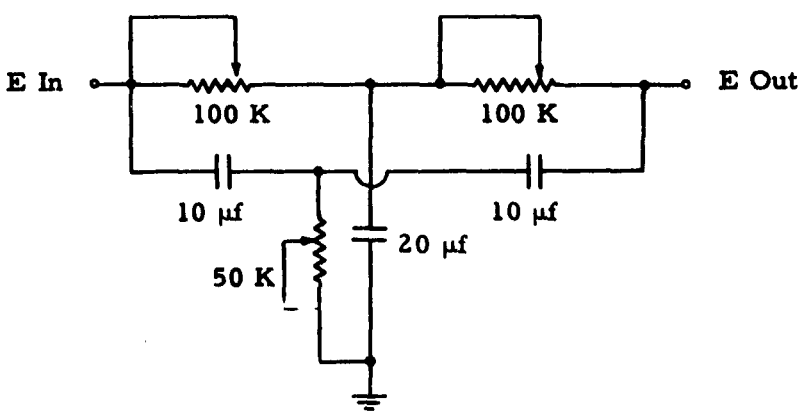

Figure E-4
Variable Twin-T Notch Filter (0.16 cps to 10 cps)

e. Preamplifier

Several breadboard configurations of the variable gain amplifier were evaluated. A Philbrick model P-2 and a TI reactance amplifier provided specifications with the most significance from a low noise and gain stability standpoint.

Binary gain steps for the P-2 amplifier are obtained by a group of feedback resistors as shown on Figure E-5. Low noise requirements dictated the use of mercury contact or reed relays for the switches. Total gain range from 10 to 1280 in binary steps was under control of the digital logic. This

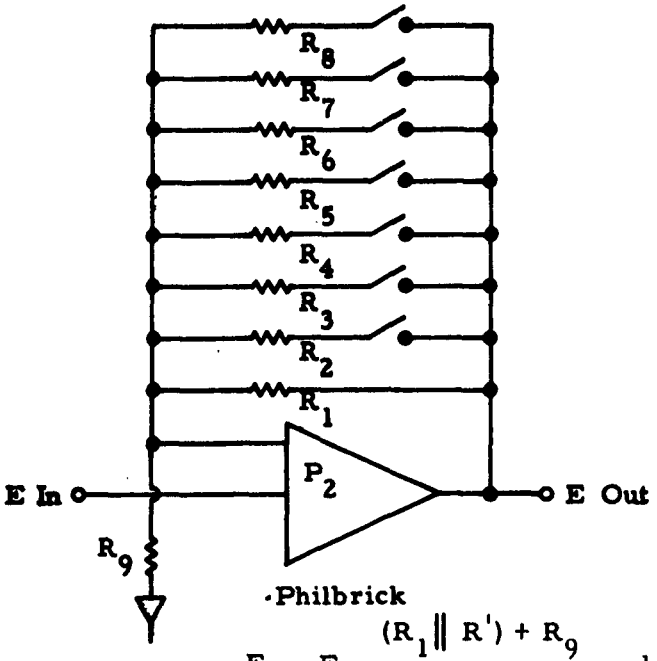

$$E_o = E_{in} \frac{(R_1 \| R') + R_9}{R_9}$$

R_1 = 1.279 M
R_2 = 1.277 M
R_3 = 637 K
R_4 = 317 K
R_5 = 157 K
R_6 = 77 K
R_7 = 37.05 K
R_8 = 17.1 K
R_9 = 1 K

The switches are controlled by the digital logic circuitry.

1240

where $\|$ means "in parallel with" and R' is the parallel combination for the switches closed.

Figure E-5
Binary Weighted Gain Switching of Operational Amplifier

gain range was required to match the output range of the sensor from 0.1 mμ to 100 μ displacement. The P-2 output would be 1.28 mv to 10 v in 8 ranges to match the input characteristics of the A-to-D converter.

Since step changes in gain are used, rise-time characteristics of the amplifier are significant. Testing showed that it required 0.5 milliseconds for the amplifier to reach 99.9% of full scale under the worst conditions. At a gain of 1000, the input broad-band noise of 4 μv rms limited the dynamic range to approximately 100:1. (Broad band is required for the logically controlled scale switching.) Smallest detectable signal or the least-significant binary bit would be 1.5 millimicrons.

The second approach utilizes the TI reactance amplifier with the following characteristics:

1) Noise level referred to the input is 0.05 μ volts rms with a frequency bandwidth of 0.8 to 10 cps.

2) Dynamic range of 80 db at gain of 2000.

3) Output voltage range 0.1 millivolts to 1 volt rms.

4) Band pass from 0.1 to 1000 cps (may be changed internally).

5) Worst condition rise time of 1.5 milliseconds.

Figure E-6 illustrates the binary weighted voltage divider switching concept required for gain change of the preamplifier system. Since the thermal noise generated in a 100,000-ohm resistor at 1 kc bandwidth is 3.6 μv peak-to-peak, minimum threshold level is limited. Assuming a signal-to-noise ratio of 2, 2.8 μv per 0.1 mμ sensor output and 6 db filter loss, the resultant least significant bit is 0.5 mμ. With this limitation, a range of 0.5 mμ to 500 μ could be realized with a resolution of 1000:1 over the entire range. A circuit modification to increase slightly the dynamic range of the reactance amplifier is also required.

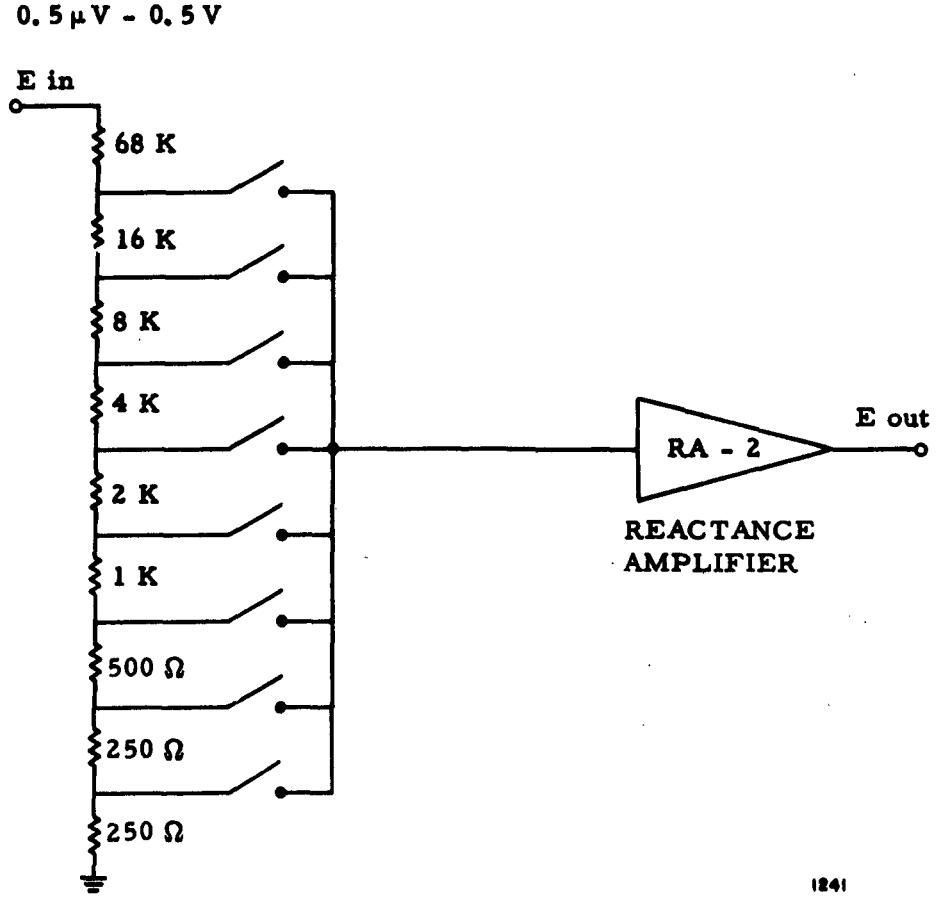

Figure E-6
Binary Weighted Voltage Divider Switching Circuit

f. Sample-And-Hold Circuit

This circuit, shown on Figure E-7 holds the sampled data point for the time required for analog to digital conversion. With the switch closed, the sample-and-hold capacitor will charge rapidly due to the low driving-circuit impedance. The time constant when the switch opens is 25 seconds, due to the 100-megohm amplifier input impedance.

The sample-and-hold circuit is actuated twice during each cycle — once for the determination of preamplifier gain setting and a second time for the 13-bit A-to-D conversion.

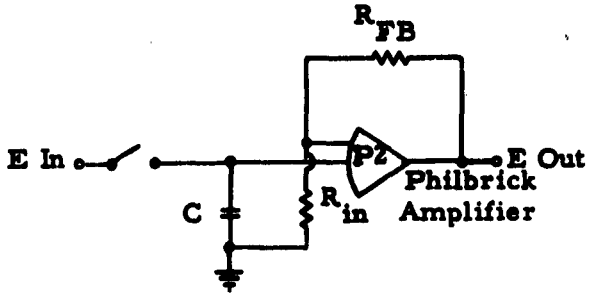

$$\frac{E_o}{E_{in}} = \frac{R_{FB} + R_{in}}{R_{in}}$$

Figure E-7
Sample-and-Hold Circuit

g. Function Delay Consideration

Time between two sample-and-hold settings within one conversion cycle allows the function amplitude to change by many significant bits. To compensate for this delay, the seismometer input signal is delayed the total time required for the preamplifier to settle after the floating-point gain determination. This concept is illustrated in Figure E-1.

2. Digital Logic Details

Figure E-8 illustrates the functional transfer of data and the generalized control required for the digital bridge. Figure E-9 is the timing diagram for the step by step sequence below.

1) Multiplexer selects the output of a sensor and stores its amplitude in the hold circuit.

2) The operational amplifier is set for minimum gain and its output is compared with the output of the voltage ladder. The reference voltage for the ladder network is provided by the same 38-kc oscillator that drives the sensors.

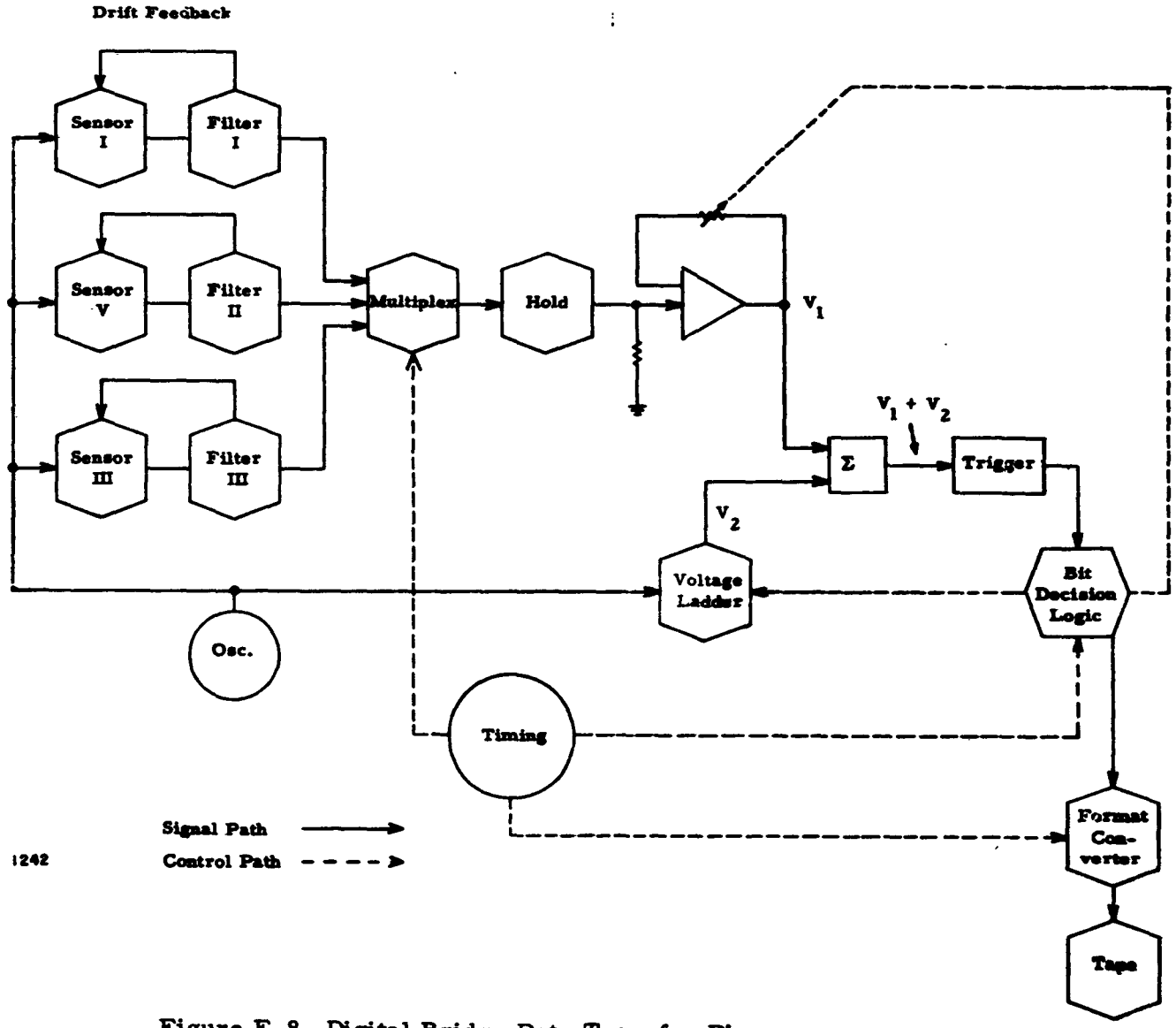

Figure E-8. Digital Bridge Data Transfer Diagram

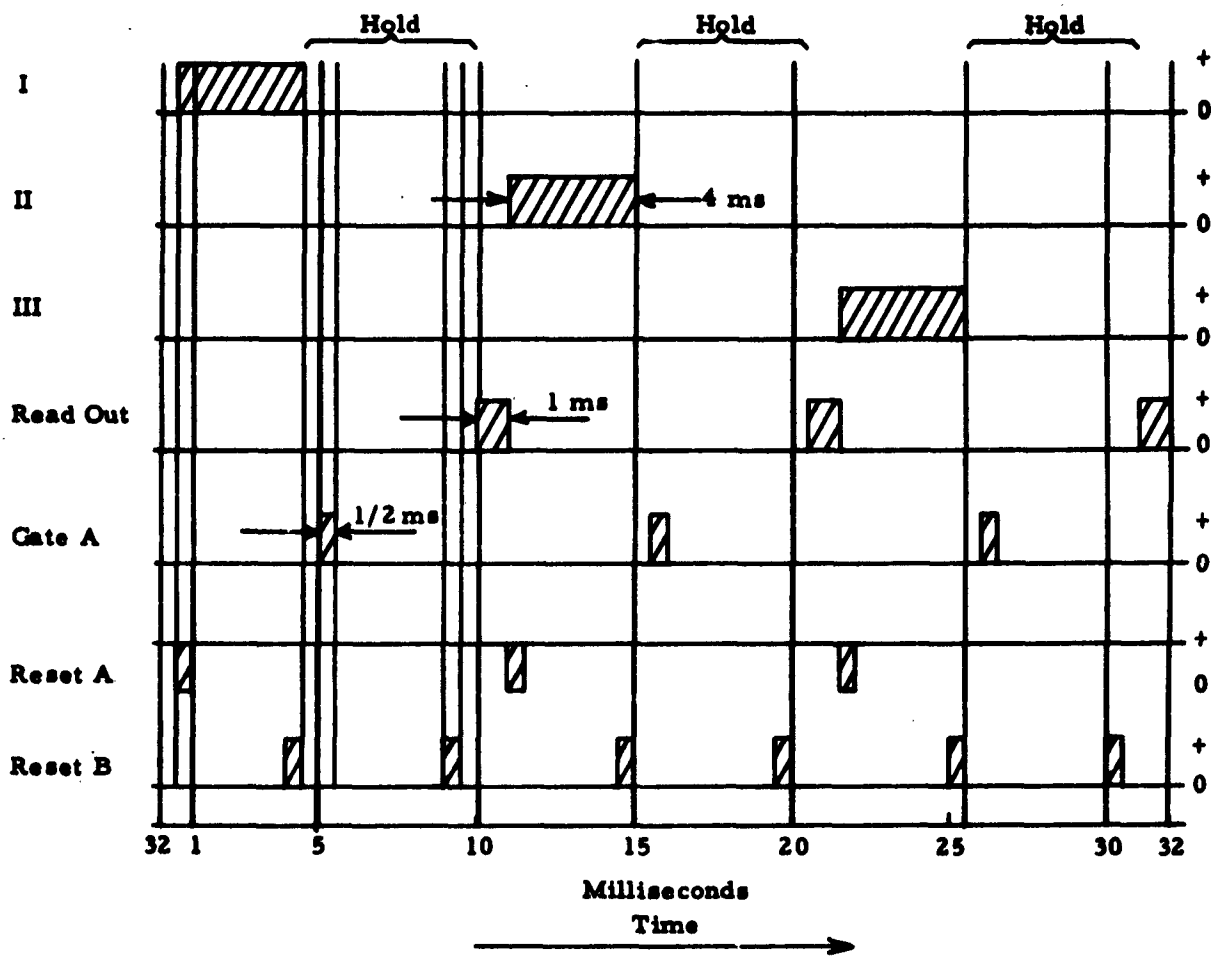

I Controls Gate to Sensor I
II Controls Gate to Sensor II
III Controls Gate to Sensor III

"Read Out" Gates Ladder and Gain Settings to Format Converter
"Gate A" Gates First Digital Ladder Reading to the Gain Register
"Reset A" Sets Gain to Minimum
"Reset B" Starts Counter 2 for 13 Bit A-to-D Conversion

1243

Figure E-9
Digital Bridge Timing Diagram

3) Bit Decision Logic adjusts the voltage ladder until a null is obtained at the Σ point.

4) Digital state of the Bit Decision Logic is transferred to the gain adjustment on the operational amplifier and a new gain is selected.

5) The voltage ladder is again adjusted by the Bit Decision Logic until a null is obtained.

6) Timing circuits transfer the digital state of the Bit Decision Logic and the gain setting of the operation amplifier to the Format Converter.

7) The Format Converter, under control of the Timing Circuit, transfers the data, with the correct format, to the tape.

8) Multiplexer selects the next sensor and the process is repeated.

a. Multiplexer

The multiplexer consists of three reed relays controlled by the timing circuit.

b. Timing Circuit

Timing for the complete digital system is tied to the 38-kc oscillator as shown in Figure E-10. Counter 1 and Decode Matrix 1 provide the timing for the total system as illustrated in Figure E-9. Figure E-11 is a detailed schematic of Decode Matrix 1, designed for a 30-cps sampling rate. Counter 2 and Decode Matrix 2 guide the Bit Decision Logic through its cycle.

Figure E-12 is a detailed schematic of the tie between Counter 1, Counter 2, and the 38-kc oscillator. This circuit doubles the frequency to 76 kc, shapes the pulses, and provides an automatic stop at the completion of the Counter 2 cycle. "Reset B" pulse delivered from Matrix 1 starts Counter 2. Note that Counter 2 supplies a sequence of 32 pulses in one cycle of operation but only 26 pulses are used in the Analog-to-Digital converter section described below.

Thirty-two pulses were the nearest economical number to twenty-six pulses and left six additional pulses for possible future use.

c. Analog-to-Digital Converter

The A-to-D converter uses the one-half approximation method of conversion. A voltage equal to the most significant bit is compared with the input amplitude to be digitized. If the output of the summing network is too high, the most significant bit is reset. By successive approximations, sequencing from the most significant bit to the least significant bit, the conversion is accomplished.

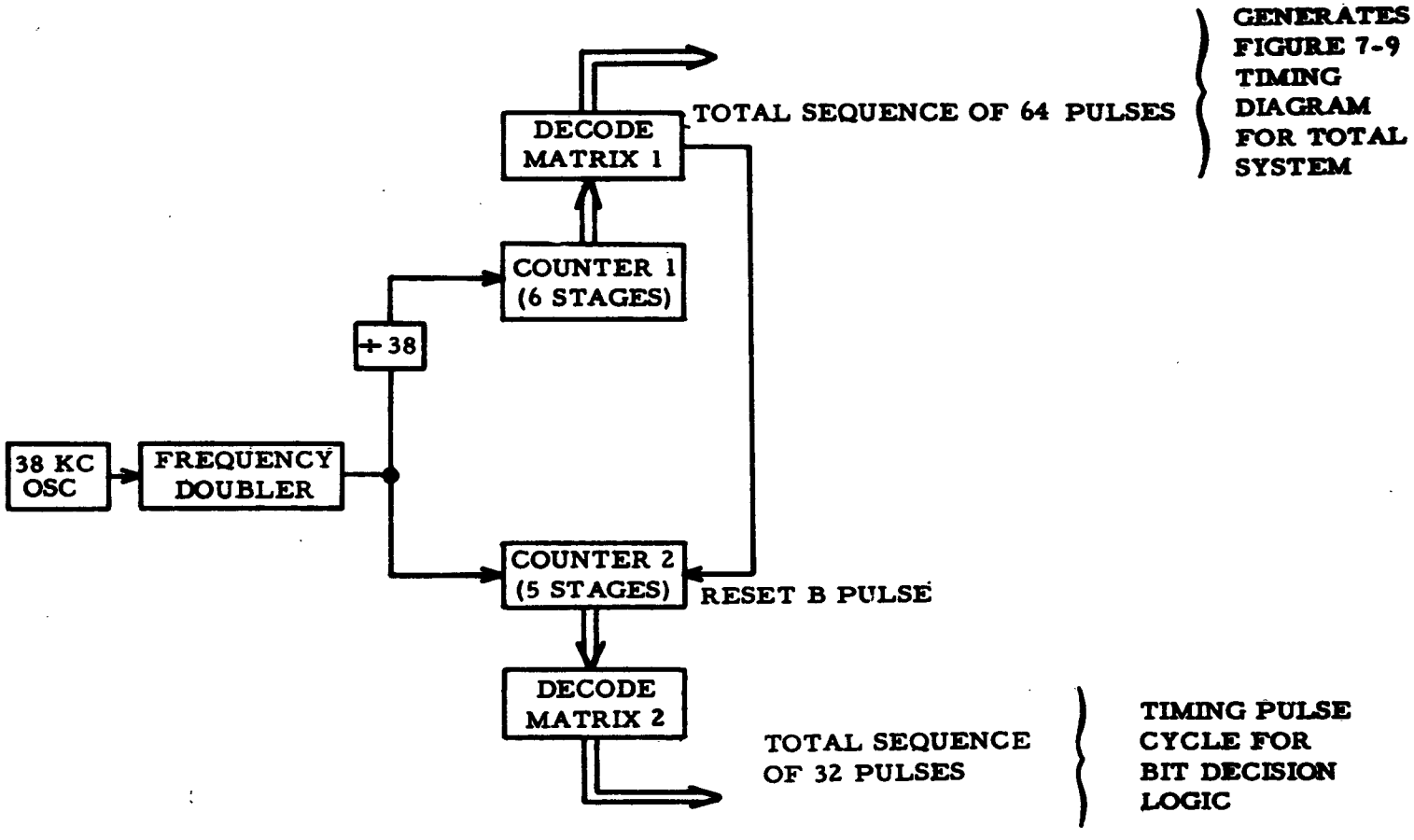

Figure E-10. Timing Block Diagram

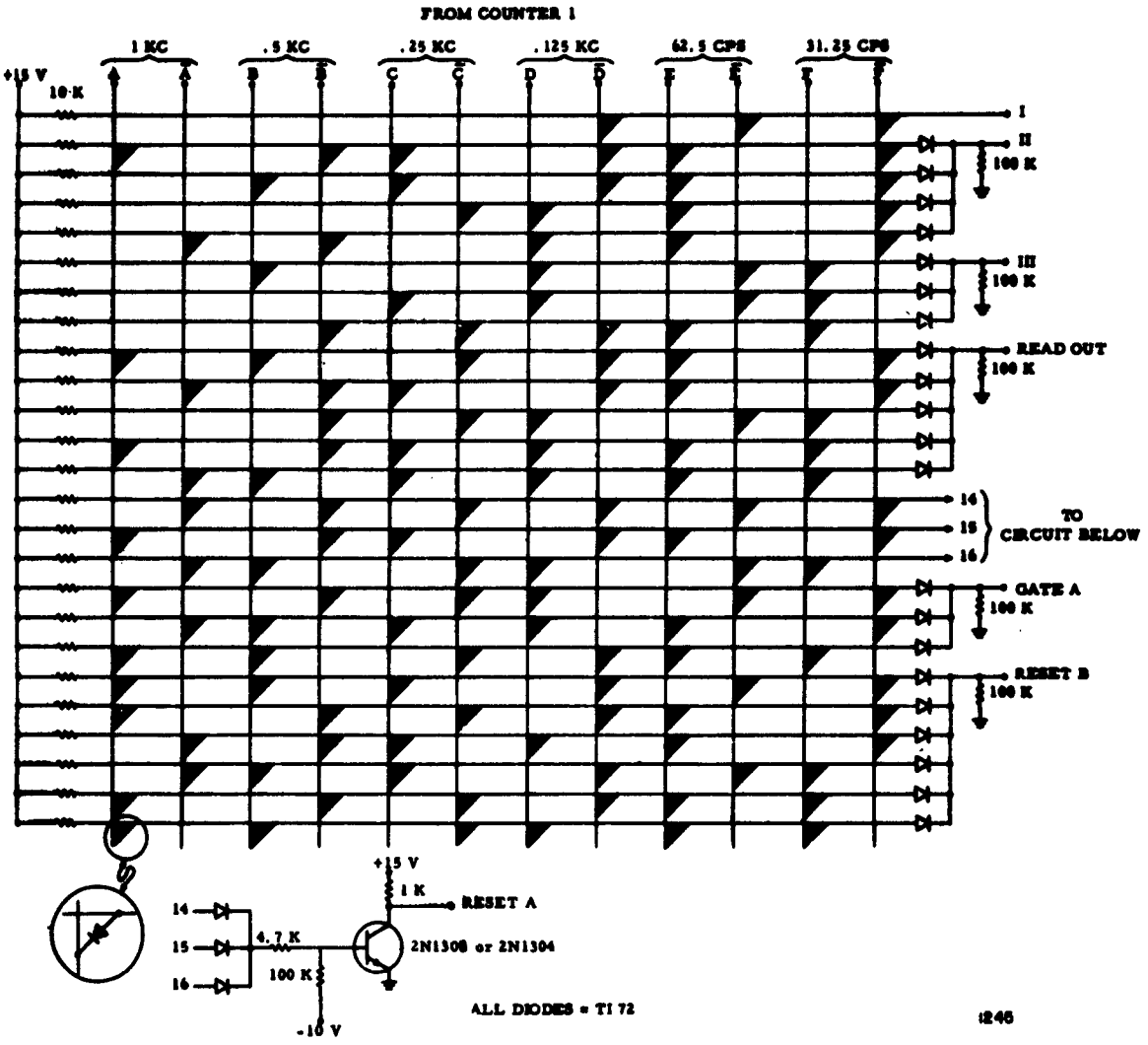

Figure E-11. Decode Matrix 1 Schematic

As previously stated, two A-to-D conversions are made for each sample. Timing pulses from the timing units generate the control pulses for the digital conversion.

Figure E-13 illustrates the symbol notation used in the logic diagrams. The Bit Decision Logic (Figure E-14) controls the conversion sequence. The sequence of pulses from the Counter and Decode Matrix 2 control the A-to-D Converter voltage ladder and summing junction. Steps in the converter sequence are:

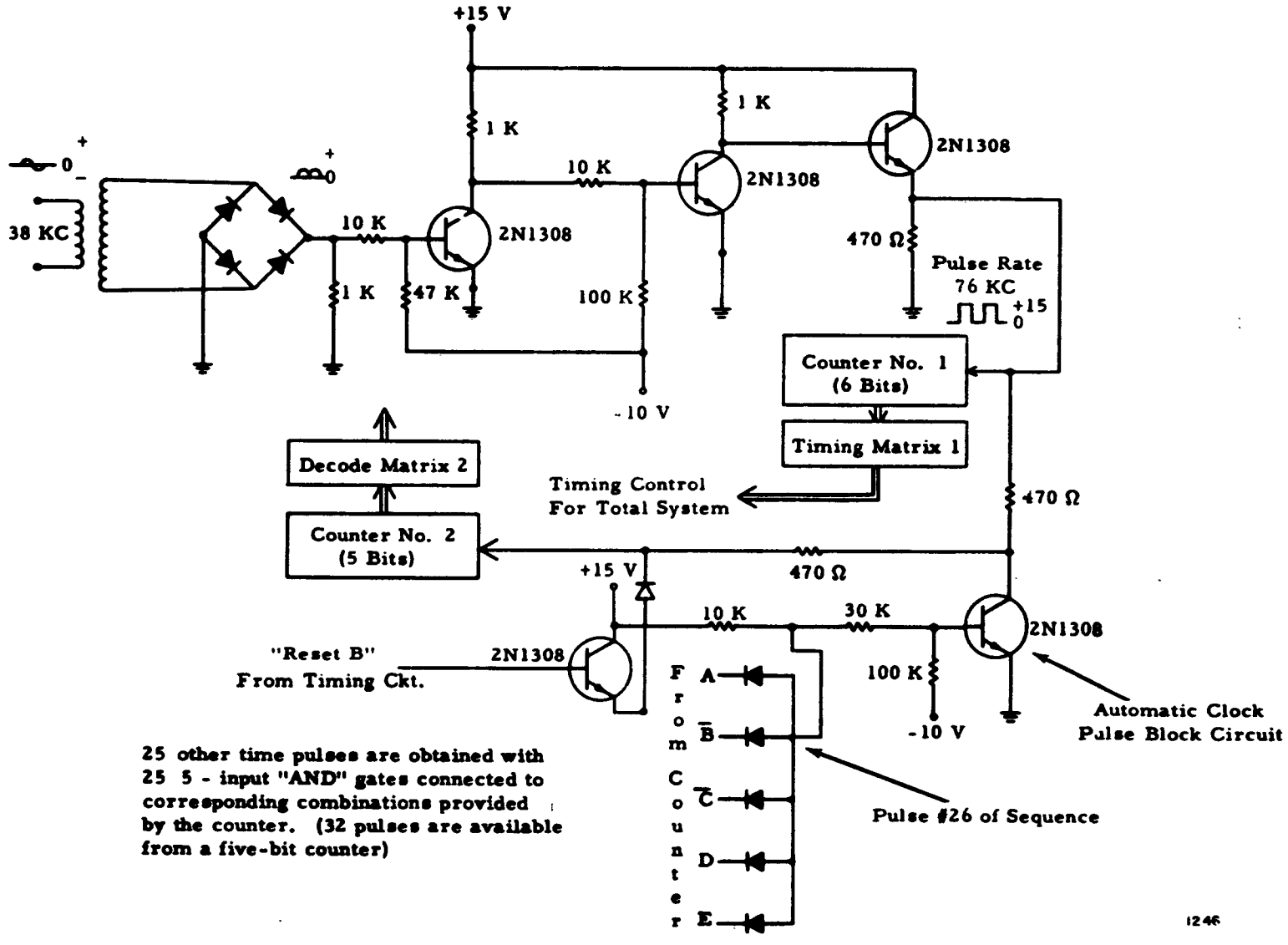

Figure E-12. Sequence Generation and Control in Bit Decision Logic

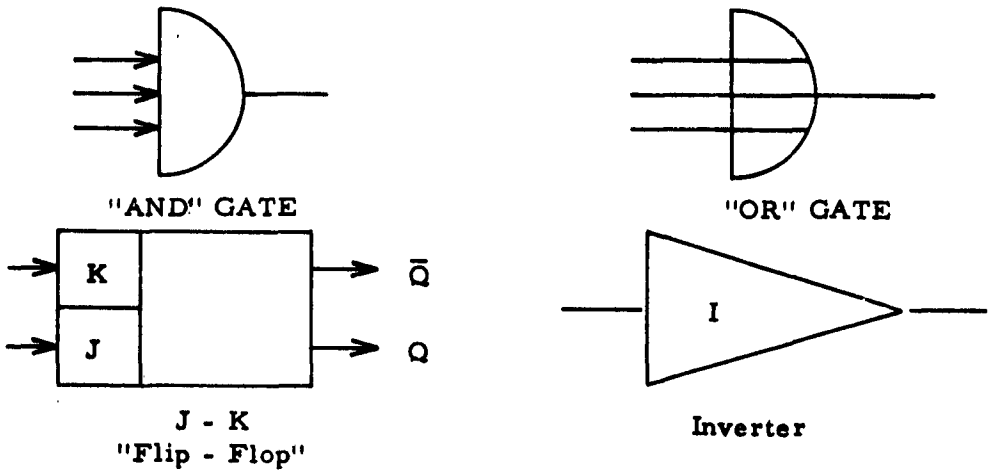

J - K "Flip - Flop"

A Negative pulse excursion on K gives a "1" output on $\bar{Q}$.

A Negative pulse excursion on J gives a "1" output on Q.

1247

Figure E-13. Symbol Notation for Logic Diagrams

1) "A" resets the Gain Register. "B" resets Counter 2 and the A-to-D Converter Register. (Gain of the preamplifier is now set at the lowest value.)

2) The 76-kc clock drives Counter 2 for sequencing the A-to-D Converter Register, which controls the switches of the ladder attenuator.

3) As the one-half approximation sequence is made, the threshold sensing amplifier output (at the summing network output) provides the control signal for resetting the appropriate binary of the A-to-D Converter Register.

4) After sequencing through the 13 bits of conversion, Gate A signal from the timing system, gates out 7 bits of the A-to-D Register to the Gain Register. The Gain Register controls the range switch selection for the preamplifier.

5) After an appropriate delay for the switches and preamplifier to settle (3.5 milliseconds) reset B is again applied and the A-to-D Converter Register is again sequenced through 13 bits.

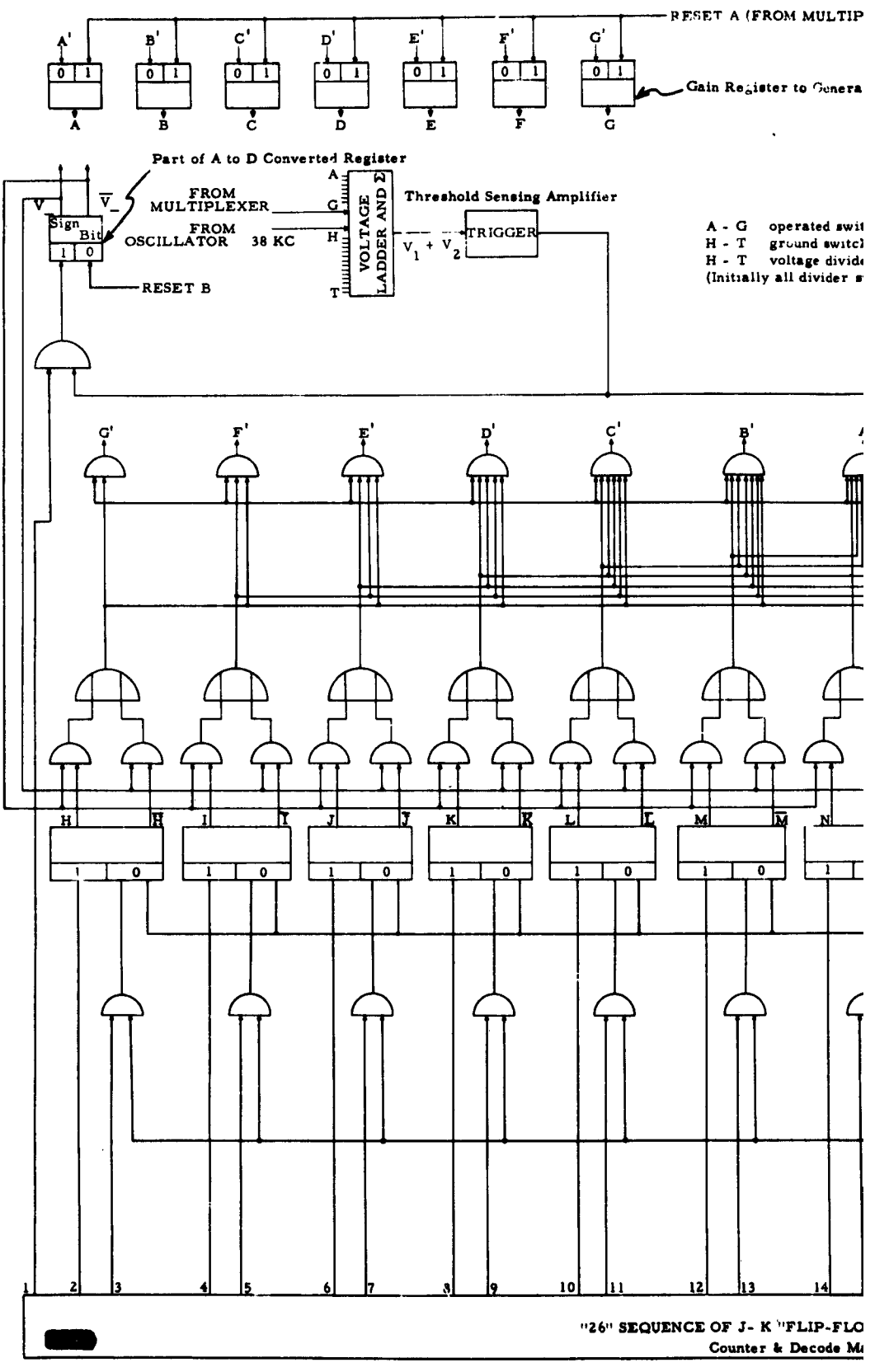
RESET A (FROM MULTIP
A' B' C' D' E' F' G'
0 1
A B C D E F G
Gain Register to Genera
Part of A to D Converted Register
FROM MULTIPLEXER
FROM OSCILLATOR 38 KC
Threshold Sensing Amplifier
VOLTAGE LADDER AND Σ
TRIGGER
$V_1 + V_2$
Sign Bit
RESET B
A - G operated swit
H - T ground switch
H - T voltage divide
(Initially all divider s
G' F' E' D' C' B'
H I J K L M N
1 0
1 2 3 4 5 6 7 8 9 10 11 12 13 14
"26" SEQUENCE OF J- K "FLIP-FLO
Counter & Decode M

FROM MULTIPLEXER)

,ister to Generate Floating Point

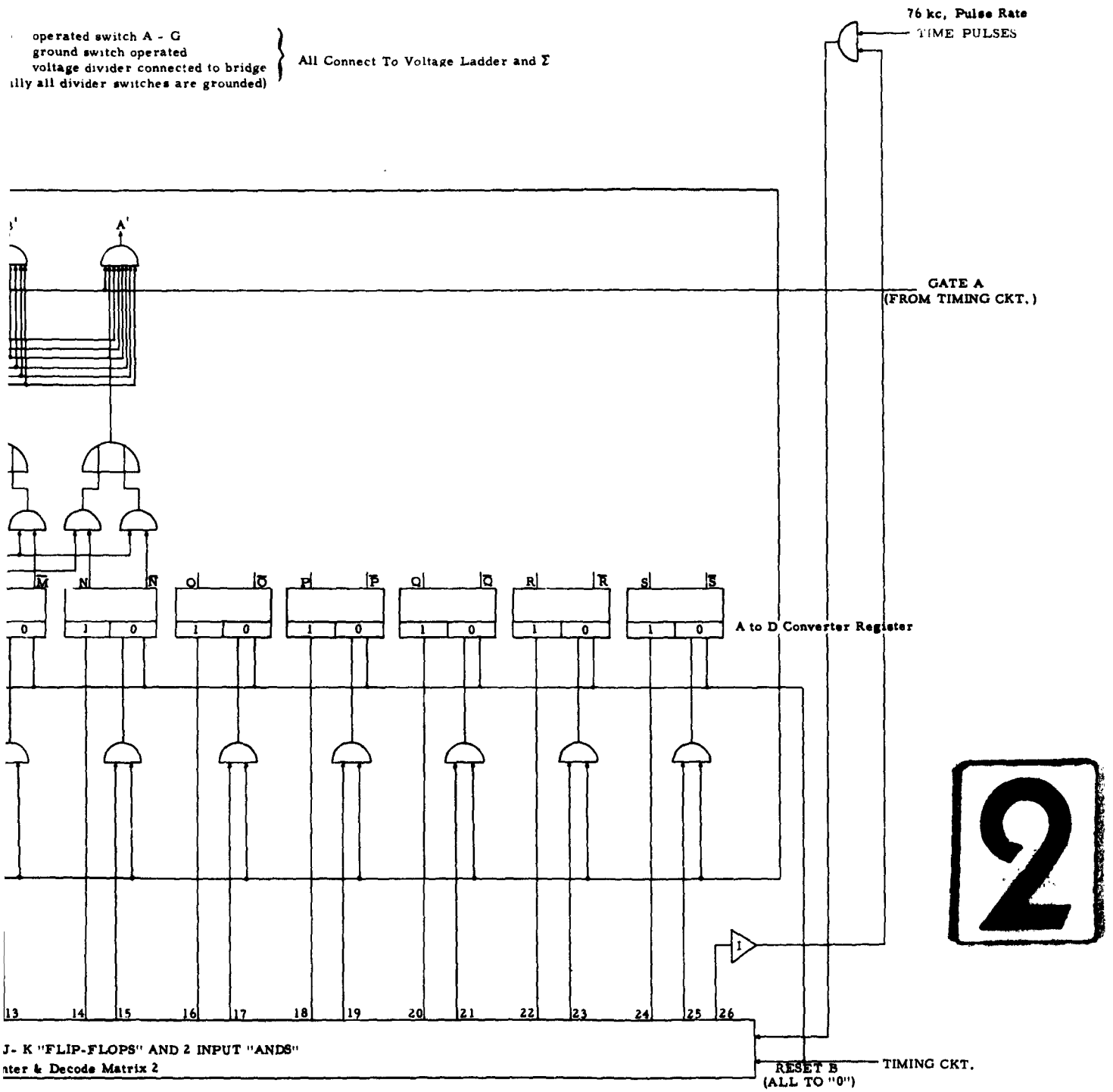

Figure E-14. Bit Decision Logic

The conversion of a sample is complete and the output of the Gain Register is gated to the output format converter for the floating point information. The A-to-D Converter Register is gated out as the 13-bit binary presentation of the input signal.

Figure E-15 illustrates the connection of the voltage ladder and summing junction into the system. Analog switches are under logic control of the Gain Register and the A-to-D Converter Register. Gain switches are reed relays. Ladder switches are conventional two-transistor switches connected for cancellation of V_{CE}.

Major parts of the system described above were fabricated and evaluated. Even though the concept is significant, the variable resolution factor was considered a disadvantage for this application. The FM-Digital approach was chosen for complete engineering and fabrication.

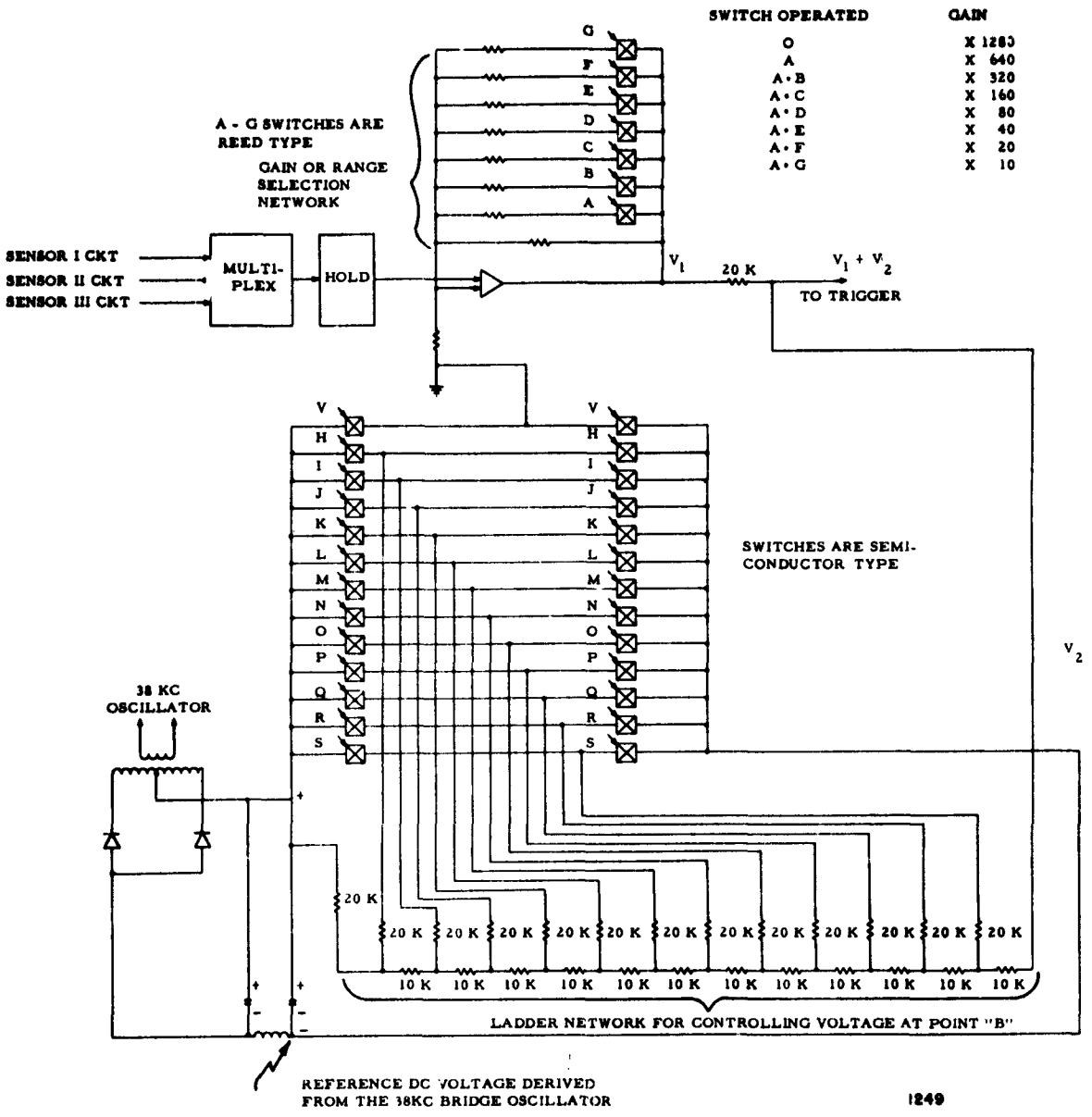

Figure E-15. Voltage Ladder and Summation Network

APPENDIX F

RICE UNIVERSITY RESEARCH CONTRIBUTIONS

During the course of this contract, it has been necessary to give consideration to many factors affecting spring-mass systems, sensor systems, and output formats. The contributions of Rice University have been especially helpful in this regard. Much of their work is included in the appropriate sections of this report.

In addition, we have included the following sections on ancillary topics:

a. Schemes to extend the dynamic range of a system without having to redesign the digital readout instrumentation.

b. Certain considerations of sampling theory aimed at minimizing the aliasing errors of a sampled data system.

c. Special tests performed on the Rice University digital systems leading to unusual measuring capabilities such as a very high-precision tidal gravimeter.

d. A possible way of obtaining high-density recording of digital data.

These topics are discussed in a specially prepared section by Dr. J. Cl. De Bremaecker of the Geology Department of Rice University.

TECHNICAL DISCUSSION

by

Dr. J. Cl. De Bremaecker*

Rice University

A. EXTENSION OF THE DYNAMIC RANGE

Suppose that the scaler (binary counter) of any of the three components of a seismograph system can count up to n. If the number of cycles, k, during the time that the gate of the scaler is open is smaller

* De Bremaecker, J. Cl., Donoho, P., Michel, J. G., "A Direct Digitizing Seismograph," Bull. Seism. Soc. Am., 52: 661-672.

than n, k will be read as such. If $2n > k > n$ then the scaler will read k-n. In general, the scaler will read k - rn where r is not a priori known.

If there are enough readings in every range so that the difference between successive readings, S_i, is smaller than $\sim n/3 = S_o$, then a jump from one range to the next will result in a difference between readings greater than S_o. This difference can be detected by the computer and the readings can be increased (or decreased) by n. This can be done any number of times provided only that in any one range $S_i < S_o$. Everytime an overflow occurs a counter is increased by 1; everytime an underflow occurs the counter is decreased by 1.

For both overflow and underflow to be possible, it is, of course, necessary that the scaler normally overflow at least once. In our practice it overflows twice.

A program has been written and tested on the Rice University computer which performs these operations. The computer possesses the additional feature that no testing takes place if the readings are near the center of the range. In this way, no time is wasted in useless testing of differences.

B. EXTENSION OF THE SAMPLING THEOREM

It is sometimes suggested that a cyclic, but not equally spaced, sampling might reduce aliasing. It has been shown that such is not the case. Cyclic sampling does produce information which differs from that produced by conventional sampling, but it does not produce more information or reduce the aliasing problem. This can easily be shown by expanding the function near one set of points and taking the orthogonality of the sine and cosine series into account.

C. INSTRUMENTAL NOISE

The transistorized Clapp oscillators are now enclosed inside the seismometers in a constant temperature environment. Extensive tests have been run to determine the noise of the instruments, by removing the boom from its hinges and setting it on supports. Under the circumstances the short-term noise is so low that it cannot be measured by conventional electronic counters. The drift does not exceed about ten c.p.s. per hour. As a consequence, the vertical instrument can be used as a very high-precision tidal gravimeter. The need for a low-noise instrument is apparent from recent papers; for instance, Ben-Menahem's measurement of directivity in Pasadena* could not be repeated using the same record because of the relatively wide line made by the spot of the galvanometer.

* Ben-Menahem, A., and Toksöz, M. N., "Source-Mechanism from Spectra of Long-Period Seismic Surface-Waves," J. Geophys. Research, 67: 1943-1955.

D. OUTPUT FORMAT

Some thought has been given and correspondence exchanged on the subject of recording at extremely high packing density on photographic film. It appears possible that, in the fairly near future it will be possible to pack one complete day's record (3 instruments, 20 words/second, 16 bits/word) on 2.5 m (8 feet) of 35 mm. film. This supposes a packing density of 10^6 bits/square inch. Such a density is possible and Eastman Kodak is investigating it. Even at a density 10 times smaller, only 25 m of film per day would be used.

It would appear that the small cost, permanence, impossibility of "correction" of the record and ease of transportation would more than justify the development of such a method.

APPENDIX G

COMMENTS ON MASS-LIMITED SENSITIVITY OF SEISMOMETERS

Because only 250 grams is used for the mass on the Millis-Romberg seismometer, it is appropriate to present a discussion relative to the mass-limited sensitivity of seismometers. This discussion is presented from two viewpoints. The first discussion states that ambient noise earth motion is larger than the effect due to classical theory Brownian movement for a long-period instrument with a small mass. The second discussion relates the output noise power spectrum of the seismometer as a function of the electrical constants, the mechanical constants, and temperature.

A. BROWNIAN MOTION OF A LIGHT WEIGHT SEISMOMETER

1. Introduction

The theory of the Brownian motion is based on the kinetic theory of gases, which explains the observed behavior of gases with the hypothesis that a gas consists of free elastic particles. The particles are in motion and collide with each other according to the laws of dynamics. They do not influence each other except through collisions, and their velocities are so great as to make the effect of earth gravity negligible. When a large number of such particles are confined in a container, their collisions with the walls of the container result in what is grossly measured as pressure. From the way a gas behaves at normal pressures, and from the behavior of gases of different molecular weights, it is deduced that the average kinetic energy of an elastic particle, regardless of its mass, is 3/2 kT, where T is the absolute temperature and k is Boltzmann's constant ($k = 1.36 \times 10^{-16}$ ergs/deg. K).

Brownian motion is "the perpetual irregular motions exhibited by small grains or particles of colloidal size immersed in a fluid. As is now well known, we witness in Brownian movement the phenomenon of molecular agitation on a reduced scale by particles very large on a molecular scale -- so large in fact as to be readily visible in an ultramicroscope. The perpetual motions of the Brownian particles are maintained by fluctuations in the collisions with the molecules of the surrounding fluid. Under normal conditions, in a liquid, a Brownian particle will suffer about 10^{21} collisions per second." (Chandrasekhar, 1943)

The observations of Brownian particles provide the link between the kinetic theory of gases and the motion of gross particles under molecular bombardment. Perrin (1916) watched Brownian particles and found that their behavior conformed with that predicted by theory. The theory of Brownian motion was applied to seismometers by Wolf (1942). This review does not attempt to modify Wolf's treatment; its purpose is merely to refer to the history of the problem, to describe the physics of it plausibly, and to correct a minimum-mass requirement he gave which was based on an underestimate of the amplitude of earth noise at long periods.

2. Brownian Motion of a Free Particle

If a free particle is suspended in a liquid it will move in response to the impact of the molecules of the liquid against it. These impacts will come from no particular direction, but even though their direction and strength are completely random, the particle will move about in such a way that its present movement is not influenced by its past location. According to the theory of probability, it will not favor its starting point, so that at some time t its most probably displacement from where it was at t_o can be calculated. The problem was solved by Einstein (1905) who found the average square of the displacement, $\overline{s}^2$, to be given by

$$\overline{s}^2 = \frac{2kT}{f} t \qquad \text{(G-1)}$$

where f is the coefficient of friction.

3. Extension to a Bound Particle

The solution of the problem can be generalized for particles under the influence of potential-field or harmonic forces. One approach to this generalization is described by Uhlenbeck and Ornstein (1930) who say that for a harmonically bound particle the mean square of the displacement x will be given by

$$\overline{x}^2 = \frac{kT}{m\omega^2} + Fe^{-\beta t} \qquad \text{(G-2)}$$

where m is the mass, ω the angular velocity, β the damping, and F a function of the other terms; F is not required for our purposes because the term containing it decreases with time. We may thus use the well-known expression

$$\overline{x}^2 = \frac{kT}{m\omega^2} \qquad \text{(G-3)}$$

which is equivalent to the original kinetic energy principle which is written

$$\frac{m\bar{v}^2}{2} = \frac{kT}{2} \qquad \text{(G-4)}$$

for the case of one degree of freedom instead of three.

4. Dependence of Motion on Mass and Period

Suppose a particle surrounded by air were constrained to move in one horizontal dimension, but otherwise free to respond to the impact of molecules of gas. It would be likely to be found, after a time, at a little distance from its starting point, just as a colloidal particle is seen to move at random away from any point where it is first observed. The distance it will have traveled can be expressed as a probability, and the probable displacement will vary directly with the square root of the time and inversely with the square root of the mass. Now suppose a restoring force is applied, as though the particle were hung from a string to form a pendulum. It will still move away from its starting point, but the restoring force will continually draw it back, so that it will not now wander away permanently. Its average displacement, considering the algebraic sign, will be zero, but it will still have an absolute displacement, usually expressed as the root mean square. The displacement obviously would be large for a weak restoring force and small for a strong one. This fact is expressed quantitatively in Equation G-3.

5. Quantitative Examples

As a numerical example, consider a mechanical oscillating system with a mass of 100 grams and a period of 1 second, at an absolute temperature of 300°. According to Equation G-3, it will have a root mean square displacement of

$$\sqrt{\bar{x}^2} = 0.33 \times 10^{-8} \text{cm} \qquad \text{(G-5)}$$

or one-thirtieth millimicron. This would limit its usefulness as a sensor of earth motion if the motion to be sensed were small enough in amplitude. According to Frantti and others (1962) the minimum peak-to-peak amplitude of one-second earth noise, from observations at about 30 sites, was one millimicron, or 10^{-7} cm. This would be a root mean square level of about 0.35×10^{-7} cm, larger than the Brownian motion in the proposed oscillating system by a factor of 10. Wolf (1942) points out that this is barely a sufficient margin, for three reasons. First, the Brownian movement ought to be smaller than the movements to be observed by a factor of four or five.

Second, a ground motion at a one-second period is reproduced at only half the amplitude in a seismometer with the same period. Third, the frequency boundary of the receiving system may affect the balance. Using Wolf's formula for a displacement seismometer, which is

$$m\bar{x}^2 \geq (16.7 \times 10^{-14})\, \tau_o^2 \qquad \text{(G-6)}$$

where τ_o is the period of the seismometer and $\bar{x}^2$ is the mean square ground motion to be expected, we arrive at a minimum mass of 133 gm for a one-second seismometer. A one-hundred-gram, one-second seismometer would thus, according to Wolf, be slightly lighter than the safe minimum.

The minimum mass required for sensing earth motions at longer periods can be found by putting into Equation G-6 the period desired and the amplitude of minimum earth noise at that period. Wolf's inference that a mass of 10^4gm would be required at a period of 10 seconds was based on an underestimate of the level of earth noise at that period. The amplitude of earth noise in the range 0.5 to 5 seconds increases faster than its period, according to the observations of Frantti and others (1962). Brune and Oliver (1959) show a minimum of 3×10^{-6} cm at a period of 7 seconds, a thirty-fold increase in amplitude for a seven-fold increase in period. Since period and amplitude appear to the same power in Equations G-6 and G-3, it is plain that masses in the 150 to 200-gm range are large enough even for periods of 20 seconds. Earth noise at longer periods has not been extensively observed, but the earth is known to be in continuous motion, with an amplitude of several centimeters, due to the tidal forces. The periods are greater than those of one-second motion by a factor of 5×10^4, and the amplitudes by a factor of 10^8, showing that the tendency of amplitude to increase faster than period generally continues.

Observations of Brownian motion on gross masses were reviewed by Barnes and Silverman (1934). The Brownian motion of a mirror weighing 0.2 mg was reported by Gerlach and Lehrer (1927) and confirmed by Kappler (1931), who used the results to check the computation of Avogadro's number. An interesting experiment would be to record earth motion simultaneously with three one-second seismometers whose suspended masses were 10 gm, 150 gm, and 300 gm. According to the theory, the two seismometers with the heavy masses should record earth movement without perceptible Brownian movement and therefore give similar recordings. The seismometer with the light mass should record the same earth movement plus its own Brownian motion, which should be detectable by comparing its recording with those of the heavy-mass seismometers. In order to avoid differences in the recordings caused by differences in the level of amplification, the displacements of the seismometers should be sensed by a method whose

sensitivity is largely independent of the suspended mass. (The angular-displacement transducer described by Hasty and Penn in a recent TI report would be such a method.)

REFERENCES

Barnes, R. B., and Silverman, S., 1934 Brownian motion as a natural limit to all measuring processes; Rev. Mod. Phys. v. 6, p. 162-192.

Brune, J. N., and Oliver, Jack, 1959, The seismic noise of the earth's surface; Seismol. Soc. Amer. Bull., v. 49, p. 349-353.

Chandrasekhar, S., 1943, Stochastic problems in physics and astronomy; Rev. Mod. Phys. v. 15, p. 1-89.

Einstein, Albert, 1905 Uber die molekular-kinetische Theorie der geforderten Bewegung von in ruhenden Flussigkeiten suspendierten Teilchen; Ann. d. Physik, v. 17, p. 549-560.

Frantti, G. E., Willis, D. E., and Wilson, J. T., 1962, The spectrum of seismic noise; Seismol. Soc. Amer. Bull. v. 52, p. 113-121.

Gerlach, W., and Lehrer, E., 1927 Uber die Messungen der rotatorischen Brownschen Bewegung mit Hilfe einer Drehwage; Naturwiss, v. 15, p. 15.

Kappler, E., 1931 Versuche zur Messung der Avogadro-Loschmidtschen Zahl aus der Brownschen Bewegung einer Drehwaage; Ann. d. Physik, vol. 11, p. 233.

Uhlenbeck, G. E. and Ornstein, L. S., 1930 On the theory of the Brownian motion; Phys. Rev. v. 36, p. 823-841.

Wolf, Alfred, 1942 The limiting sensitivity of seismic detectors; Geophysics, v. 7, p. 115-122.

B. THERMAL NOISE IN SEISMOMETERS

1. Introduction

Present day seismometers are sensitive enough that it is felt they are capable of detecting random motion caused by thermal agitation. This random motion, which is always present in a system whose temperature is above absolute zero, is called by many names, such as, Brownian motion, thermal noise, Johnston noise, and Nyquist noise. These names all refer to the same basic thermal phenomenon of matter which is dealt with in the fluctuation-dissipation theorem of irreversible thermodynamics.

The purpose of this technical note is to consider the important parameters in the design of a seismometer whose limiting noise is due to thermal agitation.

2. Fluctuation-Dissipation Theorem of Irreversible Thermodynamics

In thermostatics, or as it is more commonly called, thermodynamics, thermodynamical processes are not considered directly. Instead, only equilibrium, stationary states of a system are considered. Thus the name thermostatics. Processes are dealt with indirectly by considering only the initial and final equilibrium states of the system and attributing the change in the system to the process. In the theory of irreversible thermodynamics, the process of change in the thermodynamic system is dealt with directly. From this theory, two main theorems have been derived. The first of these is the Onsager reciprocity theorem. A practical example of the use of the Onsager theorem occurs in the design of thermocouples, where a heat flow produces an electric potential and vice-versa, an electric current flow produces a temperature gradient. The second theorem is the fluctuation-dissipation theorem, which shows that resistance and thermal fluctuation are inseparable phenomena.

In thermostatics, the equilibrium state of a system is commonly specified in terms of sets of conjugate variables. Examples of such pairs of variables are pressure and volume, voltage and electric charge, and force and distance. In these examples, the quantities pressure, voltage, and force are called intensive variables and are denoted in general by F. The quantities volume, electric charge, and distance are called extensive variables and are denoted by Q. In all cases, the product of the intensive variable F and its conjugate extensive variable Q has the dimensions of energy.

In thermodynamics, if the energy of the system and the values of all of the extensive variables Q are known, then the intensive variables F are determined - that is, assuming that the system is in equilibrium. However, if the system is not in equilibrium but is undergoing a process, then knowledge of the energy and the Q's is insufficient to determine the F's. In practice,

it is often found that if the process is not too violent, there is an additional force ΔF over and above the thermostatic force F and that this additional force is proportional to the rate of change of the extensive variable Q. That is,

$$\Delta F = R\dot{Q} \qquad \text{(G-7)}$$

Examples of this are common. When F and Q are force and distance, an example is the slow motion of an object through air, there being a frictional reacting force proportional to the velocity. Likewise, when F and Q are voltage and electric charge, a voltage is produced across a resistor proportional to the current. In the linear form of the fluctuation-dissipation theorem, equation G-7 is assumed to be valid.

In order to speak in familiar terms, the results of the fluctuation-dissipation theorem will be expressed by talking about the special case of voltage, current, and resistance. These results for this special case were first derived by Nyquist.

When a current I is passed through a resistance R, there is a voltage V produced where

$$V = RI. \qquad \text{(G-8)}$$

In this case, electrical power of amount VI is being dissipated into thermal heat in the resistor. From the microscopic point of view, the flowing electrons are colliding with the elementary particles of the resistor and transferring their kinetic energy to these particles. Now, if these resistor particles were rigidly fixed, then the electrons hitting them could not transfer any energy to them. Thus, the resistor particles must be free to move and are in fact moving around in a random manner. Otherwise the resistor would not have any resistance. But, if the resistor particles are in motion, then they have the capability of hitting electrons and transferring their thermal energy to the electrons. This produces a random noise voltage across the resistor. Thus, the fact that a resistor has resistance implies that there is a random noise voltage across it.

Nyquist derived the power spectrum of the noise voltage across an open circuit resistance and found this power spectrum to be white and equal to

$$4kRT, \qquad \text{(G-9)}$$

where k is Boltzmann's constant (1.3804×10^{-23} joules/oK), R is the resistance in ohms and T is the temperature of the resistor in degrees centigrade.

This means that in the frequency range Δf in cycles per second, the mean square voltage across the resistor in volts^2 is given by

$$4kRT\Delta f. \qquad (G\text{-}10)$$

In order to perform noise calculations in an electrical circuit, it is only necessary to put a fictitious voltage generator in series with each resistor in the circuit, where the voltage power spectrum is given by

$$4kRT. \qquad (G\text{-}11)$$

This procedure is valid even when the resistors are at different temperatures.

Likewise, for example, if the frictional force, F, of an object moving through the air with velocity v is given by

$$F = Kv \qquad (G\text{-}12)$$

where Fv is measured in watts, then the force power spectrum is given by

$$4kKT. \qquad (G\text{-}13)$$

That is, the mean square value of F in the frequency range Δf is given by

$$4kKT\Delta f. \qquad (G\text{-}14)$$

We will now use Nyquist's formulation of thermal noise in an electric circuit and show its consistency and derive some well-known results.

3. Thermal Noise in an Electric Circuit

The first problem will be to derive the noise voltage in a circuit consisting of two resistors R_1 and R_2, each at the same temperature T and hooked in parallel. In particular, what is the voltage power spectrum between A and B?

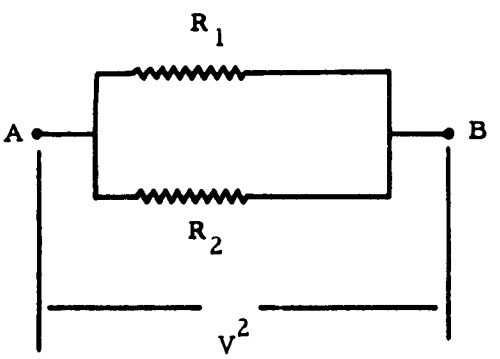

Figure G-1

Fictitious generators are placed in series with each of the resistors to give the following diagram.

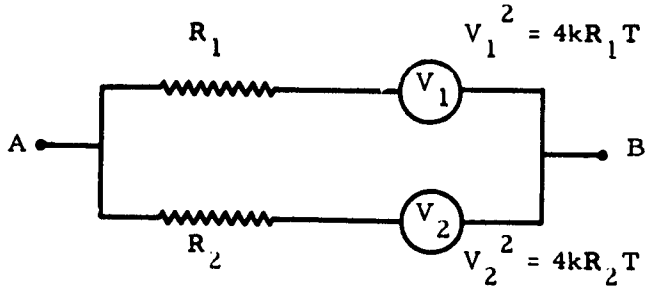

Figure G-2

Now the voltage across A and B due to V_1 alone is given by

$$\frac{R_2}{R_1 + R_2} \quad V_1, \tag{G-15}$$

and the voltage power spectrum due to V_1 is thus given by

$$\left(\frac{R_2}{R_1 + R_2}\right)^2 \overline{V_1^2} = \left(\frac{R_2}{R_1 + R_2}\right)^2 4kR_1T. \tag{G-16}$$

Likewise the voltage power spectrum across A and B due to V_2 alone is given by

$$\left(\frac{R_1}{R_1 + R_2}\right)^2 \overline{V_2^2} = \left(\frac{R_1}{R_1 + R_2}\right)^2 4kR_2T. \tag{G-17}$$

Now, the fictitious voltage generators are taken to be uncorrelated in their voltage outputs, so that the total mean square voltage across A and B is the sum of the individual mean square voltages from V_1 and V_2. Thus the total voltage power spectrum across A and B is

$$4kT\left[\left(\frac{R_2}{R_1 + R_2}\right)^2 R_1 + \left(\frac{R_2}{R_1 + R_2}\right)^2 R_2\right] = 4kt\,\frac{R_1R_2}{R_1 + R_2}.$$

But this result could have been derived directly, since the total resistance across A and B is given by

$$\frac{R_1R_2}{R_1 + R_2} \tag{G-18}$$

and thus the voltage power spectrum across A and B is

$$4kT \frac{R_1 R_2}{R_1 + R_2} . \qquad \text{(G-19)}$$

This problem was set up to show that the Nyquist formulation does lead to consistent answers.

Consider now the following problem. We have a circuit made up of a pure resistance R and a pure inductor L in parallel.

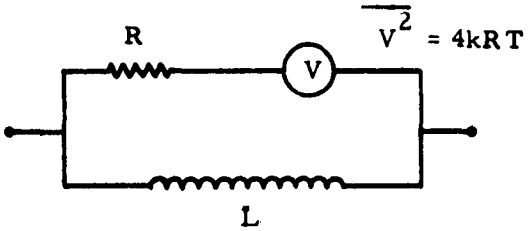

Figure G-3

Here the fictitious noise voltage generator is already shown in series with the resistor. What is the noise voltage power spectrum across L?

The voltage across L at frequency f due to the generator is given by

$$\frac{i2\pi fL}{R + i2\pi fL} V \qquad \text{(G-20)}$$

and the voltage power spectrum at frequency f is thus given by

$$\left| \frac{i2\pi fL}{R + i2\pi fL} \right|^2 \overline{V^2} = \frac{(2\pi fL)^2}{R^2 + (2\pi fL)^2} 4kRT. \qquad \text{(G-21)}$$

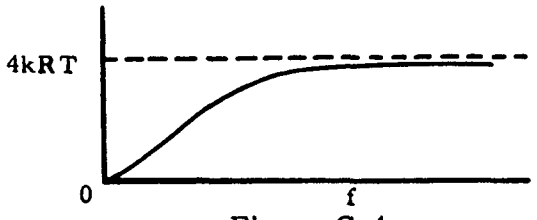

Figure G-4

Now, what is the average energy contained in L? That is, what is the average energy contained in the magnetic field of the inductor?

An expression for this energy is given by

$$\frac{1}{2} L \overline{I^2} \qquad \text{(G-22)}$$

where $\overline{I^2}$ is the total average square current in the inductor. Since the current in L at frequency f due to V is given by

$$\frac{V}{R + i2\pi fL}, \qquad \text{(G-23)}$$

we find that the power spectrum of I is given by

$$\frac{\overline{V^2}}{R^2 + (2\pi fL)^2} = \frac{4kRT}{R^2 + (2\pi fL)^2} . \qquad \text{(G-24)}$$

The total average square current is given by integrating the frequency power spectrum I from 0 to ∞.

$$\overline{I^2} = \int_0^\infty \frac{4kRT}{R^2 + (2\pi fL)^2} \, df = 4kRT \, \frac{1}{2\pi RL} \tan^{-1} \frac{f2\pi RL}{R} \Bigg|_0^\infty$$

$$= \frac{4kRT}{2\pi RL} \left(\frac{\pi}{2} - 0\right) = \frac{kT}{L} . \qquad \text{(G-25)}$$

Thus the total average energy in L is given by

$$\frac{1}{2} L \overline{I^2} = \frac{1}{2} kT . \qquad \text{(G-26)}$$

This is a well-known result. Note that it depends only on the temperature of the circuit and is independent of the resistance of the resistor and the inductance of the inductor.

If the inductor were replaced by a condenser of capacitance C, the average energy contained in the electric field of the condenser would be found to be 1/2 kT also. Mathematically, the inductor and the capacitor both correspond to one degree of freedom, and a familiar result in statistical mechanics is that the average energy is 1/2 kT, at temperature T, in each degree of freedom of a system. In the seismometer system, where there is a mass on a spring, the motion of the mass is a degree of freedom and the average thermal noise kinetic energy of the mass is 1/2 kT, depending only on the temperature of the seismometer and not on its mass. Likewise the spring is a degree of freedom and its average potential energy is 1/2 kT, independent of its spring constant.

It must be realized, however, that while the total average kinetic energy of the mass, M, of a seismometer is 1/2 kT and is independent of the parameters of the seismometers, this does not mean that the power spectrum P(v) of its velocity is independent of design parameters of the seismometer. These 1/2 kT statements only mean that

$$\frac{1}{2}M \int_0^\infty P(v)\, df = \frac{1}{2} kT. \qquad \text{(G-27)}$$

That is, P(v) is contained to satisfy this equation, but otherwise P(v) is free to be any arbitrary positive function of frequency.

4. The Thermal Noise in a Simple Seismometer System

Suppose that we have a simple seismometer system made up of a mass on a spring and where the motion of the mass is detected by a coil which has a damping resistor across it.

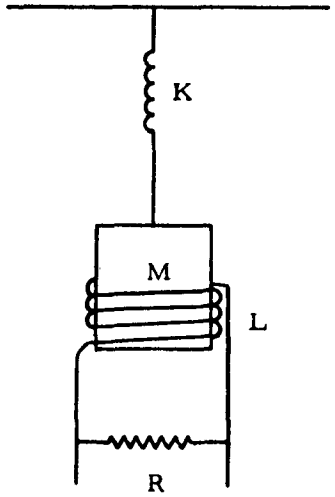

Figure G-5

Let K be the spring constant, M the mass of the seismometer, L the inductance of the coil and R the resistance of the damping resistor. Furthermore, let r be the mechanical damping factor, where the frictional force is given by r times the velocity v of the seismometer mass.

In connecting the mechanical and electrical parts of this system, let the open circuit voltage E_c across the coil be given by C times the velocity of the mass. That is,

$$E_c = Cv. \qquad \text{(G-28)}$$

This equation implies that a current I through the coil produces a force on the mass of magnitude CI. This can be derived by assuming that while the mass is moving with velocity v and producing a voltage E_c across the coil, a current I is made to flow along with the voltage so that the coil puts out power equal to IE_c. This power comes from the mass moving against the reacting force, F_c, due to the current. Now

$$IE_c = ICv = F_c v,$$

and thus,

$$F_c = CI. \tag{G-29}$$

Using Newton's law of motion, the mechanical equation for the displacement X of the mass from its equilibrium point under a mechanical force F(t) is given by

$$M\ddot{x} = -KX - r\dot{x} - F_c + F(t), \text{ or}$$
$$M\ddot{x} + r\dot{x} + KX + CI = F(t). \tag{G-30}$$

The electrical equation for the current through the circuit due to a voltage generator E(t) in series with the resistor is given by

$$E(t) = IR + L\dot{I} - E_c, \text{ or}$$
$$IR + L\dot{I} - C\dot{x} = E(t). \tag{G-31}$$

The following diagram illustrates these equations.

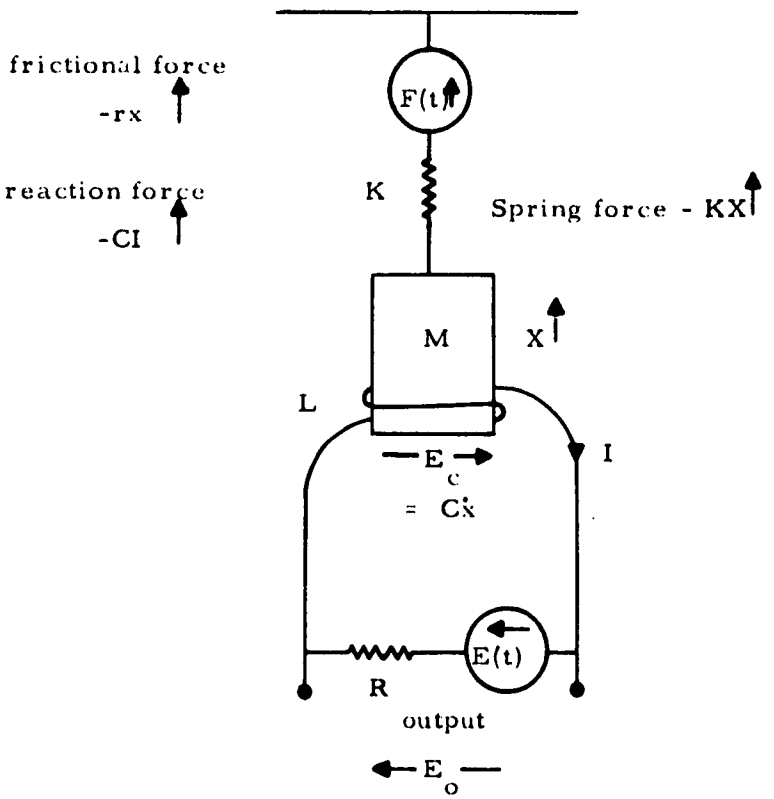

Figure G-6

Let us first assume that $E(t) = 0$, and find the output E_o due to $f(t)$. Letting $f(t) = e^{i\omega t}$ and assuming that

$$X = Ae^{i\omega t}$$

and $$I = Be^{i\omega t}$$

we have from equations G-30 and G-31

$$e^{i\omega t} = -M\omega^2 Ae^{i\omega t} + ir\omega\, Ae^{i\omega t} + KAe^{i\omega t} + CBe^{i\omega t}, \text{ or}$$

$$(-M\omega^2 + ir\omega + K)\, A + CB = 1 \qquad \text{(G-32)}$$

and

$$BRe^{i\omega t} + i\omega LBe^{i\omega t} - i\omega CAe^{i\omega t} = 0, \text{ or}$$

$$-i\omega CA + (R + i\omega L)\, B = 0. \qquad \text{(G-33)}$$

Solving for A and B gives

$$A = \frac{R + i\omega L}{(-M\omega^2 + K + ir\omega)(R + i\omega L) + i\omega C^2}$$

and

$$B = \frac{-i\omega C}{(-M\omega^2 + K + ir\omega)(R + i\omega L) + i\omega C^2}$$

Now, since $E_o = RI$, we have

$$E_o = \frac{-i\omega CR}{(-M\omega^2 + K + ir\omega)(R + i\omega \ell) + i\omega C^2}\, \rho^{i\omega t}. \qquad \text{(G-34)}$$

Assuming next that $f(t) = 0$, $E(t) = e^{i\omega t}$, $X = Ae^{i\omega t}$ and $I = Be^{i\omega t}$, we obtain from equations G-30 and G-31

$$(-M\omega^2 + ir\omega + K)\, A + CB = 0$$

and

$$-i\omega CA + (R + i\omega L)\, B = \ell.$$

The solution for B is

$$B = \frac{-M\omega^2 + ir\omega + K}{(-M\omega^2 + ir\omega + K)(R + i\omega L) + i\omega C^2} .$$

Now, since $E_o = E(t) - IR$, we have

$$E_o = e^{i\omega t} - \frac{(-M\omega^2 + ir\omega + K) R^{i\omega t}}{(-M\omega^2 + ir\omega + K)(R + i\omega L) + i\omega C^2}$$

$$= \frac{(-M\omega^2 + ir\omega + K) i\omega L + i\omega C^2}{(-M\omega^2 + ir\omega + K)(R + i\omega L) + i\omega C^2} \rho^{i\omega t} . \qquad (G\text{-}35)$$

To find the power spectrum of E_o due to the thermal noise from the resistances r and R, we only need note that the power spectrum of the noise force due to r is given by

$$4krT$$

and the power spectrum of the noise voltage due to R is given by

$$4\ kRT.$$

From equations G-34 and G-35 we find that the total power spectrum of E_o is given by

$$\frac{\left|- i\omega CR\right|^2 \ 4krT}{\left|(-M\omega^2 + K + ir\omega)(R + i\omega L) + i\omega C^2\sqrt{2}\right|} + \frac{\left|(-M\omega^2 + ir\omega + K) i\omega L + i\omega C^2\right|^2 \ 4kRT}{\left|(-M\omega^2 + ir\omega + K)(R + i\omega L) + i\omega C^2\right|^2}$$

assuming that the whole seismometer system is at temperature T.

APPENDIX H

SYSTEM EVALUATION

This appendix presents a technical discussion of the proposed system evaluation techniques for determining frequency response, linearity and dynamic range, and response to environmental variations. Background information on time domain mapping explains certain theoretical concepts that will be utilized.

PART I

FREQUENCY RESPONSE

The frequency response of the digital seismograph will be determined in two ways: by absolute calibration of the system, and by shake-table data. Here absolute calibration is understood to mean calibration of the system for both phase and amplitude response while shake-table calibration is meant to imply only amplitude response determination.

A. ABSOLUTE CALIBRATION

The substance of the method exists in the Fourier analysis of the system output pulse (derived either from a weight lift or a calibration coil pulse) and appropriate modifications of the resulting spectrum that both convert it into the system transfer function and assign absolute values.

1. Technical Discussion

Consider first the familiar model of a seismometer shown in Figure H-1. It is possible to excite the mass, M, into motion either by applying a force, f(t), directly to the mass of by displacing the base of the system. The equation of motion may be written

$$M\frac{d^2x}{dt^2} + B\frac{dx}{dt} + Kx = M\frac{d^2y}{dt^2} + f(t) \qquad \text{(H-1)}$$

or in terms of the Laplace transform variable, $s = \sigma + j\omega$

$$(Ms^2 + Bs + K)\,X(s) = Ms^2\,Y(s) + F(s). \qquad \text{(H-2)}$$

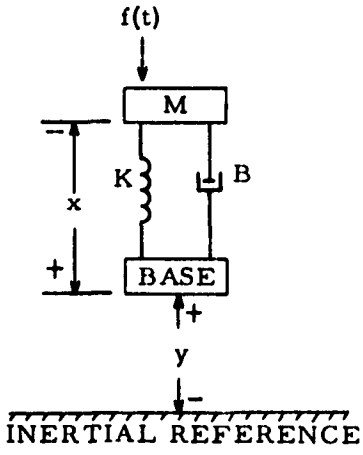

Figure H-1
Simple Model of a Seismometer

Under the assumption of no base input motion, that is, y(t) and all its derivatives are zero, the transformed displacement $X_1(s)$ is given by

$$X_1(s) = \frac{F(s)}{Ms^2 + Bs + K} \qquad \text{(H-3)}$$

when the mass is excited by the force f(t) whose transform is F(s).

If now it is assumed that no force is applied to the mass, f(t) is zero and that the mass is excited by a frame displacement, y(t), the transformed mass displacement, $X_2(s)$, is then given by

$$X_2(s) = \frac{Ms^2}{Ms^2 + Bs + K} Y(s) \qquad \text{(H-4)}$$

Thus, the frame displacement, $Y_e(s)$, that would give the same mass displacement, X(s), as the application of the force F(s), is

$$Y_e(s) = \frac{F(s)}{Ms^2} \qquad \text{(H-5)}$$

from setting $X_1(s)$ equal to $X_2(s)$. Note that the system function, $Ms^2 + Bs + K$, cancels in the formation of Equation H-5. Consequently, neither the detailed form of the mechanical system nor the comparative values of its parameters influence this relation.

The transfer function desired is that of the entire system with $0_1(jf)$ regarded as the spectrum of the system output and $Y_e(jf)$ as the spectrum of the earth-motion displacement input. Hence

$$H_o(jf) = \frac{0_1(jf)}{Y_e(jf)} \qquad \text{(H-6)}$$

Evaluating Equation 6 by means of Equation 5 gives, for $s = j2\pi f$,

$$H_o(jf) = -0_1(jf) \frac{4\pi^2 f^2 M}{F(jf)} \qquad \text{(H-7)}$$

A weight lift (or equivalent calibration coil pulse) imparts to the mass a step function of force given by

$$F(jf) = - \frac{mg}{j2\pi f} \qquad \text{(H-8)}$$

where m is the mass of the weight and g is the acceleration of gravity. Consequently,

$$H_o(jf) = j0_1(jf) \frac{8\pi^3 M}{mg} f^3 \qquad \text{(H-9)}$$

and the output pulse spectrum is modified as desired into the system transfer function and placed on an absolute basis. It is convenient to write Equation 9 as

$$\left|H_o(jf)\right| = \frac{8\pi^3 f^3 M}{mg} \left| 0_1(jf) \right| \qquad \text{(H-10)}$$

the system amplitude response, and

$$\angle H_o(jf) = \angle 0_1(jf) + \frac{\pi}{2} \qquad \text{(H-11)}$$

the system phase response.

The model of an actual seismometer operated in a system comprising, for example, a Phototube Amplifier (PTA) and other amplifiers and electrical filters is much more involved than the simple system just considered. Nonetheless, the foregoing development illustrates that regardless of the system complexity, it is possible to relate the effect produced by a weight lift to that produced by earth motion of the seismometer base. Of equal importance is the fact that no particular relation among the system parameters need be assumed; i.e., undamped resonant frequency and damping factors are not required to have any particular values. A third advantage of considerable practical importance is that complete amplitude and phase response data are obtainable from a short, simple field operation, and the lengthy procedure of measuring frequency response (which fails to give accurate phase data) is avoided.

2. An Actual System Example

The block diagram in Figure H-2 illustrates a portion of the field setup employed in the Rome field experiment * in which the proposed calibration procedure was used.

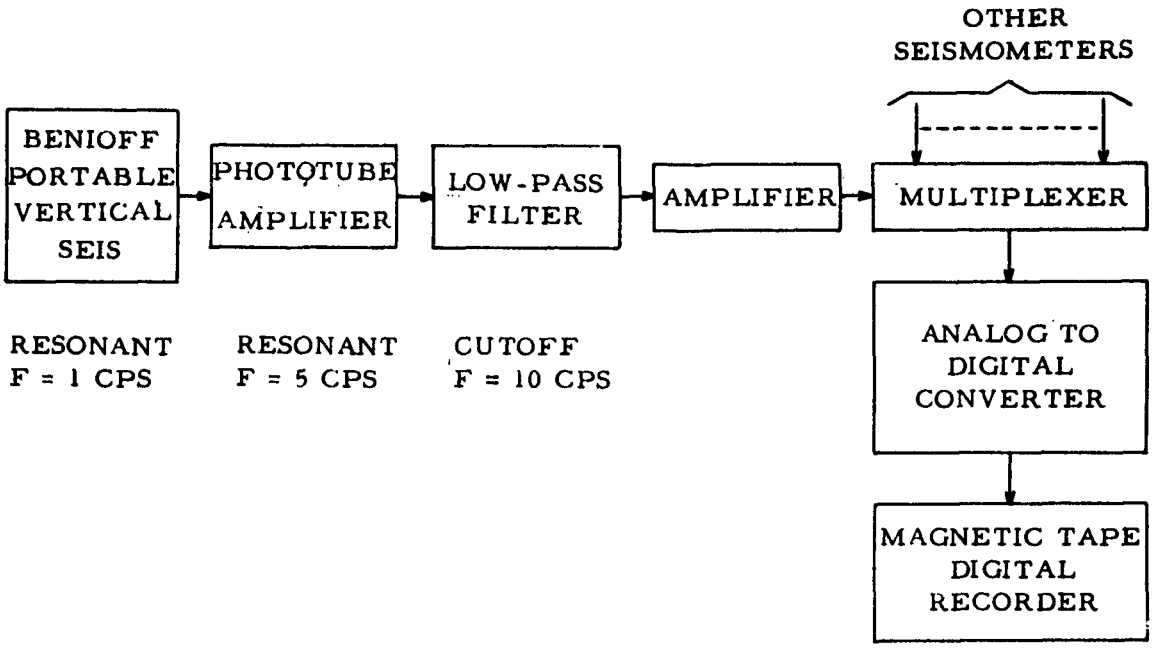

Figure H-2. Block Diagram of a Typical Seismometer Channel of the Rome Field Experiment

Figure H-3 presents a plot of the digitized weight-lift output pulse as obtained from the digitally recorded field magnetic tape. The units of the ordinate are the decimal numbers produced by the analog-to-digital converter. The waveform shown was reconstructed from 40 samples taken at 50-millisecond intervals.

The amplitude density spectrum of the pulse is presented in Figure H-4. Because the pulse is an aperiodic function, its Fourier transform has the dimensions of a density function (Energy/cps). The ordinate, therefore, is in arithmetic units per unit of frequency (cps) and is dimensionally the square root of energy density.

The shape of the system transfer function, $H_o(jf)$, is shown in Figure H-5 for PTA gain setting of 0 db and the remainder of the system in the Record Mode.

* Rock Strata Propagation Studies, Final Report, Contract No. AF 30(602)-2113 for RADC (20 October 1962).

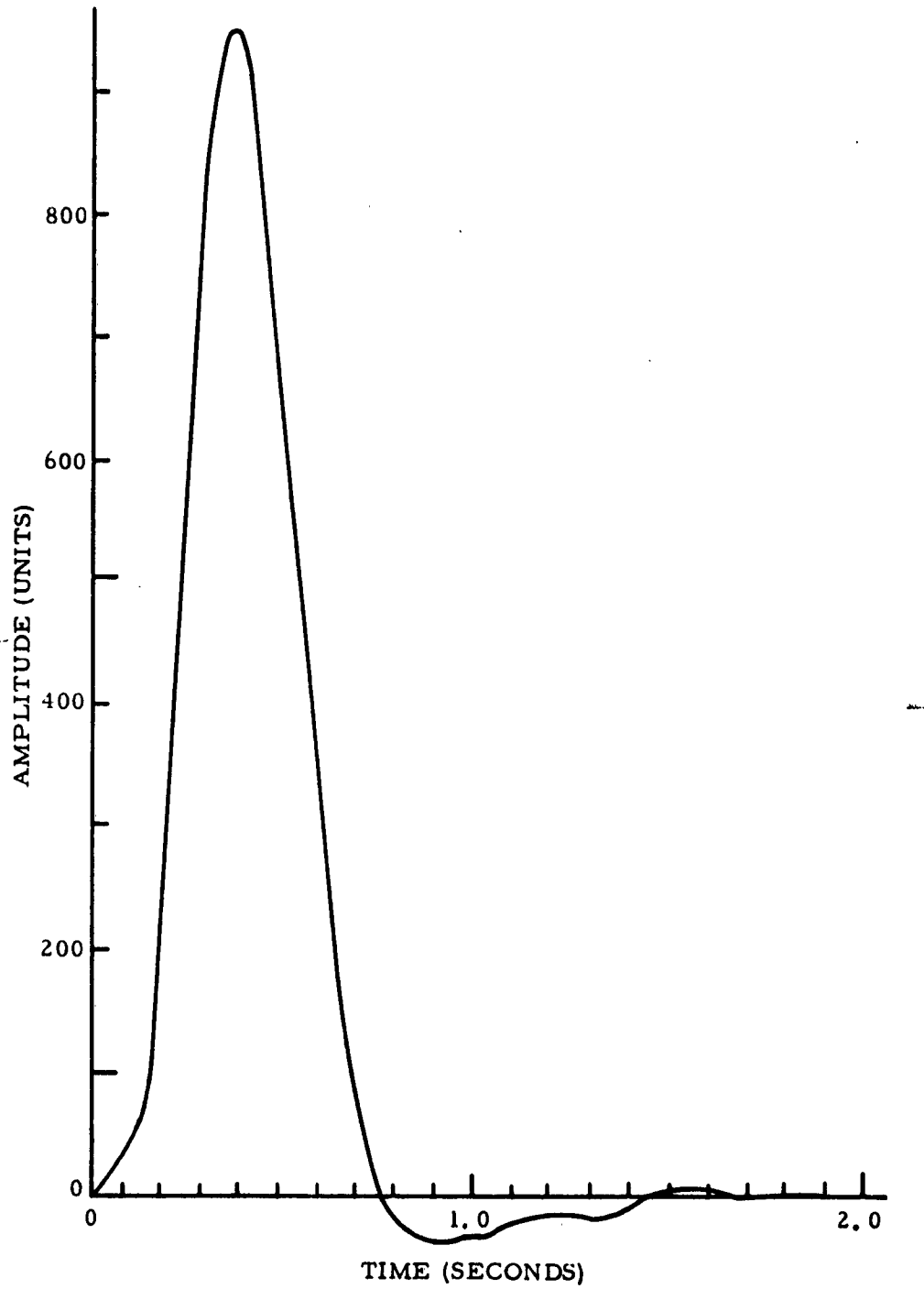

Figure H-3. Plot of Digitized Weight-Lift Output Pulse

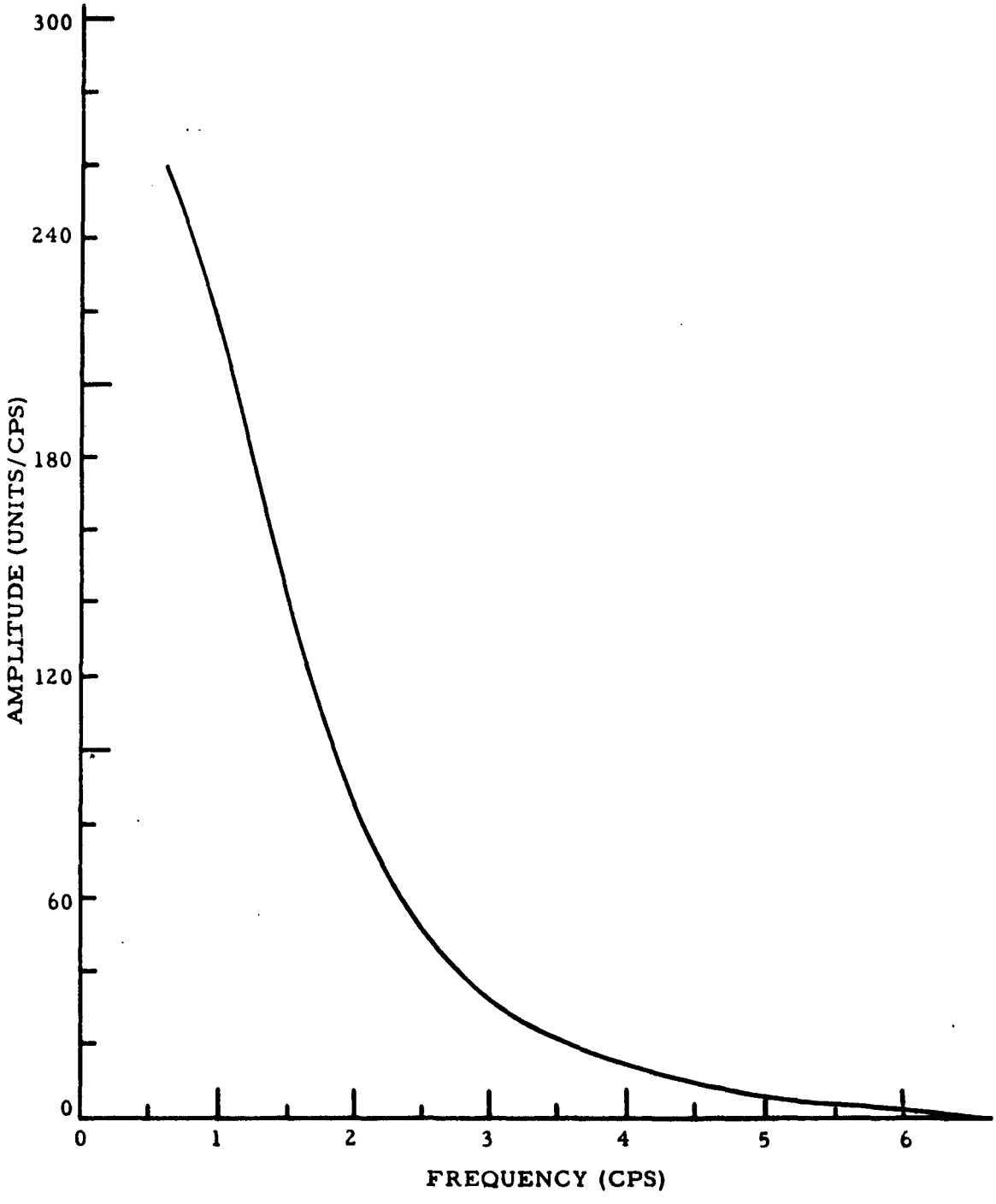

Figure H-4. Amplitude Density Spectrum of Weight-Lift Output Pulse

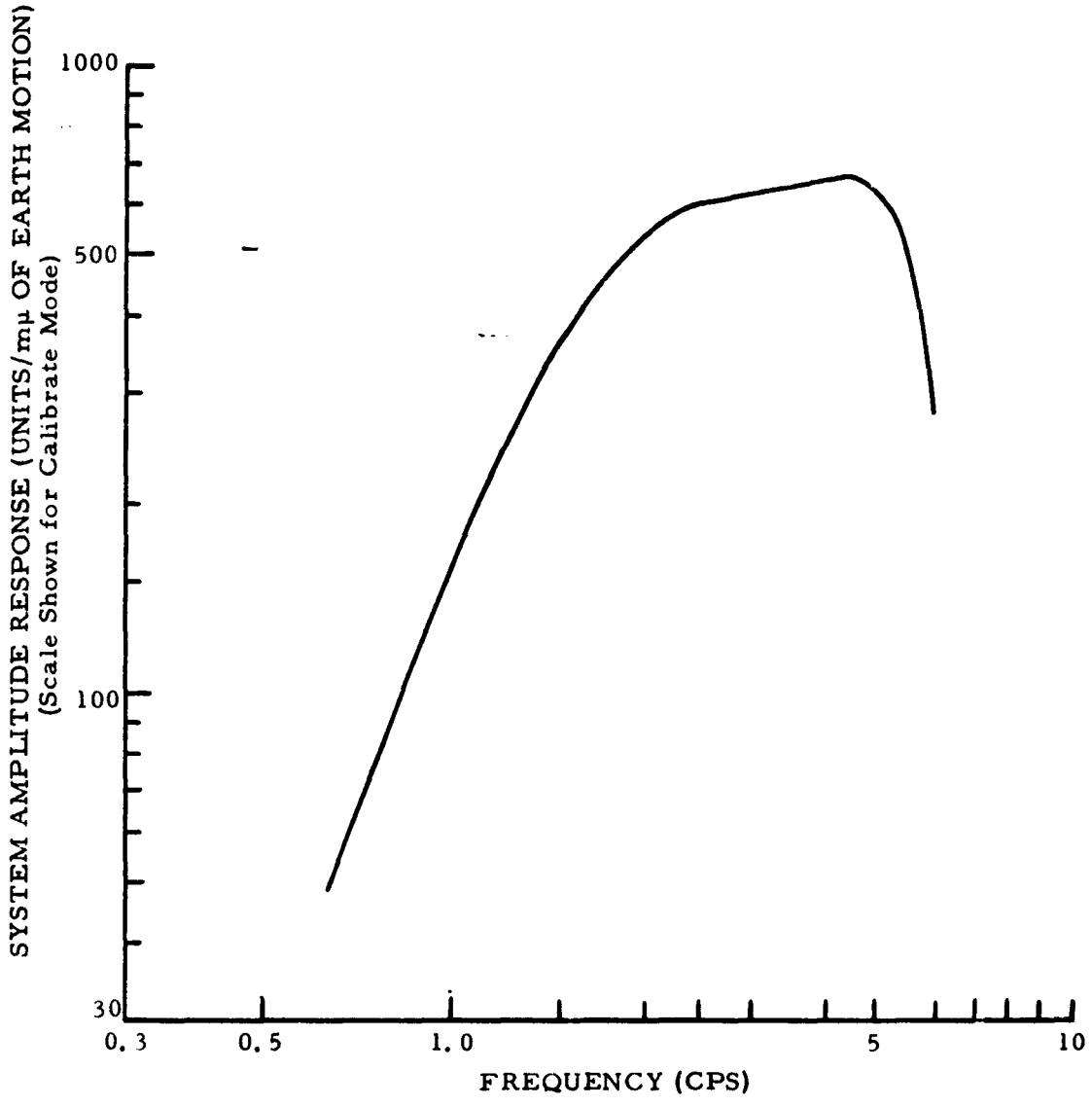

Figure H-5. System Transfer Function, $H_o(jf)$

The numerical values for the ordinates for Figures H-5 and H-6 were obtained by evaluating Equations H-10 and H-11 for

M = 15 Kg

m = 200 mg

g = 980 cm/sec^2

PTA gain = -36 db

System mode * = "Calibrate"

and then are obtained from Equation

* The field system contains a provision for changing certain amplifier gains by a factor of 6 for either calibrating or recording.

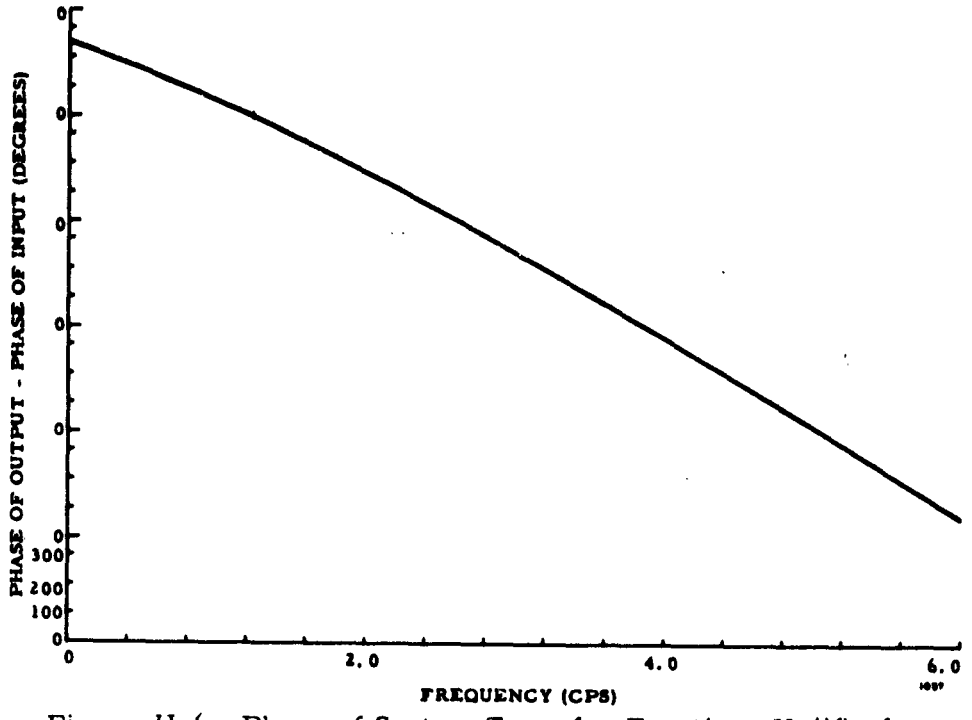

Figure H-6. Phase of System Transfer Function, $H_o(jf)$, for Phototube Amplifier Gain of 0 db and the System in Record Mode

$$\left|H_o(jf)\right| = 1.9 \times 10^{-3} f^3 \left|0_1(jf)\right| \text{ units/m}\mu \qquad \text{(H-12)}$$

or, for a PTA gain of 0 db and the system in the Record Mode (total gain ratio increase of 384) as shown in Figures H-5 and H-6,

$$\left|H_o(jf)\right| = 0.73 f^3 \left|0_1(jf)\right| \text{ units/m}\mu \qquad \text{(H-13)}$$

3. Comparison of Results and Discussion

It is of interest to compare these results with shake-table data provided by the Geotechnical Corporation in the Operation and Maintenance Manual for the Benioff Portable Seismometers. These data show that a 200 milligram weight-lift produces the same output pulse peak amplitude as a 2150 millimicron peak-to-peak displacement of the seismometer base at a frequency of 1 cps.

From the data comprising Figure H-3, the peak amplitude of the digitized weight-lift output pulse is found to be 951 units. Because the system gain was 384 times lower for the recording of the weight-lift pulse than the gain used for determining the ordinate values for Figures H-5 and H-6, the equivalent pulse peak amplitude to use with those curves is 951 x 384 or 365,500 units. From Figure H-5, the magnitude of the system response at 1 cps is seen to be 161 units/millimicron of earth-motion displacement. Consequently, the equivalent peak-to-peak steady-state sinusoidal earth-motion displacement of the seismometer frame would be 365,500/161 or 2270 millimicrons, as compared with 2150 millimicrons from the Geotech data. These

two results yield a 3.2 per cent deviation, which is an exceptional agreement in consideration of the possibility, among others, that the field seismometer may not have been adjusted the same as the laboratory unit.

B. SHAKE TABLE DATA

As a secondary check of the method of determining the absolute system response of the digital seismograph system, shake table data will be recorded using the Texas Instruments designed and built shake table shown in Figure H-7. The 11-inch by 15-inch table is supported by three vertically mounted steel leaf springs. A direct-coupled transistor amplifier feeding about three watts to a loudspeaker mounted on the base provides the driving force.

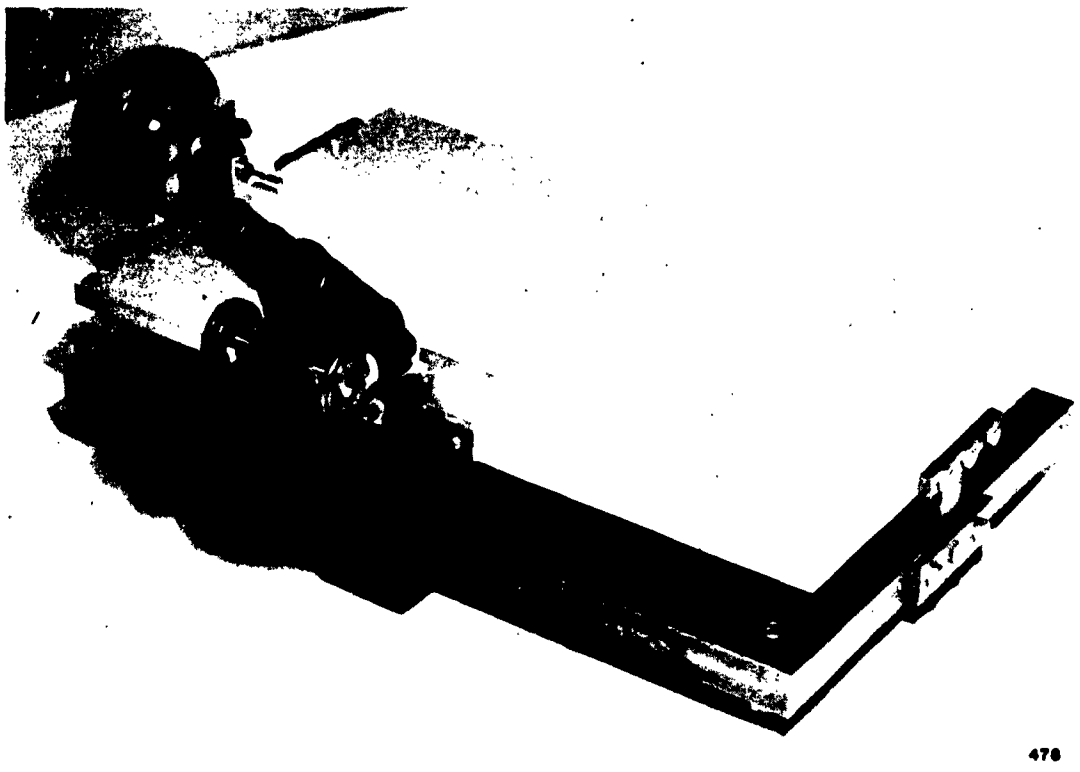

Figure H-7. Shake Table

The shake table is calibrated by means of a microscope focused on a microscope stage micrometer slide mounted on the table, and displacements of about 2 microns can be measured for slides with 10-micron divisions. A strobe light enables the amplitudes to be measured at frequencies higher than a few cycles per second. In addition to this method, a linear differential transducer will be used as a monitor of non-periodic excitations.

With the seismometer in place, the table has a usable frequency range from about 0.1 up to about 20 cycles per second. By maintaining a constant amplitude at each test frequency, a curve of seismometer output versus frequency for constant input can be measured. This method will only be used as a secondary check of the absolute method presented above, however, since it is limited at the low frequency end and phase response is not readily obtainable.

PART II

DETERMINATION OF LINEARITY AND DYNAMIC RANGE

The determination of linearity and dynamic range of the digital seismograph will be made by testing the input-output relationship for the frequency range of interest. Ideally, the linearity and dynamic range would be completely determined by a family of curves similar to those presented in Figure H-8a. This figure is a schematic example of a plot of the output numbers as a function of input base displacement for a system having a response like the schematic example presented in Figure H-8b. Each curve represents the relationship for a constant frequency and extends from the lower dynamic limit, limited by the noise of the system, to the maximum dynamic limit set by the digital system. The curves indicate that this example system is linear over the frequency band f_1 to f_n for an input base motion varying over the range A to B. The range A to B is, therefore, the dynamic range for which the system is linear for the indicated band of frequencies. If the input motion were band limited, however, to include only those frequencies extending from f_3 to f_{n-2}, which coincide in the figure due to a constant system response over this region, the system would be linear over the dynamic range A to C.

Curves such as those presented in Figure H-8a will be obtained for the digital seismometer by exciting the seismometer mass with a force function that has a known equivalent base displacement spectrum and computing the transform of the system output. The process will be repeated for a number of values of the forcing function to give two families of curves for input motion and output numbers.

Figure H-9 presents a schematic in which the equivalent input base displacement spectrum was chosen to be white for the purpose of demonstrating how the method will work. The force function will be applied to the mass a number of times with different magnitude for each trial, A through B. The output for each trial will be recorded on an Ampex FR 400 with formatting compatible with the TIAC computer. Next, the transform of the output will be computed to give the family of curves presented in Part III of Figure H-9. From the input amplitude spectrum in Part I of the figure and the output spectrum, an input-output curve like that in Figure H-8a can be determined by plotting the output as a function of input for a constant frequency.

The mass exciting function for obtaining data like that presented in Figure H-9 will be a step function in force, which can be easily implemented

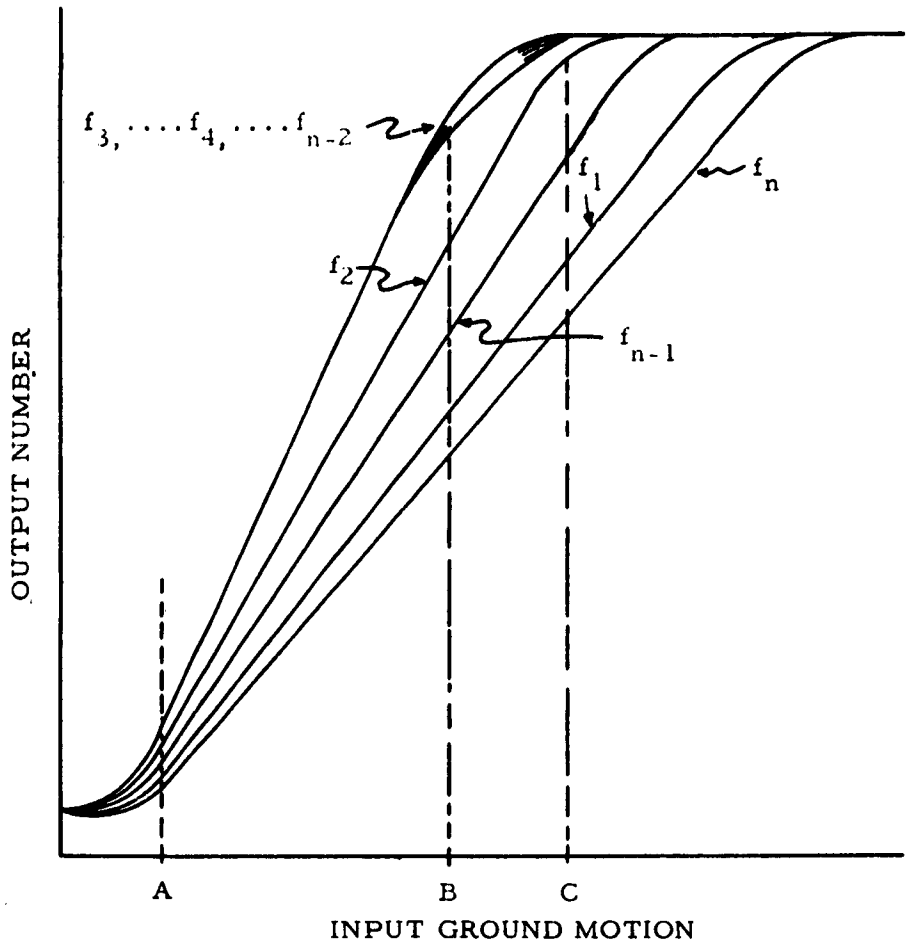

Figure H-8a. Schematic Example of Linearity and Dynamic Range Curves

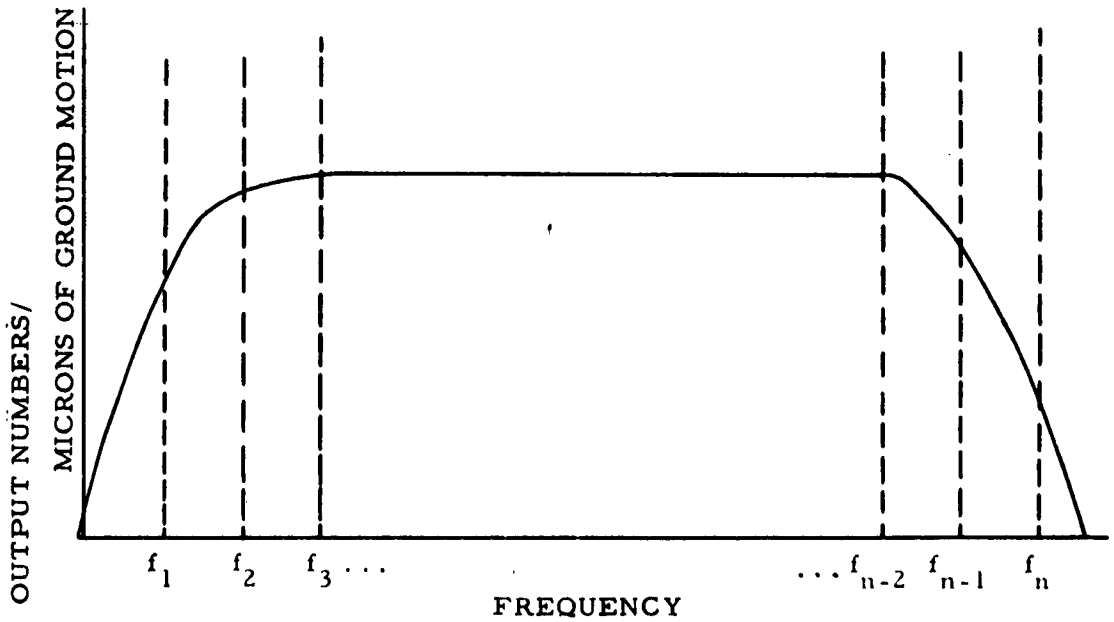

Figure H-8b. Schematic Example of System Response

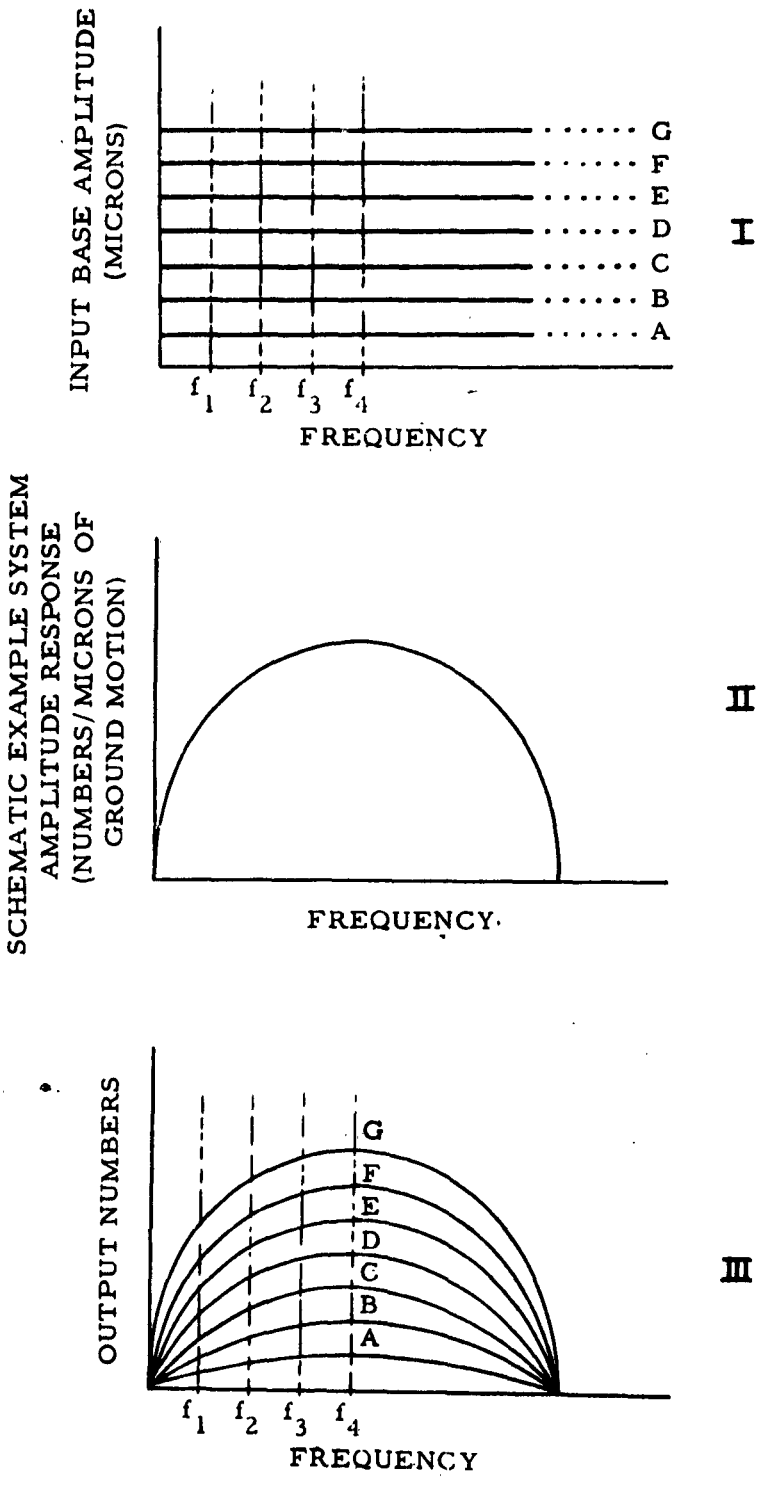

Figure H-9. Schematic Example of Curves to be used for Linearity and Dynamic Range Determination

by a weight-lift on the vertical instrument and by displacing the boom of the horizontal instrument a known distance and releasing it. It can be shown by Equations H-5 and H-8 that the step function of force at the mass has an equivalent base displacement spectrum

$$Y(jf) = -j \frac{mg}{M 8 \pi^3 f^3}$$

where m is the mass of the weight lifted and M is the prime mass of the seismometer. The input spectra can easily be incremented in magnitude by changing the weight of the mass m. This particular method of exciting the mass was chosen because of the simplicity of operation and because the same data can be used to determine absolute seismometer response as outlined eariler. It may be that since the equivalent input spectrum falls off as a function of the inverse of the cube of frequency for a step function, the possible input magnitude at higher frequencies will not yield all of the information needed over the desired dynamic range. If this proves to be true, the prime mass will be driven with a force function such as blue noise (spectral amplitude is proportional to the square of the frequency) or a sine wave, to extend the higher frequency linearity curves to the desired magnitude. Such forces would be applied by means of a calibration coil (calibrated by a weight-lift) attached to the prime mass of the seismometer.

The shake table will be used as a secondary test of linearity and dynamic range but will not be used for the complete test since it is limited in lower frequency to 0.1 cps and lower amplitude to 2 microns.

It is also proposed to perform a static linearity test by displacing the prime mass in small increments between the equilibrium position and 100 microns displacement. The mass will be displaced by adding weights to the vertical and applying known horizontal forces to the boom of the horizontal instruments. Displacement will be determined by optical methods or computational procedures relating displacement to applied force.

PART III

TIME DOMAIN MAPPING

In addition to characteristic determinations, the system evaluation will include a demonstration of the usefulness of the digital seismometer. Since the bandpass and dynamic range of this system overlaps and exceeds that of most of the conventional seismometers in use today, it will be possible to obtain a least-mean-square estimate of the output of any of these instruments by proper numerical filtering of the digital seismometer output. Probably the most important possibility offered by the wide bandpass and dynamic range, however, is that of being able to estimate the output of a seismometer having any desired response even though a seismometer having such a response is not physically realizable. An example of such an application would be to simulate a seismometer having negligible response to 6-second-period seismic noise and phase distortion in that period range.

Obtaining the output of a conventional seismometer, like a Benioff, will be demonstrated by digitally recording seismic signals simultaneously with the digital seismometer and conventional seismometers located on the same pier. Filters to be applied to the digital seismometer output which will yield least-mean-square estimates of the conventional outputs will then be computed. The development of such filters is discussed in the following section.

LEAST-MEAN-SQUARE CRITERION APPLIED TO FILTER DESIGN

The development of a filter to yield a least-mean-square estimate of a recording from a conventional seismometer when applied to the broad-band digital seismometer can best be discussed with the aid of Figure H-11.

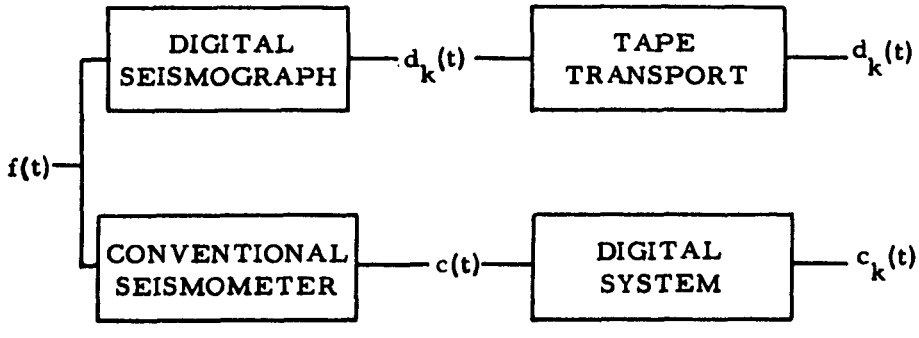

Figure H-10. Simultaneous Recording Block Diagram

The seismic signal, f(t), is fed into both the digital seismograph and the conventional system and the output of the conventional instrument is converted into a sequence of numbers, $c_k(t)$, through a digital system so that it is comparable with the output sequence of the digital seismometer, $d_k(t)$.

Due to the broad bandpass of the digital seismometer, it can be assumed that all of the information contained in the conventional output, $c_k(t)$ is also contained in the output $d_k(t)$. Therefore, there exists a linear filter having the proper transfer function to map the sequence $d_k(t)$ into $c_k(t)$. While the convolution operator of such a filter might be infinite in length, it is possible to develop a time-sampled operator consisting of a finite number of weights, N, that will give a least-mean-square-error estimation (for that number of operator points) of $c_k(t)$ when applied to $d_k(t)$. The computation of such weights can be carried out as follows.

Let $b_k(t)$ be the estimated value of $c_k(t)$ obtained from operating on $d_k(t)$ with the operator weights $A_1, A_2, \ldots A_n$.

$$b_k = \sum_{n=o}^{N} A_n d_{k-n} \tag{H-14}$$

(The function of time notation will be omitted from this point on in this development and it will be understood that d_k is the k^{th} sample of $d_k(t)$, equal to $d(k\Delta t)$ where Δt is the sample interval).

The error, e_k, between the estimated value of c_k and the true value can be written as

$$e_k = c_k - b_k \tag{H-15}$$

or

$$e_k = c_k - \sum_{n=o}^{N} A_n d_{k-n} \tag{H-16}$$

Thus the mean square error between the estimated signal and the actual conventional seismometer output for a time interval $-M\Delta t$ to $+M\Delta t$ expressed as,

$$E = \lim_{M \to \infty} \frac{1}{2M+1} \sum_{k=-m}^{+M} \left(c_k - \sum_{n=o}^{+M} A_n d_{k-n} \right)^2 \tag{H-17}$$

which can be expanded to the form

$$E = \lim_{M\to\infty} \frac{1}{2M+1} \sum_{k=-M}^{M} c_k^2 - 2 \sum_{n=o}^{N} A_n \lim_{M\to\infty} \frac{1}{2M+1} \sum_{k=-M}^{M} c_k d_{k-n}$$

$$+ \sum_{n=o}^{N} \sum_{m=o}^{M} A_n A_m \lim_{M\to\infty} \frac{1}{2M+1} \sum_{k=-M}^{M} d_{k-n}\, d_{k-m} \qquad \text{(H-18)}$$

If E is to be a least-mean-square error for N operator weights, the A_n must be chosen to minimize E, or

$$\frac{\partial E}{\partial A_j} = 0 \quad \text{for } j = 0,\ 1,\ 2, \ldots N \qquad \text{(H-19)}$$

Thus,

$$\frac{\partial E}{\partial A_j} = -2 \lim_{M\to\infty} \frac{1}{2M+1} \sum_{k=-M}^{M} c_k\, d_{k-j}$$

$$+ 2 \sum_{n=o}^{N} A_n \lim_{M\to\infty} \frac{1}{2M+1} \sum_{k=-M}^{M} d_{k-n}\, d_{k-j} = 0 \qquad \text{(H-20)}$$

or

$$\sum_{n=o}^{N} A_n \lim_{M\to\infty} \frac{1}{2M+1} \sum_{k=-M}^{M} d_{k-n}\, d_{k-j} = \lim_{M\to\infty} \frac{1}{2M+1} \sum_{k=-M}^{M} c_k\, d_{k-j} \qquad \text{(H-21)}$$

Equation 8 is a necessary condition on A_n for the error, E, to be a minimum, and it can be shown that this equation also meets the sufficiency conditions for a minimum mean square error. Thus it is possible to solve for the A_n operator points by solving the matrix equation specified by Equation 8.

APPENDIX I

LOGIC CARD SCHEMATICS

The following material is attached to this report for the sake of completeness. It contains the schematic drawings for the logic cards. The most significant design is the high-speed logic flip-flop card. Logic speeds as high as 50 megacycles are encountered for the first stage. Complete documentation for this design was made, but it is not included, because of the bulk of material.

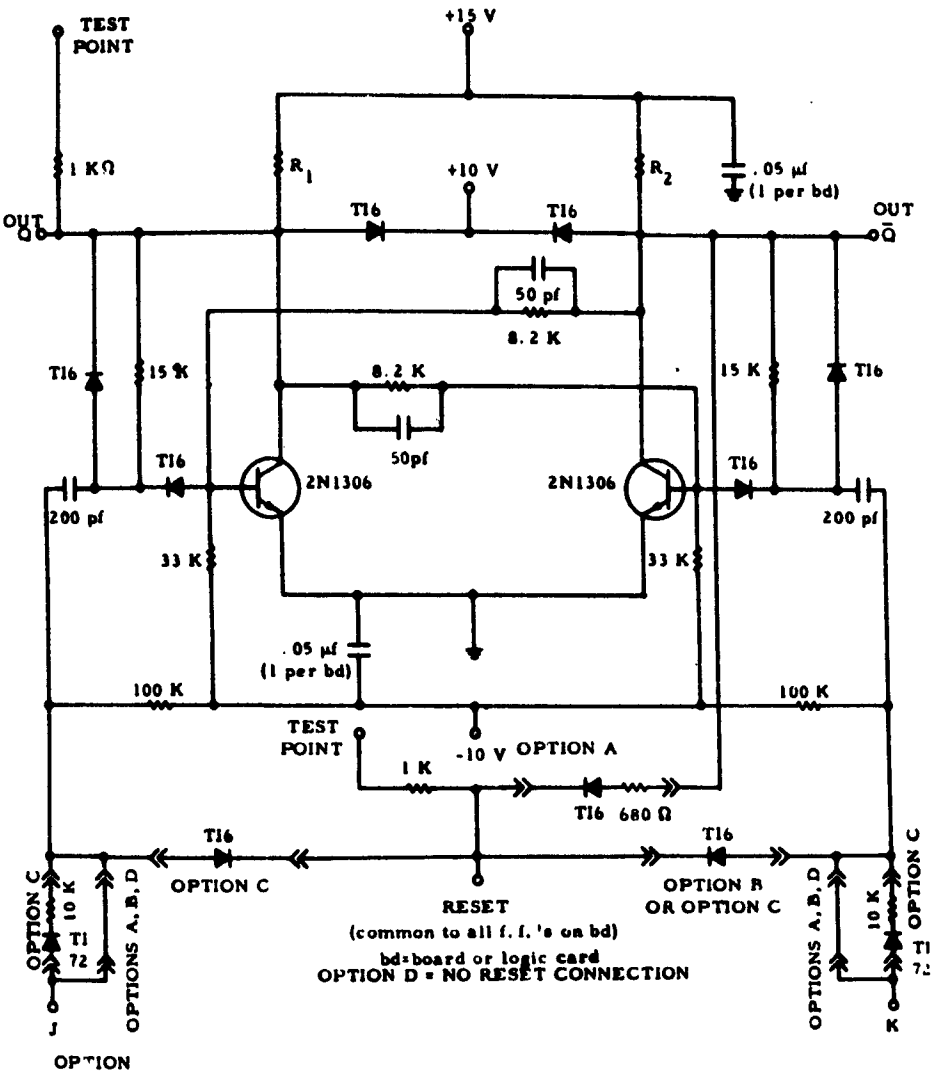

OPTION

A Used in 20-bit Counter: 23A, 24A, 25A, 26A, 14A, 15A, 16A, 17A, 5A, 6A, 7A, 8A
R_1 & R_2=2.7 K

B Used in Memory: 9B, 10B, 11B, 12B, 13B
R_1 & R_2=1.2 K

C Used in "Shift Register type" wiring: (1/2) 25B, 26B
R_1 & R_2=1.2 K

D Used in frequency divider: (1/2) 25B
R_1 & R_2=1.2 K

1250

Figure I-1. Low Speed Flip-Flop (1Mc.) (4 Per Board)

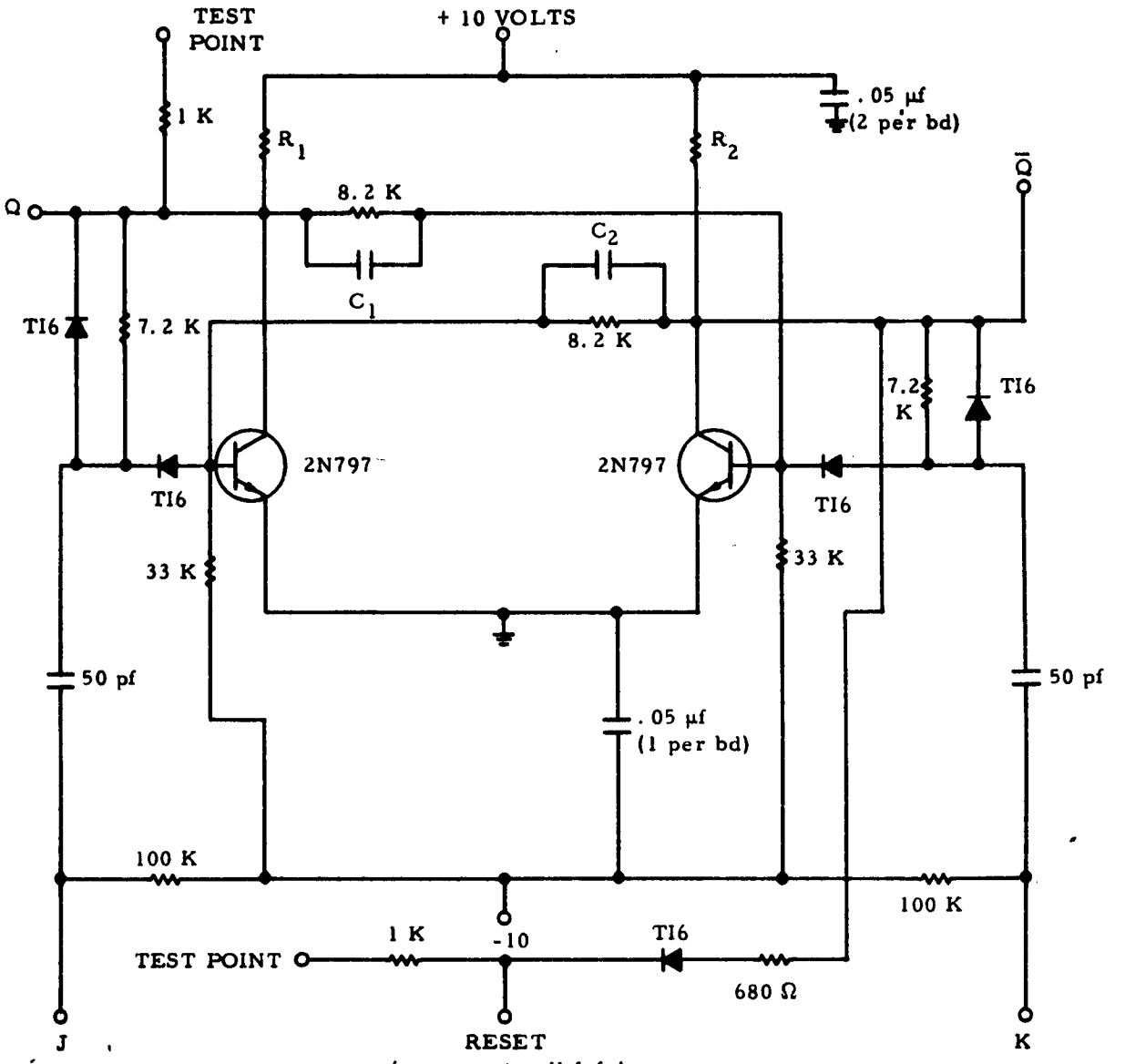

Note: Used in 22A, 13A, & 4A.

R_1 & R_2 = 470Ω
C_1 & C_2 = 50 pf
} In faster two counting stages

R_1 & R_2 = 1.2K
C_1 & C_2 = 20pf
} In slower two counting stages

1251

Figure I-2. Medium Speed Flip-Flop (To 5 MC) (4 Per Board)

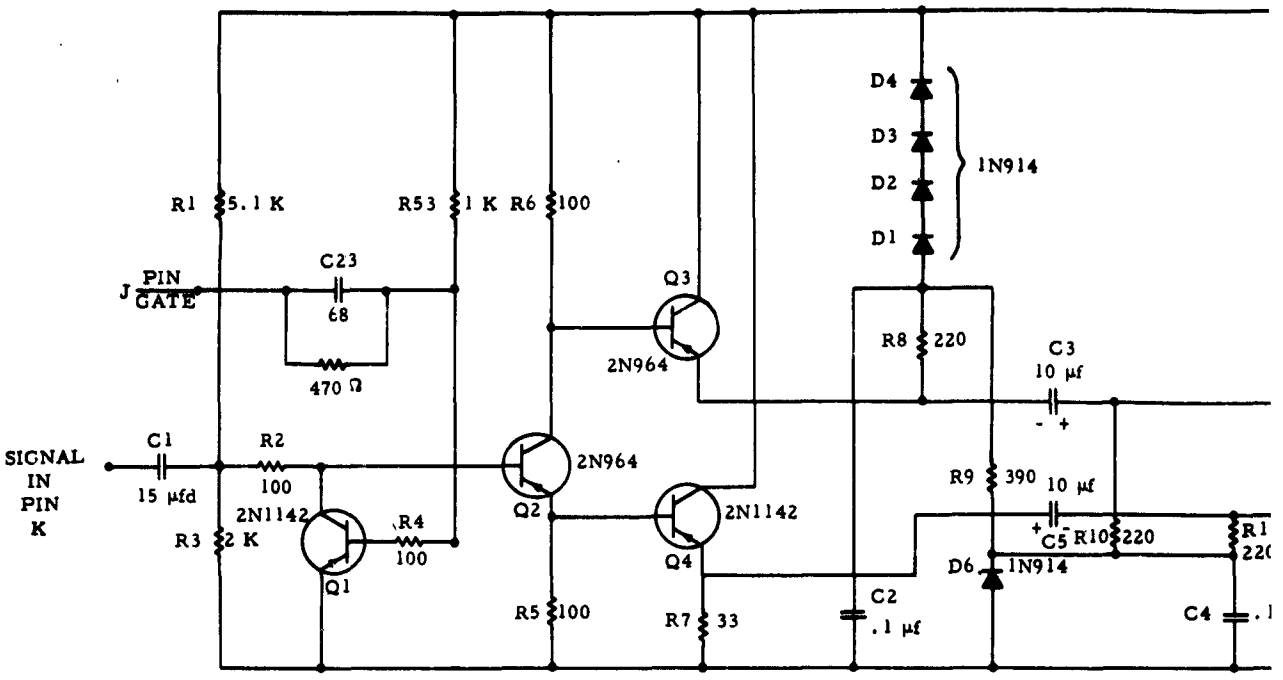
D4
D3
D2
D1
1N914
R1 5.1 K
R53 1 K
R6 100
PIN J GATE
C23
68
470 Ω
Q3
2N964
R8 220
C3
10 μf
SIGNAL IN PIN K
C1
15 μfd
R2
100
2N1142
R3 2 K
R4
100
Q1
2N964
Q2
2N1142
Q4
R9 390
10 μf
C5
R10 220
D6 1N914
R5 100
R7 33
C2
.1 μf
C4

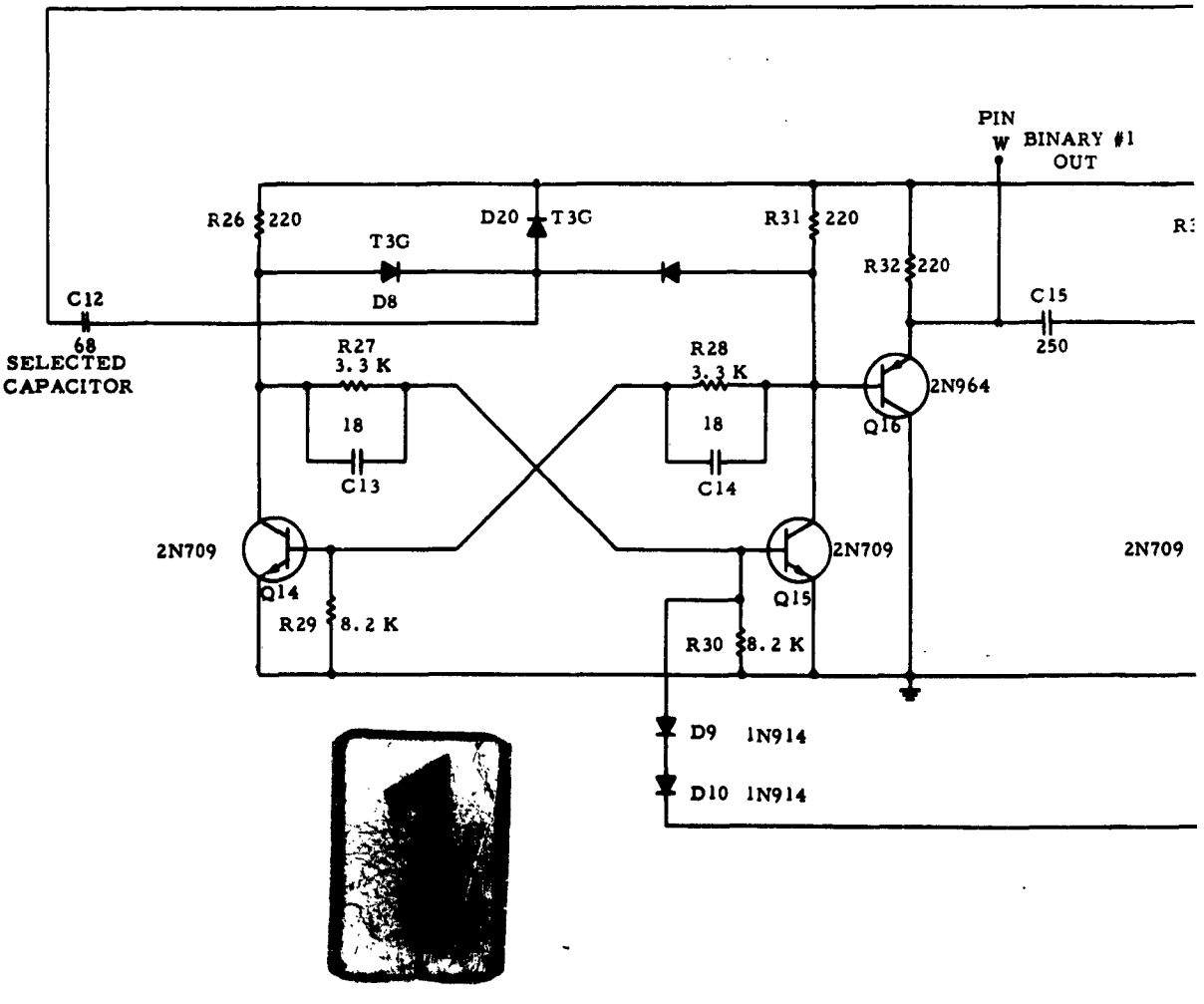
PIN W BINARY #1 OUT
R26 220
D20 T3G
T3G
D8
R31 220
R32 220
C12
68
SELECTED CAPACITOR
C15
250
R27
3.3 K
18
C13
R28
3.3 K
18
C14
2N964
Q16
2N709
Q14
2N709
Q15
2N709
R29 8.2 K
R30 8.2 K
D9 1N914
D10 1N914

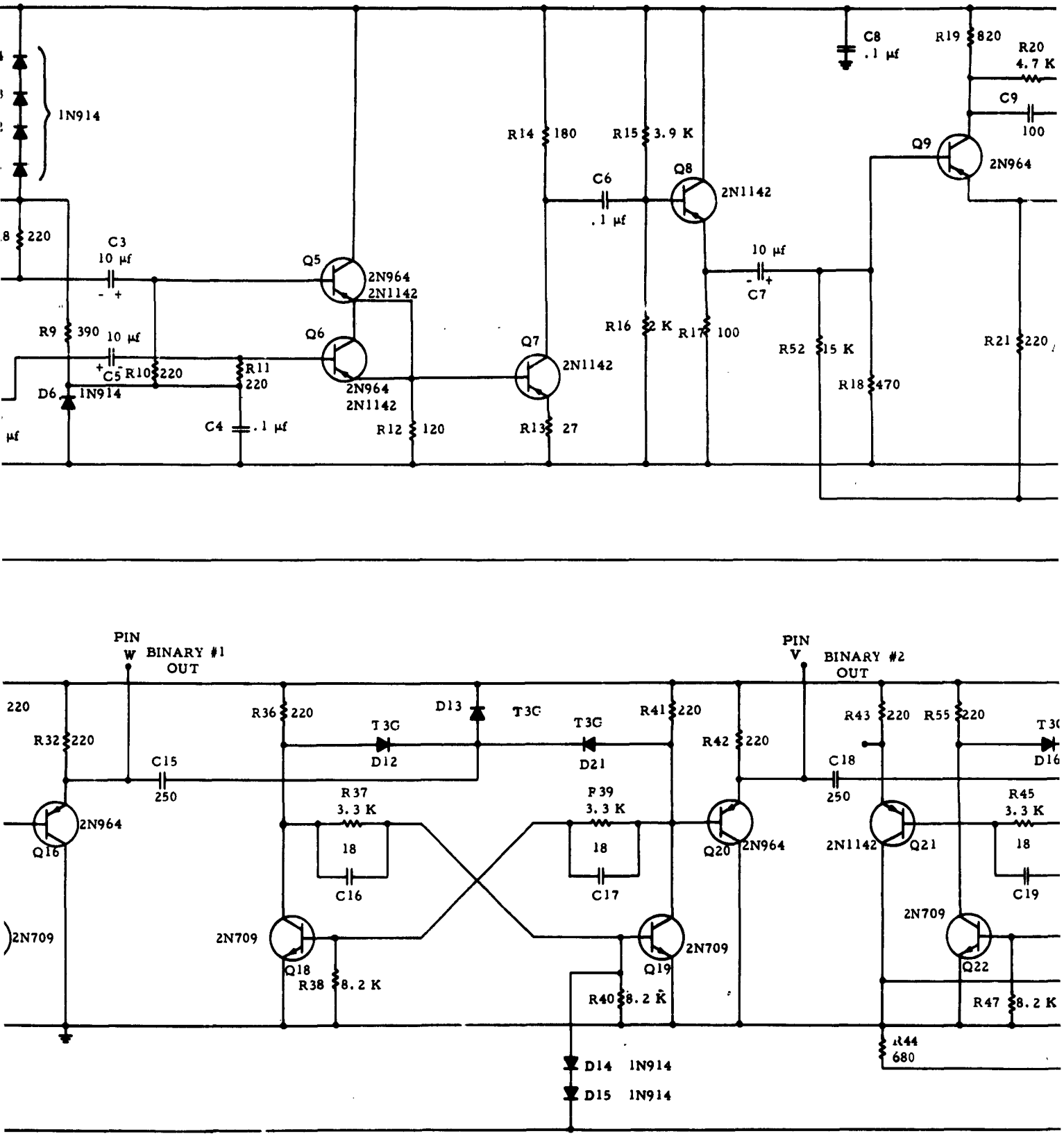

2

Figure I-3. Hig

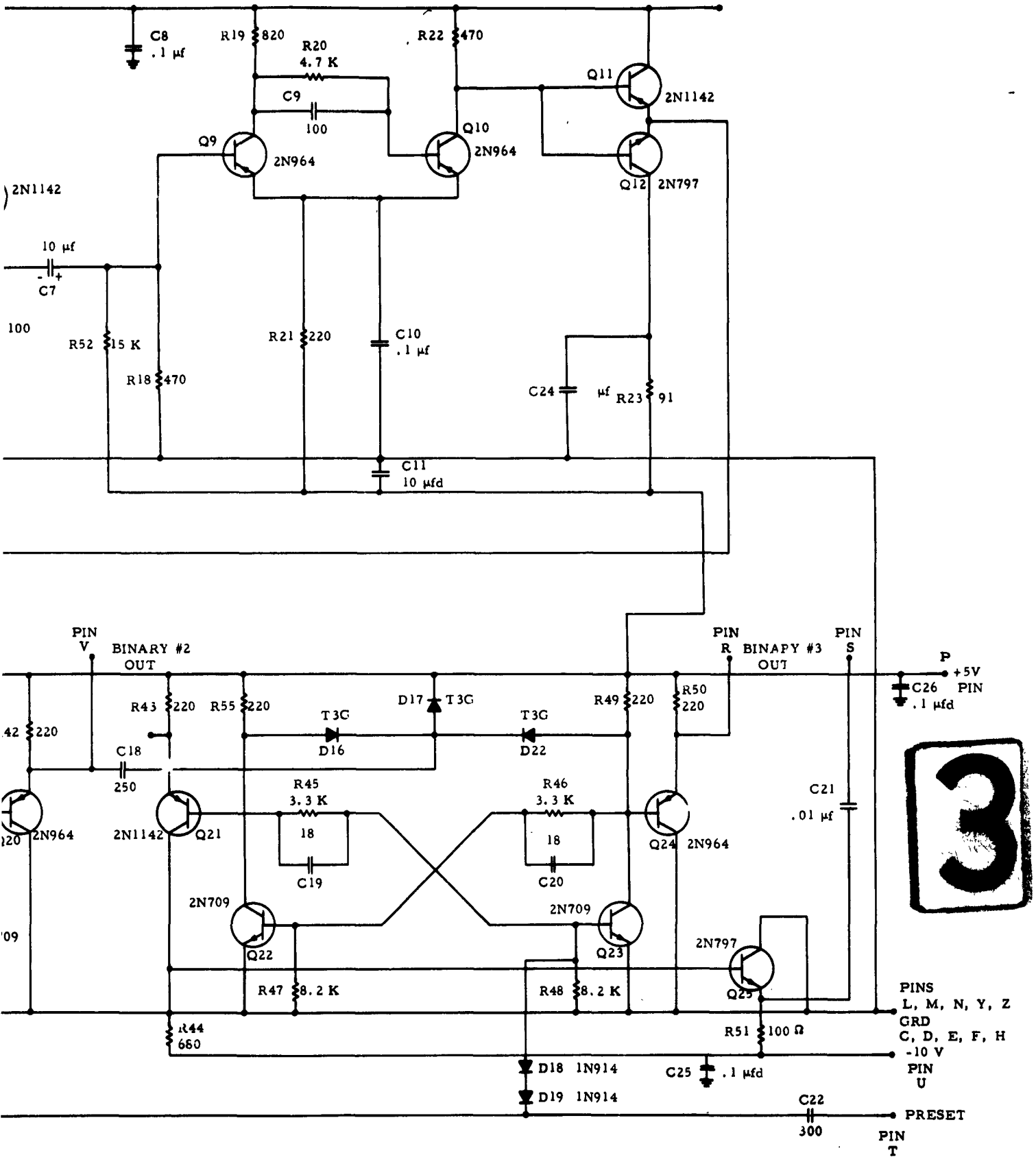

Figure I-3. High Speed Logic Board (To 50 MC) (1 Per Board)

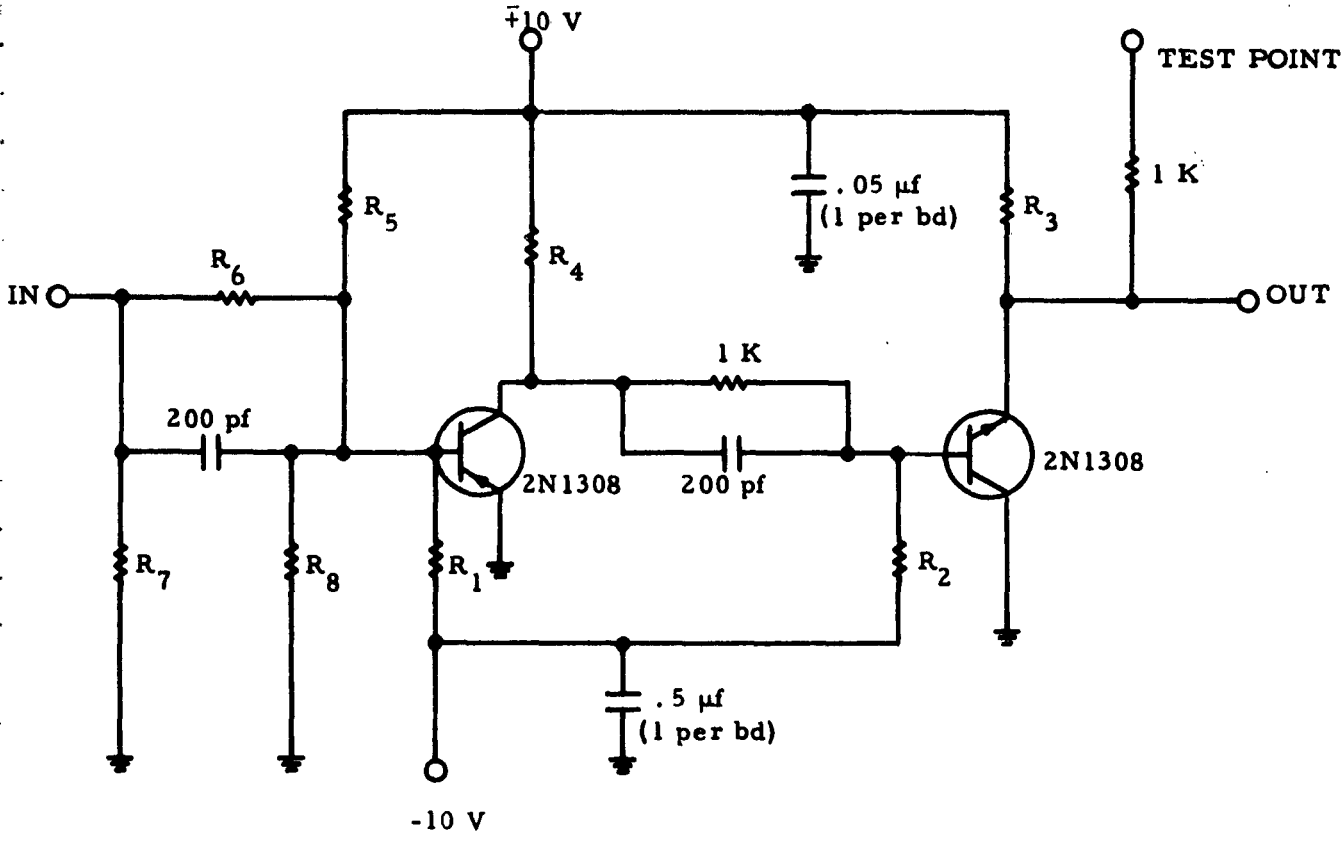

OPTIONS

POSITION	R_1	R_2	R_3	R_4	R_5	R_6	R_7	R_8	APPLICATION
6B	470 K	6.8 K	220 Ω	470 Ω	∞	47 K	10 K	∞	Counter Output
1/8 21B	∞	100 K	470	470	100 K	∞	∞	20 K	Timing Preset
3/8 21B	∞	6.8 K	220	680	∞	47 K	∞	∞	"1", "2", "3" pulses
3/8 21B	∞	6.8 K	1 K	1.5 K	∞	47 K	∞	∞	I, II, III pulses

Note: Used in positions 6B & 21B.

1283

Figure I-4. Logic Amplifier (8 Per Board)

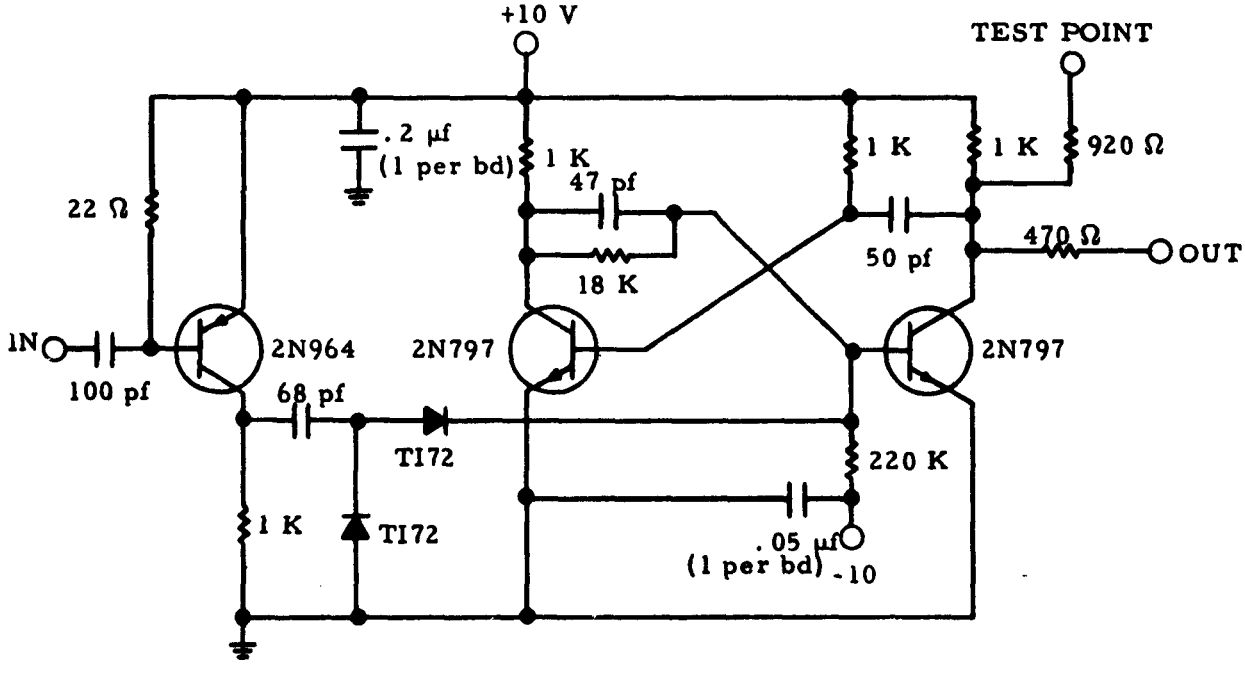

Note: Used in position 24B.

1254

Figure I-5. One-Shot Multivibrator (4 Per Board)

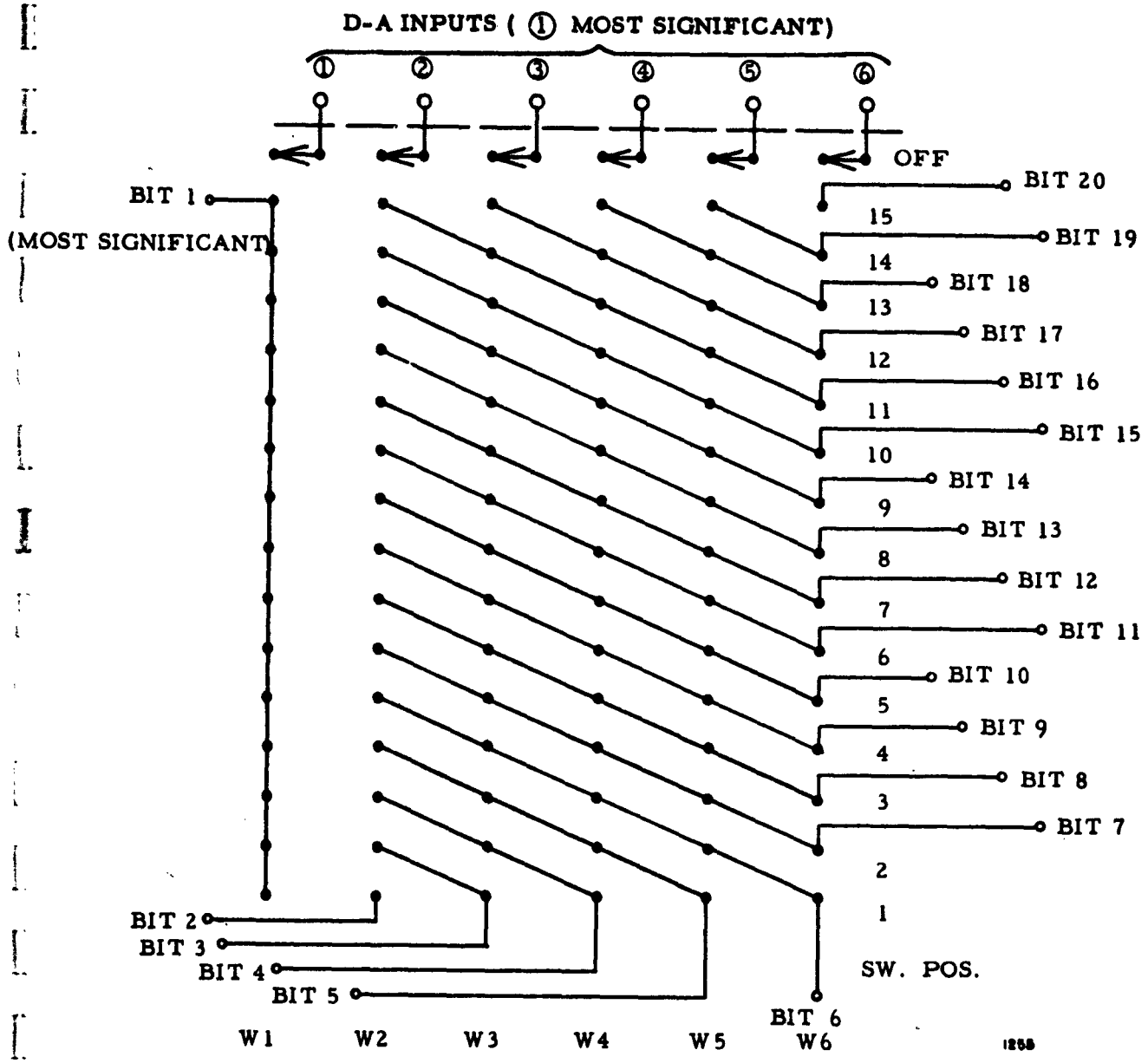

Figure I-6. Sliding Bit Gain Switch

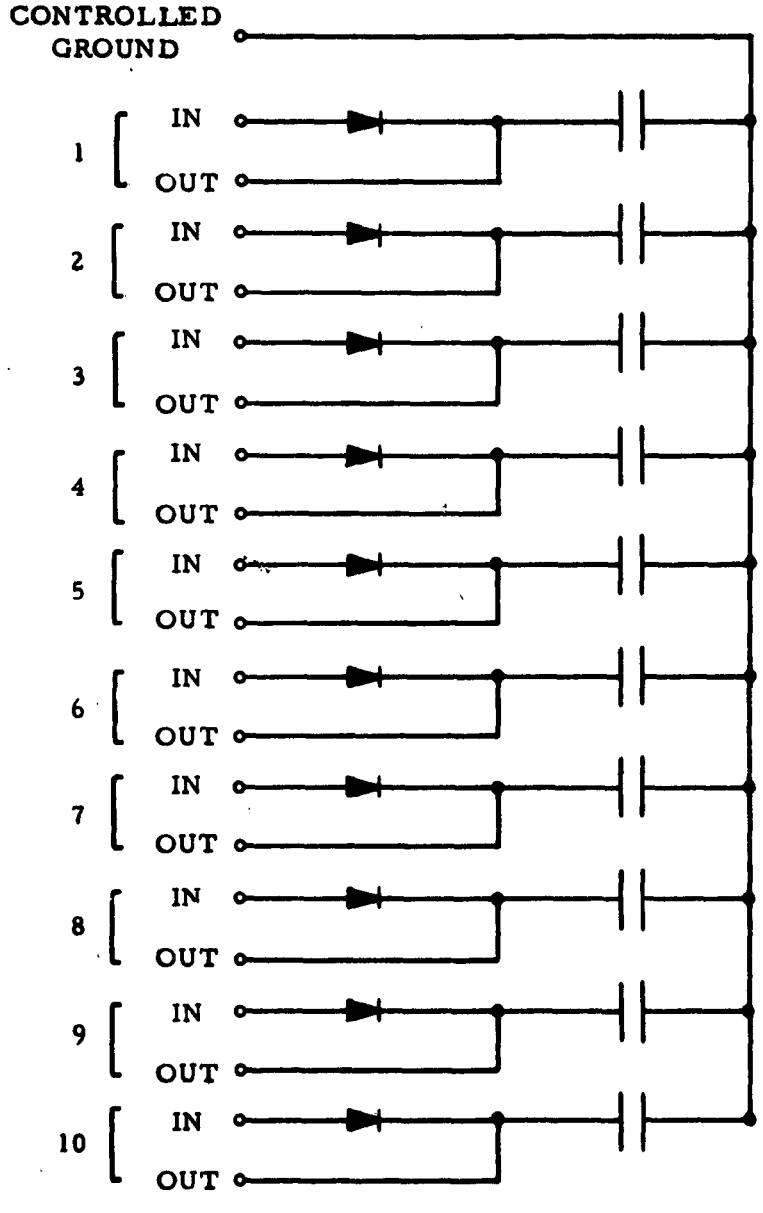

All diodes = TI6
All capacitors = .0015 μf

Note: Used in 1B, 2B.

1256

Figure I-7. Digital Indicator Storage

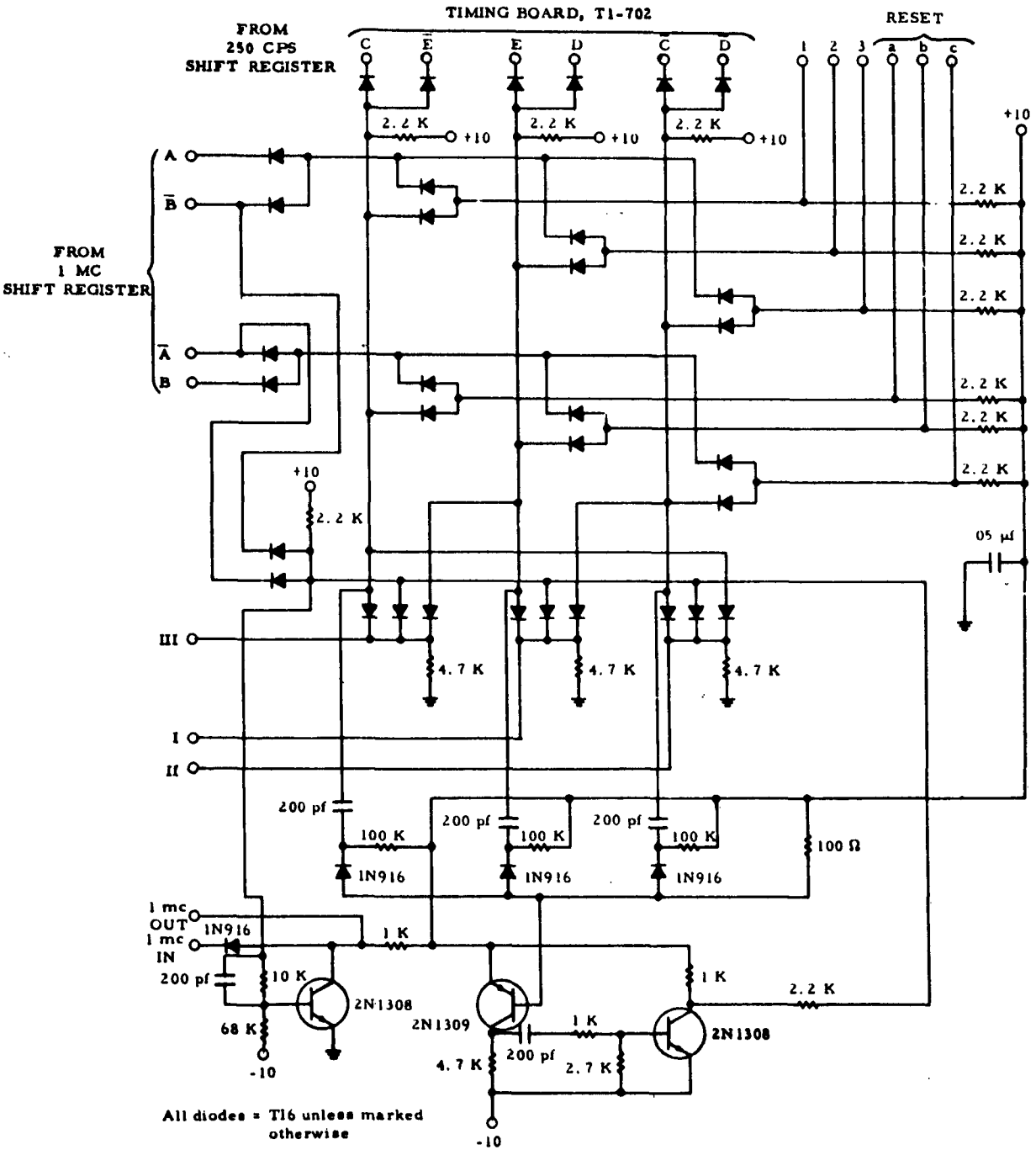

Figure I-8. Timing Board, TI-702

1257

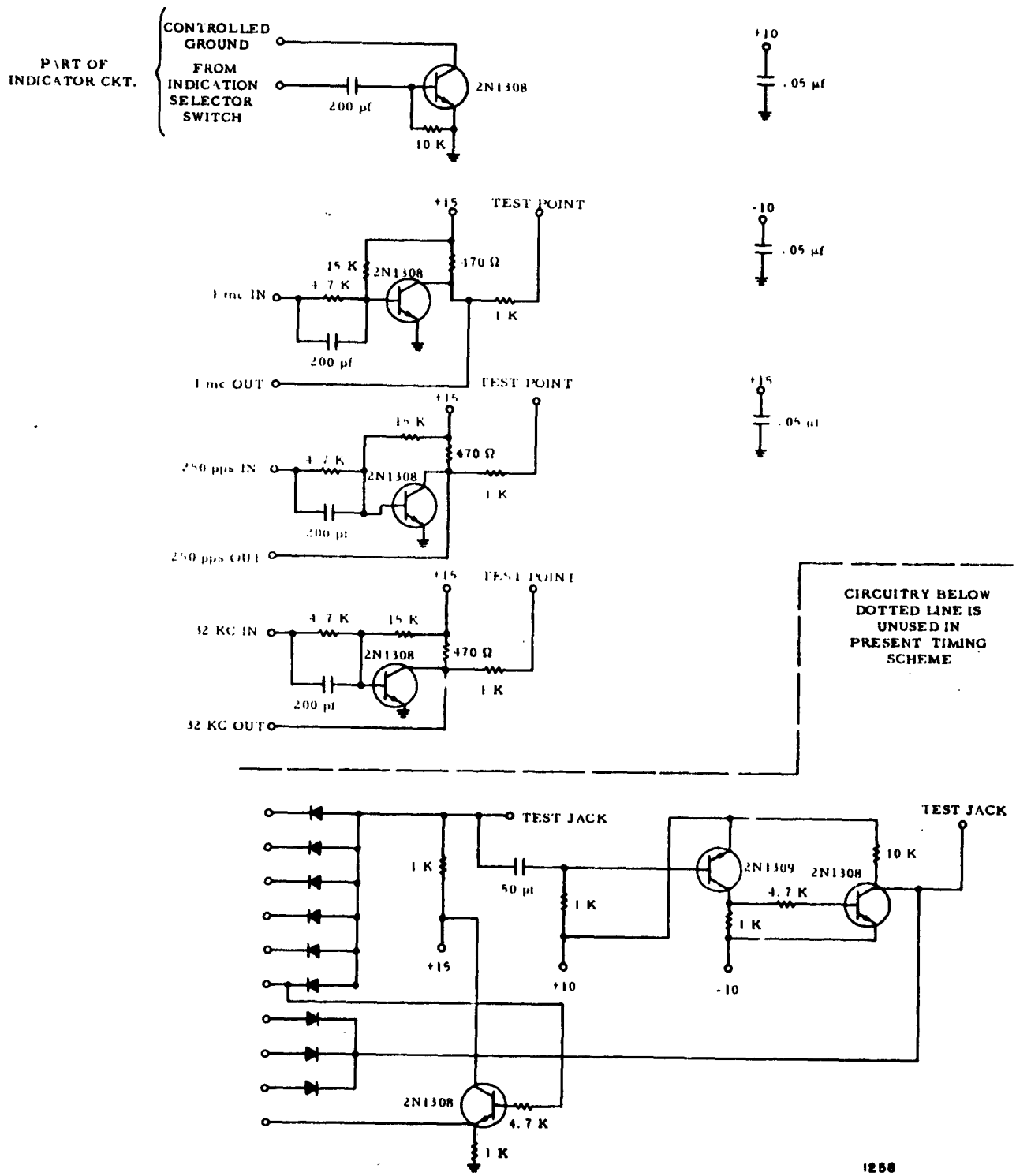

Figure I-9. Clock Converter

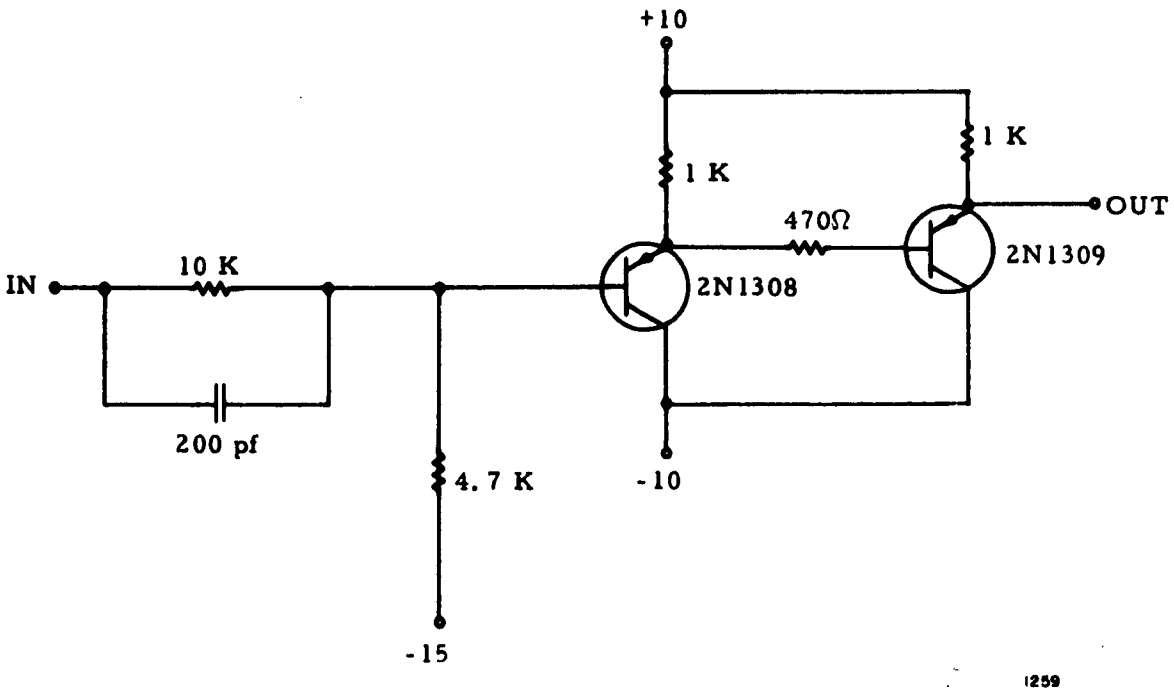

Figure I-10. Reset Driver (4 Per Board)

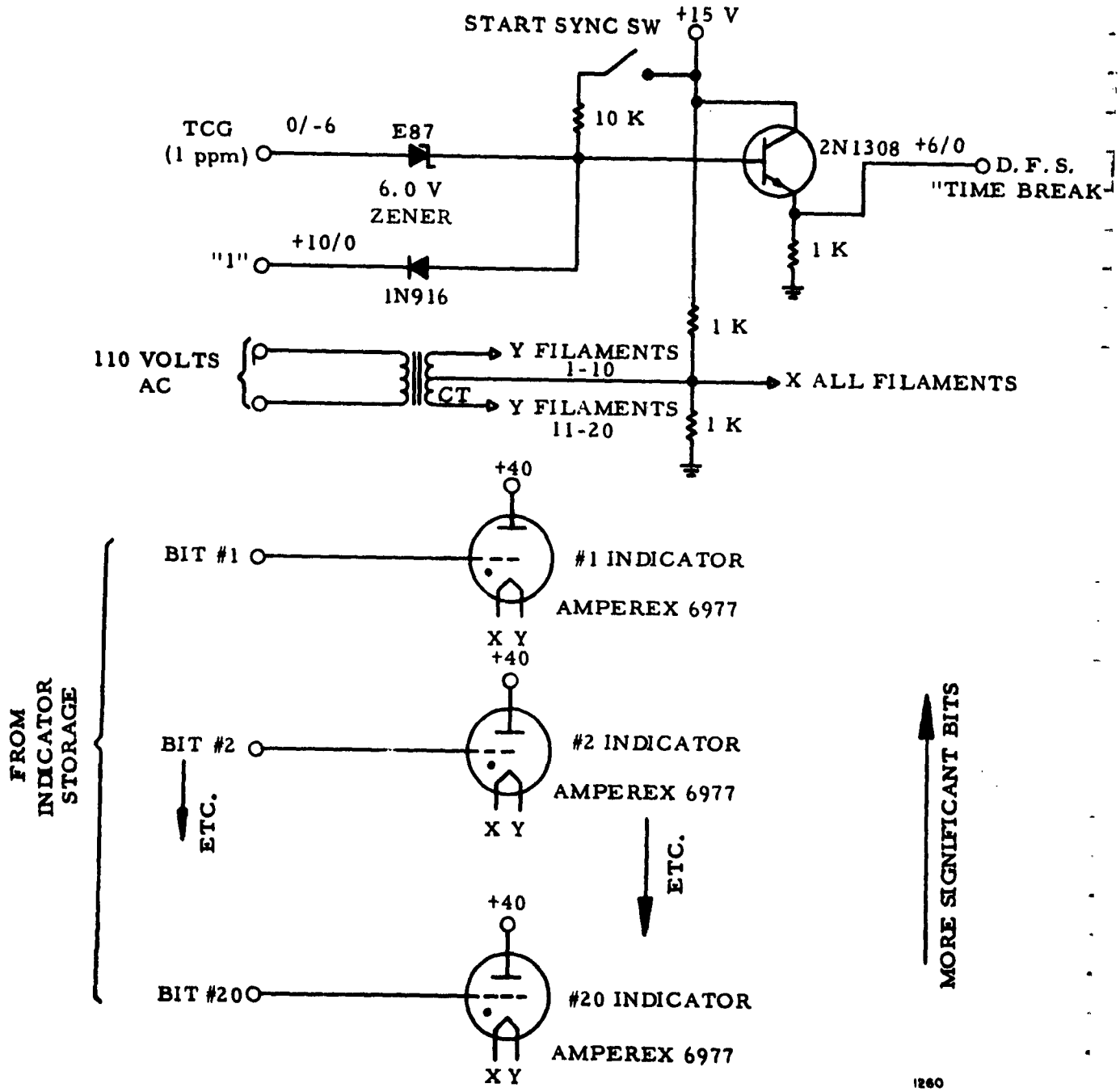

Figure I-11. Digital Display Panel

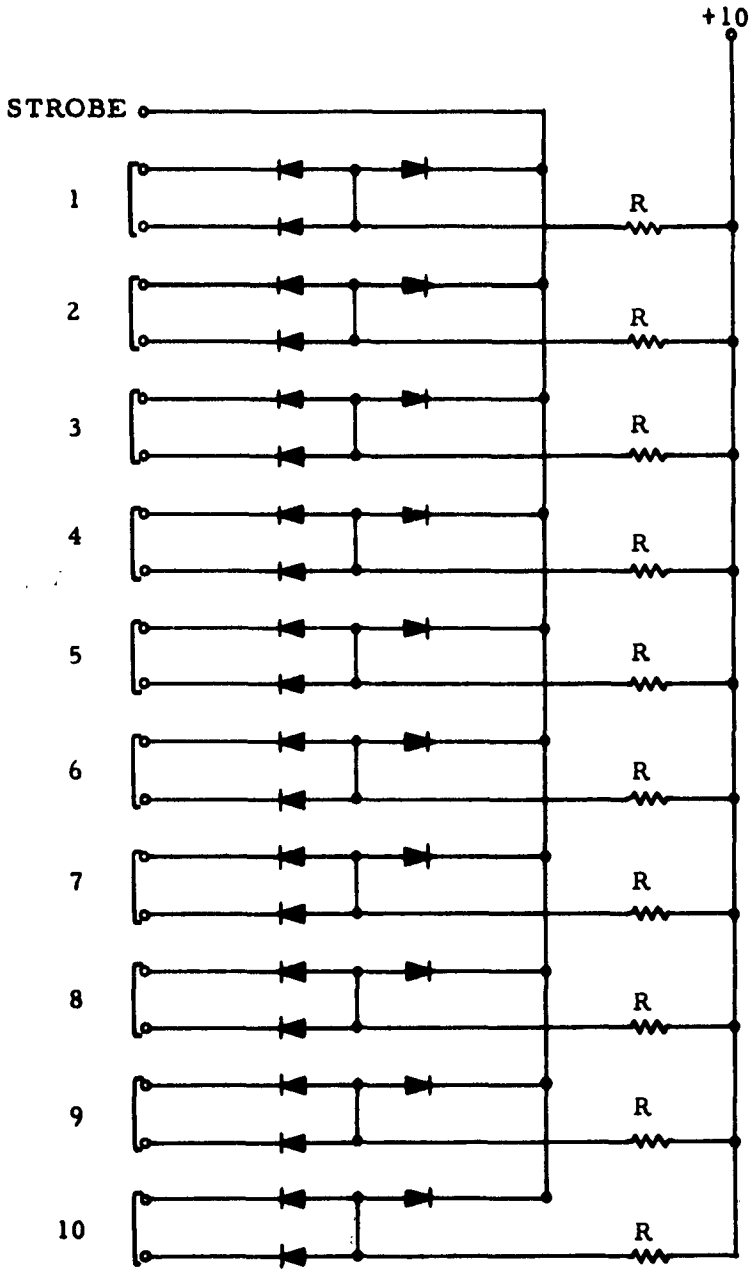

All diodes = T16

Option: Where "Or" gating of outputs is not required (as gate to D. F. S.) each output diode is replaced with a shorting bar.

With Diode: 21A, 27A, 12A, 18A, 3A, 9A, R = 1K

With Shorting Bar: 14B, 15B, R = 8.2K

1261

Figure I-12. "And" Gate

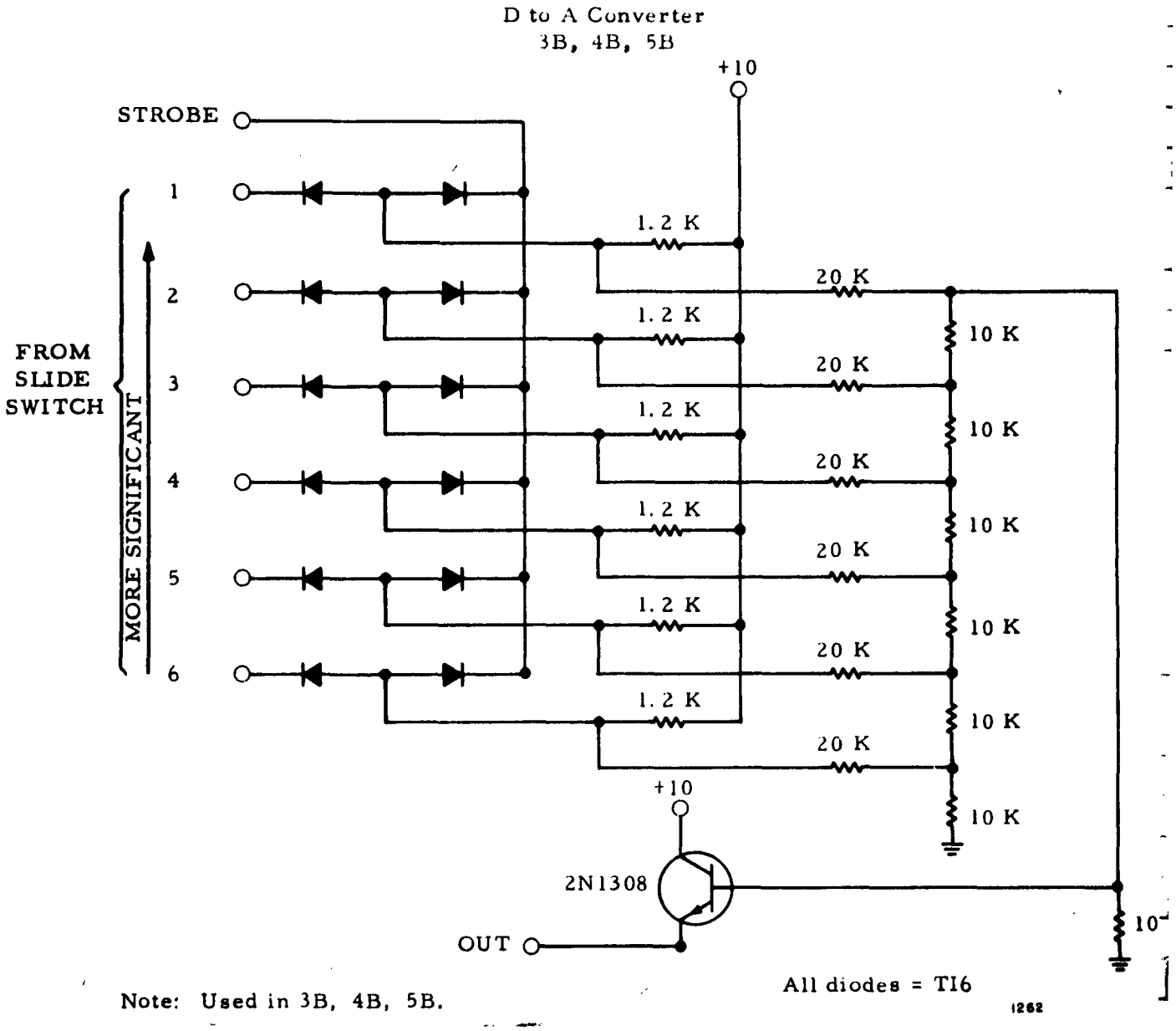

Figure I-13. Digital To Analog Converter

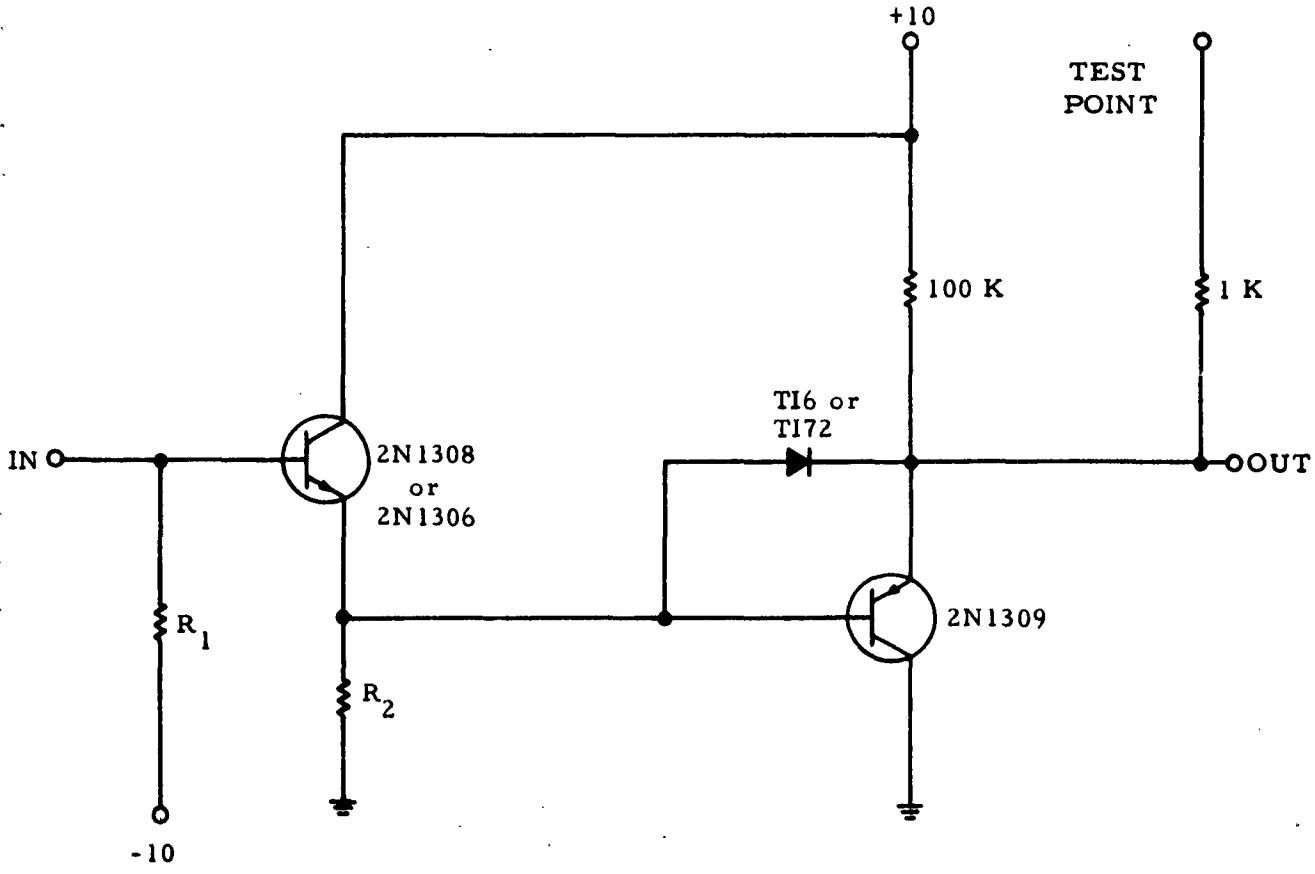

POSITION	R_1	R_2	CIRCUIT APPLICATION
7B, 8B	4.7 K	2.7 K	Counter Output Driver
17B, 18B	100 K	2.7 K	Recorder Driver
2/8 19B	100 K	2.7 K	Recorder Driver
3/8 19B	4.7K	470	Pulse "1", "2", & "3" Driver
3/8 19B	Not in use		

1263

Figure I-14. Logic Driver (8 per board)

Air Force Cambridge Research Laboratories, U. S. Air Force, Bedford, Mass.
Rpt. No. AFCRL-63-433, DIGITAL SEISMOGRAPH SYSTEM, Final Report, 29 March 1963, 176 p., incl., illus., tables.

Unclassified Report

This report describes the research, design, and development of a prototype three-component Digital Seismograph System having an output compatible with modern high-speed computers. It also describes the assembly and evaluation of a working model. The development included selection of an optimum system for digitizing the motion of seismometer masses. It was the intention of this program to develop a system of greater dynamic range (120 db), a broad frequency band (0.1 to 10 cps), good linearity, and other characteristics within the tolerance limits of comparable conventional instruments.

1. Geology & Seismology
2. Seismographs
3. Digital Recording Systems

I. AFCRL Project 8652, Task 865205
II. Contract AF 19(628)-472
III. Texas Instruments Incorporated, Dallas, Texas
IV. Bruce M. Williams
V. In ASTIA collection

Air Force Cambridge Research Laboratories, U. S. Air Force, Bedford, Mass.
Rpt. No. AFCRL-63-433, DIGITAL SEISMOGRAPH SYSTEM, Final Report, 29 March 1963, 176 p., incl., illus., tables.

Unclassified Report

This report describes the research, design, and development of a prototype three-component Digital Seismograph System having an output compatible with modern high-speed computers. It also describes the assembly and evaluation of a working model. The development included selection of an optimum system for digitizing the motion of seismometer masses. It was the intention of this program to develop a system of greater dynamic range (120 db), a broad frequency band (0.1 to 10 cps), good linearity, and other characteristics within the tolerance limits of comparable conventional instruments.

1. Geology & Seismology
2. Seismographs
3. Digital Recording Systems

I. AFCRL Project 8652, Task 865205
II. Contract AF 19(628)-472
III. Texas Instruments Incorporated, Dallas, Texas
IV. Bruce M. Williams
V. In ASTIA collection

Air Force Cambridge Research Laboratories, U. S. Air Force, Bedford, Mass.
Rpt. No. AFCRL-63-433, DIGITAL SEISMOGRAPH SYSTEM, Final Report, 29 March 1963, 176 p., incl., illus., tables.

Unclassified Report

This report describes the research, design, and development of a prototype three-component Digital Seismograph System having an output compatible with modern high-speed computers. It also describes the assembly and evaluation of a working model. The development included selection of an optimum system for digitizing the motion of seismometer masses. It was the intention of this program to develop a system of greater dynamic range (120 db), a broad frequency band (0.1 to 10 cps), good linearity, and other characteristics within the tolerance limits of comparable conventional instruments.

1. Geology & Seismology
2. Seismographs
3. Digital Recording Systems

I. AFCRL Project 8652, Task 865205
II. Contract AF 19(628)-472
III. Texas Instruments Incorporated, Dallas, Texas
IV. Bruce M. Williams
V. In ASTIA collection

Air Force Cambridge Research Laboratories, U. S. Air Force, Bedford, Mass.
Rpt. No. AFCRL-63-433, DIGITAL SEISMOGRAPH SYSTEM, Final Report, 29 March 1963, 176 p., incl., illus., tables.

Unclassified Report

This report describes the research, design, and development of a prototype three-component Digital Seismograph System having an output compatible with modern high-speed computers. It also describes the assembly and evaluation of a working model. The development included selection of an optimum system for digitizing the motion of seismometer masses. It was the intention of this program to develop a system of greater dynamic range (120 db), a broad frequency band (0.1 to 10 cps), good linearity, and other characteristics within the tolerance limits of comparable conventional instruments.

1. Geology & Seismology
2. Seismographs
3. Digital Recording Systems

I. AFCRL Project 8652, Task 865205
II. Contract AF 19(628)-472
III. Texas Instruments Incorporated, Dallas, Texas
IV. Bruce M. Williams
V. In ASTIA collection